Szkoła Doktorska Nauk Ścisłych i Przyrodniczych
Uniwersytetu Łódzkiego

Kamil Płuciennik

Zmiany strukturalne i funkcjonalne błon erytrocytów człowieka oraz białka modelowego albuminy narażonych na działanie nanocząstek polistyrenu o różnych średnicach (*in vitro*)

Structural and functional changes in human erythrocyte membranes and model albumin protein exposed to polystyrene nanoparticles of various diameters (*in vitro*)

Praca doktorska wykonana
pod kierunkiem promotora
prof. dr hab. Bożeny Bukowskiej
oraz promotora pomocniczego
dr hab. Pauliny Sicińskiej

w Katedrze Biofizyki Skażeń Środowiska,
Wydziału Biologii i Ochrony Środowiska,
Uniwersytetu Łódzkiego

Łódź, 2025

Serdecznie dziękuję moim oddanym promotorkom ***prof. dr hab. Bożenie Bukowskiej*** *oraz* ***dr hab. Paulinie Sicińskiej*** *za życzliwość, cierpliwość, zaangażowanie, wskazówki, poświęcony czas i nieocenioną pomoc w realizacji niniejszej pracy.*

Bardzo dziękuję również pracownikom Katedry Biofizyki Skażeń Środowiska, a w szczególności ***dr hab. Anicie Krokosz prof. UŁ*** *oraz* ***dr hab. Piotrowi Duchnowiczowi,*** *za podzielenie się swoją wiedzą i doświadczeniem oraz cenne wskazówki, które przyczyniły się do powstania niniejszej pracy.*

Dziękuję także ***doktorantkom Katedry Biofizyki Skażeń Środowiska*** *za wszelką pomoc i wspaniałą atmosferę w pracy.*

Szczególnie chciałabym podziękować ***Rodzicom*** *za ich wsparcie i wiarę we mnie podczas całej mojej drogi edukacji, oraz* ***mojej siostrze Karolinie****, która jest nieocenionym wsparciem.*

SPIS TREŚCI

WSPÓŁPRACA NAUKOWA

Część badań przedstawionych w zbiorze opublikowanych artykułów stanowiących podstawę rozprawy doktorskiej, przeprowadzono we współpracy z poniższymi jednostkami naukowymi:

- Uniwersytet Przyrodniczy we Wrocławiu
  - Katedra Fizyki i Biofizyki

    Wydział Biotechnologii i Nauk o Żywności

UNIWERSYTET PRZYRODNICZY WE WROCŁAWIU

- Uniwersytet Warmińsko-Mazurski w Olsztynie
  - Katedra Fizyki i Biofizyki.

    Wydział Nauki o Żywności

UNIWERSYTET WARMIŃSKO-MAZURSKI W OLSZTYNIE

- Uniwersytet Radomski im. Kazimierza Pułaskiego
  - Katedra Podstawowych Nauk Medycznych.

    Wydział Nauk Medycznych i Nauk o Zdrowiu

UNIWERSYTET RADOMSKI im. Kazimierza Pułaskiego

ŹRÓDŁA FINANSOWANIA

Badania przeprowadzone w niniejszej pracy sfinansowano z następujących źródeł:

- Dofinansowanie Działalności Doktorantów z budżetu Szkoły Doktorskiej Nauk Ścisłych i Przyrodniczych Uniwersytetu Łódzkiego w latach 2022-2025.

SZKOŁA DOKTORSKA
NAUK ŚCISŁYCH
I PRZYRODNICZYCH
Uniwersytet Łódzki

- Subwencja Katedry Biofizyki Skażeń Środowiska Uniwersytetu Łódzkiego.

SPIS PUBLIKACJI WCHODZĄCYCH W SKŁAD ROZPRAWY DOKTORSKIEJ

Publikacja przeglądowa:

Płuciennik K., Sicińska P., Misztal W., Bukowska B.*, I*mportant Factors Affecting Induction of Cell Death, Oxidative Stress and DNA Damage by Nano- and Microplastic Particles In Vitro.* Cells 2024; 13(9):768, https://doi.org/10.3390/cells13090768
Punkty MNiSW: 140, IF: 6,1 (5-letni)

Publikacje doświadczalne:

Płuciennik K., Sicińska P., Duchnowicz P., Bonarska-Kujawa D., Męczarska K., Solarska-Ściuk K., Miłowska K., Bukowska B.*, *The effects of non-functionalized polystyrene nanoparticles with different diameters on human erythrocyte membrane and morphology.* 2023; Toxicology in Vitro 91(1):105634, https://doi.org/10.1016/j.tiv.2023.105634
Punkty MNiSW: 100, IF: 3,0 (5-letni)

Płuciennik K., Szabelski M., Miłowska K., Ciepluch K., Duchnowicz P., Krokosz A., Sicińska P., Bukowska B.*, *The interactions of non-functionalized polystyrene nanoparticles with human albumin and erythrocyte proteins: implications and potential consequences*. Scientific Reports 2025; 15: 30076, https://doi.org/10.1038/s41598-025-15422-w
Punkty MNiSW: 140, IF: 4,3 (5-letni)

Nieopublikowany manuskrypt artykułu doświadczalnego:

Płuciennik K., Bukowska B., Sicińska P.*, *Polystyrene nanoparticles and death of erythrocytes: does exposure induce eryptosis?* 2025; wysłany do czasopisma Nanotoxicology.
Punkty MNiSW: 140, IF: 4,2 (5-letni)

Bibliometria:

Sumaryczna liczba punktów MNiSW cyklu prac opublikowanych wynosi: **380 pkt**

Sumaryczny IF cyklu publikacji opublikowanych wynosi: **13,4**

Indeks Hirscha = (Według Scopus): **2**

Liczba cytowań (bez autocytowań) (Według Scopus): **62**

STRESZCZENIE

Zwiększająca się od wielu lat światowa skala produkcji tworzyw sztucznych wraz z nieprawidłową gospodarką odpadami i niskim poziomem recyklingu prowadzi do zanieczyszczenia środowiska plastikiem. Tworzywa sztuczne pod wpływem czynników fizyko-chemicznych (np. promieniowania UV), biodegradacji mikrobiologicznej czy degradacji chemicznej rozkładają się do mniejszych mikroplastików o średnicy <5000 μm, a w dalszej konsekwencji nanocząstek, których średnica wynosi poniżej 0,100 μm. Skala zanieczyszczenia środowiska mikro- i nanoplastikami prowadzi do narażenia na te związki organizmów żywych, o czym świadczą oznaczenia poziomu tych cząstek w różnych tkankach człowieka, w tym również we krwi. Jednym z najczęściej produkowanych tworzyw sztucznych, jest polistyren, który znalazł wykorzystanie m.in. jako materiał izolacyjny tzw. styropian. Materiał ten znajdował się nawet w próbkach pochodzących z organizmu człowieka. Przewlekłe narażenie ludzi na cząstki plastiku oraz ich wykrycie w tkankach człowieka, a zwłaszcza we krwi, skłania do oceny wpływu nanocząstek polistyrenu na poszczególne elementy morfotyczne, w tym erytrocyty będące najliczniejszymi komórkami nie tylko krwi, ale także organizmu człowieka. W związku z powyższym celem badań przedstawionych w niniejszej pracy doktorskiej była ocena wpływu niefunkcjonalizowanych nanocząstek polistyrenu (PS-NPs) o różnych średnicach (~30 nm, ~45 nm i ~70 nm) na strukturę i funkcję erytrocytów człowieka. Ponadto ze względu na obecność we krwi licznych białek, które mogą wchodzić w interakcje z PS-NPs, w badaniach uwzględniono także wpływ nanocząstek na najobficiej występujące we krwi człowieka białko, albuminę ludzką. W pracy analizowano potencjał hemolityczny PS-NPs, ich wpływ na płynność błony komórkowej erytrocytów oraz na kształt badanych komórek. Określono także oddziaływanie tych nanocząstek z białkiem modelowym albuminą oraz białkami erytrocytarnymi. Ponadto poddano ocenie wpływ nanocząstek polistyrenu na generowanie reaktywnych form tlenu i utlenianie lipidów oraz oznaczono parametry związane z występowaniem eryptozy w krwinkach czerwonych. W badaniach wykorzystano następujące techniki: elektronowy rezonans paramagnetyczny, spektrofluorymetrię, cytofluorymetrię, spektrofotometrię, metodę dichroizmu kołowego (CD), metodę dynamicznego rozpraszania światła (DLS) oraz mikroskopię optyczną. Początkowo oceniono potencjał hemolityczny nanocząstek polistyrenu, przy czym wykazano, że PS-NPs w wysokich stężeniach indukują zależną od średnicy hemolizę erytrocytów. W dalszej kolejności przeprowadzone eksperymenty dowiodły, że PS-NPs prowadzą do usztywnienia regionów hydrofobowych błony komórkowej

erytrocytów oraz indukują zmiany reologiczne krwinek czerwonych. W kolejnym etapie badań określono wpływ nanocząstek polistyrenu na białko modelowe albuminę człowieka (HSA) oraz białka erytrocytarne. W przypadku wpływu PS-NPs na albuminę wykazano tworzenie się stabilnej korony białkowej na nanoczastkach, która może mieć wpływ *in vivo* na interakcje PS-NPs z komórkami krwi. Z kolei w przypadku oddziaływania tych samych nanocząstek na białka erytrocytarne zaobserwowano zmianę mikrolepkości wnętrza krwinek czerwonych, a także utlenianie białek błonowych. Stwierdzony wzrost poziomu grup karbonylowych mógł wynikać z mechanicznych oddziaływań PS-NPs z błoną komórkową i wykazanych pod ich wpływem zmian reologicznych krwinek czerwonych. Nie stwierdzono natomiast utleniania hemoglobiny przez PS-NPs ani zmian w aktywności acetylocholinoesterazy. Przeprowadzone w ostatnim etapie eksperymenty wykazały, że PS-NPs nie indukują tworzenia się reaktywnych form tlenu, w wysokim stężeniu powodują natomiast utlenianie lipidów. Nie obserwowano zmian w aktywności kaspazy-3. Eksternalizację fosfatydyloseryny oraz wzrost poziomu wewnątrzkomórkowych jonów wapnia zaobserwowano jedynie w najwyższym z badanych stężeń, które jest stężeniem hemolitycznym. Z kolei aktywację kalpain, zaobserwowano już przy stężeniach przedhemolitycznych PS-NPs (od 1 do 50 μg/ml) co może mieć związek ze zmianami mechanicznymi wywoływanymi przez te nanocząstki. Zatem analiza wszystkich zbadanych parametrów eryptotycznych wskazuje na brak indukcji programowanej śmierci krwinek czerwonych pod wpływem PS-NPs.

Podsumowując wszystkie wyniki uzyskane w pracy doktorskiej niefunkcjonalizowane PS-NPs wywierały niewielki szkodliwy wpływ na erytrocyty człowieka zależny od wielkości PS-NPs. Prowadziły do zmian we właściwościach mechanicznych błony komórkowej, takich jak jej usztywnienie i zaburzenia reologiczne, co ostatecznie skutkowało hemolizą erytrocytów przy wysokich stężeniach PS-NPs (100–250 μg/ml). Stwierdzono, że PS-NPs nie wykazywały bezpośrednich właściwości prooksydacyjnych wobec hemoglobiny ani nie zwiększały poziomu reaktywnych form tlenu, jedynie przy wysokich stężeniach (100 μg/ml) indukowały peroksydację lipidów oraz wzrost poziomu grup karbonylowych w białkach błonowych. Wykazano, że PS-NPs, niezależnie od wielkości, nie inicjują eryptozy w stężeniach przedhemolitycznych, lecz wywołują subtelne zmiany strukturalne błony, prawdopodobnie o charakterze mechanicznym, co potwierdza zwiększona aktywność kalpain już przy niskich stężeniach nanocząstek. Ponadto udowodniono, że PS-NPs tworzą stabilną koronę białkową z albuminą, która ulega modyfikacjom strukturalnym pod wpływem interakcji z tymi cząstkami, a modyfikacja ta może prawdopodobnie wpływać na prawidłowe funkcjonowanie erytrocytów w układzie *in vivo.*

ABSTRACT

The increasing global production of plastics over many years, combined with improper waste management and low recycling rates, has led to widespread plastic pollution. Under the influence of various physico-chemical factors (e.g., UV radiation), as well as microbiological biodegradation and chemical degradation, plastics break down into smaller microplastics (<5,000 μm) and, subsequently, into nanoparticles with diameters below 0.1 μm. The extent of environmental contamination with micro- and nanoplastics results in exposure of living organisms to these particles, as evidenced by their detection in various human tissues, including blood. One of the most commonly produced plastics is polystyrene, used, among other applications, as an insulating material known as Styrofoam. This material has also been detected in human-derived samples. Chronic human exposure to plastic particles, together with their presence in human tissues, particularly in blood, highlights the need to examine the effects of polystyrene nanoparticles on individual morphotic elements, including erythrocytes, which are the most abundant cells not only in the blood but also in the entire human body. Accordingly, this doctoral thesis aimed to assess the impact of non-functionalized polystyrene nanoparticles (PS-NPs) of different diameters (~30 nm, ~45 nm, and ~70 nm) on the structure and function of human erythrocytes. Moreover, given the presence in blood of numerous proteins capable of interacting with PS-NPs, the study also included an evaluation of the effects of these nanoparticles on the most abundant human blood protein, human serum albumin (HSA). Specifically, the haemolytic potential of PS-NPs was assessed, together with their effects on erythrocyte membrane fluidity and cell morphology. The interactions of PS-NPs with the model protein albumin and with erythrocyte proteins were also examined. In addition, the research evaluated the effects of PS-NPs on reactive oxygen species (ROS) generation and lipid oxidation, as well as parameters associated with the occurrence of eryptosis in red blood cells. The following techniques were employed: electron paramagnetic resonance, flow cytometry, spectrofluorometry, spectrophotometry, circular dichroism (CD), dynamic light scattering (DLS), and optical microscopy. Initial analyses demonstrated that PS-NPs at high concentrations induce diameter-dependent haemolysis of erythrocytes. Subsequent experiments showed that PS-NPs stiffen the hydrophobic regions of the erythrocyte membrane and induce rheological changes in red blood cells. Further studies revealed that PS-NPs interact with both HSA and erythrocyte proteins.

With respect to HSA, PS-NPs were shown to induce the formation of a stable protein corona, which may influence in vivo interactions of PS-NPs with blood cells. In erythrocyte proteins, exposure was associated with altered intracellular microviscosity and oxidation of membrane proteins. The observed increase in carbonyl group levels may result from mechanical interactions between PS-NPs and the membrane, as well as from the rheological alterations induced by these nanoparticles. No oxidation of haemoglobin or changes in acetylcholinesterase activity were detected. Experiments carried out in the final stage of the study demonstrated that PS-NPs do not induce ROS generation, although at high concentrations they do cause lipid oxidation. No changes in caspase-3 activity were observed. Phosphatidylserine externalization and increased intracellular calcium levels were detected only at the highest concentration tested, which was haemolytic. In contrast, calpain activation was already observed at pre-haemolytic concentrations (1–50 μg/ml), which may be associated with mechanically induced alterations caused by PS-NPs. Overall, analysis of all proeryptotic erythrocyte parameters examined indicates that PS-NPs do not induce programmed red blood cell death. In summary, non-functionalized PS-NPs exert a relatively mild, size-dependent detrimental effect on human erythrocytes. Exposure led to alterations in erythrocyte membrane mechanical properties, such as membrane stiffening and rheological disturbances, which ultimately resulted in haemolysis at high concentrations (100–250 μg/ml). PS-NPs did not exhibit direct pro-oxidative effects on haemoglobin and did not increase ROS levels; however, at high concentrations (100 μg/ml) they induced lipid peroxidation and increased carbonyl groups in membrane proteins. PS-NPs, regardless of size, did not initiate eryptosis at pre-haemolytic concentrations but caused subtle structural membrane changes, likely mechanical in nature, as supported by calpain activation already at low concentrations. Furthermore, the study demonstrated that PS-NPs form a stable protein corona with albumin, which undergoes structural modifications upon interaction with the nanoparticles; such modifications may potentially affect proper erythrocyte function *in vivo*.

WPROWADZENIE

Tworzywa sztuczne, ze względu na szerokie zastosowanie w licznych gałęziach przemysłu oraz istotny wpływ na poprawę komfortu życia codziennego, są wytwarzane na masową skalę. Obecnie ich roczna produkcja wynosi około 460 milionów ton rocznie (Źródło internetowe 1; Li and Liu, 2024). Szacuje się że do 2060 roku produkcja plastiku może wzrosnąć trzykrotnie (Yates et al., 2025). Jednak tylko około 9% tworzyw sztucznych poddawanych jest recyklingowi, a więcej niż 60% światowej produkcji plastiku trafia do środowiska powodując trwałe zanieczyszczenie (Anwar et al., 2025). Plastik zanieczyszczający środowisko, pod wpływem czynników fizycznych, chemicznych i biologicznych, takich jak promieniowanie UV, degradacja termiczna czy biodegradacja, ulega rozkładowi do mikrocząstek (MP <5000 μm), a w dalszej kolejności do nanocząstek (NP <1 μm) (Li and Liu, 2024; Shen et al., 2019). Cząstki plastiku produkowane są także komercyjnie i wykorzystywane w wielu gałęziach przemysłu. Mikroplastik znalazł zastosowanie w przemyśle kosmetycznym (dodatki do mydeł, past do zębów i środków złuszczających), z kolei nanoplastik w przemyśle elektronicznym oraz budowlanym (farby, kleje), a także jako nośnik leków (Koelmans et al., 2015; Wright and Kelly, 2017). Ze względu na pochodzenie cząstki plastiku dzieli się na wtórne powstające w środowisku w wyniku degradacji większych fragmentów tworzyw oraz pierwotne, które są celowo produkowane do zastosowań komercyjnych (Kik et al., 2020). Cząstki plastiku są powszechnie obecne w środowisku. Występują w wodzie, glebie i powietrzu co sprzyja ich przenikaniu do łańcucha pokarmowego, w tym do żywności, w której również są wykrywane (Bhat et al., 2023; Gondal et al., 2023). W produktach spożywczych cząstki plastiku zostały wykryte m.in.: w owocach morza, mięsie drobiowym, mleku, soli kuchennej, wodzie butelkowanej oraz kranowej i piwie (Li and Liu, 2024).

Powszechność cząstek plastiku w środowisku oraz w produktach spożywczych i wodzie sprawia, że ludzie są na nie stale narażeni. Zarówno mikro- jak i nanocząstki plastiku mogą przedostawać się do organizmu człowieka. Główną drogą wnikania cząstek jest droga pokarmowa za pomocą, której mogą przedostawać się cząstki zanieczyszczające żywność oraz wodę. Innymi drogami przedostawania się cząstek plastiku są droga oddechowa, skórna oraz dożylna. Ta ostatnia jest istotna w przypadku procedur medycznych (Kik et al., 2020; Li and Liu, 2024). Badania przeprowadzone w ostatnich latach wskazują na obecność tych cząstek w wielu tkankach ludzi. Udokumentowano ich występowanie w wydalinach człowieka: kał (Schwabl et al., 2019), mocz (Pironti et al., 2022), wydzielinach: nasienie (Zhao et al.,

2023), mleko kobiece (Ragusa et al., 2022), a także tkankach i narządach ludzi: łożysko (Ragusa et al., 2021), płuca (Amato-Lourenço et al., 2021; Jenner et al., 2022), jelito grube (Ibrahim et al., 2021), mózg (Nihart et al., 2025), serce (Yang et al., 2023), żyły (Jenner et al., 2022) i krew (Lee et al., 2024; Leslie et al., 2022; Salvia et al., 2023; V. L. Leonard et al., 2024). Ze względu na ograniczenia metodyczne jedynie nieliczne badania wskazują na obecność nanocząstek plastiku w organizmie człowieka. Nanocząstki plastiku zostały wykryte we krwi ludzi u wszystkich 196 badanych ochotników (Salvia et al., 2023). Badania, w których wykryto mikroplastik we krwi człowieka, wskazują na obecność tworzyw sztucznych w organizmach większości ludzi. Cząstki plastiku stwierdzono średnio u 85% badanych ochotników (Lee et al., 2024; Leslie et al., 2022; V. L. Leonard et al., 2024).

Wykrycie cząstek plastiku w organizmie człowieka wskazuje na konieczność dokładnego określenia ich wpływu na zdrowie i życie ludzi. Dotychczas przeprowadzone badania, zarówno *in vivo* na modelach zwierzęcych, jak i *in vitro* na ludzkich tkankach i komórkach wykazały, że cząstki plastiku mogą wywoływać negatywne skutki zdrowotne, działając zarówno pośrednio, jak i bezpośrednio. Pośrednio, tworzywa sztuczne mogą pełnić rolę nośników drobnoustrojów, takich jak bakterie, grzyby czy pierwotniaki, a także zanieczyszczeń, w tym metali ciężkich, pestycydów, leków oraz uniepalniaczy. Bezpośrednia toksyczność cząstek zależy natomiast od rodzaju tworzywa, jego rozmiaru, kształtu oraz dodatków stosowanych podczas przetwórstwa (Płuciennik et al., 2024).

Z kolei obecność cząstek plastiku we krwi człowieka jest ważnym sygnałem do przeprowadzenia szczegółowych badań nad ich oddziaływaniem na komórki krwi, które nie tylko transportują cząstki tworzyw sztucznych do różnych tkanek i narządów, ale także same mogą ulec negatywnym zmianom pod ich wpływem. To z kolei może mieć dalekosiężne konsekwencje dla całego organizmu i zdrowia ludzi.

O ile istnieją już liczne badania dotyczące wpływu cząstek nanoplastiku na jednojądrzaste komórki krwi obwodowej (PBMCs), które wykazały wzrost poziomu reaktywnych form tlenu, uszkodzenia oksydacyjne białek i lipidów (Kik et al., 2021), uszkodzenia DNA (Malinowska et al., 2025), a także indukcję apoptozy (Malinowska et al., 2023) oraz niewielkie zmiany epigenetyczne (Malinowska et al., 2024), to brakuje wystarczających danych dotyczących wpływu nanocząstek plastiku na erytrocyty człowieka (Płuciennik et al., 2023a). Erytrocyty odgrywają kluczową rolę w organizmie człowieka, odpowiadając za transport gazów oddechowych i składników odżywczych, a także uczestnicząc w utrzymaniu homeostazy układu sercowo-naczyniowego m.in. poprzez udział w kaskadzie

krzepnięcia i procesie tworzenia skrzepów, co ma szczególne znaczenie w kontekście zakrzepicy żylnej (Byrnes and Wolberg, 2017).

Nieliczne badania wykazały, że cząstki plastiku mogą być toksyczne także dla erytrocytów człowieka. Najwięcej informacji dotyczy hemolizy, którą mogą indukować zarówno niefunkcjonalizowane PS-NPs jak i te posiadające grupę funkcyjną (Barshtein et al., 2011; Gopinath et al., 2019; Kim et al., 2022). Cząstki plastiku wpływają także na agregację tych komórek i adhezję do komórek śródbłonka (Barshtein et al., 2016; Kim et al., 2022; Tian et al., 2021).

W związku z powyższym konieczne było przeprowadzenie dalszych badań dotyczących wpływu cząstek różnych tworzyw sztucznych na erytrocyty człowieka, w tym polistyrenu produkowanego na szeroką skalę. Tworzywo to jest wykorzystywane m.in. w formie styropianu do izolacji termicznej opakowania do żywności, a także w oprawkach okularowych i sprzęcie elektrycznym (Anwar et al., 2025). Roczna produkcja polistyrenu wynosi obecnie około 16 mln ton, z czego ok. 45% stanowi jego forma spieniona (Źródło internetowe 2). Udział tego materiału w odpadach z tworzyw sztucznych dochodzi do 10%, co stanowi ogromne ilości i wskazuje na polistyren jako plastik najrzadziej recyklingowany (Hidalgo-Crespo et al., 2022).

Należy podkreślić, że polistyren został wykryty we krwi ludzi w większości dotychczasowych badań toksykologicznych skierowanych na nanocząstki plastiku. W badaniach Lee i wsp. było to najczęściej oznaczane tworzywo sztuczne, które stanowiło aż 58,3% wykrytych cząstek, z kolei badania Leslie i wsp., wykazały stężenie polistyrenu wynoszące średnio 1,6 μg/ml krwi, a w 1 przypadku osiągające wartość nawet 4,8 μg/ml krwi (Lee et al., 2024; Leslie et al., 2022; V. L. Leonard et al., 2024).

W związku z powyższym w niniejszej pracy doktorskiej podjęto się analizy wpływu niefunkcjonalizowanych nanocząstek polistyrenu o różnych średnicach ~30 nm, ~45 nm i ~70 nm na erytrocyty człowieka. Ze względu na obecność we krwi licznych białek, które mogą ulegać interakcjom z tymi nanocząstkami, w badaniach uwzględniono także wpływ nanocząstek na najobficiej występujące we krwi człowieka białko, albuminę człowieka. W badaniach określono hemolizę erytrocytów pod wpływem nanocząstek, a następnie zbadano oddziaływania nanocząstek z błoną komórkową erytrocytów. W dalszej części badań określono oddziaływania tych samych nanocząstek z białkami erytrocytarnymi i białkiem modelowym albuminą. Ostatni etap miał z kolei na celu ustalenie czy niefunkcjonalizowane PS-NPs mogą wywoływać programowaną śmierć erytrocytów czyli eryptozę oraz ustalenie ewentualnego aktywowanego szlaku w tym procesie.

ZAŁOŻENIA I CELE PRACY

Wykrycie cząstek polistyrenu w komórkach krwi ludzi oraz brak wystarczających danych dotyczących ich potencjalnej szkodliwości skłania do podjęcia badań ich wpływu na strukturę i funkcję tych komórek. W związku z powyższym, celem rozprawy doktorskiej było określenie potencjalnych zmian w strukturze i funkcji erytrocytów człowieka narażonych na nanocząstki polistyrenu (PS-NPs) o różnych średnicach. Zbadano także rolę albuminy ludzkiej, najobficiej występującego białka osocza w potencjalnych interakcjach z tymi nanocząstkami. Aspekt ten jest również bardzo istotny, ponieważ modyfikacja albuminy przez PS-NPs może wpływać na prawidłowe funkcjonowanie erytrocytów w układzie *in vivo.*

Badania szczegółowe przeprowadzone w niniejszej rozprawie doktorskiej miały na celu:

1. Analizę wpływu badanych PS-NPs na indukcję hemolizy.
2. Określenie oddziaływania PS-NPs na płynność błony erytrocytarnej oraz morfologię badanych komórek.
3. Ocenę zmian powodowanych przez nanocząstki polistyrenu w wybranych białkach erytrocytarnych oraz albuminie, w tym: analizę poziomu utleniania białek błonowych i hemoglobiny, zmian w aktywności acetylocholinoesterazy, a także zaburzeń w strukturze przestrzennej oraz utlenianiu tryptofanu w albuminie.
4. Zbadanie wpływu PS-NPs na proces eryptozy oraz określenie mechanizmu tego procesu.

MATERIAŁY I METODY

Materiał badawczy

- Materiał badawczy stanowiły erytrocyty człowieka wyizolowane z kożuszków leukocytarno-płytkowych zakupionych w Regionalnym Centrum Krwiodawstwa i Krwiolecznictwa w Łodzi, które posiada odpowiednią akredytację Ministerstwa Zdrowia (BA/2/2004). Badania zrealizowane w niniejszej pracy posiadały zgodę komisji bioetycznej Uniwersytetu Łódzkiego Uchwała Nr 1/KEBN-UŁ/I/2022-23 .
- Niefunkcjonalizowane cząstki polistyrenu o określonych przez producenta firmę Bangs Laboratories (skąd) średnicach ~ 30 nm, ~ 45nm, ~ 70 nm, zakupiono w firmie Polysciences Europe GmbH.
- Albumina surowicy człowieka (HSA) (czystość ≥98%) zakupiono w firmie Sigma-Aldrich (Saint Louis, Michigan, USA).

Przygotowanie prób

Każdorazowo przed rozpoczęciem eksperymentu przeprowadzano izolację erytrocytów z kożuszka leukocytarno-płytkowego. Erytrocyty doprowadzano do hematokrytu 5%, a następnie dodawano PS-NPs o różnych średnicach do odpowiedniego stężenia. Nanocząstki były analizowane w zakresie stężeń od 0,001 do 200 µg/ml w zależności od stosowanej metody i jej uwarunkowań (np. szereg metod analizowano w stężeniach przedhemolitycznych). Schemat badań zaprezentowano na rysunku 1.

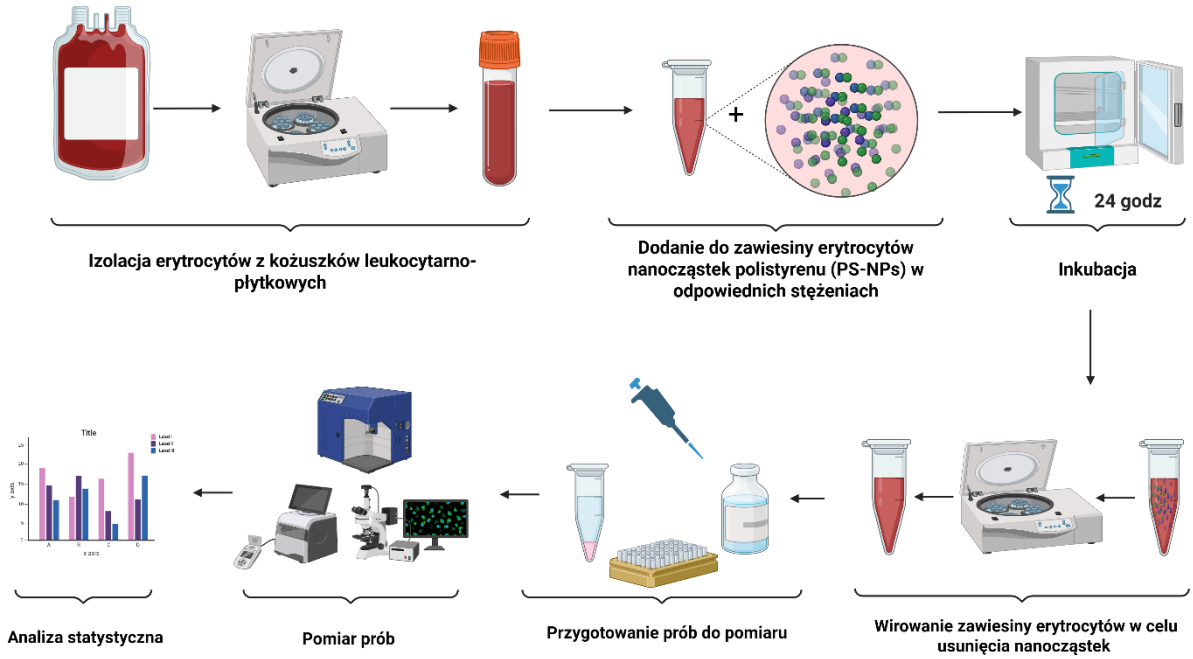

Rys. 1. Schemat przygotowania eksperymentów realizowanych w pracy doktorskiej

Metody badawcze

A) Zastosowane w badaniach erytrocytów:

- Określenie potencjału zeta PS-NPs w buforze Ringera pH = 7,4.
- Zbadanie stopnia hemolizy erytrocytów z wykorzystaniem metody spektrofotometryczej.
- Ocena płynności błony komórkowej erytrocytów:
  - Metodą elektronowego rezonansu paramagnetycznego z zastosowaniem następujących znaczników spinowych kwasu 5-doksylostearynowego i 16-doksylostearynowego.
  - Metodą fluorymetryczną z zastosowaniem znaczników 1-(4-trimetyloamono-fenylo)-6-fenylo-1,3,5-heksatrien p-toluenosulfonianu (TMA-DPH) i 1,6-difenylo-1,3,5-heksatrienu (DPH).
- Analiza kształtu erytrocytów za pomocą mikroskopii świetlnej.
- Oznaczenie lepkości wewnątrzkomórkowej erytrocytów metodą elektronowego rezonansu paramagnetycznego z zastosowaniem znacznika tempoaminy.

- Wyznaczenie aktywności acetylocholinoesterazy erytrocytarnej metodą spektrofotometryczną Ellmana.
- Izolacja błon komórkowych erytrocytów zmodyfikowaną metodą Dodge'a.
- Ocena poziomu grup karbonylowych w białkach błony erytrocytarnej za pomocą testu fluorometrycznego (Cayman Chemical Company, MI, USA).
- Określenie poziomu reaktywnych form tlenu za pomocą sondy fluorescencyjnej dioctanu 2',7'-dichlorodihydrofluoresceiny ($DCFH_2$-DA).
- Ocena peroksydacji lipidów za pomocą sondy fluorecencyjnej BODIPY 581/591 C11.
- Ocena eksternalizacji fosfatydyloseryny z użyciem aneksyny V wyznakowanej izotiocyjanianiem fluoresceiny (FITC).
- Oznaczenie poziomu wewnątrzkomórkowego wapnia za pomocą znacznika fluorescencyjnego tj. estru fluoro-3-acetoksymetylowego (Fluo3-AM).
- Określenie aktywności kaspazy-3 z wykorzystaniem substratu DEVD-FMK sprzężonego z izotiocyjanianem fluoresceiny (FITC).
- Oznaczenie aktywności kalpain przy pomocy komercyjnego zestawu QIA 120.

B) Zastosowane w badaniach albuminy człowieka (HSA)

- Ocena wpływu różnych stężeń albuminy na tworzenie się korony białkowej na PS-NPs metodą dynamicznego rozpraszania światła (DLS).
- Określenie wpływu PS-NPs na konformację albuminy ludzkiej (HSA) metodą dichroizmu kołowego (CD).
- Analiza widm fluorescencji tryptofanowej albuminy człowieka poddanej oddziaływaniu PS-NPs.
- Analiza kinetyki zaniku fluorescencji tryptofanowej albuminy po działaniu PS-NPs.

OMÓWIENIE PRAC WCHODZĄCYCH W SKŁAD ROZPRAWY DOKTORSKIEJ

Cykl publikacji wchodzących w skład niniejszej rozprawy doktorskiej otwiera praca przeglądowa „*Important Factors Affecting Induction of Cell Death, Oxidative Stress and DNA Damage by Nano- and Microplastic Particles In Vitro”* opublikowana w czasopiśmie *Cells.* W pracy tej omówiono czynniki zwiększające toksyczność mikro i nanoplastików w badaniach *in vitro*, w odniesieniu do żywotności komórek, różnych rodzajów śmierci komórkowej, indukcji reaktywnych form tlenu (ROS) oraz genotoksyczności. Dokonując przeglądu literatury skupiono się na szeregu czynników, do których należą te związane z cząstkami plastiku: rozmiar cząstek, ich stężenie, czas ekspozycji, wartość potencjału zeta, a także obecność grup funkcyjnych, czy czynniki środowiskowe, jak i te związane z rodzajem komórek używanych w badaniach (linie komórkowe nowotworowe lub pierwotne, komórki krwi).

Powyższe czynniki zostały omówione w aspekcie ich wpływu na indukcję różnych rodzajów śmierci komórkowej tj. zarówno nieprogramowanej śmierci komórkowej (nekrozy i hemolizy) jak i programowanej śmierć komórkowej (autofagii, apoptozy i ferroptozy). Przeanalizowano także wpływ różnych czynników zmieniających toksyczność nanocząstek w odniesieniu do indukcji stresu oksydacyjnego poprzez wzrost poziomu reaktywnych form tlenu oraz zmiany aktywności enzymów antyoksydacyjnych i poziomu niskocząsteczkowych antyoksydantów w komórkach. Analiza przeglądowa dotyczyła również ich działania genotoksycznego obejmującego jedno- i dwuniciowe uszkodzenia DNA oraz oksydacyjne zmiany zasad purynowych i pirymidynowych.

Na podstawie przeanalizowanych badań *in vitro* stwierdzono, że najważniejszym czynnikiem decydującym o toksyczności mikro i nanoplastików jest wielkość cząstek plastiku (Rys. 2). Wpływa ona na szybsze przenikanie do komórek cząstek mniejszych, a także na ich zwiększoną reaktywność, która związana jest z większym stosunkiem powierzchni do objętości. Na wzrost toksyczności nanocząstek polistyrenu wpływa zarówno czas narażenia komórek jak i stężenie zastosowanych nanocząstek, a także obecność grup funkcyjnych nadających nanocząstkom ładunek powierzchniowy decydujący o oddziaływaniu z błoną komórkową. Nanocząstki o dodatnim potencjale zeta są bardziej cytotoksyczne niż te o ujemnym potencjale zeta, ponieważ błony komórkowe mają ładunek ujemny, a to decyduje o rodzaju oddziaływania. Stwierdzono również, że występowanie korony białkowej na nanocząstkach istotnie nasila hemolizę erytrocytów. Toksyczność nanocząstek wzrasta także po naświetleniu ich promieniowaniem UV, które powoduje zmniejszenie wielkości nanocząstek

plastiku oraz tworzenie różnych grup funkcyjnych na ich powierzchni. Wykazano również, że komórki prawidłowe są bardziej wrażliwe na cząstki plastiku niż komórki nowotworowe. Co więcej cząstki plastiku pokryte koroną białkową np. białkami osocza charakteryzują się większą cytotoksycznością.

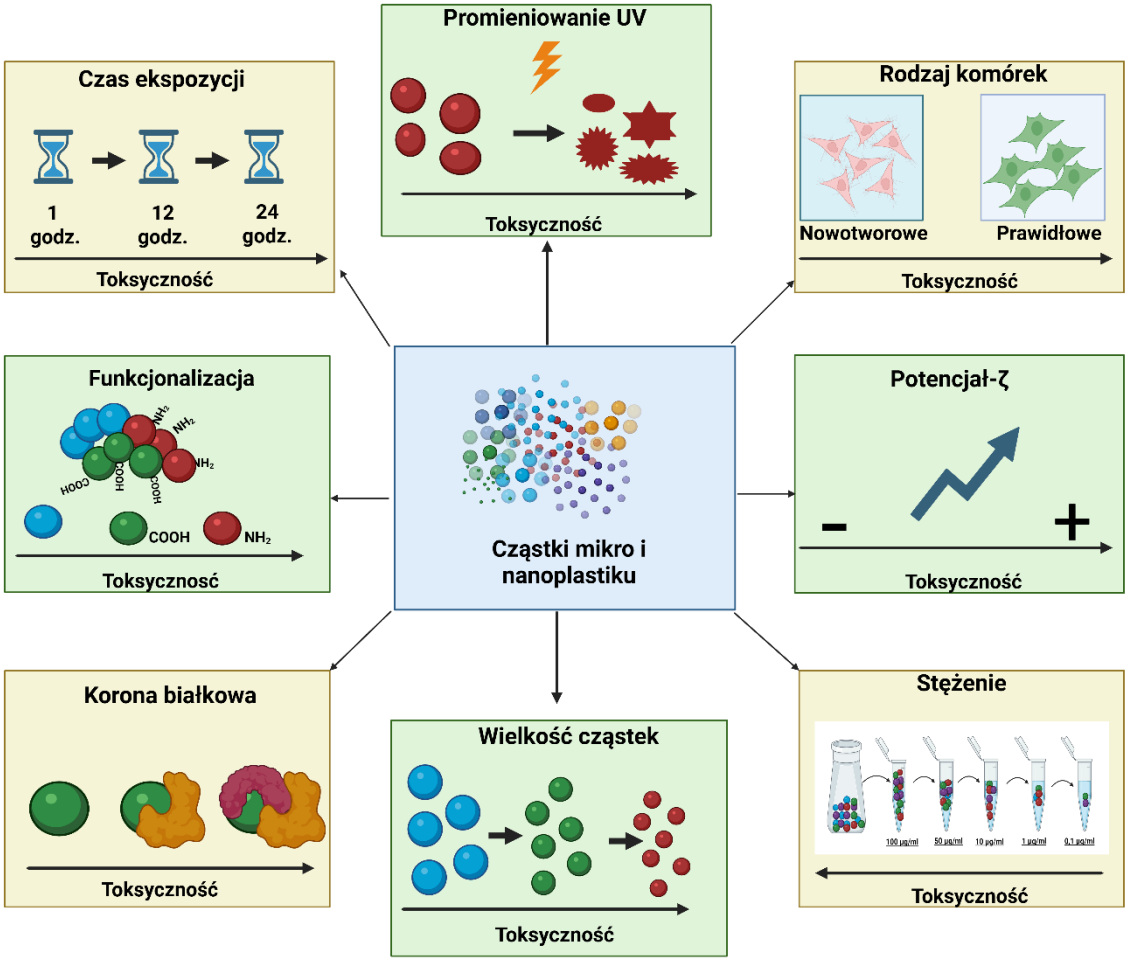

Rys. 2. Czynniki wpływające na toksyczność nano- i mikrocząstek plastiku w badaniach *in vitro* (na podstawie Płuciennik i wsp., 2024).

W związku z tym, że wielkość cząstek jest głównym czynnikiem odpowiadającym za ich toksyczność w badaniach *in vitro*, do realizacji części eksperymentalnej pracy doktorskiej wybrano PS-NPs w trzech różnych rozmiarach: ~30 nm, ~45 nm i ~70 nm, co pozwoliło na ocenę zależności pomiędzy rozmiarem a toksycznością w obrębie nanoskali. Część eksperymentalna prezentowanej rozprawy doktorskiej została opisana w dwóch opublikowanych pracach doświadczalnych i trzeciej wysłanej do czasopisma *Nanotoxicology.*

Pierwsza z publikacji pt. *„The effects of non-functionalized polystyrene nanoparticles with different diameters on human erythrocyte membrane and morphology”* opublikowana w czasopiśmie *Toxicology in vitro* miała na celu określenie wpływu PS-NPs na hemolizę erytrocytów, ich morfologię oraz płynność błony komórkowej.

Do badań wybrano niefunkcjonalizowane komercyjnie produkowane do celów naukowych cząstki polistyrenu o średnicach ~30 nm, ~45 nm i ~70 nm. Początkowym etapem badań było określenie stopnia hemolizy erytrocytów po 24 godzinnej inkubacji komórek z nanocząstkami. Aktywność hemolityczną cząstek plastiku badano w szerokim zakresie stężeń od 0,001 do 200 µg/ml obejmującym także maksymalne stężenie wykryte we krwi człowieka wynoszące 4,8 µg/ml (Leslie et al., 2022). Statystycznie istotny wzrost stopnia hemolizy zaobserwowano dla nanocząstek we wszystkich badanych średnicach, ale tylko przy największych stężeniach tj. 100 µg/ml i 200 µg/ml. Wykazano istotne statystycznie różnice pomiędzy hemolizą indukowaną przez nanocząstki o różnych średnicach. Stwierdzono, że największą hemolizę powodowały najmniejsze z badanych nanocząstek polistyrenu o średnicy wynoszącej ~30 nm. Dane uzyskane z badania hemolizy pozwoliły na określenie stężeń przedhemolitycznych, które zostały użyte w kolejnych eksperymentach.

Stosując metodę elektronowego rezonansu paramagnetycznego (EPR) oraz metodę fluorymetryczną dokonano analizy płynności różnych regionów dwuwarstwy fosfolipidowej błony komórkowej erytrocytów człowieka po 24-godzinnej inkubacji z PS-NPs. Badania te prowadzono w zakresie przedhemolitycznych stężeń od 0,001 do 10 µg/ml. W metodzie EPR wykorzystano dwa znaczniki lokujące się na różnych głębokościach błony komórkowej, kwas 5-doksylostearynowy (5-DSA) oraz kwas 16-doksylostearynowy. Natomiast w przypadku metody fluorymetrycznej wykorzystano znaczniki TMA-DPH i DPH, lokujące się w zbliżonych rejonach błony komórkowej erytrocytów do tych użytych w metodzie EPR (rys. 3).

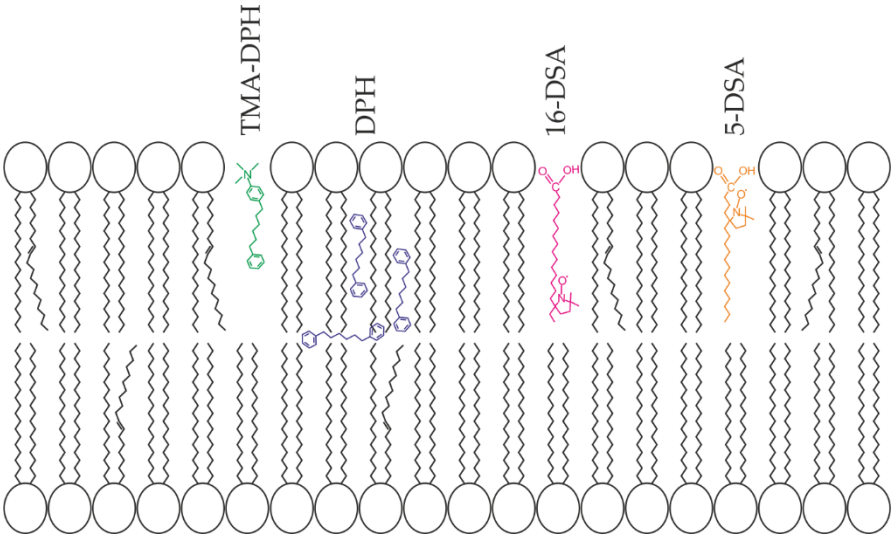

Rys. 3. Miejsce lokowania się poszczególnych znaczników fluorymetrycznych i spinowych w błonie komórkowej erytrocytów (opracowano na podstawie Płuciennik i wsp., 2023).

W płytkich regionach dwuwarstwy fosfolipidowej jakimi są szkielet glicerolowy i górne segmenty łańcuchów acylowych fosfolipidów zaobserwowano istotny statystycznie wzrost

parametru S wyznaczonego dla znacznika 5-DSA (kwas 5-doksylostearynowy), lokującego się na poziomie 5 atomu węgla łańcucha kwasów tłuszczowych. Różnice były istotne statystycznie dla nanocząstek o średnicy ~30 nm i ~45 nm od stężenia 0,1 μg/ml, zaś dla największych badanych cząstek (~70 nm) od stężenia 0,001 μg/ml. W badaniach wykonanych metodą fluorymetryczną nie zaobserwowano jednak zmian anizotropii fluorescencji dla znacznika TMA-DPH. Z kolei w przypadku głębokich regionów hydrofobowych błony komórkowej erytrocytów zaobserwowano zmiany w przypadku zastosowania zarówno znacznika spinowego jak i sondy fluorescencyjnej. Dla znacznika spinowego, kwasu 16-doksylostearynowego, który lokuje się na poziomie 16-atomu węgla łańcucha kwasów tłuszczowych wyznaczono czasy korelacji: τ_B i τ_C, których wydłużenie, świadczące o usztywnieniu błony komórkowej w rdzeniu hydrofobowym erytrocytów zaobserwowano w przypadku narażenia na wszystkie badane nanocząsteki polistyrenu. Istotne statystycznie zmiany wartości czasu korelacji τ_B występowały odpowiednio dla PS-NPs o średnicy ~30 nm od stężenia 0,001 μg/ml, dla ~45 nm od stężenia 0,01 μg/ml i ~70 nm od stężenia 0,1 μg/ml. Natomiast w przypadku czasu korelacji τ_C dla cząstek o średnicy ~30 nm i ~45 nm od stężenia 1 μg/ml, a dla największych badanych cząstek w stężeniach 0,001 i 0,1 μg/ml. Z kolei w przypadku metody fluorymetrycznej dla znacznika DPH, istotny statystycznie wzrost anizotropii fluorescencji wykazano dla cząstek o średnicy ~30 i ~70 nm od stężenia 0,01 μg/ml. W przypadku cząstek o średnicy ~45 nm istotny statystycznie wzrost anizotropii fluorescencji zaobserwowano już od stężenia 0,1μg/ml.

W ostatnim etapie pracy za pomocą mikroskopii optycznej oceniono również wpływ PS-NPs na kształt erytrocytów. Zaobserwowano istotny statystycznie spadek procentowy dyskocytów. Towarzyszył temu jednoczesny wzrost odsetka stomatocytów. Zmiany te występowały dla nanocząstek o średnicy ~70 nm już od najniższego badanego stężenia 0,001 μg/ml. Z kolei dla mniejszych PS-NPs o średnicy ~45 nm odpowiednio od stężenia 0,01 μg/ml i 0,1 μg/ml, zaś dla najmniejszych nanocząstek (~30 nm). Powstawanie stomatocytów pod wpływem nanocząstek plastiku wskazuje na zmiany w wewnętrznej monowarstwie błony komórkowej erytrocytów przy bardzo małych stężeniach badanych nanocząstek. Przy niskich stężeniach nanocząstek, dzięki większej mobilności i mniejszej agregacji, mogą oddziaływać z wewnętrzną monowarstwą, co prowadzi do względnego zwiększenia powierzchni tej monowarstwy i powstawania stomatocytów. Zjawisko to odzwierciedla klasyczny mechanizm bilayer-coupling wyjaśniający, jak różnice w powierzchni dwóch monowarstw błony komórkowej prowadzą do zmiany kształtu komórki.

Kolejny etap badań, który został zwieńczony pracą pt. *„The interactions of non-functionalized polystyrene nanoparticles with human albumin and erythrocyte proteins: implications and potential consequences”* opublikowanej w czasopiśmie *Scientific Reports* miał na celu zbadanie wpływu nanocząstek polistyrenu na albuminę surowicy człowieka (HSA) będącą głównym białkiem osocza oraz na białka erytrocytów w układzie *in vitro*, co pozwoliło na łączną analizę dwóch uzupełniających się systemów biologicznych. Albumina odgrywa kluczową rolę w utrzymaniu integralności strukturalnej i funkcjonalnej erytrocytów, szczególnie w ich bezpośrednim środowisku, czyli osoczu. Jest to najliczniej występujące białko w osoczu, niezbędne do zachowania dwuwklęsłego kształtu czerwonych krwinek, co jest kluczowe dla zachowania ich odkształcalności i przenikania przez naczynia włosowate włosowate (Kamada et al., 1988; Van De Wouw and Joles, 2022). Stwierdzono, że krystaliczna albumina surowicy bydlęcej zwiększa odporność erytrocytów na uszkodzenia mechaniczne i chroni przed hemolizą oksydacyjną lub fizyczną (Williams, 1973).

Ze względu na to, że białka adsorbujące się na powierzchni cząstek plastiku zmieniają ich właściwości biologiczne, ułatwiając translokację tych cząstek z krwioobiegu do narządów oraz wydłużając czas ich utrzymywania się w krążeniu, oceniono proces tworzenia się korony białkowej HSA na nanocząstkach polistyrenu. W tym celu zostały wykorzystane metody: dynamicznego rozpraszania światła, dichroizmu kołowego i spektroskopii fluorescencyjnej.

Metodą dynamicznego rozpraszania światła (DLS) wykazano tworzenie się korony białkowej HSA na nanocząstkach polistyrenu. Dla nanocząstek o średnicy ~45 nm w obecności albuminy ludzkiej w stężeniu 50 µg/ml średnica hydrodynamiczna wynosiła 52 ± 20 nm, a przy stężeniu HSA 150 µg/ml średnica wzrosła do 136 ± 40 nm. Natomiast średnica tych nanoczastek oznaczona bez albuminy jak i z albuminą w stężeniu 10 µg/ml wynosiła 33 ± 6 nm. W przypadku największych z badanych nanocząstek o średnicy deklarowanej przez producenta wynoszącej ~70 nm, pomiar średnicy hydrodynamicznej cząstek bez albuminy wskazał średnicę 60 ± 10 nm, z kolei z albuminą w stężeniu 10 µg/ml było to 74 ± 16 nm. Natomiast przy stężeniu albuminy 50 µg/ml obserwowano dwie populacje nanoczastek o rozkładzie wielkości 70 ± 10 nm i 228 ± 50 nm. Pomiar średnicy hydrodynamicznej dla stężenia 150 µg/ml nie był możliwy ze względu na tworzące się agregaty. Zaobserwowany w tym badaniu wzrost średnicy hydrodynamicznej świadczy o tworzeniu się korony białkowej z HSA na nanocząstkach polistyrenu o średnicy ~45 nm i ~70 nm, co jest związane z większą powierzchnią całkowitą oraz większą krzywizną tych nanocząstek w stosunku do nanocząstek o średnicy ~30 nm. Wynikać to może także z korzystniejszej energii

adsorpcji na większych PS-NPs, co umożliwia skuteczniejsze przyłączanie się białek do tych nanocząstek plastiku.

W związku z tym w kolejnym etapie badań przy wykorzystaniu metody dichroizmu kołowego określono zmiany w strukturze przestrzennej albuminy po inkubacji z nanocząstkami. Zaobserwowano zmiany struktury drugorzędowej tego białka pod wpływem nanocząstek we wszystkich testowanych średnicach (~30 nm, ~45 nm i ~70 nm) w dwóch najwyższych badanych stężeniach, 50 μg/ml i 100 μg/ml. Określenie składu struktury drugorzędowej wykazało, że PS-NPs powodowały spadek zawartości α-helisy, nieznaczny wzrost zawartości β-harmonijki, a także wzrost zawartości zwojów losowych. Powyższe zmiany w strukturze drugorzędowej zgodnie z danymi literaturowymi (Kihara et al., 2019) wskazują na tworzenie się twardej korony białkowej na nanocząstkach polistyrenu.

Oddziaływanie niefunkcjonalizowanych PS-NPs z albuminą ludzką (HSA) określono także za pomocą metod fluorescencyjnych. Wykonano widma emisji fluorescencji HSA oraz dokonano analizy kinetyki zaniku fluorescencji, co pozwoliło zaobserwować zarówno wzrost fluorescencji pochodzącej od tyrozyny i tryptofanu w albuminie ludzkiej, jak i wydłużenie czasów życia stanów wzbudzonych tych aminokwasów aromatycznych w albuminie inkubowanej z nanocząstkami polistyrenu. Oba efekty zostały zaobserwowane dla nanocząstek polistyrenu o średnicach ~30 nm i ~45 nm, przy czym większe oddziaływanie zostało zaobserwowane dla najmniejszych z badanych nanocząstek.

Zatem uzyskane wyniki wskazują na zmiany w strukturze albuminy w układzie *in vitro* pod wpływem PS-NPs, które w przeniesieniu na układ *in vivo* mogą mieć istotne znaczenie prowadzące do ograniczenia funkcji ochronnych tego białka wobec erytrocytów. Prawdopodobnie PS-NPs poprzez modyfikacje struktury albuminy mogą pośrednio nasilać uszkodzenia erytrocytów wywołane przez nanoplastik *in vivo*. Zmiany w strukturze białka mogą bowiem prowadzić do jego denaturacji i w konsekwencji do destabilizacji błony komórkowej erytrocytów.

W drugiej części pracy określono wpływ PS-NPs na białka erytrocytarne. Określono mikrolepkość wnętrza erytrocytów, utlenianie hemoglobiny i aktywność acetylocholinoesterazy erytrocytarnej, oraz zbadano poziom grup karbonylowych w białkach błony erytrocytarnej. Ocena mikrolepkości wewnętrznej erytrocytów wykazała, że wszystkie badane PS-NPs po 24-godzinnej inkubacji z erytrocytami powodują wzrost względnej mikrolepkości. Zmiany mikrolepkości wnętrza erytrocytów dla najmniejszych z badanych nanocząstek (~30 nm) zaobserwowano już od stężenia 0,1 μg/ml, z kolei dla pozostałych badanych NPs od stężenia 1 μg/ml. Może świadczyć to o interakcji PS-NPs z głównym białkiem

tych komórek, którym jest hemoglobina, co w rezultacie prowadzi do reorganizacji cytoszkieletu, czego konsekwencją jest tworzenie się stomatocytów, obserwowanych w pierwszej pracy. Dokonano również analizy utleniania hemoglobiny do methemoglobiny, w erytrocytach wystawionych na działanie PS-NPs w zakresie stężeń 0,001–100 μg/ml przez 24 godziny. Nie stwierdzono utleniania tego białka co przyczyniałoby się do usuwania erytrocytów z krwioobiegu. Po 24 godzinnej inkubacji erytrocytów z PS-NPs w zakresie stężeń 0,001-100 μg/ml nie zaobserwowano z kolei zmian aktywności acetylocholinoesterazy erytrocytarnej będącej biomarkerem integralności błony komórkowej erytrocytów oraz starzenia się tych komórek. Zaobserwowano z kolei zależne zarówno od stężenia, jak i średnicy PS-NPs zwiększenie zawartości grup karbonylowych w białkach błony erytrocytarnej po 24 godzinnej inkubacji z nanocząstkami polistyrenu. Stwierdzono że PS-NPs o najmniejszej średnicy (~ 30 nm) indukowały zmiany istotne statystycznie w stężeniach 10 μg/ml i 100 μg/ml, natomiast nanocząstki o średnicach ~45 nm i ~70 nm tylko w najwyższym stężeniu wynoszącym 100 μg/ml. Prawdopodobny wzrost zawartości grup karbonylowych w białkach błony erytrocytarnej związany jest z naciskiem cząstek na błonę komórkową erytrocytów, co wiąże się także ze zmianą płynności ich błony komórkowej jak i zmianami morfologii tych komórek.

Dotychczasowe badania sugerują, że wybrane ksenobiotyki oraz dodatki do tworzyw sztucznych mogą indukować eryptozę czyli programowaną śmierć krwinek czerwonych. Zjawisko to ma szczególne znaczenie toksykologiczne, ponieważ zmiany w podatności na utlenianie, równowadze jonowej i integralności błony erytrocytów mogą przyczyniać się do dysfunkcji krążeniowych, przewlekłego stanu zapalnego i zaburzeń mikrokrążenia. Z tego względu w niniejszej rozprawie podjęto się określenia wpływu PS-NPs na ten proces, a uzyskane wyniki przedstawiono w manuskrypcie pracy: *Polystyrene nanoparticles and death of erythrocytes: does exposure induce eryptosis?* wysłanej do recenzji w czasopiśmie Nanotoxicology.

Programowana śmierć komórkowa w przypadku erytrocytów, które są komórkami nie posiadającymi jądra i innych organelli komórkowych, nie może przebiegać na skutek apoptozy. Komórki te wykształciły własny rodzaj śmierci komórkowej jakim jest eryptoza. Proces ten charakteryzuje się przede wszystkim wzrostem wewnątrzkomórkowego poziomu jonów wapnia, co przyczynia się do wycieku jonów K^+ z erytrocytów, a także eksternalizacji fosfatydyloseryny. Od poziomu jonów Ca^{2+} zależna jest także aktywacja proteazy cysteinowej-kalpainy-1, która w procesie eryptozy może przyczyniać się do rozpadu cytoszkieletu.

Proces ten niezależne od jonów wapnia może zostać uruchomiony także przez ROS, które aktywują kaspazę-3, a to prowadzi do eksternalizacji fosfatydyloseryny (Tkachenko et al., 2025) (rys. 4).

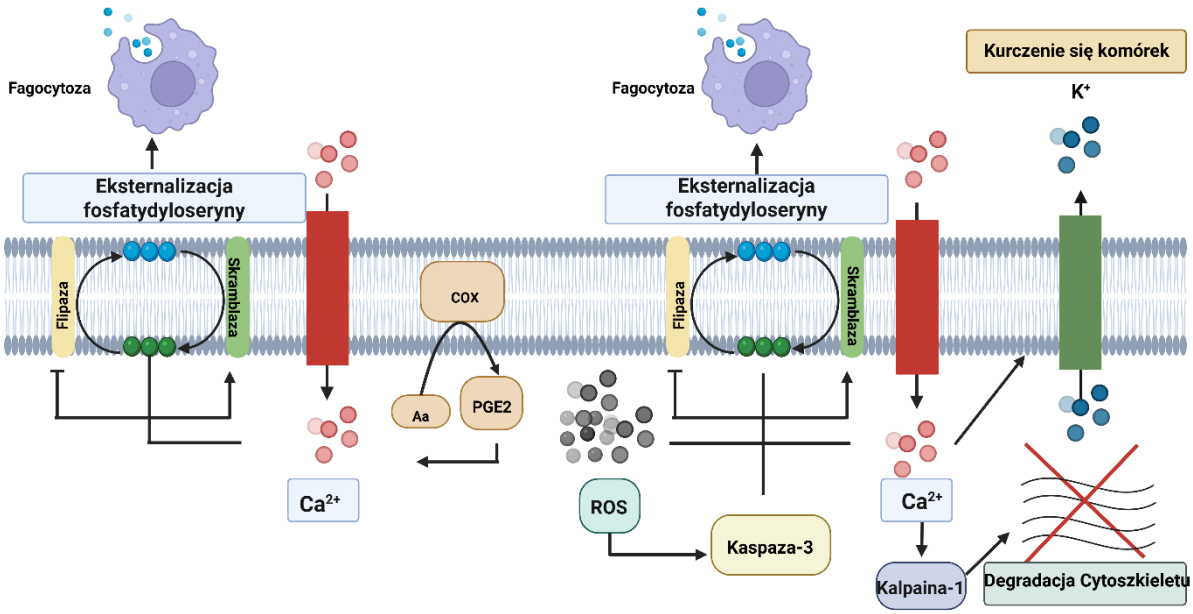

Rys. 4. Szlaki eryptozy (w oparciu o pracę Tkachenko et al., 2025).

W celu określenia czy eryptoza jest indukowana przez PS-NPs oznaczano wcześniej omawiane parametry wykorzystując odpowiednie znaczniki fluorescencyjne. Poziom reaktywnych form tlenu zbadano za pomocą sondy fluorescencyjnej dioctanu 2',7'-dichlorodihydrofluoresceiny (H_2DCF-DA), peroksydację lipidów oceniono przy użyciu znacznika BODIPY 581/591 C11, oceniono eksternalizację fosfatydyloseryny przy użyciu aneksyny V wyznakowanej izotiocyjanianiem fluoresceiny (FITC), z kolei poziom wapnia wewnątrzkomórkowego oznaczono stosując znacznik fluorescencyjny Fluo3-AM, natomiast aktywność kaspazy-3 zbadano przy użyciu testu z substratem specyficznym dla kaspazy-3 – DEVD-FMK sprzężonym z izotiocyjanianem fluoresceiny (FITC), a aktywność kalpain oznaczono przy pomocy komercyjnego zestawu QIA 120 z wykorzystaniem znacznika fluorescencyjnego 7-amino-4-metylokumaryny (AMC).

Uzyskane wyniki wskazują, że 24-godzinna inkubacja erytrocytów z PS-NPs o średnicach ~30 nm, ~45 nm i ~70 nm nie powodowała istotnych statystycznie zmian w poziomie reaktywnych form tlenu względem kontroli, co może być związane z budową tych komórek, które pozbawione są mitochondriów, i w związku z tym mogą być mniej podatne na mechanizmy oksydacyjnych uszkodzeń niż komórki jądrzaste. Mimo braku zmian w poziomie ROS, zaobserwowano istotny statystycznie wzrost peroksydacji lipidów pod wpływem nanocząstek o średnicach ~30 nm i ~70 nm w stężeniach 50 i 100 µg/ml,

a dla nanocząstek o średnicy ~45 nm przy najwyższym badanym stężeniu, przy czym najmniejsze nanocząstki najbardziej zwiększały peroksydację lipidów.

Jednym ze wskaźników eryptozy jest eksternalizacja fosfatydyloseryny. Wzrost tego parametru może być obserwowany zarówno w związku z podwyższeniem poziomu wewnątrzkomórkowych jonów Ca^{2+} jak i aktywacją kaspazy-3. W niniejszej pracy istotny statystycznie wzrost tego wskaźnika zaobserwowano jedynie w przypadku PS-NPs o średnicy ~30 nm przy najwyższym stężeniu 100 µg/ml, w związku z czym zmiany te mogą być związane z hemolityczną dezintegracją błony komórkowej a nie bezpośrednio z procesem eryptozy. Przy tym stężeniu obserwowano już ponad 10% hemolizy (Płuciennik et al., 2023). Zaobserwowano także wzrost poziomu wewnątrzkomórkowych jonów wapnia Ca^{2+}, który występował w hemolitycznym stężeniu 100 µg/ml w przypadku nanocząstek o średnicy ~30 nm i ~45 nm. Podobnie jak w przypadku eksternalizacji fosfatydyloseryny zmiany te mogły być związane z hemolizą. Nie wykazano aktywacji kaspazy-3. Przedstawione wyniki wskazują na brak indukcji eryptozy przez PS-NPs we wszystkich badanych średnicach w zakresie przedhemolitycznych stężeń. Zaobserwowano natomiast wzrost aktywności kalpainy-1, w niskich przedhemolitycznych stężeniach PS-NPs tj. od 1 do 50 µg/ml, co może wiązać się z zaburzeniami strukturalnymi w błonie erytrocytów powodowanymi przez te nanocząstki (praca pierwsza doświadczalna). W literaturze także podkreśla się, że PS-NPs mogą fizycznie oddziaływać z błoną poprzez adsorpcję, częściowe wnikanie w dwuwarstwę lipidową lub generowanie lokalnych naprężeń (Hollóczki and Gehrke, 2019; Łazarski et al., 2025). Tego typu mechaniczna interakcja może prowadzić do mikrodefektów cytoszkieletu erytrocytu. Natomiast kalpainy jako proteazy o wysokiej wrażliwości na zaburzenia organizacji cytoszkieletu prawdopodobnie mogą być uwrażliwione na aktywację w warunkach odkształcenia błony (np. reorganizację ankiryny lub spektryny), co obniża próg aktywacji wapniowej (Suzuki and Sorimachi, 1998; Von Reyn et al., 2012; Wieschhaus et al., 2012).

Podsumowując brak zmian w parametrach charakteryzujących indukcję eryptozy tj. poziomu reaktywnych form tlenu (ROS) i Ca^{2+}, aktywności kaspazy-3 i eksternalizacji fosfatydyloseryny (PS) sugeruje brak zachodzenia eryptozy w stężeniach przedhemolitycznych niezależnie od ich stężenia i średnicy. Natomiast wzrost aktywności kalpain dotyczy prawdopodobnie mikromechanicznej odpowiedzi cytoszkieletu na oddziaływanie nanocząstek.

PODSUMOWANIE

- Badane nanocząstki polistyrenu (PS-NPs) o średnicach ~30 nm, ~45 nm i ~70 nm powodują wzrost hemolizy erytrocytów człowieka zależny od wielkości cząstek.
- PS-NPs przyczyniają się do usztywnienia błony komórkowej erytrocytów w regionach hydrofobowych dwuwarstwy lipidowej.
- Obserwowano powstawanie stomatocytów, co wskazuje na wpływ PS-NPs na właściwości reologiczne krwinek czerwonych.
- PS-NPs nie indukują wzrostu poziomu reaktywnych form tlenu ani utleniania hemoglobiny wewnątrz erytrocytów.
- PS-NPs powodują utlenianie białek i lipidów błon erytrocytarnych w bardzo wysokich stężeniach natomiast nie wpływają na aktywność błonowej acetylocholinoesterazy.
- PS-NPs w stężeniach przedhemolitycznych nie indukują eryptozy.
- Prawdopodobnie PS-NPs działają mechanicznie na błonę erytrocytu, prowadząc do zmian w cytoszkielecie manifestujących się zwiększoną aktywnością kalpain już przy stężeniu PS-NPs 1 μg/mL.
- Oddziaływanie PS-NPs z albuminą manifestuje się zmianą struktury drugorzędowej białka oraz wydłużeniem czasów życia fluoresencji HSA, które są zależne od wielkości PS-NPs. Zmieniona albumina przez PS-NPs może prawdopodobnie wpływać na prawidłowe funkcjonowanie erytrocytów w układzie *in vivo.*

WNIOSKI

1. Niefunkcjonalizowane PS-NPs wywierają szkodliwy wpływ na erytrocyty człowieka, prowadząc do hemolizy zależnej od wielkości nanocząstek oraz do zmian we właściwościach mechanicznych błony komórkowej, takich jak jej usztywnienie i zaburzenia reologiczne.

2. PS-NPs nie wykazują bezpośrednich właściwości prooksydacyjnych wobec hemoglobiny ani nie zwiększają poziomu reaktywnych form tlenu, jednak przy wysokich stężeniach indukują peroksydację lipidów oraz utlenianie białek błonowych.

3. Nanocząstki polistyrenu nie inicjują eryptozy w stężeniach przedhemolitycznych, lecz wywołują subtelne zmiany strukturalne błony, prawdopodobnie o charakterze mechanicznym, co potwierdza zwiększona aktywność kalpain już przy niskich stężeniach ekspozycji.

4. Na niefunkcjonalizowanych PS-NPs tworzy się stabilna korona białkowa z albuminy, która ulega modyfikacjom strukturalnym pod wpływem interakcji z PS-NPs, co potwierdzają zmiany w strukturze drugorzędowej albuminy oraz w czasie życia fluorescencji jej aminokwasów aromatycznych.

BIBLIOGRAFIA

Publikacje naukowe

- Amato-Lourenço, L.F., Carvalho-Oliveira, R., Júnior, G.R., Dos Santos Galvão, L., Ando, R.A., Mauad, T., 2021. Presence of airborne microplastics in human lung tissue. J. Hazard. Mater. 416, 126124. https://doi.org/10.1016/j.jhazmat.2021.126124
- Anwar, M., Konnova, M.E., Dastgir, S., 2025. Circular plastic economy for sustainable development: current advances and future perspectives. RSC Sustain. 10.1039.D5SU00225G. https://doi.org/10.1039/D5SU00225G
- Barshtein, G., Arbell, D., Yedgar, S., 2011. Hemolytic Effect of Polymeric Nanoparticles: Role of Albumin. IEEE Trans. NanoBioscience 10, 259–261. https://doi.org/10.1109/TNB.2011.2175745
- Barshtein, G., Livshits, L., Shvartsman, L.D., Shlomai, N.O., Yedgar, S., Arbell, D., 2016. Polystyrene Nanoparticles Activate Erythrocyte Aggregation and Adhesion to Endothelial Cells. Cell Biochem. Biophys. 74, 19–27. https://doi.org/10.1007/s12013-015-0705-6
- Bhat, M.A., Gedik, K., Gaga, E.O., 2023. Atmospheric micro (nano) plastics: future growing concerns for human health. Air Qual. Atmosphere Health 16, 233–262. https://doi.org/10.1007/s11869-022-01272-2
- Byrnes, J.R., Wolberg, A.S., 2017. Red blood cells in thrombosis. Blood 130, 1795–1799. https://doi.org/10.1182/blood-2017-03-745349
- Gondal, A.H., Bhat, R.A., Gómez, R.L., Areche, F.O., Huaman, J.T., 2023. Advances in plastic pollution prevention and their fragile effects on soil, water, and air continuums. Int. J. Environ. Sci. Technol. 20, 6897–6912. https://doi.org/10.1007/s13762-022-04607-9
- Gopinath, P.M., Saranya, V., Vijayakumar, S., Mythili Meera, M., Ruprekha, S., Kunal, R., Pranay, A., Thomas, J., Mukherjee, A., Chandrasekaran, N., 2019. Assessment on interactive prospectives of nanoplastics with plasma proteins and the toxicological impacts of virgin, coronated and environmentally released-nanoplastics. Sci. Rep. 9, 8860. https://doi.org/10.1038/s41598-019-45139-6
- Hidalgo-Crespo, J., Moreira, C.M., Jervis, F.X., Soto, M., Amaya, J.L., Banguera, L., 2022. Circular economy of expanded polystyrene container production: Environmental benefits of household waste recycling considering renewable energies. Energy Rep. 8, 306–311. https://doi.org/10.1016/j.egyr.2022.01.071
- Hollóczki, O., Gehrke, S., 2019. Nanoplastics can change the secondary structure of proteins. Sci. Rep. 9, 16013. https://doi.org/10.1038/s41598-019-52495-w
- Ibrahim, Y.S., Tuan Anuar, S., Azmi, A.A., Wan Mohd Khalik, W.M.A., Lehata, S., Hamzah, S.R., Ismail, D., Ma, Z.F., Dzulkarnaen, A., Zakaria, Z., Mustaffa, N., Tuan Sharif, S.E., Lee, Y.Y., 2021. Detection of microplastics in human colectomy specimens. JGH Open 5, 116–121. https://doi.org/10.1002/jgh3.12457
- Jenner, L.C., Rotchell, J.M., Bennett, R.T., Cowen, M., Tentzeris, V., Sadofsky, L.R., 2022. Detection of microplastics in human lung tissue using μFTIR spectroscopy. Sci. Total Environ. 831, 154907. https://doi.org/10.1016/j.scitotenv.2022.154907

- Kamada, T., McMillan, D.E., Sternlieb, J.J., Björk, V.O., Otsuji, S., 1988. Albumin prevents erythrocyte crenation in patients undergoing extracorporeal circulation. Scand. J. Thorac. Cardiovasc. Surg. 22, 155–158. https://doi.org/10.3109/14017438809105949
- Kihara, S., Van Der Heijden, N.J., Seal, C.K., Mata, J.P., Whitten, A.E., Köper, I., McGillivray, D.J., 2019. Soft and Hard Interactions between Polystyrene Nanoplastics and Human Serum Albumin Protein Corona. Bioconjug. Chem. 30, 1067–1076. https://doi.org/10.1021/acs.bioconjchem.9b00015
- Kik, K., Bukowska, B., Krokosz, A., Sicińska, P., 2021. Oxidative Properties of Polystyrene Nanoparticles with Different Diameters in Human Peripheral Blood Mononuclear Cells (In Vitro Study). Int. J. Mol. Sci. 22, 4406. https://doi.org/10.3390/ijms22094406
- Kik, K., Bukowska, B., Sicińska, P., 2020. Polystyrene nanoparticles: Sources, occurrence in the environment, distribution in tissues, accumulation and toxicity to various organisms. Environ. Pollut. 262, 114297. https://doi.org/10.1016/j.envpol.2020.114297
- Kim, E.-H., Choi, S., Kim, D., Park, H.J., Bian, Y., Choi, S.H., Chung, H.Y., Bae, O.-N., 2022. Amine-modified nanoplastics promote the procoagulant activation of isolated human red blood cells and thrombus formation in rats. Part. Fibre Toxicol. 19, 60. https://doi.org/10.1186/s12989-022-00500-y
- Koelmans, A.A., Besseling, E., Shim, W.J., 2015. Nanoplastics in the Aquatic Environment. Critical Review, in: Bergmann, M., Gutow, L., Klages, M. (Eds.), Marine Anthropogenic Litter. Springer International Publishing, Cham, pp. 325–340. https://doi.org/10.1007/978-3-319-16510-3_12
- Łazarski, G., Rajtar, N., Romek, M., Jamróz, D., Rawski, M., Kepczynski, M., 2025. Interaction of Polystyrene Nanoplastic with Lipid Membranes. J. Phys. Chem. B 129, 4110–4122. https://doi.org/10.1021/acs.jpcb.5c00738
- Lee, D.-W., Jung, J., Park, S., Lee, Y., Kim, J., Han, C., Kim, H.-C., Lee, J.H., Hong, Y.-C., 2024. Microplastic particles in human blood and their association with coagulation markers. Sci. Rep. 14, 30419. https://doi.org/10.1038/s41598-024-81931-9
- Leslie, H.A., Van Velzen, M.J.M., Brandsma, S.H., Vethaak, A.D., Garcia-Vallejo, J.J., Lamoree, M.H., 2022. Discovery and quantification of plastic particle pollution in human blood. Environ. Int. 163, 107199. https://doi.org/10.1016/j.envint.2022.107199
- Li, P., Liu, J., 2024. Micro(nano)plastics in the Human Body: Sources, Occurrences, Fates, and Health Risks. Environ. Sci. Technol. 58, 3065–3078. https://doi.org/10.1021/acs.est.3c08902
- Malinowska, K., Sicińska, P., Michałowicz, J., Bukowska, B., 2023. The effects of non-functionalized polystyrene nanoparticles of different diameters on the induction of apoptosis and mTOR level in human peripheral blood mononuclear cells. Chemosphere 335, 139137. https://doi.org/10.1016/j.chemosphere.2023.139137
- Malinowska, K., Tarhonska, K., Foksiński, M., Sicińska, P., Jabłońska, E., Reszka, E., Zarakowska, E., Gackowski, D., Górecka, K., Balcerczyk, A., Bukowska, B., 2024. Impact of Short-Term Exposure to Non-Functionalized Polystyrene Nanoparticles on DNA Methylation and Gene Expression in Human Peripheral Blood Mononuclear Cells. Int. J. Mol. Sci. 25, 12786. https://doi.org/10.3390/ijms252312786

- Malinowska, K., Tarhonska, K., Górecka, K., Tokarz, P., Jabłońska, E., Balcerczyk, A., Reszka, E., Sicińska, P., Mokra, K., Bukowska, B., 2025. Exploring the effect of short-term exposure to non-functionalized polystyrene nanoparticles on selected chromatin determinants in human immune cells and plasmid DNA integrity. Nanotoxicology 1–14. https://doi.org/10.1080/17435390.2025.2556865
- Nihart, A.J., Garcia, M.A., El Hayek, E., Liu, R., Olewine, M., Kingston, J.D., Castillo, E.F., Gullapalli, R.R., Howard, T., Bleske, B., Scott, J., Gonzalez-Estrella, J., Gross, J.M., Spilde, M., Adolphi, N.L., Gallego, D.F., Jarrell, H.S., Dvorscak, G., Zuluaga-Ruiz, M.E., West, A.B., Campen, M.J., 2025. Bioaccumulation of microplastics in decedent human brains. Nat. Med. https://doi.org/10.1038/s41591-024-03453-1
- Pironti, C., Notarstefano, V., Ricciardi, M., Motta, O., Giorgini, E., Montano, L., 2022. First Evidence of Microplastics in Human Urine, a Preliminary Study of Intake in the Human Body. Toxics 11, 40. https://doi.org/10.3390/toxics11010040
- Płuciennik, K., Sicińska, P., Duchnowicz, P., Bonarska-Kujawa, D., Męczarska, K., Solarska-Ściuk, K., Miłowska, K., Bukowska, B., 2023a. The effects of non-functionalized polystyrene nanoparticles with different diameters on human erythrocyte membrane and morphology. Toxicol. In Vitro 91, 105634. https://doi.org/10.1016/j.tiv.2023.105634
- Płuciennik, K., Sicińska, P., Duchnowicz, P., Bonarska-Kujawa, D., Męczarska, K., Solarska-Ściuk, K., Miłowska, K., Bukowska, B., 2023b. The effects of non-functionalized polystyrene nanoparticles with different diameters on human erythrocyte membrane and morphology. Toxicol. In Vitro 91, 105634. https://doi.org/10.1016/j.tiv.2023.105634
- Płuciennik, K., Sicińska, P., Misztal, W., Bukowska, B., 2024. Important Factors Affecting Induction of Cell Death, Oxidative Stress and DNA Damage by Nano- and Microplastic Particles In Vitro. Cells 13, 768. https://doi.org/10.3390/cells13090768
- Ragusa, A., Notarstefano, V., Svelato, A., Belloni, A., Gioacchini, G., Blondeel, C., Zucchelli, E., De Luca, C., D'Avino, S., Gulotta, A., Carnevali, O., Giorgini, E., 2022. Raman Microspectroscopy Detection and Characterisation of Microplastics in Human Breastmilk. Polymers 14, 2700. https://doi.org/10.3390/polym14132700
- Ragusa, A., Svelato, A., Santacroce, C., Catalano, P., Notarstefano, V., Carnevali, O., Papa, F., Rongioletti, M.C.A., Baiocco, F., Draghi, S., D'Amore, E., Rinaldo, D., Matta, M., Giorgini, E., 2021. Plasticenta: First evidence of microplastics in human placenta. Environ. Int. 146, 106274. https://doi.org/10.1016/j.envint.2020.106274
- Salvia, R., Rico, L.G., Bradford, J.A., Ward, M.D., Olszowy, M.W., Martínez, C., Madrid-Aris, Á.D., Grífols, J.R., Ancochea, Á., Gomez-Muñoz, L., Vives-Pi, M., Martínez-Cáceres, E., Fernández, M.A., Sorigue, M., Petriz, J., 2023. Fast-screening flow cytometry method for detecting nanoplastics in human peripheral blood. MethodsX 10, 102057. https://doi.org/10.1016/j.mex.2023.102057
- Schwabl, P., Köppel, S., Königshofer, P., Bucsics, T., Trauner, M., Reiberger, T., Liebmann, B., 2019. Detection of Various Microplastics in Human Stool: A Prospective Case Series. Ann. Intern. Med. 171, 453–457. https://doi.org/10.7326/M19-0618
- Shen, M., Zhang, Y., Zhu, Y., Song, B., Zeng, G., Hu, D., Wen, X., Ren, X., 2019. Recent advances in toxicological research of nanoplastics in the environment: A review. Environ. Pollut. 252, 511–521. https://doi.org/10.1016/j.envpol.2019.05.102
- Suzuki, K., Sorimachi, H., 1998. A novel aspect of calpain activation. FEBS Lett. 433, 1–4. https://doi.org/10.1016/S0014-5793(98)00856-4

- Tian, Y., Tian, Z., Dong, Y., Wang, X., Zhan, L., 2021. Current advances in nanomaterials affecting morphology, structure, and function of erythrocytes. RSC Adv. 11, 6958–6971. https://doi.org/10.1039/D0RA10124A
- Tkachenko, A., Alfhili, M.A., Alsughayyir, J., Attanzio, A., Al Mamun Bhuyan, A., Bukowska, B., Cilla, A., Quintanar-Escorza, M.A., Föller, M., Havranek, O., Jilani, K., Onishchenko, A., Pretorius, E., Prokopiuk, V., Restivo, I., Tesoriere, L., Virzì, G.M., Wieder, T., 2025. Current understanding of eryptosis: mechanisms, physiological functions, role in disease, pharmacological applications, and nomenclature recommendations. Cell Death Dis. 16, 467. https://doi.org/10.1038/s41419-025-07784-w
- V. L. Leonard, S., Liddle, C.R., Atherall, C.A., Chapman, E., Watkins, M., D. J. Calaminus, S., Rotchell, J.M., 2024. Microplastics in human blood: Polymer types, concentrations and characterisation using μFTIR. Environ. Int. 188, 108751. https://doi.org/10.1016/j.envint.2024.108751
- Van De Wouw, J., Joles, J.A., 2022. Albumin is an interface between blood plasma and cell membrane, and not just a sponge. Clin. Kidney J. 15, 624–634. https://doi.org/10.1093/ckj/sfab194
- Von Reyn, C.R., Mott, R.E., Siman, R., Smith, D.H., Meaney, D.F., 2012. Mechanisms of calpain mediated proteolysis of voltage gated sodium channel α-subunits following *in vitro* dynamic stretch injury. J. Neurochem. 121, 793–805. https://doi.org/10.1111/j.1471-4159.2012.07735.x
- Wieschhaus, A., Khan, A., Zaidi, A., Rogalin, H., Hanada, T., Liu, F., De Franceschi, L., Brugnara, C., Rivera, A., Chishti, A.H., 2012. Calpain-1 knockout reveals broad effects on erythrocyte deformability and physiology. Biochem. J. 448, 141–152. https://doi.org/10.1042/BJ20121008
- Williams, A.R., 1973. The effect of bovine and human serum albumins on the mechanical properties of human erythrocyte membranes. Biochim. Biophys. Acta BBA - Biomembr. 307, 58–64. https://doi.org/10.1016/0005-2736(73)90024-2
- Wright, S.L., Kelly, F.J., 2017. Plastic and Human Health: A Micro Issue? Environ. Sci. Technol. 51, 6634–6647. https://doi.org/10.1021/acs.est.7b00423
- Yang, Y., Xie, E., Du, Z., Peng, Z., Han, Z., Li, L., Zhao, R., Qin, Y., Xue, M., Li, F., Hua, K., Yang, X., 2023. Detection of Various Microplastics in Patients Undergoing Cardiac Surgery. Environ. Sci. Technol. 57, 10911–10918. https://doi.org/10.1021/acs.est.2c07179
- Yates, J., Deeney, M., Muncke, J., Carney Almroth, B., Dignac, M.-F., Castillo, A.C., Courtene-Jones, W., Kadiyala, S., Kumar, E., Stoett, P., Wang, M., Farrelly, T., 2025. Plastics matter in the food system. Commun. Earth Environ. 6, 176. https://doi.org/10.1038/s43247-025-02105-7
- Zhao, Q., Zhu, L., Weng, J., Jin, Z., Cao, Y., Jiang, H., Zhang, Z., 2023. Detection and characterization of microplastics in the human testis and semen. Sci. Total Environ. 877, 162713. https://doi.org/10.1016/j.scitotenv.2023.162713

Źródła Internetowe

Źródło internetowe 1 – https://iucn.org/sites/default/files/2024-05/plastic-pollution-issues-brief-may-2024-update.pdf (dostęp 04.09.2025 r)

Źródło internetowe 2 – https://www.marketreportsworld.com/market-reports/polystyrene-market-14718057 (dostęp 10.09.2025 r).

DOROBEK NAUKOWY

Publikacje

Płuciennik K., Sicińska P., Misztal W., Bukowska B.*, . I*mportant Factors Affecting Induction of Cell Death, Oxidative Stress and DNA Damage by Nano- and Microplastic Particles In Vitro.* Cells 2024; 13(9):768. https://doi.org/10.3390/cells13090768
Punkty MNiSW: 140, IF: 6,1 (5-letni)
Płuciennik K., Sicińska P., Duchnowicz P., Bonarska-Kujawa D., Męczarska K., Solarska-Ściuk K., Miłowska K., Bukowska B.*, *The effects of non-functionalized polystyrene nanoparticles with different diameters on human erythrocyte membrane and morphology.* 2023; Toxicology in vitro 91(1):105634
Punkty MNiSW: 100, IF: 3,0 (5-letni)
Płuciennik K., Szabelski M., Miłowska K., Ciepluch K., Duchnowicz P., Krokosz A., Sicińska P., Bukowska B.*, *The interactions of non-functionalized polystyrene nanoparticles with human albumin and erythrocyte proteins: implications and potential consequences*. Scientific Reports 2025; 15: 30076,
Punkty MNiSW: 140, IF: 4,3 (5-letni)

Doniesienia konferencyjne w języku polskim

Płuciennik K.*, Duchnowicz P., Sicińska P., Bukowska B, VII Ogólnopolska Konferencja Doktorantów Nauk o Życiu BioOpen 2022, *Wpływ nanocząstek polistyrenu na płynność błony komórkowej erytrocytów człowieka.* Łódź 7–8.04.2022 r. – poster
Płuciennik K.*, Duchnowicz P., Sicińska P., XV Interdyscyplinarna Konferencja Naukowa TYGIEL 2023 „Interdyscyplinarność kluczem do rozwoju", *Zmiany strukturalne w obszarze hydrofobowym w dwuwarstwie lipidowej błony erytrocytów człowieka pod wpływem nanocząstek polistyrenu o różnych średnicach*. Lublin 23–26.03.2023 r. – poster
Płuciennik K.*, Sicińska P., Bukowska B., VIII Ogólnopolska Konferencja Doktorantów Nauk o Życiu BioOpen 2023, *Wpływ niefunkcjonalizowanych nanocząstek polistyrenu o różnych średnicach na hemolizę i utlenianie hemoglobiny w erytrocytach człowieka w warunkach in vitro.* Łódź 13–14.04.2023 r – poster
Hofman M.*, **Płuciennik K.,** Bukowska B., VIII Ogólnopolska Konferencja Doktorantów Nauk o Życiu, 11–12 kwietnia 2023. *Wpływ niefunkcjonalizowanych nanocząstek polistyrenu o różnych średnicach na indukcję ferroptozy w jednojądrzastych komórkach krwi obwodowej*. Łódź, 13–14.04.2023 r. – poster
Bukowska B.*, **Płuciennik K.,** XIV Konferencja Naukowo Szkoleniowa Polskiego Towarzystwa Toksykologicznego, *Czynniki wpływające na toksyczność mikro i nanoplastiku.* Poznań, 4–6 09 2024 r. – prezentacja ustna

Doniesienia konferencyjne w języku angielskim

Płuciennik K.*, Sicińska P., Bukowska B., 5th BIO Congres 2023, *Changes in human erythrocyte morphology under the influence of non-funcionalized polystyrene nanoparticles with different diameters ,* Szczecin, 13–16.09.2023 r.
Płuciennik K.*, Sicińska P., Bukowska B., 58th Congress of the European Societies of Toxicology- Eurotox 2024, *Proeryptotic effects of non-functionalized polystyrene nanoparticles with different diameters* , Kopenhaga (Dania), 08–11. 09. 2024 r.

Pluciennik K.*, Miłowska K., Duchnowicz P., Szabelski M., Ciepluch K., Sicińska P., Krokosz A., Bukowska B., 59th Congress of the European Societies of Toxicology- Eurotox 2025, *The effect of non-functionalized polystyrene nanoparticles with varying diameters on human albumin (in vitro),* Ateny (Grecja), 14–17.09.2025 r.

Staże

Staż naukowy z zakresu fluorescencji w Katedrze Fizyki i Biofizyki, Wydział Nauk o Żywności, Uniwersytet Warmińsko-Mazurski w Olsztynie 23.11–02.12.2022 r. – opiekun stażu dr hab. Mariusz Szabelski prof. UWM.

Organizacja Konferencji

- Członek komitetu naukowego *Ogólnopolskiej Konferencji Doktorantów Nauk o Życiu BioOpen* organizowanej przez Wydział Biologii i Ochrony Środowiska Uniwersytetu Łódzkiego:
  - Sesja „Mikrobiologia i Immunologia" – VIII edycja w 2023 r., 13–14.04.2023 r.
  - Sesja „Biologia Molekularna i Medyczna" – IX edycja w 2024 r., 11–12.04.2023 r.
- Członek komitetu naukowego *10th International PhD Students' Conference in Life Sciences – BioOpen* organizowanej przez Wydział Biologii i Ochrony Środowiska Uniwersytetu Łódzkiego:
  - Sesja „Molecular and medical biology" – X edycja w 2025 r., 15–16.05.2025 r.

Popularyzacja nauki

- Współprowadzenie warsztatów: *3,2,1- START! Woda jako baza fascynujących, naukowych eksperymentów* w ramach Nocy Biologów 2023, 13.01.2023 r.
- Prezentacja Instytutu Biofizyki z krótkimi pokazami, podczas pobytu licealistów spoza Łodzi w ramach akcji „Zasmakuj studiowania w Łodzi" – 17.11.2023 r.
- Prowadzenie warsztatów *W świecie komórek krwi – widzimy Was! "* oraz współprowadzenie warsztatów : *„ Świat DNA – zobacz to na własne oczy." W ramach Nocy Biologów 2024* – 12.01.2024 r.
- Współprowadzenie warsztatów : *„Izolacja składników morfotycznych krwi"* w ramach III Drzwi Otwartych Wydziału Biologii i Ochrony Środowiska UŁ- 05.04.2024 r.

Szkolenia Naukowe

- Szkolenie naukowe *„Analiza danych biologicznych- wprowadzenie do statystyki"* – organizowane przez dr hab. Magdalenę Łabieniec- Watałę prof. UŁ, Wydział Biologii i Ochrony Środowiska Uniwersytetu Łódzkiego, Łódź, 7-10. 02.2023 r
- Warsztaty Organizowane przez firmę Anton Paar, Analiza wielkości cząstek i spektroskopia Ramana, Łódź, 04.06.2025 r

Pozostałe

- Członek Polskiego Towarzystwa Biofizycznego od 07.2023 r.

KOPIE PRAC WCHODZĄCYCH W SKŁAD ROZPRAWY DOKTORSKIEJ

cells

MDPI

Review

Important Factors Affecting Induction of Cell Death, Oxidative Stress and DNA Damage by Nano- and Microplastic Particles In Vitro

Kamil Płuciennik, Paulina Sicińska, Weronika Misztal and Bożena Bukowska *

University of Lodz, Faculty of Biology and Environmental Protection, Department of Biophysics of Environmental Pollution, Pomorska 141/143, 90-236 Lodz, Poland; kamil.pluciennik@edu.uni.lodz.pl (K.P.); paulina.sicinska@biol.uni.lodz.pl (P.S.); weronika.misztal@edu.uni.lodz.pl (W.M.)
* Correspondence: bozena.bukowska@biol.uni.lodz.pl

Abstract: We have described the influence of selected factors that increase the toxicity of nanoplastics (NPs) and microplastics (MPs) with regard to cell viability, various types of cell death, reactive oxygen species (ROS) induction, and genotoxicity. These factors include plastic particle size (NPs/MPs), zeta potential, exposure time, concentration, functionalization, and the influence of environmental factors and cell type. Studies have unequivocally shown that smaller plastic particles are more cytotoxic, penetrate cells more easily, increase ROS formation, and induce oxidative damage to proteins, lipids, and DNA. The toxic effects also increase with concentration and incubation time. NPs with positive zeta potential are also more toxic than those with a negative zeta potential because the cells are negatively charged, inducing stronger interactions. The deleterious effects of NPs and MPs are increased by functionalization with anionic or carboxyl groups, due to greater interaction with cell membrane components. Cationic NPs/MPs are particularly toxic due to their greater cellular uptake and/or their effects on cells and lysosomal membranes. The effects of polystyrene (PS) vary from one cell type to another, and normal cells are more sensitive to NPs than cancerous ones. The toxicity of NPs/MPs can be enhanced by environmental factors, including UV radiation, as they cause the particles to shrink and change their shape, which is a particularly important consideration when working with environmentally-changed NPs/MPs. In summary, the cytotoxicity, oxidative properties, and genotoxicity of plastic particles depends on their concentration, duration of action, and cell type. Also, NPs/MPs with a smaller diameter and positive zeta potential, and those exposed to UV and functionalized with amino groups, demonstrate higher toxicity than larger, non-functionalized and environmentally-unchanged particles with a negative zeta potential.

Keywords: cytotoxic; DNA damage; functionalization; oxidative stress; UV radiation; zeta potential

Citation: Płuciennik, K.; Sicińska, P.; Misztal, W.; Bukowska, B. Important Factors Affecting Induction of Cell Death, Oxidative Stress and DNA Damage by Nano- and Microplastic Particles In Vitro. *Cells* **2024**, *13*, 768. https://doi.org/10.3390/cells13090768

Academic Editor: Mark R. Wilson

Received: 16 March 2024
Revised: 26 April 2024
Accepted: 28 April 2024
Published: 30 April 2024

1. Introduction

Plastic production has remained at a high level since 2000, with a global production of 400.3 million tons in 2022 [1]. As waste management is currently insufficient, with only 9% of material being recycled and 12% incinerated, most plastics end up as waste in the natural environment [2], where they are exposed to inter alia UV radiation, mechanical abrasion, temperature or biological agents. As a result, the plastics are degraded to microparticles (MPs) smaller than ≤5000 µm, and then to nanoparticles (NPs) smaller than 1 µm [2,3]. Approximately 90% of the total amount of plastics consists of high-density polyethylene (HDPE), low-density polyethylene (LDPE), polyvinyl chloride (PCV), polystyrene (PS), polypropylene (PP), and polyethylene terephthalate (PET) [4]. Of these, polystyrene particles are the most commonly used in in vitro studie because they are commercially available from various manufacturers, such as Bangs Laboratories (Fishers, IN, USA), Kisker Biotech (Steinfurt, Germany), and Alpha Nanotech Inc. (Vancouver, BC, Canada) [5].

MPs and NPs are widespread throughout the environment and pose a potential threat to living organisms. They have been found to enter living organisms and accumulate in the trophic chain [6–8]. Due to their persistent nature, MPs and NPs can accumulate in various organs and tissues and may induce the long-term development of various diseases. Clearly, the toxic effects of NPs/MPs require further research, especially in regard to human health.

A number of studies have indicated the presence of MPs in humans, but unfortunately, little data have been acquired regarding NPs. Nevertheless, MPs have been detected in human stool [9], urine [10], sputum [11], and lung sections [12]. They have also been found in the male reproductive system [13] and in human blood [14]. Other reports have mentioned a higher number of MPs in the tumor tissue of patients with colorectal adenocarcinoma [15].

Only one study to date has assessed the level of NPs in the human body. Blood samples from 196 subjects, a mixture of healthy donors and patients, were found to contain NPs [16]. The mean NP concentration was 667 events/μL in healthy donors (n = 37). Among the patients, the highest level was found in those with acute lymphoblastic leukemia (n = 46, m = 648.3 events/μL) and the lowest in patients with type 1 diabetes (n = 10, m = 368.2 events/μL).

Studies have shown that due to their accumulation in cells and tissues, NPs/MPs can induce cytotoxicity [17], oxidative stress [18], genotoxicity [19], inflammation [20], and neurotoxicity [21], among others [22,23]. Hence, the aim of the present work was to describe the factors that increase the cytotoxicity of plastic NPs/MPs in vitro, with regard to cell viability, cell death, reactive oxygen species (ROS) induction, and genotoxicity. It focuses on the size, zeta potential, exposure time, concentration, and functionalization of the particles, as well as the influence of environmental factors and target cell type. Most of the reviewed studies were published from 2019 to 2024. They were identified by searches of Elsevier, Frontiers, PubMed, and Springer databases, as well as Google Scholar.

2. Effects of Plastic Particles on Cells

2.1. Plastic Particles Penetrate Cells

Numerous studies have indicated that NPs/MPs have cytotoxic effects against various cell types. These particles have been found to penetrate the cell, and this correlates with their cytotoxic effects. Studies based on fluorescent polystyrene NPs found that their penetration into the cells depended on their concentration; particles with a diameter of 0.04–0.09 μm penetrated 59% of Caco-2 cells at a concentration of 25 μg/mL, and 86% of cells at a concentration of 100 μg/mL [24].

Other studies have identified effective cellular uptake of fluorescent NPs/MPs with diameters ranging from 200 nm to 6 μm. Schmidt et al. [25] found a higher relative accumulation of smaller particles compared to larger particles, and polystyrene NPs (PS-NPs) accumulated mainly in the cytoplasm around the cell nucleus. Microscope observation [26] found the lysosomal membrane in HT29 cells to be more permeable to smaller MPs, i.e., with a diameter of 3 μm, than those with a diameter of 10 μm. In contrast, another study showed that PS-NPs with a size of 50 nm were internalized by human HepG2 cells and localized intracellularly, especially in the lysosomal compartment [27].

Annangi et al. [28] reported the uptake and intracellular localization of 50 nm and 500 nm diameter PS-NPs at 100 μg/mL after 24 h incubation in primary human nasal epithelial cells. Confocal microscopy identified a greater internalization of PS of 50 nm compared to PS of 500 nm, indicating that the effect was dependent on particle size. The authors indicate that the process of internalization was similar to phagocytosis, and that the PS particles entered the nucleus, inhibiting cell proliferation and inducing cell apoptosis [28].

2.2. Cytotoxicity—Plastic Particles Decreased Cell Viability and Their Metabolic Activity

Cytotoxicity is the ability of a specific agent to disturb the functioning of cells, i.e., to damage or destroy them, by disturbing the continuity of cell membranes or the cytoskeleton, or by disturbing the processes of metabolism and cell division, among others [29].

2.2.1. Plastic Particles with Smaller Size, Higher Concentration, and Longer Exposure Time Are More Cytotoxic

Studies indicate that the cytotoxicity of plastic NPs is associated with their size, concentration, and time of action, irrespective of target cell type.

Visalli et al. [26] assessed the effect of 3 μm and 10 μm diameter PS particles on the viability of HT-29 intestinal epithelial cells after 24 h of incubation using the MTT assay. At concentrations of 100–1600 particles mL^{-1}, the microparticles showed moderate cytotoxicity. Smaller particles were shown to be more cytotoxic. At the tested concentrations, cell mortality rates were between 6.7% and 21.6% for the 10 μm PS, and between 6.1% and 29.6% for the 3 μm PS. Yan et al. [30] evaluated the effect of 20 nm and 1 μm PS-NPs on the viability of AGS gastric adenocarcinoma cells after 24 h of incubation. The MTT test confirmed that at 10 μg/mL, the NP treatment resulted in lower cell viability, while the MP treatment did not. Clearly, the cytotoxicity of NPs/MPs depends on their size.

Another study [31] examined the effects of polystyrene (PS) MPs measuring 3 μm and PS-NPs of 20 nm and 80 nm, at a concentration range of 0.001–100 μg/mL, on CT26.WT mouse colon cancer cells using the Cell Counting Kit-8 (CCK-8) assay. The smallest NPs (20 nm) showed a cytotoxic effect from a concentration of 0.1 μg/mL, the 80 nm particles from a concentration of 50 μg/mL, and the 3 μm microparticles of from 100 μg/mL.

Malinowska et al. [19] examined the impact of non-functionalized PS-NPs (29 nm, 44 nm, and 72 nm in diameter) on the metabolic activity (MTT assay) of human peripheral blood mononuclear cells (PBMCs) at concentrations from 100 to 1000 μg/mL. It was found that the smallest 29 nm NPs demonstrated the greatest decrease in metabolic activity relative to controls, which was significant from 300 μg/mL. However, the NPs (44 nm and 72 nm) caused a significant decrease in activity from 500 μg/mL. Kik et al. [17] reported various reductions of PBMC viability following exposure to NPs. Propidium iodide and calcein AM staining, and flow cytometry measurement, indicated that the 29 nm and 44 nm NPs decreased cell viability at 500 μg/mL, and the largest NPs (72 nm) at 1000 μg/mL.

The literature data also suggest that NP/MP cytotoxicity depends on the duration of their action. In one study, colon epithelial HRT-18 (human) and rectal epithelial CMT-93 (mouse) cells were treated with the same concentration of MPs, i.e., 1 mg/mL, for 6, 24, or 48 h. The results indicate that the MPs exhibited a time-dependent cytotoxic effect on the tested cell lines; 18.4% at 6 h, 24.9% at 24 h, and 42.8% at 48 h [32].

Steckiewicz et al. [33] found that amino group-modified PS-NPs with a diameter of 100 nm caused time-dependent cytotoxicity in HT-29 colon cancer cell lines. A cytotoxic effect was noted at NP concentrations of 250 μg/mL and 500 μg/mL after 48 h of incubation, and the effect was greater after 24 h.

In conclusion, NPs definitely demonstrate greater cytotoxicity than MPs. In both cases, the cytotoxicity also increases with decreasing diameter, so smaller NPs demonstrate greater toxic effects. Although the cytotoxicity also depends on the concentration of the NPs/MPs and the time of their action, particle size seems to be the most crucial factor.

2.2.2. Functionalized Plastics Particles Are More Cytotoxic

The presence of a functional group in plastic NPs affects cell penetration and cytotoxicity. Nanoparticle surface functionalization was found to facilitate internalization of PS-NPs by HepG2 cells. Indeed, HepG2 cells exposed to PS-COOH and $PSNH_2$ particles demonstrated significantly more intense fluorescence compared to non-functionalized PS-NPs [27]. This study determined the cytotoxic effect of PS-NPs of about 50 nm in

diameter against HepG2 liver cancer cell lines using the MTT assay. It was shown that both non-functionalized PS-NPs and those containing a functional group (PS-COOH, PS-NH_2) induced a cytotoxic effect after 24 h incubation, but the effect depended on particle concentration and the presence of the functional group. For non-functionalized NPs, the reduction in cell viability was 2.94% at 10 μg/mL, 16.44% at 50 μg/mL, and 24.82% at 100 μg/mL. The cytotoxicity was higher for PS-COOH and PS-NH_2 functionalized particles. PS-COOH particles at 10, 50, and 100 μg/mL reduced HepG2 cell viability by 2.79, 2.11, and 1.83 times, respectively, compared to non-functionalized PS and by 2.42, 1.50, and 1.86 times, respectively, in PS-NH_2 particles [27].

Chen et al. [34] also evaluated the impact of non-functionalized PS-NPs, and positively (PS-NH_2) and negatively (PS-COOH) charged PS-NPs on RAW 264.7 macrophage cells after 24 h incubation. The PS particles had no cytotoxic effect at concentrations of 0.5 to 100 μg/mL, while PS-COOH particles caused a 6% decrease in viability, and PS-NH_2 particles as much as 70% at 20 μg/mL. Positively-charged particles caused greater cell cytotoxicity, most likely because they had the ability to penetrate the phospholipid bilayer and could cause greater damage to the cytoplasmic membrane.

The absorption coefficient of positively-charged NPs is much higher than that of negatively-charged particles [35]. Cationic NPs are generally more toxic than anionic NPs, partly due to their greater cellular uptake and/or their deleterious effects on cells and lysosomal membranes [36]. Positively-charged NPs can affect cell membranes by changing the orientation of phospholipid groups, reducing lipid density, thus increasing membrane permeability [37]. This may promote passive diffusion of NPs and membrane bending associated with endocytosis and phagocytosis, while encouraging cells to rapidly absorb positively-charged PS-NH_2.

According to Wang et al. [38], processes such as cytotoxicity and apoptosis induced by cationic particles are mainly due to the positive cationic charge on the particle surface and interference with the proton pump. Cationic NPs exert a toxic effect via their strong electrostatic attraction to negatively-charged cell membrane bilayers, which enhances their interaction with the cell membrane [34,39,40]. Shao et al. [41] suggested that negatively-charged NPs have relatively weak interactions with negatively-charged biomembranes, thus induce low cytotoxicity.

2.2.3. Plastic Particles with Positive Zeta Potentials Are More Cytotoxic

The zeta potential, which depends on the surface charge, is a very important parameter for the initial adsorption of NPs on the cell membrane [42]. It is known that the rate of endocytotic uptake also depends on particle size [43]. Thus, zeta potential and size affect the toxicity of NPs [44].

Shao et al. [41] investigated how zeta potential affected the cytotoxicity of polymer NPs. They used four types of NPs with similar sizes and zeta potential gradients. MTT assay against mouse L929 fibroblasts was carried out using nanoparticles (poly-3-hydroxybutyrate-co-3-hydroxyhexanoate biopolymer) (PHBHHx) with a zeta potential gradient ranging from −30 mV to +40 mV. NPs with positive zeta potentials were found to be more toxic than those with negative potentials. Such particles react more strongly with the negatively-charged cell membrane.

Malinowska et al. [19] found the smallest NPs (29 nm), suspended in RPMI medium to exhibit the strongest cytotoxicity against human PBMCs, had the lowest absolute negative zeta potential (−40.86 ± 2.77 mV). In contrast, the largest particles were characterized by the highest absolute negative zeta potential (−56 ± 2 mV) and the lowest cytotoxicity. The zeta potential is important in the interaction of NPs with cells, due to the fact that cell membranes are negatively charged. It is possible that the lower absolute value of the zeta potential of the smallest NPs may indirectly induce stronger electrostatic interactions between these particles and the negatively-charged membrane.

In summary, among plastic NPs of the same diameter, cytotoxicity is significantly affected by their zeta potential. Certainly, NPs with a positive zeta potential exhibit

stronger toxicity than those with a negative zeta potential, which is due to a stronger interaction with the negatively-charged cell membrane and easier penetration of the particles into the cell.

2.2.4. Plastic Particles Are More Toxic to Normal Cells than Cancer Cells

An interesting study was published by Xu et al. [45]. Their findings, based on direct cell counting, indicate that at concentrations of 1 to 100 μg/mL, plastic NPs had a greater cytotoxic effect on normal HIEC-6 cells than human intestinal cancer cells (RKO, HT-29, HCT-116 lines). Exposure to PS-NPs 100 nm in diameter resulted in a reduction in the cell growth of colon cancer cells at 100 μg/mL, and of normal cells from 10 μg/mL.

2.2.5. The Toxicity of Plastic Particles Is Different for Different Cell Types

Rubio et al. [46] investigated the effects of 50 nm PS-NPs on the immune cell population using three human leukocyte lines: Raji-B (B lymphocytes), TK6 (lymphoblasts), and THP-1 (monocytes). It was shown that although monocytic THP-1 cells revealed the highest internalization of the particles, no adverse effects were noticed in this cell type. In contrast, Raji-B and TK6 cells showed lower uptake of PS-NPs, but also weak toxicity, ROS production, and genotoxic effects. These results underscore the importance of cell line selection when evaluating the biological effects of PS-NPs; the effects of PS can vary between cell lines, even among the three leukocyte cell line types.

2.2.6. UV Radiation Increases the Toxicity of Plastic Particles

As reported by Lins et al. [47], the toxicity of nanoplastics to organisms varies significantly over ecologically relevant ranges of temperature and salinity. Hence, environmental conditions have a strong influence on the toxicity of these particles.

An important environmental factor affecting plastic properties and performance is UV radiation. In in vitro studies, non-functionalized PS-NPs (50 nm) were exposed to ultraviolet radiation for one or two months. Unlike the initial spherical-shaped nanoparticles, those exposed to UV radiation were irregularly shaped and smaller, and their size decreased with exposure time. The study also showed that with UV exposure time, the ratio of oxygen atoms to carbon atoms increased, as did the absolute value of the zeta potential, indicating exposure of the carbonyl group [48]. It was observed that unlike the untreated NPs, UV-exposed PS-NPs decreased the viability of the A549 alveolar adenocarcinoma line at a concentration of 100 μg/mL after a 24 h incubation. Cytotoxicity assays were performed using a colorimetric assay to count CCK-8 cells [49].

In summary, the aged plastic NPs exhibited greater cytotoxicity than the untreated NPs and this toxicity increased with treatment time.

2.2.7. Cytotoxicity Induced of Plastic Particles—Summary

It can be concluded that the cytotoxicity of NPs/MPs depends on their size, i.e., with size being inversely related to cytotoxicity and functionalization, with positively-charged NPs having greater harmful effects. It also depends on time and concentration, with greater cytotoxicity observed at longer incubation times and higher NP/MP concentration. It is also influenced by cell type, with normal intestinal cells being more sensitive to plastic particles than cancer cells, and the effect of UV radiation, which causes the breakdown of NPs/MPs into smaller irregular shapes and more toxic particles (Table 1).

The plastic particles may exert their cytotoxic activity by escaping from the endosome and interfering with cellular processes, such as mitosis. They may also cross the membrane in a passive manner, damaging the phospholipid bilayer and impairing transport signals. In addition, MPs and NPs that have entered the cytoplasm may also make direct contact with cell organelles [50].

Table 1. Cytotoxicity of NPs/MPs depending on their size, zeta potential, time of incubation, concentration, functionalization, type of cell line, and the effect of UV radiation.

Cells/Exposure Time	Type of Particle /Factors/Concentration	Cytotoxic Concentration	Decrease in Cell Viability	References
	Size			
Caco-2 cells 24 h	PS-NPs 20 nm 1000 nm	 500 µg/mL 500 µg/mL	 90% No changes	[30]
HT-29	PS-MPs 3 µm 10 µm	200 particles/mL	 15.99 6.31	[26]
PBMCs 24 h (test MTT)	PS-NPs 29 nm 44 nm 72 nm	500 µg/mL	 53% 17% 14%	[19]
	Zeta potential			
L929 fibroblasts 24 h	20 nm PHBHHx NP-1 (−21 mV) NP-2 (−28 mV) NP-3 (+20 mV) NP-4 (+44.9 mV)	100 µg/mL	 31% 33% 46% 52%	[41]
PBMCs 24 h (PI/calcein AM)	PS-NPs 29 nm (−41 mV) 44 nm (−45 mV) 72 nm (−56 mV)	700 µg/mL	 41% 24% 17%	[17]
	Time of incubation			
CMT 93 6 h 24 h 48 h	4.8–5.8 µm mixture of PS-MPs	1 mg/mL	 16% 23% 25%	[32]
TK6 24 h 48 h	40–90 nm mixture of PS-NPs	100 µg/mL	 15% 26%	[46]
HT-29 48 h 72 h	100 nm PS-NPs	250 µg/mL 500 µg/mL 250 µg/mL 500 µg/mL	7% 41% 15% 45%	[33]
	Concentration			
Caco-2 cells 24 h (test MTT)	20 nm PS-NPs	10 µg/mL 50 µg/mL 100 µg/mL 500 µg/mL	16% 80% 93% 90%	[30]
RAW 264.7 24 h	100 nm PS-NH_2	10 µg/mL 20 µg/mL 50 µg/mL	21% 70% 96%	[34]
L929 fibroblasts 24 h	20 nm PHBHHx NP-4 (+44.9 mV)	12.5 µg/mL 50 µg/mL 100 µg/mL 200 µg/mL	28% 39% 47% 52%	[41]

Table 1. *Cont.*

Cells/Exposure Time	Type of Particle /Factors/Concentration	Cytotoxic Concentration	Decrease in Cell Viability	References
PBMCs 24 h (PI/calcein AM)	PS-NPs 29 nm	300 µg/mL 500 µg/mL 700 µg/mL 1000 µg/mL	11% 17% 41% 54%	[17]
	Functionalization			
HepG2 24 h	50 nm PS-NPs 50 nm PS-COOH 50 nm PS-NH_2	100 µg/mL 100 µg/mL 100 µg/mL	24.82% 45.42% 46.16%	[27]
Raw 264.7 24 h	100 nm PS-COOH 100 nm PS-NH_2	20 µg/mL 20 µg/mL	6% 70%	[35]
A 549 24 h	80 nm PS-NPs 80 nm PS-COOH 80 nm PS-NH_2	100 µg/mL 100 µg/mL 100 µg/mL	16.1% 26.89% 33.97%	[49]
RAW 264.7 24 h	100 nm PS-NPs 100 nm PS-COOH 100 nm PS-NH_2	20 µg/mL	No changes 8% 70%	[34]
	Type of cell line			
CaCo-2 CCD 841 CoN 72 h	100 nm PS-NH_2	500 µg/mL 500 µg/mL	56% 33%	[33]
Raji-B/24 h TK6 THP-1	40–90 nm mixture of PS-NPs	100 µg/mL 100 µg/mL -	19% 15% No changes	[46]
CMT 93 HRT-18 24 h/(test MTT)	4.8–5.8 µm mixture of PS-MPs	1 mg/mL	23% 4%	[32]
HIEC 6—normal cells RKO, HCT116, HT-29—cancer cells 48 h	100 nm PS-NPs	10 µg/mL	17% decrease in cell growth No changes	[45]
	UV radiation			
A549 24 h	50 nm PS-NPs UVPS1 UVPS1	- 100 µg/mL 100 µg/mL	No changes 17.19% 21.12%	[49]

3. Type of Cell Death

Cell death is generally divided into two types: accidental cell death (ACD), which is a biologically uncontrolled process, and regulated cell death (RCD) or programmed cell death (PCD), which involve precise signaling cascades and molecularly-defined effector mechanisms. ACD involves hemolysis in anucleated erythrocytes and necrosis in nucleated cells. In turn, PCD concerns various other types of cell death, such as autophagy, apoptosis, and ferroptosis [51]. As the induction of cell death by plastic particles has been broadly covered in previous studies, the subsequent chapters will examine the effects of plastic particle size, concentration, duration of action, and functionalization on the types of cell death and DNA damage (Figure 1).

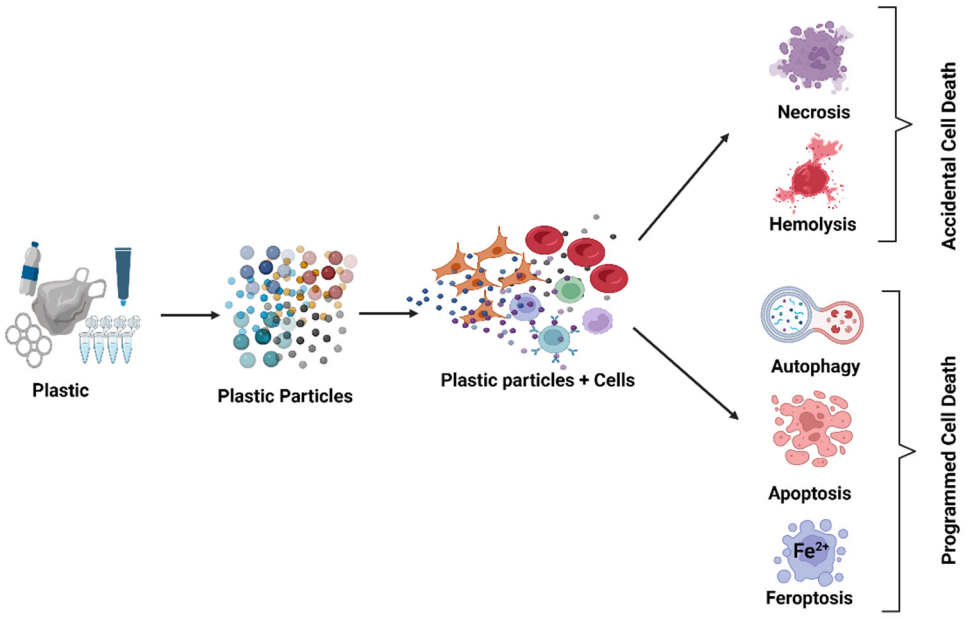

Figure 1. Plastic particles induce various kinds of cell death. Created with BioRender.com. Agreement number WY26OLGRVX on 10 April 2024.

3.1. Accidental Cell Death (ACD)

3.1.1. Necrosis Accidental Death in Nucleated Cells

Necrosis is a type of premature cell death resulting from autolytic processes. Necrosis is caused by the effect of various external factors, such as infection, trauma, or xenobiotics. Studies have examined the effect of PS-NPs on epidermal growth factor (EGF) in the human epithelial carcinoma cell line A431. The tested cells lost viability after treatment with PS-NPs or a combination of PS-NPs and EGF, which was attributed to PS-NP-induced cell death. The results also suggest that when used alone, PS-NPs became internalized in the cells and induced cell death by necrosis (Figure 1). In contrast, EGF accelerated the uptake ratio of PS-NPs, and PS-NPs in the cytoplasm, as well as with EGF-EGFR complexes; this may have inhibited the recycling of receptors, thus triggering apoptosis [52]. Without EGF, PS-NPs internalized to the cells by caveolin-mediated endocytosis, resulting in cell death by necrosis. Xia et al. [53] showed that NH_2-labeled PS nanospheres 60 nm in diameter were toxic to macrophage (RAW 264.7) and epithelial (BEAS-2B) cells. Whereas the death pathway in RAW 264.7 cells involved caspase activation, so the cytotoxic response in BEAS-2B cells was more necrotic. NH_2-PS in BEAS-2B were taken up by caveolae and their toxicity could be disrupted by cholesterol extraction from the surface membrane.

In summary, different cell-specific uptake mechanisms and pathways may increase sensitivity or resistance to particle toxicity.

3.1.2. Hemolysis, Accidental Death in Anucleated Cells

Hemolysis involves the rupture (lysis) of red blood cells (erythrocytes) and the release of their contents (cytoplasm) into the surrounding fluid (e.g., blood plasma).

Płuciennik et al. [54] reported that in vitro hemolysis of human erythrocytes induced by non-functionalized PS-NPs was influenced by NP size (Figure 1). It was noticed that the smallest NPs (30 nm) triggered the greatest alterations in the integrity of the cell membrane, i.e., the largest degree of hemolysis, which was likely related to their easy penetration into the tested cells. They also showed that particles with a higher absolute negative zeta potential (−42 mV) and larger size (~70 nm) demonstrated a lower cytotoxic effect (i.e., lower hemolysis) compared to smaller NPs (30 nm) with a lower negative zeta potential (−29.68 mV). It is likely that the smaller particles triggered greater hemolysis due to a higher number of unitary interactions with erythrocyte membranes.

Sarma et al. [55] studied the effect of 50 nm PS-NPs at concentrations from 500 to 2000 µg/mL on hemolysis in human erythrocytes. The highest level of hemolysis (93%) was observed at 2000 µg/mL, compared to 1000 µg/mL (15.3%), and 500 µg/mL (6.5%). In turn, Gopinath et al. [56] studied the effect of virgin, coronated and environmentally-released PS-NPs with a diameter of 100 nm in a slightly lower concentration range (1 to 25 µg/mL). They found that coronated NPs (with protein) at 5 µg/mL caused the highest rate of hemolysis (91%), followed by isolated NPs from facial peels (40%), and virgin NPs (22%). Hence, the coronation of the protein significantly affects the hemolytic activity of NPs, and isolated NPs may be contaminated with chemical additives that increase their toxicity.

Therefore, the induction of hemolysis increased with the concentration of the tested particles and was inversely proportional to their diameter. Additionally, the smallest PS-NPs, with the smallest absolute negative zeta potential, caused the strongest hemolysis. Moreover, the presence of proteins and impurities may increase the hemolytic effect of the particles (Table 2).

Table 2. Hemolysis in human erythrocytes incubated for 24 h with NPs/MPs, with regard to particle size, concentration, and zeta potential.

Type Particle/Size/Zeta Potential mV	Hemolytic Concentrations	Hemolysis [%]	References
PS-NPs in Ringer buffer			
~30 nm (−29.68 mV)	100 µg/mL	13.50%	[54]
~45 nm (−35.03 mV)	200 µg/mL	10.42%	
~70 nm (−42.00 mV)	200 µg/mL	9.31%	
PS-NPs in culture medium	500 µg/mL	6.5%	[55]
50 nm	1000 µg/mL	15.3%	
	2000 µg/mL	93%	
PS-NPs in PBS	5 µg/mL	22%	[56]
	7.5 µg/mL	36%	
PS-NPs with protein	5 µg/mL	91%	
	7.5 µg/mL	83%	
Isolated-NPs from face scrubs	5 µg/mL	40%	
100 nm	25 µg/mL	70%	

3.2. Programmed Cell Death (PCD)

3.2.1. Induction of Autophagy

Autophagy is a process activated in all cells in response to stress conditions, with the aim of maintaining the homeostasis of the cytoplasm, organelles, and proteins. The mechanism is based on the degradation of damaged or redundant cytoplasmic proteins or the elimination of the entire organelles. Although the process is designed to allow the cell to survive, it leads to cell death when pathological changes occur [57]. Studies on mammalian cell lines have found that the autophagy–lysosome pathway plays an important role in toxicity induced by NPs/MPs [28] (Figure 1). PS-NPs have been shown to cause accumulation of intracellular autophagosomes.

To detect autophagy in vitro, it is important to determine the expression of the LC3 protein, whose conjugated form, LC3-II, is involved in the formation of the autophagosomal membrane and/or disruption of autophagic flow. Indeed, several studies have examined effect of PS-NPs on the expression of this protein in mammalian cells. Annangi et al. [28] found an increase in the level of LC3-II protein in the presence of 50 nm and 500 nm PS-NPs, with the 50 nm particles being slightly more responsive than 500 nm, and chloroquine, an inhibitor of autophagosomal and lysosomal fusion. Xu et al. [45] observed an increase in LC3-II protein expression in both the RKO colon cancer cell line and normal intestinal epithelial cells (HIEC-6) exposed to 100 nm diameter PS-NPs; these findings, similarly to Annangi et al. [28], confirm that NPs that enter cells induce autophagy and autophagosome formation. Both studies found p62 protein to be degraded in the process of autophagy, but also that the level increased in

cells exposed to PS-NPs, indicating that autophagic flow was disrupted. Therefore, it can be concluded that PS-NPs have the potential to trigger autophagy.

Furthermore, studies on human bronchial epithelial BEAS-2B cells found three differently charged PS-MPs to induce autophagy by increasing the expression of the p62 and LC-3 proteins. The amount of autophagosome was also noted to increase as MPs entered the lysosome. The results also depended on particle charge; only positively-charged particles (NH_2-PS-MPs) triggered mechanisms that led to the initiation of different types of cell death. The results demonstrated that NH_2-PS-MPs induced autophagic cell death in bronchial epithelial cells, leading to inflammatory responses in the lungs [58].

A study by Lu et al. [59] examined the effects of NPs/MPs on human umbilical vein endothelial cells (HUVECs). The HUVECs were treated with unmodified NPs/MPs with diameters of 100 nm and 500 nm. Both sets of PS particles caused damage to the cell membrane, as indicated, among other things, by increased LDH release. However, the smaller particles also induced autophagosome formation, confirmed by the detection of LC3-I to LC3-II conversion. Lentivirus infection assay also showed impaired autophagic flow, as indicated by altered expression of the LAMP-2 and CTSB proteins.

Seca et al. [60] evaluated the impact of functionalized PS-NH_2 PS-NPs (30 nm) on OVCAR3 and OAW42 ovarian cancer cell lines. The results demonstrate progressive toxicity with incubation time, resulting in autophagy. The effect of these NPs on the autophagy process varied according to the cell line tested. Autophagy was observed in the OVCAR3 line, as evidenced by inter alia increased expression of LC3 and ATG4, and decreased levels of p62/SQSTM1, which was also confirmed by the conversion of LC3-I to LC3-II, as determined by Western blot. However, the process was inhibited in the OAW42 line, as indicated by a decrease in LC3 expression and the accumulation of undegraded p62, indicating impaired autophagosome formation.

In conclusion, the effect of the particles on autophagy depends on their size, with smaller particles causing a greater effect, as well as the degree of functionalization, with the amine group increasing autophagy. The type of target cell line also plays a role, with treatment inducing or inhibiting autophagy.

3.2.2. Induction of Apoptosis

Apoptosis is a crucial process implicated in hormone-dependent atrophy, embryonic development, the cell cycle, normal immune function, and cell death induced by xenobiotics [61]. Some research works indicate that PS-NPs interact with cell membranes, causing changes in their integrity, disrupting ion transport and signal transduction [54,62,63].

Several studies have found the effects of plastic NPs on apoptosis to depend on the size of the NPs and their concentration (Figure 1). Steckiewicz et al. [33] noted an increase in the expression of phosphatidylserine (a marker of apoptotic changes) on the surface of HT-29 colon adenocarcinoma cell lines incubated with PS-NPs-NH2 nanoparticles at 500 μg/mL. In contrast, Wang et al. [31] found smaller particles to induce apoptosis more effectively in CT26.WT colon cancer cells, noting a rise in apoptosis after treatment with small NPs (20 nm) at a concentration of 0.1 μg/mL, by larger NPs (80 nm) at 50 μg/mL, and by MPs (3 μm) at 100 μg/mL.

Similarly, Malinowska et al. [63] examined the impact of non-functionalized PS-NPs of 29 nm, 44 nm, and 72 nm in diameter on induction of apoptosis in PBMCs. All studied PS-NPs triggered apoptosis by the intrinsic pathway via a rise in cytosolic Ca^{2+} level, and a reduction in transmembrane mitochondrial potential and caspase-9 and -3 activation. Moreover, the smallest NPs (29 nm), activated caspase-8, confirming the induction of the extrinsic apoptotic pathway. The authors suggest that the smallest particles demonstrated the greatest potential to induce ROS generation. However, all tested PS-NPs increased ROS levels, induced protein damage and lipid peroxidation [17], and promoted damage to DNA [19]. It is probable that tested NPs triggered apoptosis by driving an increase in p53 levels, which is a DNA damage response (DDR) protein. DDR promotes apoptosis and prevents proliferation of abnormal cells. Indeed, p53 is a tumor suppressor protein that is crucial for controlling DNA damage.

P53 is able to trigger apoptosis by interacting with the apoptotic protein Bax, and block this process by the anti-apoptotic factor BCL2. Baran et al. [64] and Schmidt et al. [25] have revealed that acute exposure to PS nanoplastics and microplastics elevated the expression of the tumor suppressor protein p53 in mouse skin cells.

Hence, it appears that NPs/MPs activate both intrinsic (mitochondrial) and extrinsic apoptotic pathways. Smaller particles have a stronger apoptotic potential and activate both apoptotic pathways, which is probably due to the induction of ROS formation and p53 protein activation. This process also associated with the increase of NP/MP concentrations.

3.2.3. Induction of Ferroptosis

Ferroptosis is a type of iron-dependent planned cell death, characterized by lipid peroxidation, and is genetically and biochemically different from other forms of regulated cell death types [65]. It is caused by the failure of the glutathione-dependent antioxidant defense, leading to uncontrolled lipid peroxidation and cell death [66].

A study investigated ferroptosis in the BEAS-2B human lung bronchial epithelial cell line. Cells were treated for 24 h with 100 nm and 200 nm PS-NPs at concentrations from 100 μg/mL to 400 μg/mL [67]. It was observed that malondialdehyde, Fe^{2+}, and ROS levels were elevated, while the glutathione level decreased. Moreover, it was found that ferroptotic protein expression levels were substantially changed. The findings indicate that exposure to PS-NPs caused cell damage by ferroptosis (Figure 1).

Sun et al. [68] found that NPs of 44 nm in diameter entered microglial cells (BV2) and induced oxidative stress and inflammation reactions at 25–100 μg/mL. Based on ROS level, SOD activity and the levels of GSH, cell iron, and ferroptosis-related proteins, it was found that NPs compromised the antioxidative mechanisms of microglial (BV2) cells, increased intracellular lipid peroxidation and Fe^{2+} concentration, triggering inflammation reactions and ferroptosis. These changes were exacerbated at higher NP concentrations. Pretreatment with N-acetylcysteine, an ROS inhibitor, alleviated the induction of inflammatory reactions and cell ferroptosis. Furthermore, c Jun N terminal kinase (JNK) inhibition increased the expression of heme oxygenase (HO1), resulting in a reduction in ferroptosis, indicating that the signal pathway of JNK/HO1 was involved in the effects NPs induced on ferroptosis in BV2 cells.

Microplastic particles can also function as heavy metal (HMs) carriers, and this is accompanied by considerable health risk. Heavy metals and NPs/MPs are known to play important roles in ferroptosis. In recent years, cadmium (Cd), iron (Fe), arsenic (As), and copper (Cu), among others, have been proven to induce ferroptosis. MPs can function as carriers of HMs to aggravate damage to the body [69].

In summary, NPs/MPs appear to induce ferroptosis, and the process is intensified with the concentration of NPs/MPs.

4. Induction of Oxidative Stress by Plastic Particles

Most studies have shown that the deleterious effects of NPs/MPs are associated with ROS formation and oxidative stress induction. It is believed that the particles stimulate the production of ROS through an oxidative burst, and that the particles activate various cytokines. These, in turn, activate nicotinamide dinucleotide oxidase, resulting in changes in mitochondrial membrane potential and hence, alterations in mitochondrial function [50].

ROS are involved in many pathological processes, such as cellular aging and the immune response. A number of studies conducted on mammalian cell lines have found NPs/MPs to cause excessive production of intracellular ROS. This is most likely related to the effect of NPs/MPs on mitochondrial membrane potential. Annangi et al. [28] showed an increase in intracellular ROS production by PS-NPs of 50 nm and 500 nm in diameter in a nasal epithelial cell line (HNEpCs). Cells treated with PS-50 had a slightly elevated ROS level compared to those induced by PS-500, which could probably be attributed to greater cellular internalization and localization to different intracellular areas of the smaller particles. Also, Chen et al. [34] determined the effects of 10–100 μg/mL PS, PS-COOH, and

PS-NH_2 nanoparticles on a RAW 264.7 cell line. At the highest concentration, the negatively-charged NPs demonstrated a 1.3-fold increase in ROS level after six hours of incubation, relative to non-functionalized NPs. In contrast, the positively-charged PS-NH_2 particles exhibited 23-times greater ROS formation against non-functionalized particles at the same concentration (100 μg/mL). These studies show that functionalized NPs, especially the positivel-charged ones, have a much greater oxidative effect, probably resulting from the intensification of interactions occurring between their functional group and the cell and mitochondrial membrane.

In contrast, Shi et al. [48] examined the effects of a six-hour incubation with 80 nm and 2 μm NPs/MPs on A549 cells, at concentrations of 100, 200, and 400 μg/mL. The treatment with 80 nm NPs resulted in increased ROS production at each concentration; the production itself also increases with increasing concentration, being 1.64, 1.79, and 2.10-times greater than control values, depending on concentration. Incubation with 2 μm MPs increased to about 1.6-fold greater ROS production, but no correlation with concentration was noted. In the same study, using the fluorescence method, PS-NPs containing the amine group at 100 μg/mL were found to cause the strongest oxidative damage compared to non-functionalized PS-NPs and NPs containing the carboxyl group (PS-NP-COOH).

Poma et al. [70] examined the effect of NPs of 100 nm on induction of ROS in cells of the HS27 human fibroblast line. Depending on the incubation time, a concentration-dependent increase in ROS level was observed. A statistically significant increase in ROS level was noted after 15 min of incubation at 5 μg/mL, as well as after 30 min at 25 μg/mL, and after one hour at 50 μg/mL. However, ROS production was depleted to control values after 24 h, for which detoxification processes were responsible.

The effect of both NPs/MPs on ROS formation was also evaluated by Wang et al. [31]. The findings indicate that ROS production was inversely proportional to particle size, i.e., smaller particles caused greater ROS induction.

Rubio et al. [46] examined the induction of oxidative stress in various human hematopoietic cell lines using 50 nm PS-NPs at concentrations of 5–50 μg/mL after 3 h and 24 h of incubation. The results indicate that the time of exposure to the particles played an important role, as an increase in ROS level was associated with incubation time. After three hours, an increase in ROS was observed in TK-6i Raji-B cells at the highest concentration of tested NPs. In contrast, for the TK-6 line, an increase in ROS production was observed at all tested concentrations after 24 h. A differential response was also observed, depending on the cell line.

Shi et al. [49] also showed an increase in ROS production in cells exposed to PS-NPs and to UV radiation. Unaltered PS particles with regular shapes and a diameter of 100 nm induced lower ROS formation (1.68 and 1.91 times lower, respectively), compared to particles aged by UV for one month (UVPS1) and two months (UVPS2) at a concentration of 100 μg/mL. Compared to the untreated particles, the UV-treated particles had irregular shapes and smaller diameters.

Kik et al. [17] reported a significant increase in ROS level in PBMCs, as well as highly-reactive forms such as hydroxyl radicals, after incubation with 29 nm, 44 nm, and 72 nm PS-NPs. The smaller NPs increased ROS generation at 0.01 μg/mL and the largest (72 nm) at 0.1 μg/mL. The smallest NPs (29 nm) induced the formation of highly reactive species from a concentration of 1 μg/mL, and the other particles from a concentration of 10 μg/mL. Thus, the smallest NPs were able to induce the formation of ROS and highly reactive ROS at lower concentrations.

Since the increase in ROS level is accompanied by damage to cellular macromolecules, this research also assessed oxidative damage to proteins and lipids. They found that the particles enhanced lipid peroxidation and protein oxidation, again with the strongest changes detected in cells incubated with the smallest NPs (29 nm) [17].

Oxidative stress was also studied by Domenech et al. [71]. The study examined the effect of eight-week incubation with 50 nm NPs on human CaCo-2 intestinal cells, at concentrations of 0.0006, 0.26, 1.3 and 6.5 μg/mL. Another set of analyses were also

performed after 24 h incubation. The study examined the expression of antioxidant enzyme genes, i.e., HO1 encoding heme oxygenase, SOD2 encoding superoxide dismutase, GSTP1 encoding glutathione S-transferase, and HSP70 encoding heat shock proteins. No significant changes were observed after one day, but after eight weeks, significant abnormalities associated with increased expression of HO1 and SOD2 were shown. No differences were observed for the two other tested genes. These results showed that under long-term exposure, NPs were able to significantly alter the expression of genes associated with oxidative stress. Interestingly, this study showed no statistically significant changes in ROS production or oxidative DNA damage (Table 3).

Table 3. Oxidative effects of plastic particles in selected cell lines.

Cells/Time Incubation	Type, Particle Functionalization the Effect of UV	Concentration at Which Statistically Significant Changes in ROS Level Begin	Literature
	Size		
PBMCs 24 h	29 nm PS-NPs 44 nm PS-NPs 72 nm PS-NPs	0.01 µg/mL 0.01 µg/mL 0.1 µg/mL	[17]
HNEpCs 24 h	 50 nm PS-NPs 500 nm PSNPs	100 µg/mL Increase by 30% Increase by 22%	[28]
	Time incubation		
HCT116 15 min 1 h	100 nm PS-NPs	 400 µg/mL 100 µg/mL	[72]
Hs27 15 min 30 min 45 min	100 nm PS-NPs	5 µg/mL 5/25 µg/mL No changes	[69]
	Concentration		
RAW 264.7 24 h	100 nm PS-NH_2 10 µg/mL 20 µg/mL 50 µg/mL 100 µg/mL	 Increase by 51% Increase by 135% Increase by 276% Increase by 2610%	[34]
PBMCs 24 h	29 nm PS-NPs 0.1 µg/mL	 Increase by 27%	[17]
	1 µg/mL 10 µg/mL	Increase by 37% Increase by 46%	
	Functionalization		
Lung cancer cells A549 6 h	80 nm PS-NPs 80 nm PS-COOH 80 nm PS-NH_2	100 µg/mL 200 µg/mL 400 µg/mL	[48]
RAW 264.7 24 h	 100 nm PS -NPs 100 nm PS-COOH 100 nm PS-NH_2	100 µg/mL Increase by 22% Increase by 45% Increase by 2610%	[34]
	Cell type		
THP-1 Raji-B/TK6 3 h THP-1/Raji-B TK6 24 h	50 nm PS-NPs	No effects 50 µg/mL No effects 5 µg/mL	[46]
	UV radiation		
A549 24 h	50 nm PS-NPs UVPS1 UVPS1	No effects 100 µg/mL 50 µg/mL	[49]

He et al. [27] examined antioxidant enzyme activity in HepG2 cells after 48 h incubation with 50 nm PS-NPs at concentrations of 10–100 μg/mL. The NPs used in this study were both non-functionalized (PS-NPs), and those containing an amine (PS-NH_2) or carboxyl (PS-COOH) group. The cells exposed to the NPs at 10 μg/mL demonstrated 1.68 times greater SOD activity compared to control for non-functionalized nanoparticles, and 1.8 times for PS-COOH nanoparticles, but no such effect was observed for PS-NH_2 particles. However, for all particles, SOD activity decreased as the concentration of PS-NPs increased. In addition, reduced glutathione (GSH) levels increased in cells exposed to all tested NPs at concentrations of 10–50 μg/mL; however, no increase in GSH level was noted at 100 μg/mL, which may indicate inhibition of detoxification processes. The largest decrease was observed for PS-NH_2.

Vecchiotti et al. [72] determined the level of ROS in cells of the colon cancer line HCT-116 exposed to 100 nm PS-NPs at concentrations of 100–1200 μg/mL. The greatest increase in ROS production was observed at 400 μg/mL and 800 μg/mL after 45 min of incubation; however, at lower concentrations (100 μg/mL and 200 μg/mL), an increase was noticed only after 60 min exposure, Thus, ROS induction was dependent on the concentration and incubation time of the cells with PS particles.

In summary, smaller plastic particles elicited greater oxidative changes in the cells. Also, oxidation processes generally increased with the applied concentration, as well as incubation time and exposure to UV radiation. However, the levels of ROS and some antioxidant markers may decrease due to the activation of detoxification processes. The presence of an amino group (positively charged) and then a carboxyl group intensifies the oxidative properties of NPs/MPs compared to those of non-functionalized NPs.

5. Genotoxic Effects of Plastic Particles

As DNA damage is a key marker of the toxic effects of xenobiotics, the review will also examine the genotoxic effects of NPs/MPs observed in in vitro studies. DNA is the storage site for genetic information. However, DNA is constantly exposed to damage through various endogenous and exogenous sources, presenting a major threat to genome stability and human health [73]. Exposure to carcinogens is associated with various forms of DNA damage, such as single-stand breaks, double-strand breaks, covalently-bound chemical DNA adducts, oxidative-induced lesions, and DNA–DNA or DNA–protein cross-links [74]. Our findings indicate that exposure to NPs/MPs can induce various changes in DNA (Figure 2). An increase in the level of micronuclei (MN) was also observed in various cell lines incubated with PS-NPs [70–72].

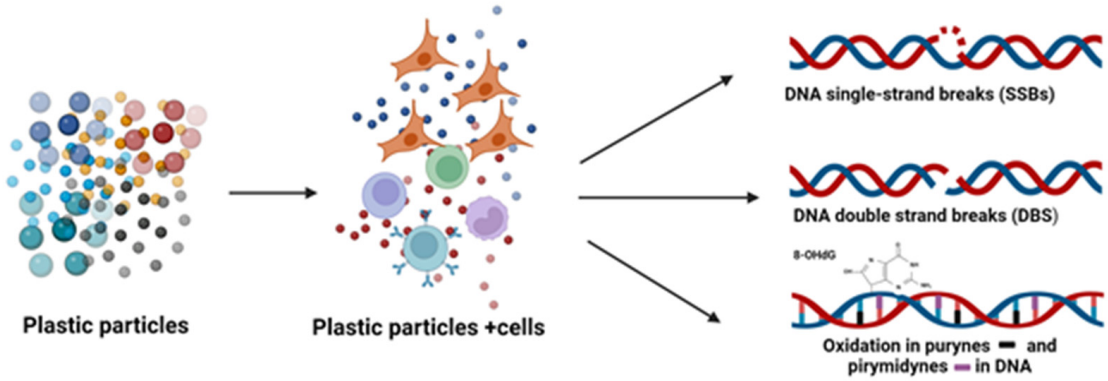

Figure 2. Plastic particles induce various forms of DNA damage. Created with BioRender.com. Agreement number IO26L11V2Z on 16 March 2024.

5.1. Single- and Double-Stranded DNA Breaks Induced by Plastic Particles

The most common type of damage is the occurrence of DNA single-strand breaks (SSBs) [73]. More than 10,000 such breaks occur in each mammalian cell every day. They involve disconnection of one of the DNA double strands, accompanied by damage or

mismatching of the 5′ or 3′ ends of the DNA or loss of single nucleotides [75]. SSBs can arise from oxidized nucleotides/nitrogen bases, disrupted cellular enzyme activity, and as intermediates of DNA repair pathways. They can also be promoted by oxidative stress, which arises from an imbalance in the production of ROS, including hydroxyl radical and hydrogen peroxide and antioxidants [73].

Unrepaired SSBs can cause DNA replication stress and inhibit transcription [75], induce chromosomal mutations, chromosomal aberrations, genome instability [75], and cell death [73]. When SSBs are not repaired, they can develop into double-strand breaks (DSBs), which are more harmful [75]. This type of damage can be induced by endogenous factors, including replication processes, e.g., when replication forks are blocked or halted, or the repair of oxidized DNA nitrogen bases is incorrect [76]. Damage to DNA also proceeds as a result of action of exogenous factors, such as various chemicals [76,77]. DSBs often become terminal lesions caused by various genotoxic agents, which, when not repaired, become the basis for genomic instability [76].

One study examined the effect of 24 h exposure to 29 nm, 44 nm, and 72 nm PS-NPs on DNA breakage in human PBMCs at concentrations of 0.0001 to 100 μg/mL. It was found that all PS-NPs induced DNA damage. The 29 nm NPs caused significant changes in DNA integrity from a concentration of 0.01 μg/mL, the 44 nm NPs from a concentration of 0.1 μg/mL, and the 72 nm NPs from 10 mg/mL. However, only the 29 nm and 44 nm NPs induced DNA DSB formation, the largest NPs did not cause such changes. It is noteworthy that the observed damage caused by the 44 nm and 72 nm NPs was completely repaired after 120 min, while the repair was not fully effective for the smaller particles (29 nm) [19]. The results indicate that the smallest tested non-functionalized PS-NPs, i.e., with a diameter of 29 nm, were the most genotoxic.

The effects of NPs on human white blood cells present in whole blood were also investigated. Whole blood from healthy donors was exposed for 72 h to NPs with diameters of 40–100 nm and at concentrations of 50 μg/mL and 100 μg/mL. Different groups of leukocytes demonstrated genotoxic effects: lymphocytes did not suffer DNA damage, monocytes showed a significant increase in DNA breaks (100 μg/mL of NPs), while granulocytes showed a significantly increase in DNA damage at both tested NP concentrations [78] (Table 2).

5.2. DNA Bases Damage Induced by Plastic Particles

The detection of oxidative DNA damage (ODD) involves oxidation of purines and pyrimidines; as such, the most important biomarkers of DNA oxidation are oxidized deoxyguanosine and guanine products. One such product is 8-oxo-2′-deoxyguanosine (8-oxodG), a highly-mutagenic and widely-studied compound formed by ODD. It erroneously binds to adenine during DNA replication, resulting in a spontaneous mutation from the guanine–cytosine pair to adenine–thymine [19].

Malinowska et al. [19] examined the formation of oxidized purine bases in PBMCs after treatment with PS-NPs. The highest degree of oxidation was achieved by the smallest particles (29 nm) at the lowest concentrations (0.1 μg/mL and above), while the 44 nm and 72 nm particles increased oxidation at concentrations of 10 μg/mL and 100 μg/mL, respectively. The levels of oxidized pyrimidines also increased at higher NP concentrations. The treatment also increased 8-oxodG levels, but only after exposure to the smallest (29 nm) particles. Purines demonstrated significantly greater damage than pyrimidines, with the most significant changes observed in purines exposed to the smallest NPs, which correlated with the production of 8-oxodG and DSBs (Table 4).

Table 4. Genotoxic effects of plastic particles in selected cell lines.

Cells/Incubation Time	Type and Size of Particles	Genotoxic Concentrations	Observed Changes	Literature
Hs-27/48 h	100 nm PS	25–75 μg/mL	Increase in MN	[70]
Caco-2/8 weeks	50 nm PS	800–1200 μg/mL	Increase in MN	[71]
HCT116/48 h	100 nm PS	800–1200 μg/mL	Increase in MN	[72]
PBMCs/24 h	29 nm PS 44 nm PS 72 nm PS 29 nm PS	0.01–100 μg/mL 0.1–100 μg/mL 10–100 μg/mL 0.1–100 μg/mL	SSBs and DSBs formation, oxidation of pyrimidine and purine bases, 8-oxodG formation	[19]
Raji-B/24 h TK6 THP1	50 nm PS	25–50 μg/mL 50 μg/mL 5–50 μg/mL No effects	Genotoxicity Oxidative DNA damage Oxidative DNA damage No effects	[46]
Monocytes/72 h Granulocytes Lymphocytes	40–100 nm PS	100 μg/mL 50–100 μg/mL No effects	DNA damage	[78]

Rubio et al. [46] reported general genotoxic damage, as well as specific oxidative damage to DNA, in TK-6 human lymphoblastic cells (lymphoblasts), RajiB (B lymphocytes), and THP-1 (monocytes) exposed to 50 nm PS particles at concentrations of 5–50 μg/mL. The RajiB line demonstrated general genotoxicity at 25 μg/mL and 50 μg/mL, and oxidative DNA damage after 24 h incubation at 50 μg/mL. Oxidative DNA damage was also noted for the TK-6 line at all tested concentrations.

Soto-Bielicka et al. [79] studied the effect of combined exposure to NPs and tetrabromobisphenol A (TBBPA), a flame-retardant additive, on fish cell lines. Within 24 h, a significant increase in oxidative DNA damage was noted after joint exposure to 10 μg/mL NPs and 25 μM TBBPA, but not after exposure to TBBPA alone. Thus, it can be concluded that NPs/MPs can enhance the harmful effects of xenobiotics.

The studies presented above indicate that NPs can induce ROS production in cells and living organisms, and that this may result in oxidative damage to DNA.

Hence, it can be concluded that genotoxic effects of NPs/MPs on cellular models depend on the same factors as the oxidative and cytotoxic effects. Smaller plastic particles elicit greater changes in DNA damage, and NPs/MPs cause significantly higher DNA damage when administered at higher concentrations with longer incubation times, and when the particles have functional groups (Table 4).

6. Conclusions

Concerns about the possible negative effects of chronic human exposure to NPs/MPs continue to grow, particularly the potential threat from NPs [72]. A number of studies have shown that NPs/MPs can be toxic to cells and, consequently, living organisms.

The toxicity of MPs and NPs depends on their size, concentration, zeta potential, exposure time, functionalization, the influence of environmental factors, and the target cell type (Figure 3). In vitro studies have shown that smaller particles are more toxic to cells than those of larger sizes [80]. Smaller NPs can penetrate cells more easily and have a larger surface area relative to their volume, which has a significant impact on their reactivity. Indeed, smaller particles are more cytotoxic, cause ROS formation, and induce oxidative damage to lipids, proteins, and DNA. The toxic effect of particles is also enhanced by their functionalization. In such cases, cationic particles are generally more toxic than anionic NPs, probably because of their greater cellular uptake and their deleterious effects on cells and lysosomal membranes. Also, NPs with positive zeta potential are more toxic than those with a negative zeta potential, probably due to their stronger interaction with the cell membrane.

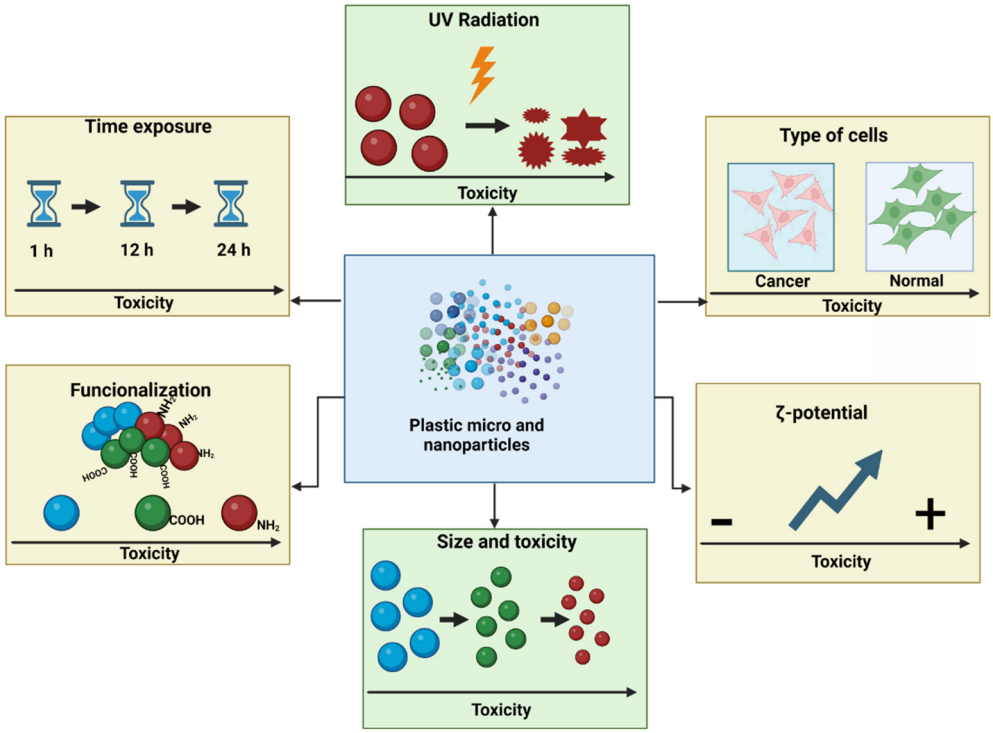

Figure 3. The influence of various factors on the toxicity of plastic particles. Created with BioRender.com. Agreement number AO26L13F22 on 16 March 2024.

The cytotoxic effect of NPs/MPs also increases with their concentration and duration of action. In addition, UV radiation can enhance toxicity by shrinking NPs/MPs and altering their shape; this is an important consideration in in vitro studies, which generally use commercial particles that are spherical, thus they do not reflect the irregular shape of particles found in the environment.

Studies conducted on three leukocyte cell lines indicate that the harmful effects of PS vary from cell line to cell line. Also, the toxicity of NPs/MPs varies between normal and cancer cells. Exposure to plastic particles, widespread in the environment, can pose a potential health risk. Many of these factors can intensify the toxic and potential genotoxic effects of NPs/MPs.

In vitro toxicity tests allowed the mechanism of action of plastic particles to be determined at the cellular level, which is an important indication of their potential harmful effects on human health. In vitro studies offer controlled laboratory conditions, speed, and relatively low cost, as well as ease of repetition and elimination of animal suffering, in accordance with the 3R principle and alternative methods. They can also indicate starting points for assessing toxicity in animal tests and determining safe exposure levels for people. However, such studies fail to consider cellular interactions and system-wide metabolism, and it can be difficult to extrapolate the results to in vivo systems.

The in vitro testing described herein clearly indicates that size, zeta potential, exposure time, concentration, functionalization, environmental factors, and target cell type should be taken into account when assessing the toxicity of plastic particles. The findings can be used in epidemiological studies.

Future studies of the effects of plastic particles in human tissues should therefore concern not only their concentration, but also their size, shape and, if possible, their functionalization. Only such holistic assessment can allow a reliable estimate of the risk of exposure to these particles.

The in vitro test results indicated that exposure may also result in DNA damage, with the effects also modulated by the above factors. These should be taken into account in further epidemiological studies, to assess their impact on human health (e.g., carcinogenicity).

Exposure to MPs/NPs is commonly associated with a decrease in metabolic activity and changes in mitochondrial potential [63], characteristic of mitochondrial damage. It is widely believed that this is the route by which NP/MP particles can induce ROS production and DNA damage. As such, it would worth conducting more in-depth research on the changes in the functioning of mitochondria and its proteins after exposure to plastic particles, as well as the formation of ATP.

While numerous studies have examined specific types of cell death in nucleated cells or the combined decline in viability and metabolic activity under the influence of MPs/NPs, few have addressed the effect on necrosis. As such, the role of necrosis in cell death induced by MPs/NPs remains unclear.

Our analysis also highlights the important role played by environmental factors such as UV radiation in enhancing the toxicity of NPs/MPs. The research carried out so far indicates an increase in the toxicity of plastic particles exposed to ultraviolet radiation, including solar radiation.

There is also no comparison of the toxicity to cells and organisms of NPs/MPs from various plastics, such as HDPE, LDPE, PVC, PS, PP, and PET, with the same physical parameters, e.g., diameter. Again, such considerations play an important role in the effect of plastic contamination on organisms following environmental exposure.

Author Contributions: Conceptualization, B.B. and K.P.; writing—original draft preparation, K.P., B.B., W.M. and P.S.; writing—review and editing, B.B. and K.P.; visualization, K.P. and B.B. All authors have read and agreed to the published version of the manuscript.

Funding: This work was funded by Research granted (B2011000000191.01) to the Department of Biophysics of Environmental Pollution, Faculty of Biology and Environmental Protection, University of Lodz.

Data Availability Statement: Not applicable.

Conflicts of Interest: The authors declare no conflicts of interest.

References

1. Plastics Europe Plastics—The Fast Facts 2023. 2023. Available online: https://plasticseurope.org/knowledge-hub/plastics-the-fast-facts-2023/ (accessed on 1 March 2024).
2. Fan, P.; Yu, H.; Xi, B.; Tan, W. A Review on the Occurrence and Influence of Biodegradable Microplastics in Soil Ecosystems: Are Biodegradable Plastics Substitute or Threat? *Environ. Int.* **2022**, *163*, 107244. [CrossRef] [PubMed]
3. Gigault, J.; Halle, A.T.; Baudrimont, M.; Pascal, P.-Y.; Gauffre, F.; Phi, T.-L.; El Hadri, H.; Grassl, B.; Reynaud, S. Current Opinion: What Is a Nanoplastic? *Environ. Pollut.* **2018**, *235*, 1030–1034. [CrossRef] [PubMed]
4. Lithner, D.; Larsson, Å.; Dave, G. Environmental and Health Hazard Ranking and Assessment of Plastic Polymers Based on Chemical Composition. *Sci. Total Environ.* **2011**, *409*, 3309–3324. [CrossRef] [PubMed]
5. Grote, K.; Brüstle, F.; Vlacil, A.-K. Cellular and Systemic Effects of Micro- and Nanoplastics in Mammals—What We Know So Far. *Materials* **2023**, *16*, 3123. [CrossRef] [PubMed]
6. Mattsson, K.; Hansson, L.-A.; Cedervall, T. Nano-Plastics in the Aquatic Environment. *Environ. Sci. Process. Impacts* **2015**, *17*, 1712–1721. [CrossRef] [PubMed]
7. Chae, Y.; Kim, D.; Kim, S.W.; An, Y.-J. Trophic Transfer and Individual Impact of Nano-Sized Polystyrene in a Four-Species Freshwater Food Chain. *Sci. Rep.* **2018**, *8*, 284. [CrossRef] [PubMed]
8. Costa, E.; Piazza, V.; Lavorano, S.; Faimali, M.; Garaventa, F.; Gambardella, C. Trophic Transfer of Microplastics From Copepods to Jellyfish in the Marine Environment. *Front. Environ. Sci.* **2020**, *8*, 571732. [CrossRef]
9. Schwabl, P.; Köppel, S.; Königshofer, P.; Bucsics, T.; Trauner, M.; Reiberger, T.; Liebmann, B. Detection of Various Microplastics in Human Stool: A Prospective Case Series. *Ann. Intern. Med.* **2019**, *171*, 453–457. [CrossRef] [PubMed]
10. Pironti, C.; Notarstefano, V.; Ricciardi, M.; Motta, O.; Giorgini, E.; Montano, L. First Evidence of Microplastics in Human Urine, a Preliminary Study of Intake in the Human Body. *Toxics* **2022**, *11*, 40. [CrossRef]
11. Huang, S.; Huang, X.; Bi, R.; Guo, Q.; Yu, X.; Zeng, Q.; Huang, Z.; Liu, T.; Wu, H.; Chen, Y.; et al. Detection and Analysis of Microplastics in Human Sputum. *Environ. Sci. Technol.* **2022**, *56*, 2476–2486. [CrossRef]
12. Jenner, L.C.; Rotchell, J.M.; Bennett, R.T.; Cowen, M.; Tentzeris, V.; Sadofsky, L.R. Detection of Microplastics in Human Lung Tissue Using MFTIR Spectroscopy. *Sci. Total Environ.* **2022**, *831*, 154907. [CrossRef]
13. Zhao, Q.; Zhu, L.; Weng, J.; Jin, Z.; Cao, Y.; Jiang, H.; Zhang, Z. Detection and Characterization of Microplastics in the Human Testis and Semen. *Sci. Total Environ.* **2023**, *877*, 162713. [CrossRef]

14. Leslie, H.A.; van Velzen, M.J.M.; Brandsma, S.H.; Vethaak, A.D.; Garcia-Vallejo, J.J.; Lamoree, M.H. Discovery and Quantification of Plastic Particle Pollution in Human Blood. *Environ. Int.* **2022**, *163*, 107199. [CrossRef]
15. Cetin, M.; Demirkaya Miloglu, F.; Kilic Baygutalp, N.; Ceylan, O.; Yildirim, S.; Eser, G.; Gul, H.İ. Higher Number of Microplastics in Tumoral Colon Tissues from Patients with Colorectal Adenocarcinoma. *Environ. Chem. Lett.* **2023**, *21*, 639–646. [CrossRef]
16. Salvia, R.; Rico, L.G.; Bradford, J.A.; Ward, M.D.; Olszowy, M.W.; Martínez, C.; Madrid-Aris, Á.D.; Grífols, J.R.; Ancochea, Á.; Gomez-Muñoz, L.; et al. Fast-Screening Flow Cytometry Method for Detecting Nanoplastics in Human Peripheral Blood. *MethodsX* **2023**, *10*, 102057. [CrossRef]
17. Kik, K.; Bukowska, B.; Krokosz, A.; Sicińska, P. Oxidative Properties of Polystyrene Nanoparticles with Different Diameters in Human Peripheral Blood Mononuclear Cells (In Vitro Study). *Int. J. Mol. Sci.* **2021**, *22*, 4406. [CrossRef]
18. Guševac Stojanović, I.; Drakulić, D.; Todorović, A.; Martinović, J.; Filipović, N.; Stojanović, Z. Acute Toxicity Assessment of Orally Administered Microplastic Particles in Adult Male Wistar Rats. *Toxics* **2024**, *12*, 167. [CrossRef] [PubMed]
19. Malinowska, K.; Bukowska, B.; Piwoński, I.; Foksiński, M.; Kisielewska, A.; Zarakowska, E.; Gackowski, D.; Sicińska, P. Polystyrene Nanoparticles: The Mechanism of Their Genotoxicity in Human Peripheral Blood Mononuclear Cells. *Nanotoxicology* **2022**, *16*, 791–811. [CrossRef] [PubMed]
20. Yin, K.; Wang, D.; Zhang, Y.; Lu, H.; Hou, L.; Guo, T.; Zhao, H.; Xing, M. Polystyrene Microplastics Promote Liver Inflammation by Inducing the Formation of Macrophages Extracellular Traps. *J. Hazard. Mater.* **2023**, *452*, 131236. [CrossRef]
21. Prüst, M.; Meijer, J.; Westerink, R.H.S. The Plastic Brain: Neurotoxicity of Micro- and Nanoplastics. *Part. Fibre Toxicol.* **2020**, *17*, 24. [CrossRef]
22. Zhao, B.; Rehati, P.; Yang, Z.; Cai, Z.; Guo, C.; Li, Y. The Potential Toxicity of Microplastics on Human Health. *Sci. Total Environ.* **2024**, *912*, 168946. [CrossRef]
23. González-Caballero, M.C.; De Alba González, M.; Torres-Ruiz, M.; Iglesias-Hernández, P.; Zapata, V.; Terrón, M.C.; Sachse, M.; Morales, M.; Martin-Folgar, R.; Liste, I.; et al. Internalization and Toxicity of Polystyrene Nanoplastics on Inmortalized Human Neural Stem Cells. *Chemosphere* **2024**, *355*, 141815. [CrossRef]
24. Cortés, C.; Domenech, J.; Salazar, M.; Pastor, S.; Marcos, R.; Hernández, A. Nanoplastics as a Potential Environmental Health Factor: Effects of Polystyrene Nanoparticles on Human Intestinal Epithelial Caco-2 Cells. *Environ. Sci. Nano* **2020**, *7*, 272–285. [CrossRef]
25. Schmidt, A.; Da Silva Brito, W.A.; Singer, D.; Mühl, M.; Berner, J.; Saadati, F.; Wolff, C.; Miebach, L.; Wende, K.; Bekeschus, S. Short- and Long-Term Polystyrene Nano- and Microplastic Exposure Promotes Oxidative Stress and Divergently Affects Skin Cell Architecture and Wnt/Beta-Catenin Signaling. *Part. Fibre Toxicol.* **2023**, *20*, 3. [CrossRef]
26. Visalli, G.; Facciolà, A.; Pruiti Ciarello, M.; De Marco, G.; Maisano, M.; Di Pietro, A. Acute and Sub-Chronic Effects of Microplastics (3 and 10 Mm) on the Human Intestinal Cells HT-29. *Int. J. Environ. Res. Public Health* **2021**, *18*, 5833. [CrossRef]
27. He, Y.; Li, J.; Chen, J.; Miao, X.; Li, G.; He, Q.; Xu, H.; Li, H.; Wei, Y. Cytotoxic Effects of Polystyrene Nanoplastics with Different Surface Functionalization on Human HepG2 Cells. *Sci. Total Environ.* **2020**, *723*, 138180. [CrossRef] [PubMed]
28. Annangi, B.; Villacorta, A.; López-Mesas, M.; Fuentes-Cebrian, V.; Marcos, R.; Hernández, A. Hazard Assessment of Polystyrene Nanoplastics in Primary Human Nasal Epithelial Cells, Focusing on the Autophagic Effects. *Biomolecules* **2023**, *13*, 220. [CrossRef]
29. Duffus, J.H.; Nordberg, M.; Templeton, D.M. Glossary of Terms Used in Toxicology, 2nd Edition (IUPAC Recommendations 2007). *Pure Appl. Chem.* **2007**, *79*, 1153–1344. [CrossRef]
30. Yan, L.; Yu, Z.; Lin, P.; Qiu, S.; He, L.; Wu, Z.; Ma, L.; Gu, Y.; He, L.; Dai, Z.; et al. Polystyrene Nanoplastics Promote the Apoptosis in Caco-2 Cells Induced by Okadaic Acid More than Microplastics. *Ecotoxicol. Environ. Saf.* **2023**, *249*, 114375. [CrossRef]
31. Wang, X.; Ren, X.; Hu, H.; Zhang, P.; Zhao, F.; Zhang, L.; He, H.; Huang, B.; Pan, X. Micro- and Nano- Polystyrene Plastic Particles Induce Apoptosis Through the Production of Intracellular ROS on CT26.WT Cells. *SSRN J.* **2022**. [CrossRef]
32. Mattioda, V.; Benedetti, V.; Tessarolo, C.; Oberto, F.; Favole, A.; Gallo, M.; Martelli, W.; Crescio, M.I.; Berio, E.; Masoero, L.; et al. Pro-Inflammatory and Cytotoxic Effects of Polystyrene Microplastics on Human and Murine Intestinal Cell Lines. *Biomolecules* **2023**, *13*, 140. [CrossRef] [PubMed]
33. Steckiewicz, K.P.; Adamska, A.; Narajczyk, M.; Megiel, E.; Inkielewicz—Stepniak, I. Fluoride Enhances Polystyrene Nanoparticles Cytotoxicity in Colonocytes in Vitro Model. *Chem. Biol. Interact.* **2022**, *367*, 110169. [CrossRef]
34. Chen, J.; Xu, Z.; Liu, Y.; Mei, A.; Wang, X.; Shi, Q. Cellular Absorption of Polystyrene Nanoplastics with Different Surface Functionalization and the Toxicity to RAW264.7 Macrophage Cells. *Ecotoxicol. Environ. Saf.* **2023**, *252*, 114574. [CrossRef]
35. Jiang, Y.; Huo, S.; Mizuhara, T.; Das, R.; Lee, Y.-W.; Hou, S.; Moyano, D.F.; Duncan, B.; Liang, X.-J.; Rotello, V.M. The Interplay of Size and Surface Functionality on the Cellular Uptake of Sub-10 Nm Gold Nanoparticles. *ACS Nano* **2015**, *9*, 9986–9993. [CrossRef] [PubMed]
36. Weiss, M.; Fan, J.; Claudel, M.; Sonntag, T.; Didier, P.; Ronzani, C.; Lebeau, L.; Pons, F. Density of Surface Charge Is a More Predictive Factor of the Toxicity of Cationic Carbon Nanoparticles than Zeta Potential. *J. Nanobiotechnol* **2021**, *19*, 5. [CrossRef] [PubMed]
37. Zhang, H.; Wei, X.; Liu, L.; Zhang, Q.; Jiang, W. The Role of Positively Charged Sites in the Interaction between Model Cell Membranes and γ-Fe_2O_3 NPs. *Sci. Total Environ.* **2019**, *673*, 414–423. [CrossRef] [PubMed]
38. Wang, F.; Salvati, A.; Boya, P. Lysosome-Dependent Cell Death and Deregulated Autophagy Induced by Amine-Modified Polystyrene Nanoparticles. *Open Biol.* **2018**, *8*, 170271. [CrossRef] [PubMed]

39. Halimu, G.; Zhang, Q.; Liu, L.; Zhang, Z.; Wang, X.; Gu, W.; Zhang, B.; Dai, Y.; Zhang, H.; Zhang, C.; et al. Toxic Effects of Nanoplastics with Different Sizes and Surface Charges on Epithelial-to-Mesenchymal Transition in A549 Cells and the Potential Toxicological Mechanism. *J. Hazard. Mater.* **2022**, *430*, 128485. [CrossRef] [PubMed]
40. Li, Y.; Xu, M.; Zhang, Z.; Halimu, G.; Li, Y.; Li, Y.; Gu, W.; Zhang, B.; Wang, X. In Vitro Study on the Toxicity of Nanoplastics with Different Charges to Murine Splenic Lymphocytes. *J. Hazard. Mater.* **2022**, *424*, 127508. [CrossRef]
41. Shao, X.; Wei, X.; Song, X.; Hao, L.; Cai, X.; Zhang, Z.; Peng, Q.; Lin, Y. Independent Effect of Polymeric Nanoparticle Zeta Potential/Surface Charge, on Their Cytotoxicity and Affinity to Cells. *Cell Prolif.* **2015**, *48*, 465–474. [CrossRef]
42. Honary, S.; Zahir, F. Effect of Zeta Potential on the Properties of Nano-Drug Delivery Systems—A Review (Part 1). *Trop. J. Pharm. Res.* **2013**, *12*, 255–264. [CrossRef]
43. Zhang, S.; Li, J.; Lykotrafitis, G.; Bao, G.; Suresh, S. Size-Dependent Endocytosis of Nanoparticles. *Adv. Mater.* **2009**, *21*, 419–424. [CrossRef] [PubMed]
44. Schwegmann, H.; Feitz, A.J.; Frimmel, F.H. Influence of the Zeta Potential on the Sorption and Toxicity of Iron Oxide Nanoparticles on S. Cerevisiae and E. Coli. *J. Colloid Interface Sci.* **2010**, *347*, 43–48. [CrossRef] [PubMed]
45. Xu, X.; Feng, Y.; Han, C.; Yao, Z.; Liu, Y.; Luo, C.; Sheng, J. Autophagic Response of Intestinal Epithelial Cells Exposed to Polystyrene Nanoplastics. *Environ. Toxicol.* **2023**, *38*, 205–215. [CrossRef] [PubMed]
46. Rubio, L.; Barguilla, I.; Domenech, J.; Marcos, R.; Hernández, A. Biological Effects, Including Oxidative Stress and Genotoxic Damage, of Polystyrene Nanoparticles in Different Human Hematopoietic Cell Lines. *J. Hazard. Mater.* **2020**, *398*, 122900. [CrossRef] [PubMed]
47. Lins, T.F.; O'Brien, A.M.; Kose, T.; Rochman, C.M.; Sinton, D. Toxicity of Nanoplastics to Zooplankton Is Influenced by Temperature, Salinity, and Natural Particulate Matter. *Environ. Sci. Nano* **2022**, *9*, 2678–2690. [CrossRef]
48. Shi, X.; Wang, X.; Huang, R.; Tang, C.; Hu, C.; Ning, P.; Wang, F. Cytotoxicity and Genotoxicity of Polystyrene Micro- and Nanoplastics with Different Size and Surface Modification in A549 Cells. *Int. J. Nanomed.* **2022**, *17*, 4509–4523. [CrossRef]
49. Shi, Q.; Tang, J.; Liu, X.; Liu, R. Ultraviolet-Induced Photodegradation Elevated the Toxicity of Polystyrene Nanoplastics on Human Lung Epithelial A549 Cells. *Environ. Sci. Nano* **2021**, *8*, 2660–2675. [CrossRef]
50. Sun, N.; Shi, H.; Li, X.; Gao, C.; Liu, R. Combined Toxicity of Micro/Nanoplastics Loaded with Environmental Pollutants to Organisms and Cells: Role, Effects, and Mechanism. *Environ. Int.* **2023**, *171*, 107711. [CrossRef]
51. Tang, D.; Kang, R.; Berghe, T.V.; Vandenabeele, P.; Kroemer, G. The Molecular Machinery of Regulated Cell Death. *Cell Res.* **2019**, *29*, 347–364. [CrossRef]
52. Phuc, L.T.M.; Taniguchi, A. Polystyrene Nanoparticles Induce Apoptosis or Necrosis With or Without Epidermal Growth Factor. *J. Nanosci. Nanotechnol.* **2019**, *19*, 4812–4817. [CrossRef] [PubMed]
53. Xia, T.; Kovochich, M.; Liong, M.; Zink, J.I.; Nel, A.E. Cationic Polystyrene Nanosphere Toxicity Depends on Cell-Specific Endocytic and Mitochondrial Injury Pathways. *ACS Nano* **2008**, *2*, 85–96. [CrossRef] [PubMed]
54. Płuciennik, K.; Sicińska, P.; Duchnowicz, P.; Bonarska-Kujawa, D.; Męczarska, K.; Solarska-Ściuk, K.; Miłowska, K.; Bukowska, B. The Effects of Non-Functionalized Polystyrene Nanoparticles with Different Diameters on Human Erythrocyte Membrane and Morphology. *Toxicol. Vitr.* **2023**, *91*, 105634. [CrossRef]
55. Sarma, D.K.; Dubey, R.; Samarth, R.M.; Shubham, S.; Chowdhury, P.; Kumawat, M.; Verma, V.; Tiwari, R.R.; Kumar, M. The Biological Effects of Polystyrene Nanoplastics on Human Peripheral Blood Lymphocytes. *Nanomaterials* **2022**, *12*, 1632. [CrossRef] [PubMed]
56. Gopinath, P.M.; Saranya, V.; Vijayakumar, S.; Mythili Meera, M.; Ruprekha, S.; Kunal, R.; Pranay, A.; Thomas, J.; Mukherjee, A.; Chandrasekaran, N. Assessment on Interactive Prospectives of Nanoplastics with Plasma Proteins and the Toxicological Impacts of Virgin, Coronated and Environmentally Released-Nanoplastics. *Sci. Rep.* **2019**, *9*, 8860. [CrossRef] [PubMed]
57. Rudnicka, K.; Szczesna, E.; Mnich, E.; Mikolajczyk-Chmiela, M. Apoptosis and autophagy—Mechanisms and detection methods. *Postep. Biol. Komorki* **2011**, *38*, 247–265.
58. Jeon, M.S.; Kim, J.W.; Han, Y.B.; Jeong, M.H.; Kim, H.R.; Sik Kim, H.; Park, Y.J.; Chung, K.H. Polystyrene Microplastic Particles Induce Autophagic Cell Death in BEAS-2B Human Bronchial Epithelial Cells. *Environ. Toxicol.* **2023**, *38*, 359–367. [CrossRef] [PubMed]
59. Lu, Y.-Y.; Li, H.; Ren, H.; Zhang, X.; Huang, F.; Zhang, D.; Huang, Q.; Zhang, X. Size-Dependent Effects of Polystyrene Nanoplastics on Autophagy Response in Human Umbilical Vein Endothelial Cells. *J. Hazard. Mater.* **2022**, *421*, 126770. [CrossRef] [PubMed]
60. Seca, C.; Ferraresi, A.; Phadngam, S.; Vidoni, C.; Isidoro, C. Autophagy-Dependent Toxicity of Amino-Functionalized Nanoparticles in Ovarian Cancer Cells. *J. Mater. Chem. B* **2019**, *7*, 5376–5391. [CrossRef]
61. Elmore, S. Apoptosis: A Review of Programmed Cell Death. *Toxicol. Pathol.* **2007**, *35*, 495–516. [CrossRef]
62. Pinsino, A.; Bergami, E.; Della Torre, C.; Vannuccini, M.L.; Addis, P.; Secci, M.; Dawson, K.A.; Matranga, V.; Corsi, I. Amino-Modified Polystyrene Nanoparticles Affect Signalling Pathways of the Sea Urchin (*Paracentrotus lividus*) Embryos. *Nanotoxicology* **2017**, *11*, 201–209. [CrossRef] [PubMed]
63. Malinowska, K.; Sicińska, P.; Michałowicz, J.; Bukowska, B. The Effects of Non-Functionalized Polystyrene Nanoparticles of Different Diameters on the Induction of Apoptosis and MTOR Level in Human Peripheral Blood Mononuclear Cells. *Chemosphere* **2023**, *335*, 139137. [CrossRef]

64. Baran, K.; Rodriguez, D.; Green, D. The DNA Damage Response Mediates Apoptosis and Tumor Suppression. In *Cell Death*; Wu, H., Ed.; Springer: New York, NY, USA, 2014; pp. 135–165, ISBN 978-1-4614-9301-3.
65. Han, C.; Liu, Y.; Dai, R.; Ismail, N.; Su, W.; Li, B. Ferroptosis and Its Potential Role in Human Diseases. *Front. Pharmacol.* **2020**, *11*, 239. [CrossRef]
66. Cao, J.Y.; Dixon, S.J. Mechanisms of Ferroptosis. *Cell. Mol. Life Sci.* **2016**, *73*, 2195–2209. [CrossRef]
67. Wu, Y.; Wang, J.; Zhao, T.; Sun, M.; Xu, M.; Che, S.; Pan, Z.; Wu, C.; Shen, L. Polystyrene Nanoplastics Lead to Ferroptosis in the Lungs. *J. Adv. Res.* **2024**, *56*, 31–41. [CrossRef]
68. Sun, J.; Wang, Y.; Du, Y.; Zhang, W.; Liu, Z.; Bai, J.; Cui, G.; Du, Z. Involvement of the JNK/HO-1/FTH1 Signaling Pathway in Nanoplastic-induced Inflammation and Ferroptosis of BV2 Microglia Cells. *Int. J. Mol. Med.* **2023**, *52*, 61. [CrossRef]
69. Chen, Q.; Liu, Y.; Bi, L.; Jin, L.; Peng, R. Understanding the Mechanistic Roles of Microplastics Combined with Heavy Metals in Regulating Ferroptosis: Adding New Paradigms Regarding the Links with Diseases. *Environ. Res.* **2024**, *242*, 117732. [CrossRef] [PubMed]
70. Poma, A.; Vecchiotti, G.; Colafarina, S.; Zarivi, O.; Aloisi, M.; Arrizza, L.; Chichiriccò, G.; Di Carlo, P. In Vitro Genotoxicity of Polystyrene Nanoparticles on the Human Fibroblast Hs27 Cell Line. *Nanomaterials* **2019**, *9*, 1299. [CrossRef] [PubMed]
71. Domenech, J.; De Britto, M.; Velázquez, A.; Pastor, S.; Hernández, A.; Marcos, R.; Cortés, C. Long-Term Effects of Polystyrene Nanoplastics in Human Intestinal Caco-2 Cells. *Biomolecules* **2021**, *11*, 1442. [CrossRef]
72. Vecchiotti, G.; Colafarina, S.; Aloisi, M.; Zarivi, O.; Di Carlo, P.; Poma, A. Genotoxicity and Oxidative Stress Induction by Polystyrene Nanoparticles in the Colorectal Cancer Cell Line HCT116. *PLoS ONE* **2021**, *16*, e0255120. [CrossRef]
73. Kim, H.J.; Jang, C.-H. Imaging DNA Single-Strand Breaks Generated by Reactive Oxygen Species Using a Liquid Crystal-Based Sensor. *Anal. Biochem.* **2018**, *556*, 1–6. [CrossRef] [PubMed]
74. Barnes, J.L.; Zubair, M.; John, K.; Poirier, M.C.; Martin, F.L. Carcinogens and DNA Damage. *Biochem. Soc. Trans.* **2018**, *46*, 1213–1224. [CrossRef] [PubMed]
75. Hossain, M.A.; Lin, Y.; Yan, S. Single-Strand Break End Resection in Genome Integrity: Mechanism and Regulation by APE2. *Int. J. Mol. Sci.* **2018**, *19*, 2389. [CrossRef] [PubMed]
76. Da Silva, M.S. DNA Double-Strand Breaks: A Double-Edged Sword for Trypanosomatids. *Front. Cell Dev. Biol.* **2021**, *9*, 669041. [CrossRef] [PubMed]
77. Cannan, W.J.; Pederson, D.S. Mechanisms and Consequences of Double-Strand DNA Break Formation in Chromatin. *J. Cell. Physiol.* **2016**, *231*, 3–14. [CrossRef] [PubMed]
78. Ballesteros, S.; Domenech, J.; Barguilla, I.; Cortés, C.; Marcos, R.; Hernández, A. Genotoxic and Immunomodulatory Effects in Human White Blood Cells after Ex Vivo Exposure to Polystyrene Nanoplastics. *Environ. Sci. Nano* **2020**, *7*, 3431–3446. [CrossRef]
79. Soto-Bielicka, P.; Tejeda, I.; Peropadre, A.; Hazen, M.J.; Fernández Freire, P. Detrimental Effects of Individual versus Combined Exposure to Tetrabromobisphenol A and Polystyrene Nanoplastics in Fish Cell Lines. *Environ. Toxicol. Pharmacol.* **2023**, *98*, 104072. [CrossRef]
80. Sökmen, T.Ö.; Sulukan, E.; Türkoğlu, M.; Baran, A.; Özkaraca, M.; Ceyhun, S.B. Polystyrene Nanoplastics (20 Nm) Are Able to Bioaccumulate and Cause Oxidative DNA Damages in the Brain Tissue of Zebrafish Embryo (Danio Rerio). *NeuroToxicology* **2020**, *77*, 51–59. [CrossRef]

Toxicology in Vitro 91 (2023) 105634

Contents lists available at ScienceDirect

Toxicology in Vitro

journal homepage: www.elsevier.com/locate/toxinvit

The effects of non-functionalized polystyrene nanoparticles with different diameters on human erythrocyte membrane and morphology

Kamil Płuciennik [a], Paulina Sicińska [a], Piotr Duchnowicz [a], Dorota Bonarska-Kujawa [b], Katarzyna Męczarska [b], Katarzyna Solarska-Ściuk [b], Katarzyna Miłowska [c], Bożena Bukowska [a,*]

[a] Department of Biophysics of Environmental Pollution, Faculty of Biology and Environmental Protection, University of Lodz, Pomorska Str. 141/143, 90-236 Lodz, Poland
[b] Department of Physics and Biophysics, Wrocław University of Environmental and Life Sciences, Norwida 25, 50-375 Wrocław, Poland
[c] Department of General Biophysics, Faculty of Biology and Environmental Protection, University of Lodz, Pomorska Str. 141/143, 90-236 Lodz, Poland

ARTICLE INFO

Editor: Dr. J Davila

Keywords:
Erythrocyte
Membrane
Membrane fluidity
Stomatocytes
Cell morphology
Haemolysis

ABSTRACT

In this study, the potential toxicity of non-functionalized polystyrene nanoparticles (PS-NPs) in human erythrocytes has been assessed. The effect of PS-NPs with different diameters (~30 nm, ~45 nm, ~70 nm) on fluidity of erythrocytes membrane, red blood cells shape, as well as haemolysis of these cells has been investigated. Erythrocytes were incubated for 24 h with non-functionalized PS-NPs in concentrations ranging from 0.001 to 200 μg/mL in order to study haemolysis and from 0.001 to 10 μg/mL to determine other parameters. Fluidity was estimated by electron paramagnetic resonance (EPR) and the fluorimetric method. It has been shown that PS-NPs induced haemolysis, caused changes in the fluidity of red blood cells membrane, and altered their shape. Non-functionalized PS-NPs increased the membrane stiffness in the hydrophobic region of hydrocarbon chains of fatty acids. The observed changes in haemolysis and morphology were dependent on the size of the nanoparticles. The smallest PS-NPs of ~30 nm (with the smallest absolute value of the negative zeta potential −29.68 mV) induced the greatest haemolysis, while the largest PS-NPs of ~70 nm (with the highest absolute value of the negative zeta potential −42.00 mV) caused the greatest changes in erythrocyte shape and stomatocytes formation.

1. Introduction

Several dozen types of plastics have been synthesised, including polystyrene (PS), polyvinyl chloride polyethylene, and terephthalate polypropylene, and most of which are very popular and used in massive amounts in the market (Kelpsiene et al., 2022). During the last century, plastic production has increased up to 390.4 million tons in 2021, while >40% is used as packaging (Plastics Europe, 2022). Plastics have numerous applications in the construction industry and medicine (Klemeš et al., 2020). Under the impact of physicochemical factors, such as biodegradation, UV irradiation, chemical or mechanical degradation, macroplastics are disintegrated into smaller microparticles (MPs) (<5 mm), and then to nanoparticles (NPs) (from 1 to 100 or 1000 nm) (Li et al., 2020). In the latest reports, the diameter of 1000 nm of NPs has been assumed as the upper limit (Jiang et al., 2020; Mitrano et al., 2021). PS is one of the most widely produced plastic, as a product of polymerization of styrene monomers (vinylbenzene). This polymer is used in storage: food, cosmetics, and drugs, as well as in toothbrush, CDs, toys, but the number of its applications is still increasing (Kik et al., 2020; Loos et al., 2014).

Small sizes, high surface curves, and large surface areas of PS nanoplastics can increase the potential risk to the environment and increase the potential for accumulation in organs (Mattsson et al., 2015). For plastic with surface charge modifications, charge seem to be a central component in determination of uptake and dispersion into tissue. Negatively and positively charged nanoplastics of the same type have been found to have different levels of uptake (Cole and Galloway, 2015), accumulation (Sun et al., 2020), and toxicity (Bergami et al., 2017), as well as different sites of accumulation within the organism (Bergami et al., 2016).

Nanoplastic particle size also plays a role in both rate of uptake and tissue distribution. Studies showed general smaller particles are internalized faster and disperse throughout the organism, while larger particles are taken up more slowly and tend to accumulate in the intestinal tract (Cole and Galloway, 2015; Lu et al., 2016; Snell and Hicks, 2011). Nano-sized plastics have a much greater surface area to volume ratio

* Corresponding author.
E-mail address: bozena.bukowska@biol.uni.lodz.pl (B. Bukowska).

https://doi.org/10.1016/j.tiv.2023.105634
Received 28 April 2023; Received in revised form 10 June 2023; Accepted 15 June 2023
Available online 17 June 2023

than larger particles, which increases their reactivity in aquatic environment, making them potentially more toxic (Tallec et al., 2019).

MPs and NPs have been detected in aquatic and terrestrial ecosystems causing pollution of the environment. Pollution with MPs also concerns food products, including sea food, honey, beer, salt, as well as tap water (Sana et al., 2020). MPs and NPs can be transferred within food chain, which was observed by Mattson et al. (Mattsson et al., 2015) demonstrating (under laboratory conditions) the movement of 53-nm-diameter PS-NPs from algae to zooplankton and, consequently to fish.

Because of their size, MPs and NPs can enter the human body through inhalation, dermal contact, and ingestion. They have been determined in human faeces (O'Neill and Lawler, 2021; Schwabl et al., 2019), human placenta (Ragusa et al., 2021), and human lungs after biopsy (Jenner et al., 2022). Recently Leslie et al. (Leslie et al., 2022) showed the presence of plastic microparticles in human blood in 17 of 22 tested donors, however, this report seems to be controversial (Kuhlman, 2022). In addition the latest study of 196 cohorts confirmed the existence of nanoplastics in the peripheral blood of all the patients (Salvia et al., 2023).

Biological membranes are the first barrier encountered by foreign particles to the cell. MPs and NPs can cross many biological barriers and come into direct contact with lipid membranes, the last cell protective barrier from the environment. Fleury and Baulin ((Fleury and Baulin, 2021) demonstrated that microplastic beads ranging from 1 to 10 μm attached to lipid membranes. This attachment led to significant stretching of the lipid bilayer without requiring any oxidative, or biological, e.g., inflammatory, reactions. This mechanical stretching can potentially lead to serious dysfunction of the cell machinery. On the other hand, Rossi et al. (Rossi et al., 2014) used coarse-grained molecular simulations to determine the effect of nanosized PS-NPs on the properties of model biological membranes. They found that PS-NPs entered easily into lipid membranes. Dissolved in the membrane core, the PS chains altered the membrane structure, significantly reduced molecular diffusion, and softened the membrane. Moreover, PS-NPs severely affected the lateral organization by stabilizing raft-like domains.

Because, the effect of non-functionalized PS-NPs on membrane fluidity and erythrocyte shape is unknown, the effect of PS-NPs on membrane of erythrocytes, which are the most abundant cells in the circulatory system, was assessed.

Because the surface functionalization is a major parameter determining the biological properties of plastics, we chose non-functionalized nanoparticles devoid of charge, such as those mainly formed in the environment as a result of plastic degradation, to check how these types of particles differing mainly in size affect human isolated erythrocytes (in vitro).

In order to verify the hypothesis that nonfunctionalized PS-NPs depending on their diameter and the value of zeta potential (determined in a Ringer buffer in which cells were suspended), may alter membrane fluidity, which can lead to different alterations in the shape of the erythrocytes and haemolysis, we have evaluated the impact of non-functionalized PS-NPs of different diameters (~30 nm, ~45 nm, ~70 nm) at concentrations ranging from 0.001 to 200 μg/mL (24 h of incubation) on haemolysis of the erythrocytes, and in concentration ranges of 0.001 to 10 μg/mL on membrane fluidity and morphology of red blood cells. Erythrocyte membrane fluidity was determined by means of electron paramagnetic resonance (EPR) and fluorimetry. As plastic NPs interact with the erythrocyte membrane, they can also alter the shape of these cells, which has been assessed using the microscopic technique. Different concentrations of PS-NPs, including those, which are likely present in the human blood were tested to account for sublethal results.

2. Materials and methods

2.1. Chemical standards

Standards of non-functionalized PS-NPs were purchased from Bangs Laboratories (Fishers, Indiana, USA). 1 g of individual nanoparticles contained: 9.24116×10^{16} nanoparticles/g (29 nm); 2.13516×10^{16} particles/g (44 nm); 5.78515×10^{15} particles/g (72 nm). The fluorescent probes, such as 1,6-diphenyl-1,3,5-hexatriene (DPH) and 1-(4-trimethylammonium-phenyl)-6-phenyl-1,3,5-hexatriene p-toluene sulfonate (TMA-DPH) were obtained from Molecular Probes (Eugene, Oregon, USA). 5-Doxylstearic acid (5-DSA) and 16-doxylstearic acid (16-DSA) were purchased from Sigma-Aldrich (Saint Louis, Mi, USA). The remaining reagents i.e. NaCl, NaOH, TRIS, sodium acetate and HEPES were purchased from POCh (Poland) and Roth (Germany).

2.2. Physico-chemical characterization of non-functionalized PS-NPs

To obtain comparable results in the study of NP, an in-depth characterization of the material (microplastics) is needed (Ramsperger et al., 2022), and therefore, we performed physicochemical tests. In our earlier work, we assessed PS-NP hydrodynamic size in water using the Dynamic Light Scattering technique (DLS), atomic force microscopy (AFM) and scanning electron microscope (SEM). The diameters of the particles indicated by the manufacturer were consistent with the results measured in water by the three methods (Malinowska et al., 2022).

Now, in this study, we marked the value of the zeta potential in Ringer buffer, in which red blood cells were incubated.

2.2.1. The zeta potentials (ζ) of the PS-NPs

The zeta potentials of the PS-NPs were measured using a Malvern Instruments Zetasizer Nano-ZS (Malvern Instruments Ltd., Malvern, UK). Samples in electric field were prepared in capillary cells (DTS1061). Measurement was carried out at 37 °C in Ringer buffer at pH 7.4 with 6 repetitions. The zeta potential value was calculated directly from the Helmholtz-Smoluchowski equation using Malvern software (Sze et al., 2003).

2.3. Isolation of erythrocytes

The erythrocytes were obtained from leucocyte buffy-coat (separated from blood) bought in the Regional Centre of Blood Donation and Blood Treatment in Łódź, Poland. Blood was collected from 20 volunteers (aged 18–55) with no symptoms of infectious disease. The investigation was approved by the Bioethics Committee of the University of Lodz (Resolution No. 12/KEBN-UŁ/I/2022–23).

The leukocyte buffy-coat was centrifuged (3000 rpm. For 10 min. at 4 °C) and washed twice with phosphate-buffered saline ($Na_2H_2PO_4$, $Na_2HPO_4 \times 12\ H_2O$, 0.9% NaCl). The erythrocytes of 5% haematocrit were suspended in Ringer buffer, and then incubated with PS-NPs from 0.001 to 200 μg/mL for haemolysis determination, and from 0.001 to 10 μg/mL for assessing other tested parameters at 37 °C for 24 h. Negative control samples contained the erythrocytes incubated with Ringer buffer consisting of 125 mM NaCl, 5 mM KCl, 1 mM $MgCl_2$, 1 mM $CaCl_2$, 10 mM glucose, 32 mM 2-[4-(2-hydroxyethyl)piperazin-1-yl]ethanesulfonic acid (HEPES), 25 mM Tris (pH 7.4).

2.4. Haemolysis

The absorbance of haemoglobin leaking from the erythrocytes was used as an indicator of haemolysis (Drabkin, 1946). The erythrocytes were incubated with non-functionalized PS-NPs with different diameters (~30 nm, ~45 nm, ~70 nm) in concentrations from 0.001 to 200 μg/mL at 37 °C for 24 h. Then, the absorbance of haemoglobin released into supernatant was measured at 542 nm in microplate absorbance reader (BioTek ELx808, BioTek). Determination of haemolysis was described in

the paper of Jarosiewicz et al. (2017). Haemolysis (100%) was obtained by diluting sample 12 times with water, and then measured by the Drabkin method, such as the undiluted test sample.

2.5. Membrane fluidity

2.5.1. Electron paramagnetic resonance (EPR)

To determine red blood cell fluidity, EPR spectroscopy was used (Brucker 300 Spectrometer, Germany), involving 5-doxylstearic acid (5-DSA) and 16-doxylstearic acid (16-DSA) spin labels. From the EPR spectra obtained for the 5-DSA spin label, the ordering parameter S was calculated, and for 16-DSA spin label correlation times τ_B and τ_C were determined. These parameters show the inverse correlation with membrane fluidity. Order parameter S and the correlation times τ_B and τ_C were calculated as described in the study of Koter et al. (2004).

2.5.2. Fluorimetry

To study the effect of non-functionalized PS-NPs on erythrocyte membrane fluidity, the measurement of fluorescent anisotropy using probes DPH and TMA-DPH, which located in different regions of the lipid bilayer was conducted (Fig. 5). Anisotropy indicates membrane fluidity by free rotation of the lipid probe in the lipid bilayer. The increase in fluorescence anisotropy is associated with a decrease in the mobility of lipid hydrocarbon chains, which shows a decrease in membrane fluidity. For the fluorimetric studies, isolated erythrocytes' membranes (ghosts erythrocytes) were used according to Dodge method (1963). Erythrocytes' membranes were suspended in phosphate-saline buffer, pH 7.4. The Bradford method was used to determine the content of membranes in the tested samples Bradford (1976). Fluorescence intensity was measured for two probes (TMA-DPH, DPH) at the final concentration in the sample of 1 μM, while non-functionalized PS-NPs concentration was in the range from 0.001 to 10 μg/mL. Measurements were made with fluorimeter (Cary Eclipse, Varian, UK) at excitation and emission wavelength respectively for DPH λex 360 nm, and λem 425 nm; TMA-DPH λex 358 nm, and λem 428 nm. Fluorescence anisotropy for DPH and TMA-DPH probes was calculated by the methods described in the study of Bonarska-Kujawa et al. (2011). In fluorimetric studies that used fluorescent probes, additional control tests were performed: autofluorescence of PS-NPs, autofluorescence of suspension of NPs and erythrocyte membranes, as well as suspension of NPs and fluorescent markers. Tested NPs did not exhibit autofluorescence, and the signal from the fluorescent probes in the presence of NPs (except concentration of 10 μg/mL) was similar to the signal of the probe from phosphate buffer. Slightly higher control values for NPs concentration of 10 mg/mL were associated with greater light scattering, as well as possibility of aggregation of NPs in solution, which was described in the studies of Barshtein et al. (2016) and Malinowska et al. (2022).

2.6. Evaluation of erythrocytes shape

The effect of non-functionalized PS-NPs on human erythrocytes shape was determined by optical microscopy. The erythrocytes after 24 h of incubation with PS-NPs (different diameters) in the range of concentrations from 0.001 to 10 μg/mL, were washed and fixed with glutaraldehyde. So prepared erythrocytes were observed under the optical microscope (Zeiss AXIO Scope. A1) equipped with a microscope camera (AxioCam MR) with magnification 600× (Carl Zeiss Microscopy, GmbH, Germany). The photos were taken, which made possible to calculate the percentage of three forms of the erythrocytes, such as discocytes, stomatocytes and echinocytes.

2.7. Statistical analysis

Data were expressed as the mean and standard deviation (SD) (for equal numbers of trials) or as median and interquartile range (IQR) (lower (25%) to upper (75%) quartile for not equal numbers of trials); $n = 3–9$ (3–9 blood donors).

Erythrocyte shapes were analysed from 5 individual experiments. From each tested erythrocyte sample, 6 images were taken and the percentage of discocytes, echinocytes and stomatocytes was calculated, and then the average of these percentages was adopted for statistical analysis. Average values obtained from 5 series were counted from about 500 cells. Statistical analysis was performed from 5 averages assigned to the controls and consecutive concentrations.

Statistical analyses were performed using Statistica v.13.1 (Dell Inc., Tulsa, OH, USA). The Shapiro-Wilk test was used to test for normality, and Brown-Forsythe'a test was used to verify variance homogeneity. All data demonstrated a normal distribution, therefore parametric tests were used for further analyses. The statistical significance of differences between homogenous groups was tested using two-way ANOVA (one-way ANOVA was only used to test potential zeta), followed by a post hoc Tukey's test. The results were considered statistically significant when $P < 0.05$.

3. Results

3.1. Differences in the ζ potential of particles

Zeta potentials at pH 7.4 of tested particles after their incubation in Ringer buffer (in which erythrocytes were incubated) (Table 1) were measured.

The obtained results showed a significant change in ζ-potential measured in Ringer buffer depending on the particle size from −29.68 ± 2.15 mV (for the smallest particles ~30 nm) to −42.0 ± 1.52 mV (for the largest particles ~70 nm) (Table 1). Statistically significant differences were found between the zeta potential values for the smallest NPs ~30 nm and NPs ~45 nm ($P < 0.01$) and ~70 nm ($P < 0.001$), and between ~45 and ~ 70 nm ($P < 0.001$).

3.2. Haemolysis

Red blood cells were treated with non-functionalized PS-NPs in the range of concentrations from 0.001 to 200 mg/mL and incubated for 24 h. PS-NPs of ~30 nm diameters from the concentration of 100 μg/mL ($P < 0.001$) and NPs of diameter ~ 70 nm and ~45 nm from the concentration of 200 μg/mL ($P < 0.001$) caused significant haemolytic changes (Fig. 1). The smallest NPs caused the greatest haemolytic changes (Fig. 1). Statistically significant differences were noted between PS-NPs of ~30 nm and PS-NPs of diameter ~ 70 nm and ~45 nm at 100 μg/mL and 200 μg/mL ($P < 0.001$).

3.3. Membrane fluidity

Haemolysis was assessed under influence of PS-NPs in order to select their concentrations that do not alter cell viability, and consequently may be used in membrane fluidity tests. Based on obtained results, electron paramagnetic resonance (EPR) and fluorescence analyses were conducted for the particles in concentrations from 0.001 to 10 μg/mL, which did not induce haemolytic changes in tested cells (Fig. 1).

Table 1
Zeta potential of non-functionalized PS-NPs in Ringer buffer, pH 7.4. Mean ± SD was calculated from 6 measurements. (*) Significantly different between PS-NPs ~30 nm and ~45 and ~70 nm and (#) between ~45 nm and ~70 nm; one-way ANOVA and post hoc Tukey's test.

	PS-NPs		
Manufacturer diameter [nm]	~30	~45	~70
ζ-potential [mV], in Ringer buffer, pH 7.4	−29.68 ± 2.15	−35.03 ± 3.31*	−42.0 ± 1.52*#

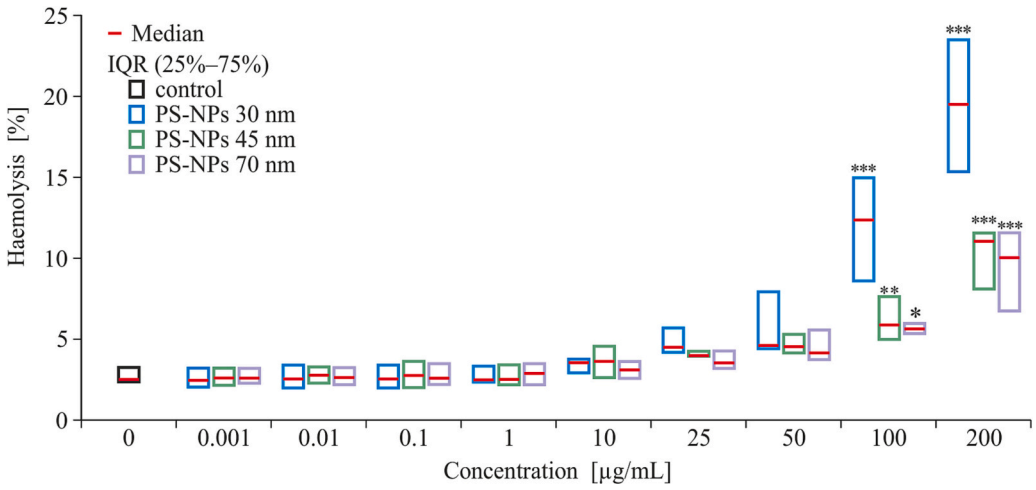

Fig. 1. Haemolysis of the erythrocytes caused by different sized non-functionalized PS-NPs. Data were presented as median and IQR. Significantly different from control (*) $P < 0.05$, (**) P < 0.0, (***) P < 0.001; n = 3–8 experiments (at 3 replications for each donor); two-way ANOVA and post hoc Tukey's test.

3.3.1. Order parameter S

Statistically significant changes were noted in the order parameter S in the erythrocytes incubated for 24 h with non-functionalized PS-NPs of diameter ~ 70 nm in concentrations from 0.001 to 10 μg/mL and incubated with PS-NPs of diameters ~30 and ~45 nm in concentrations from 0.01 to 10 μg/mL. All tested PS-NPs caused an increase in the parameter S value as compared with control (Table 2). No differences in parameter S value between different-sized NPs were found ($P > 0.05$).

3.3.2. Correlation time τ_B and time τ_C

Following incubation of the erythrocytes with non-functionalized PS-NPs for 24 h, statistically, significant changes were observed in the values of the correlation time $_{\tau B}$ and time $_{\tau C}$. For correlation time τ_B, statistically significant changes were observed for PS-NPs with diameters of ~30 nm from the concentration of 0.001 μg/mL, for PS-NPs ~45 nm from the concentration of 0.01 μg/mL and for NPs with diameter of ~70 nm from the concentration of 0.1 μg/mL (Table 3).

For correlation time τ_C, a statistically significant changes were observed after incubation of tested cells with PS-NPs with a diameter of ~70 nm at concentrations of 0.001 μg/mL and 0.1 μg/mL, and with diameters of ~30 nm and ~45 nm in concentrations from 1 to 10 μg/mL (Table 3). However, no differences in τ_B and τ_C values between different-sized PS-NPs were found ($P > 0.05$).

Table 2
Changes in order parameter S for control erythrocytes and the erythrocytes incubated with different-sized non-functionalized PS-NPs. Data were presented as median and IQR (n = 7–8, at 1 replications for each donor). Significantly different from control (*) ($P < 0.05$), (***) ($P < 0.001$); two-way ANOVA and post hoc Tukey's test.

PS-NPs diameter [nm]	Parameter S
Concentrations [μg/mL]	
~30 nm	
control	0.704 (0.701, 0.709)
0.001	0.712 (0.705, 0.715)
0.01	0.717 (0.715, 0.718)***
0.1	0.723 (0.719, 0.724)***
1	0.726 (0.722, 0.729)***
10	0.732 (0.731, 0.735)***
~45 nm	
control	0.704 (0.702, 0.710)
0.001	0.713 (0.711, 0.715)
0.01	0.717 (0.713, 0.724)***
0.1	0.722 (0.720, 0.726)***
1	0.725 (0.723, 0.729)***
10	0.732 (0.728, 0.737)***
~70 nm	
control	0.705 (0.704, 0.708)
0.001	0.714 (0.711, 0.717)*
0.01	0.717 (0.715, 0.724)***
0.1	0.726 (0.722, 0.727)***
1	0.726 (0.722, 0.729)***
10	0.734 (0.728, 0.738)***

Table 3
Changes in correlation time τ_B, and time τ_c for control erythrocytes and the erythrocytes incubated with different-sized non-functionalized PS-NPs. Data were presented as median and IQR (n = 8–9, at 1 replications for each donor). Significantly different from control (*) ($P < 0.05$), (**) ($P < 0.01$), (***) ($P < 0.001$); two-way ANOVA and post hoc Tukey's test.

PS-NPs diameter [nm]	Correlation time	Correlation time
Concentrations [μg/mL]	τ_B ($\times 10^{-9}$ s)	τ_C ($\times 10^{-9}$ s)
~30 nm		
control	17.440 (17.280, 18.127)	22.752 (21.958, 23.590)
0.001	18.405 (18.138, 19.413)**	24.038 (23.220, 25.588)
0.01	18.671 (18.138, 18.762)*	24.291 (23.902, 24.970)
0.1	18.662 (18.241, 19.119)*	24.579 (23.502, 25.166)
1	18.876 (18.369, 19.573) ***	25.055 (24.175, 26.337) ***
10	18.758 (18.452, 19.204)**	24.822 (24.293, 25.361)*
~45 nm		
control	17.404 (17.280, 18.127)	22.752 (21.958, 23.590)
0.001	18.393 (18.107, 18.673)	24.176 (23.347, 25.096)
0.01	18.346 (18.150, 19.024)*	23.776 (23.395, 24.470)
0.1	18.544 (18.256, 19.104)*	24.648 (23.303, 24.754)
1	18.755 (18.535, 19.172) ***	24.479 (24.030, 25.057)*
10	18.964 (18.254, 19,649) ***	24.467 (24.014, 25.586)*
~70 nm		
control	17.440 (17.280, 18.127)	22.752 (21.958, 23.590)
0.001	18.147 (18.041, 19.037)	24.023 (23.529, 25.848)*
0.01	18.392 (18.236, 18.615)	24.463 (23.811, 24.770)
0.1	18.806 (18.274, 19.307) ***	24.721 (23.852, 25.120)*
1	18.797 (18.384, 19.266) ***	24.106 (23.752, 25.050)
10	18.426 (18.213, 19,168)*	24.190 (23.839, 24.918)

3.4. Fluorimetric methods

There were no statistically significant changes in fluorescence anisotropy for the (1-(4-trimethylammoniumphenyl)-6-phenyl-1,3,5-hexatriene *p*-toluene sulfonate) (TMA-DPH) fluorescence probe at the level of the fourth carbon atom of the fatty acid chain in the erythrocytes membrane incubated with tested PS-NPs (Fig. 2A). Fluorescence anisotropy for the 1,6-diphenyl-1,3,5-hexatriene (DPH) probe increased (statistically significant changes) after incubation of tested cells with non-functionalized PS-NPs with diameters of ~30 nm and ~70 nm in concentrations range from 0.01 to 10 μg/mL and for PS-NPs with a diameter of ~45 nm in the concentration of 0.1 μg/mL ($P < 0.05$) (Fig. 2B). No differences in fluorescence anisotropy values between tested NPs were found ($P > 0.05$).

3.5. Impact on erythrocyte shape

Figs. 4A-C show percentages of various forms of human erythrocytes (discocytes, echinocytes and stomatocytes) after exposure to PS-NPs with diameters of ~30 nm, ~45 nm, and ~70 nm in concentrations range from 0.001 to 10 μg/mL. The exemplary photos of the erythrocytes incubated with PS-NPs are shown in Fig. 3 and all photos are deposited.

In all samples containing the erythrocytes and PS-NPs of ~45 nm and ~70 nm in diameter, a statistically significant decrease in discocytes count relative to the control sample occurred. The biggest NPs caused a decrease in echinocytes formation from the concentration of 0.001 μg/mL ($P < 0.001$), PS-NPs in diameter ~ 45 nm from the concentration of 0.01 μg/mL ($P < 0.001$), while PS-NPs in diameter ~ 30 nm from the concentration of 0.1 μg/mL ($P < 0.01$). The differences in the percentage of discocytes were statistically significant between samples containing tested NPs of ~70 nm and ~30 nm at the concentrations of 0.001 μg/mL ($P < 0.01$), 0.01 μg/mL ($P < 0.001$), and 0.1 μg/mL ($P < 0.05$), additionally between samples consisting of NPs of 70 nm and 45 nm in the concentration of 0.01 μg/mL ($P < 0.05$).

Changes in the percentage of echinocytes were not statistically significant, while the number of stomatocytes increased. Statistically significant changes in the percentage of stomatocytes were observed in samples containing NPs in diameter of ~70 nm in each of their concentration ($P < 0.001$), for PS-NPs of ~45 nm from the concentration of 0.01 μg/mL ($P < 0.001$), while for the smallest PS-NPs ~30 nm from the concentration of 0.1 μg/mL ($P < 0.001$).

The differences in the percentage of stomatocytes were statistically significant between samples containing tested NPs of 70 nm and 30 nm at the concentrations of 0.001 μg/mL and 0.01 μg/mL ($P < 0.001$), and additionally between samples consisting of NPs of 70 nm and 45 nm in the concentrations 0.001 μg/mL ($P < 0.05$) and 0.01 μg/mL ($P < 0.01$). However, there were no differences in the percentage of discocytes and stomatocytes between all tested NPs in the concentrations of 1 μg/mL and 10 μg/mL ($P > 0.05$). Compared to the other tested NPs, 70 nm PS-NPs caused the greatest changes at the lowest concentrations.

4. Discussion

Plastic particles formerly considered inert to the body are increasingly being studied for their harmful effects on living organisms. They

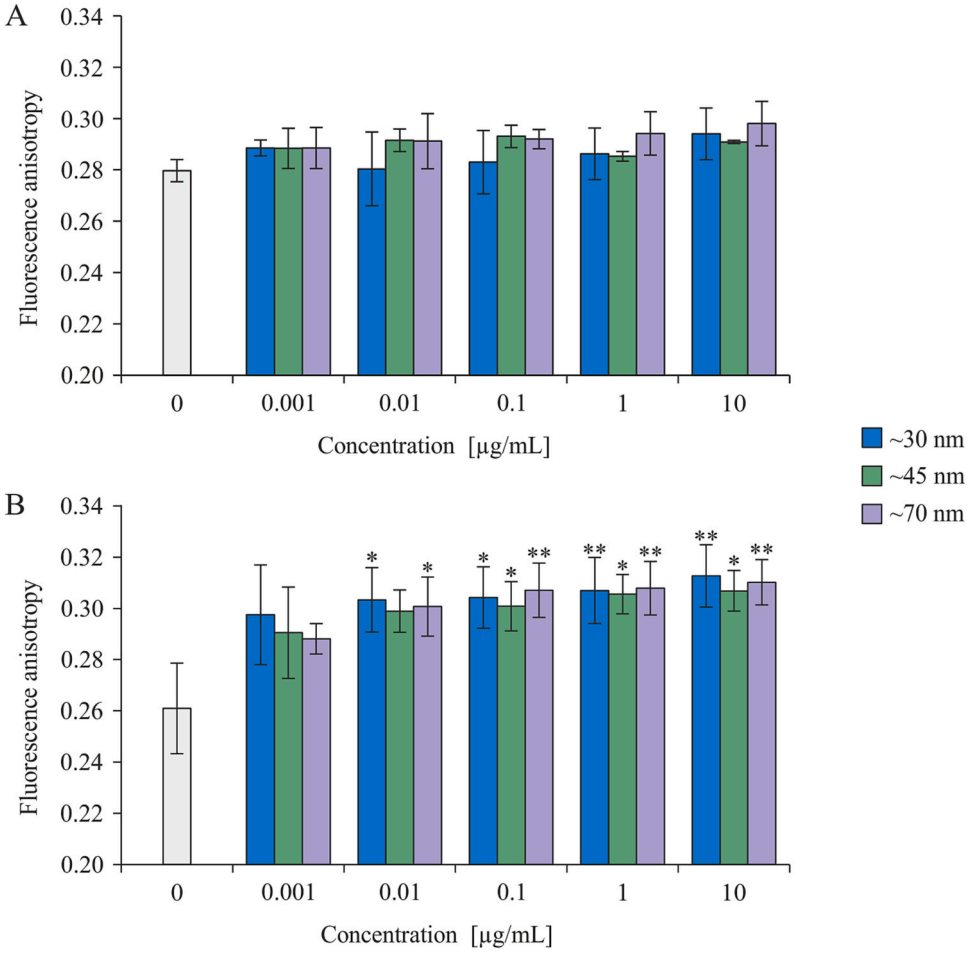

Fig. 2. Fluorescence anisotropy values of TMA-DPH probe (A) and DPH probe (B) for erythrocyte membrane incubated for 24 h with different-sized non-functionalized PS-NPs. Significantly different from control (*) ($P < 0.05$), (**) ($P < 0.01$); $n = 3$; two-way ANOVA and post hoc Tukey's test.

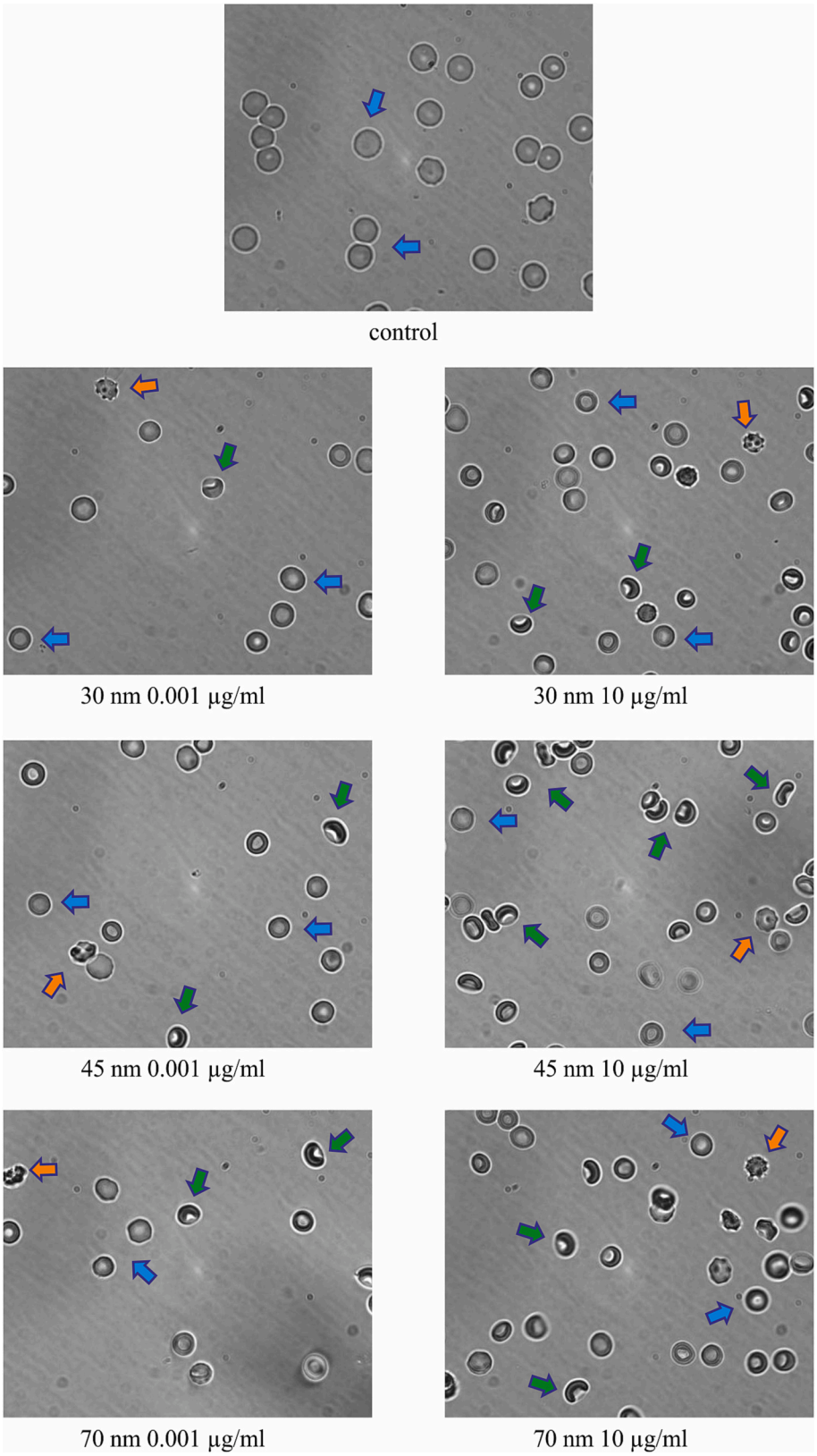

Fig. 3. The impact of PS-NPs on erythrocytes shape. Selected photos present control sample and samples with two highest concentrations of NPs of different size (blue arrow – discocytes, orange arrow – echinocytes and green arrow – stomatocytes). (For interpretation of the references to colour in this figure legend, the reader is referred to the web version of this article.)

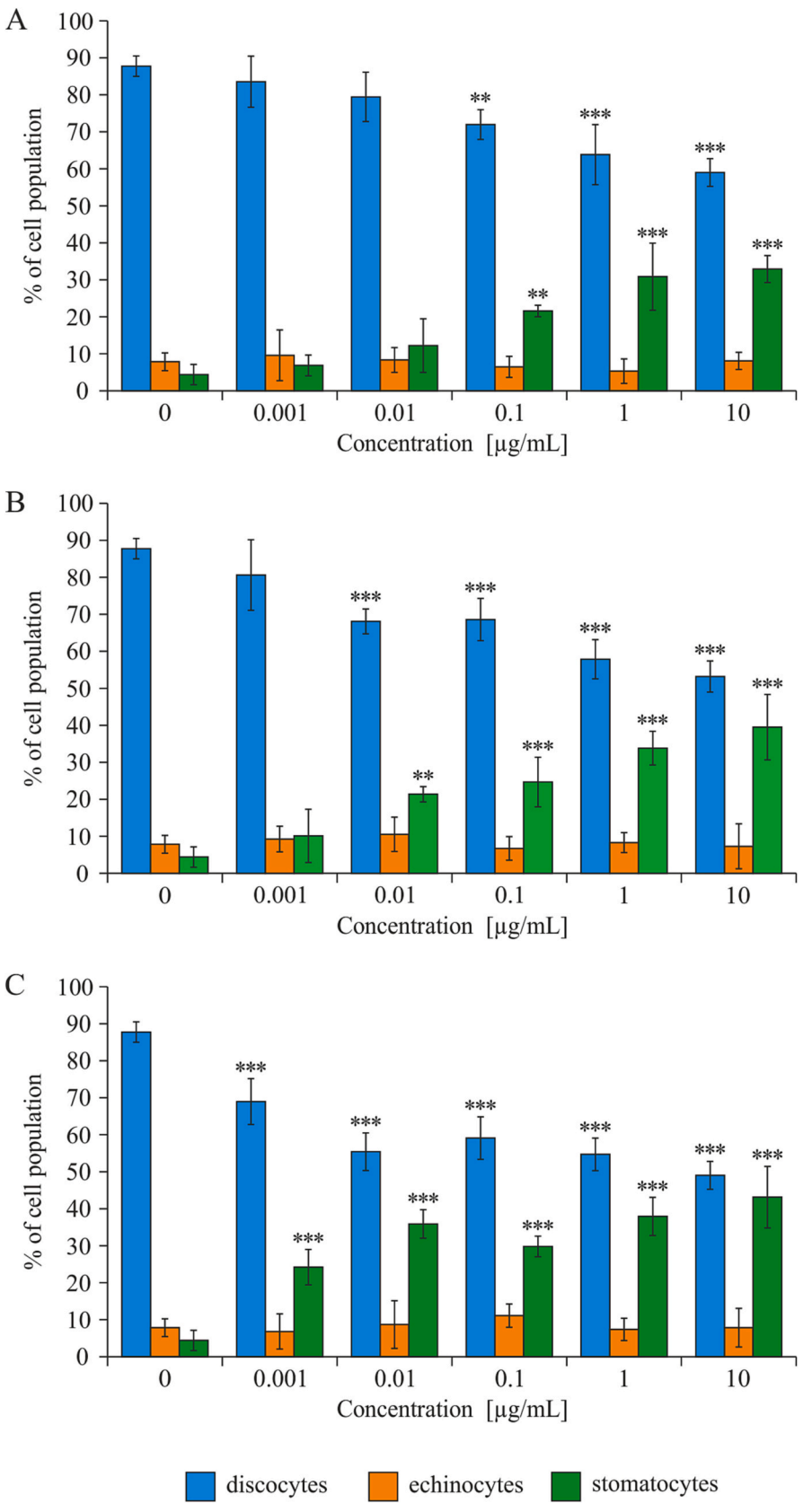

Fig. 4. Percentage of various forms of the erythrocytes: discocytes, echinocytes, stomatocytes in control samples and the samples incubated with non-functionalized PS-NPs with diameter of ~30 nm (A), ~45 nm (B) and ~70 nm (C). Significantly different from control (*) ($P < 0.05$), (**) ($P < 0.01$), (***) ($P < 0.001$); $n = 5$; two-way ANOVA and post hoc Tukey's test.

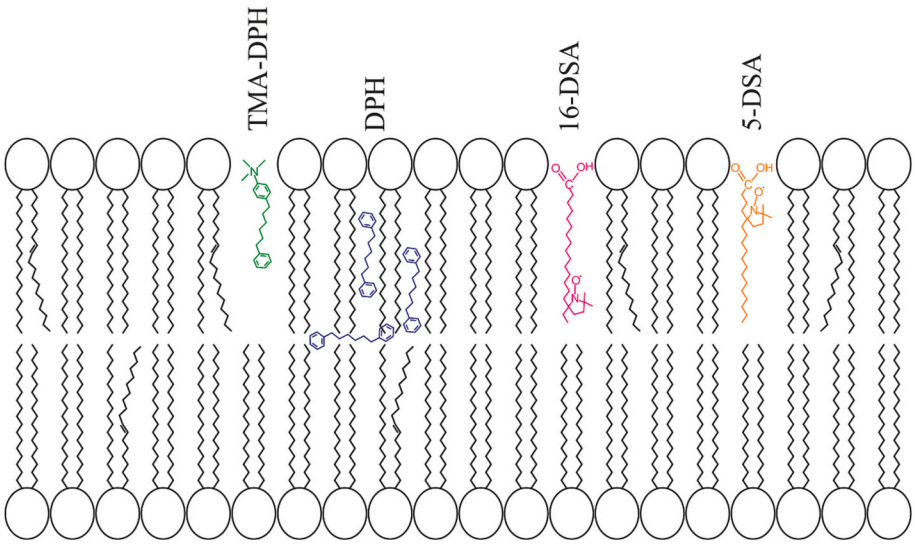

Fig. 5. Localization of markers in the cell membrane of the erythrocytes: DPH (Poojari et al., 2019); TMA-DPH (Fernandes et al., 2018); 5-DSA and 16-DSA (Gaeti et al., 2015).

can accumulate in organs and tissues, causing a sustained inflammatory response, oxidative stress, and cytotoxicity (Kik et al., 2021; Lehner et al., 2019). Particles smaller than 100 nm pose a potentially greater environmental and health risk, due to their size, which is two orders of magnitude smaller than that of eukaryote cell; they can affect cells at the subcellular and even at molecular level (Hollóczki and Gehrke, 2020). In search of associations between humans exposure to PS-NPs and the effects of their action, it is important to consider the erythrocytes, which are the most abundant cells in the human circulatory system. Because limited information on the effects of NPs on blood cells, including erythrocytes exists, and the latest results have shown plastic particles exist in the human blood (Leslie et al., 2022), we decided to evaluate the effect of non-functionalized PS-NPs of different diameters on haemolysis of erythrocytes, as well as the structure and function of erythrocyte membrane.

In preliminary haemolytic studies, the concentrations of PS-NPs that did not decrease red blood cells viability, and consequently may be used in membrane fluidity tests.

Published studies on human erythrocytes indicated haemolysis induction under the influence of PS-NPs, but at their very different doses/concentrations. Sarma et al. (Sarma et al., 2022) studied the effect of PS-NPs at diameter of 50 nm at very high concentrations from 500 μg/mL to as much as 2000 μg/mL on haemolysis. They observed the highest haemolysis (93%) in cells exposed to PS-NPs at 2000 μg/mL, in comparison to other concentrations (15.3% at 1000 μg/mL and 6.5% at 500 μg/mL). In turn, Gopinath et al. (2019) studied the effect of non-functionalized PS-NPs with a larger diameter of 100 nm in slightly lower concentration range from 1 to 10 μg/mL and found that tested NPs already at 5 μg/mL and 7.5 μg/mL caused haemolysis of 22% and 36%, respectively, and at 10 μg/mL they induced almost 50% haemolysis. Haemolysis in our study was observed at lower concentrations of PS-NPs (from 100 to 200 μg/mL) (Fig. 1) in comparison to haemolytic changes observed by Sarma et al. (2022) caused by PS-NPs of 50 nm in diameter (500, 1000 and 2000 μg/mL), as well as at slightly higher concentrations than those reported by Gopinath et al. (2019) for PS-NPs of 100 nm (from 1 to 10 μg/mL). It was observed that haemolysis caused by non-functionalized PS-NPs was concentration dependent, and the smallest NPs caused the greatest changes in cell membrane integrity. Among the non-functionalized PS-NPs tested, those with the smallest diameter exhibited the strongest haemolytic activity, which was probably associated with their easiest penetration into the cells, as reported elsewhere (Hwang et al., 2022; Xu et al., 2019). Similarly, Kim and Shin (2014) investigated the effect of the size and aspect ratio of Ag-NMs on the rheological characteristics of human erythrocytes, including haemolysis and noted that the smaller particles induced the strongest haemolysis. For PS, such a relationship was determined (Hwang et al., 2020); although it referred to MPs of much larger size than the those used in our study. Those scientists observed that induction of haemolysis depended only on particles size, but not on their concentration. PS particles, which had an average diameter of 6–8 μm, were more cytotoxic at each concentration. They also suggested that probably the adhesion of small PS particles to the erythrocytes was enhanced by weak interactive forces, such as van der Waals forces, which led to red blood cells haemolysis (Hwang et al., 2020).

It should be emphasized that these studies are carried out in an in vitro system, erythrocytes were suspended in Ringer's solution devoid of proteins. The presence of proteins and the potential formation of a protein corona, as showed Gopinath et al. (2019) may be important in the haemolytic properties of NPs. Gopinath et al. (2019) indicated that protein coronation with increased conformation greatly influenced haemolytic activity of NPs. They showed that coronate-NPs at 5 μg/mL and 7.5 μg/mL caused 91% and 83% haemolysis, respectively, as a result of higher conformational changes in plasma protein, while virgin-NPs induced 22% and 36% haemolysis. This is a very important observation, because it indicates the possibility of increase in toxicity of PS-NPs in the bloodstream as a result of reaction with proteins and the formation of hard- or soft-corona.

Zając et al. (2022) presented research in which cell membranes were exposed to plain PS and amino-functionalized PS (PS-NH_2) of two different sizes. They showed that the size and surface chemistry of the particles determined their interactions with biological membranes. They concluded that 100 nm and 200 nm PS, as well as 100 nm PS-NH_2, internalized into the cells. On the contrary, PS-NH_2 particles of 200 nm were only attached to cell membranes. These observations were confirmed by Anselmo et al. (2013). They noticed the attachment of spherical PS-NPs (200 nm in diameter) to the erythrocytes by scanning electron microscopy (SEM) and quantified this phenomenon using 3H-radiolabeled NPs. At a particle/erythrocyte ratio of 100:1, a single cell on average carried ~24 particles (200 nm in diameter). The attachment of particles to erythrocytes was also proven to the erythrocytes was mediated by electrostatic and hydrophobic interactions (Chambers and Mitragotri, 2004).

In the erythrocytes, NPs can change the structure of the phospholipid bilayer (Wang et al., 2012), which is formed by a hydrophilic outer

surface and a hydrophobic core (Hollóczki and Gehrke, 2020). The penetration ability of NPs depends on their physicochemical properties, such as size, surface area, and charge, so the hydrophobic nature of plastics will play an important role in these interactions (Hollóczki and Gehrke, 2020; Wang et al., 2012). Changes in lipid membranes caused by microplastic particles have been reported by Fleury and Baulin (2021), who proved that microplastic particles adsorbed on lipid membranes considerably increased membrane tension even at low particle concentrations. Each particle adsorbed at the membrane consumes a surface area that is proportional to the contact area between the particle and the membrane. Although lipid membranes are liquid and capable of accommodating mechanical stress, the relaxation time is much slower than the rate of adsorption; thus, the cumulative effect of the arrival of microplastic particles to the membrane leads to the global reduction of the membrane area and increased membrane tension. This, in turn, leads to a strong reduction in the lifetime of the membrane. Mechanical stress may alter the function of membrane proteins or ion channels.

Membrane fluidity is essential for maintaining cell homeostasis, because it affects cell growth, signal transduction, transport of solutes and membrane-bound enzymatic activity, therefore changes in cell membrane fluidity can disrupt function and induce pathological processes in the cell (Ammendolia et al., 2021; Rawat et al., 2021). The effect of non-functionalized PS-NPs with different diameters (~30 nm, ~45 nm, ~70 nm), on the erythrocyte cell membrane was evaluated in the non-haemolytic concentrations range of 0.001–10 μg/mL. The effect of non-functionalized PS-NPs on the fluidity of the hydrophobic region of the erythrocyte membranes was determined by changes in the fluorescence anisotropy of DPH and TMA-DPH probes, as well as EPR spectra obtained for the spin labels 5-doxylstearic acid (5-DSA) and 16-doxylstearic acid (16-DSA). We used probes, which were located in different hydrophobic parts of the membrane (Fig. 5). For 5-DSA, the ordering parameter S was calculated, for which the first statistically significant increase was observed for PS-NPs of diameter ~70 nm at a concentration of 0.001 μg/mL (Table 2) and at a concentration of 0.01 μg/mL for other nanoparticles. No differences in parameter S values between different-sized PS-NPs were found ($P > 0.05$). The increase in order parameter S is associated with a decrease in the fluidity of the cell membrane at the level of the 5th carbon atom of the fatty acid residue. However, no statistically significant changes in TMA-DPH fluorescence anisotropy were observed (Fig. 2B).

To investigate the core tail of the hydrophobic region of the erythrocyte membrane, spin label 16-DSA in EPR technique and DPH probes in a fluorimetric method were used. The correlation time τ_B determined for the spin label demonstrated statistically significant changes in these parameters after 24-h of incubation of the erythrocytes with non-functionalized PS-NPs with diameters of ~30 nm from the concentration of 0.001 μg/mL, with diameters of ~45 nm from the concentration of 0.01 μg/mL, as well as for the biggest NPs (~70 nm) from the concentration of 0.1 μg/mL. The correlation time τ_C increased at 1 μg/mL and 10 μg/mL for smaller NPs, and for the largest NPs ~70 nm, the changes were significant at the concentrations of 0.001 μg/mL and 0.1 μg/mL. No differences in the correlations time τ_B and τ_C values between different NPs were found ($P > 0.05$). These findings demonstrate the stiffening of the erythrocyte cell membrane at the 16-carbon level of the chain of fatty acid chain (Table 3). Similar results were observed for DPH (Fig. 2B), which is located in the membrane in the same region as the 16-DSA tested by the EPR technique. It can be assumed that the PS-NPs tested caused alterations in the hydrophobic part by increasing the pressure on the membrane surfaces. As a consequence, an increase in the stiffness of the internal leaflet of the red blood cell membrane was observed.

Interactions of NPs with blood morphotic elements lead to changes in the plasma membrane of the erythrocytes, and consequently to alterations in the structure of lipids and membrane proteins, which indirectly may impact the shape of the erythrocyte. The physiological human erythrocyte (discocyte) has a characteristic biconcave disk shape that gives it a higher surface-to-volume ratio than a sphere, which creates better conditions for gas exchange and increases the deformability of the cell. When specific compounds bind to the outer or inner monolayer of the discocyte membrane, echinocytes and stomatocytes are formed, respectively (Stasiuk et al., 2009). However, in the case of PS-NPs, it is more likely that these particles, due to the high pressure they exert on the cell surface and changes in the lipid-protein structure of the entire bilayer, cause volume stresses and change the shape of the cells (Fleury and Baulin, 2021). In the current study, a statistically significant increase in stomatocyte\ number was noted for NPs of ~30 nm from 0.1 μg/mL, PS-NPs of ~45 nm from 0.01 μg/mL, whereas for NPs of ~70 diameter, an increase in number was observed at all particle concentrations tested.

We observed that the smallest particles (~30 nm) with the lowest absolute value of the negative zeta potential (−29.68 ± 2.15 mV) showed the highest haemolytic properties, while the largest particles (~70 nm) with the highest absolute value of the negative zeta potential (−42.0 ± 1.52 mV) revealed the smallest haemolytic changes. All tested NPs caused the formation of stomatocytes; however, particles of 70 nm in diameter induced the strongest changes in this parameter from their lowest concentrations tested.

In the assessment of toxicity, the number of particles is also important, for example, at a haemolytic concentration of 100 μg/mL for PS-NP 29 nm it is 7.418×10^{12} in ml, for 44 nm it is 2.150×10^{12} and for 72 nm it is 5.055×10^{11}. Therefore, the smallest particles are the most in a given system, which may also contribute to an increased haemolytic. Probably, the high surface curves of the smallest nanoparticles also increased their cytotoxicity.

As suggested by Shao et al., (2015) in the case of negatively charged NPs, their interactions with biomembranes are relatively weak because the membranes are also negatively charged, and consequently NPs induces low cytotoxicity. Our research also confirmed these observations, as a higher absolute value of negative zeta potential of ~45 and a larger size of tested NPs (~70 nm) were correlated with their lower cytotoxicity compared with 30 nm NPs with lower absolute value of negative zeta potential. Therefore, the absolute value of the zeta potential plays an essential role in the effect of PS-NPs on the erythrocytes but not decisive when comparing NPs effects of different diameters. The greater haemolysis caused by the smallest particles is probably due to the greater number of unit interactions of PS-NPs with the erythrocyte membranes. Additionally, as previously suggested by Hollóczki and Gehrke (2020), the adhesion of small PS particles to erythrocytes was enhanced by weak interactive forces, such as van der Waals forces, which led to higher red blood cell haemolysis.

In the presented study, the results indicated that non-functionalized PS-NPs interacted with the erythrocyte membrane, causing increased membrane stiffness at the level of 5th and 16th carbon in the hydrophobic part of the hydrocarbon chains of fatty acids. These changes may influence the volumetric deformity of erythrocytes, as indicated by the tendency to form stomatocytes. Probably, for larger PS-NPs (~70 nm), the total surface of interaction with erythrocytes is generally smaller, but the individual contact surface is greater, and thus the pressure on the surface of larger NPs is greater, so the shape changes are more pronounced (at lower concentrations).

Pan et al. (2018) showed that PSNPs with diameter 171.1 nm induce erythrocyte agglutination and sensitize red blood cells to damage by osmotic, mechanical, and oxidative stress. In addition, they increase erythrocyte stiffening and surface exposure of phosphatidylserine, both known to accelerate red blood cell clearance in vivo. Red blood cell sedimentation, haemolysis, abnormal morphology, and agglutination appear to be related. As demonstrated in the studies (Li et al., 2008; Trpkovic et al., 2010; Wadhwa et al., 2019), when an NP attaches to the cell membrane, it changes the native properties of the membrane asymmetry due to the rearrangement of lipids in the two monolayers, which can lead to membrane breakdown and changes in cell shape.

Ultimately, impaired hemorheological parameters of RBC by NP can lead to blood microrheology alterations and result in thrombosis, which was suggested in the AG NP nanoparticles study (Bian et al., 2019).

In contrast to haemolytic changes occurring at relatively high concentrations of PS-NPs of 100 μg/mL (rather impossible to be present in the bloodstream), observed changes in membrane fluidity parameters and cell shape occurred at very low concentrations of the tested nanoparticles.

5. Conclusions

This study illustrates the effect of non-functionalized PS-NPs on the human erythrocyte membrane. We showed that PS-NPs induced haemolysis, and changed the structure of the erythrocyte membrane, as well as altered the shape of red blood cells. Changes in the erythrocyte membrane fluidity were observed in the hydrophobic regions of its lipid bilayer and were not dependent on the size of the PS-NPs tested. However, the highest PS-NPs of ~70 nm (with the highest absolute value of negative zeta potential) induced changes in the shape of the erythrocytes at lower concentrations. On the contrary, the smallest PS-NPs of ~30 nm (with the smallest absolute value of negative zeta potential) caused the strongest haemolysis. The greatest haemolysis induced by the smallest particles was probably due to the greater packing of small nanoparticles on a specific surface of the membrane and their stronger interaction with plasma membrane components compared to those of larger nanoparticles, while the most intensive formation of stomatocytes under the influence of the largest NPs resulted from a smaller contact with the cell surface, but a greater force pressure.

Funding

This manuscript was funded by research granted (B2011000000191.01) to the Department of Biophysics of Environmental Pollution, Faculty of Biology and Environmental Protection, University of Lodz Poland.

CRediT authorship contribution statement

Kamil Płuciennik: Conceptualization, Methodology, Formal analysis, Visualization, Writing – original draft. **Paulina Sicińska:** Conceptualization, Methodology, Formal analysis, Project administration, Writing – original draft. **Piotr Duchnowicz:** Methodology, Visualization. **Dorota Bonarska-Kujawa:** Supervision. **Katarzyna Męczarska:** Methodology. **Katarzyna Solarska-Ściuk:** Methodology. **Katarzyna Miłowska:** Methodology. **Bożena Bukowska:** Conceptualization, Formal analysis, Project administration, Supervision, Writing – original draft, Writing – review & editing.

Declaration of Competing Interest

The authors declare no conflict of interest.

Data availability

Data will be made available on request.

References

Ammendolia, D.A., Bement, W.M., Brumell, J.H., 2021. Plasma membrane integrity: implications for health and disease. BMC Biol. 19, 71. https://doi.org/10.1186/s12915-021-00972-y.

Anselmo, A.C., Gupta, V., Zern, B.J., Pan, D., Zakrewsky, M., Muzykantov, V., Mitragotri, S., 2013. Delivering nanoparticles to lungs while avoiding liver and spleen through adsorption on red blood cells. ACS Nano 7, 11129–11137. https://doi.org/10.1021/nn404853z.

Barshtein, G., Livshits, L., Shvartsman, L.D., Shlomai, N.O., Yedgar, S., Arbell, D., 2016. Polystyrene Nanoparticles Activate Erythrocyte Aggregation and Adhesion to Endothelial Cells. Cell Biochem. Biophys. 74 (1), 19–27. https://doi.org/10.1007/s12013-015-0705-6.

Bergami, E., Bocci, E., Vannuccini, M.L., Monopoli, M., Salvati, A., Dawson, K.A., Corsi, I., 2016. Nano-sized polystyrene affects feeding, behavior and physiology of brine shrimp Artemia franciscana larvae. Ecotoxicol. Environ. Saf. 123, 18–25. https://doi.org/10.1016/j.ecoenv.2015.09.021.

Bergami, E., Pugnalini, S., Vannuccini, M.L., Manfra, L., Faleri, C., Savorelli, F., Dawson, K.A., Corsi, I., 2017. Long-term toxicity of surface-charged polystyrene nanoplastics to marine planktonic species Dunaliella tertiolecta and Artemia franciscana. Aquat. Toxicol. 189, 159–169. https://doi.org/10.1016/j.aquatox.2017.06.008.

Bonarska-Kujawa, D., Pruchnik, H., Oszmiański, J., Sarapuk, J., Kleszczyńska, H., 2011. Changes Caused by Fruit Extracts in the Lipid Phase of Biological and Model Membranes. Food Biophys 6 (1), 58–67. https://doi.org/10.1007/s11483-010-9175-y.

Bradford, M.M., 1976. A rapid and sensitive method for the quantitation of microgram quantities of protein utilizing the principle of protein-dye binding. Anal Biochem 72, 248–254. https://doi.org/10.1006/abio.1976.9999.

Chambers, E., Mitragotri, S., 2004. Prolonged circulation of large polymeric nanoparticles by non-covalent adsorption on erythrocytes. J. Control. Release 100, 111–119. https://doi.org/10.1016/j.jconrel.2004.08.005.

Cole, M., Galloway, T.S., 2015. Ingestion of Nanoplastics and microplastics by Pacific oyster larvae. Environ. Sci. Technol. 49, 14625–14632. https://doi.org/10.1021/acs.est.5b04099.

Fernandes, E., Soares, T., Gonçalves, H., Bernstorff, S., Real Oliveira, M., Lopes, C., Lúcio, M., 2018. A molecular biophysical approach to diclofenac topical gastrointestinal damage. IJMS 19, 3411. https://doi.org/10.3390/ijms19113411.

Fleury, J.-B., Baulin, V.A., 2021. Microplastics destabilize lipid membranes by mechanical stretching. Proc. Natl. Acad. Sci. U. S. A. 118, e2104610118 https://doi.org/10.1073/pnas.2104610118.

Gaeti, M.P.N., Benfica, P.L., Mendes, L.P., Vieira, M.S., Anjos, J.L.V., Alonso, A., Rezende, K.R., Valadares, M.C., Lima, E.M., 2015. Liposomal entrapment of 4-Nerolidylcatechol: impact on phospholipid dynamics. Drug Stability and Bioactivity. j nanosci nanotechnol 15, 838–847. https://doi.org/10.1166/jnn.2015.9188.

Gopinath, P.M., Saranya, V., Vijayakumar, S., Mythili Meera, M., Ruprekha, S., Kunal, R., Pranay, A., Thomas, J., Mukherjee, A., Chandrasekaran, N., 2019. Assessment on interactive prospectives of nanoplastics with plasma proteins and the toxicological impacts of virgin, coronated and environmentally released-nanoplastics. Sci. Rep. 9, 8860. https://doi.org/10.1038/s41598-019-45139-6.

Hollóczki, O., Gehrke, S., 2020. Can Nanoplastics Alter cell membranes? ChemPhysChem 21, 9–12. https://doi.org/10.1002/cphc.201900481.

Hwang, J., Choi, D., Han, S., Jung, S.Y., Choi, J., Hong, J., 2020. Potential toxicity of polystyrene microplastic particles. Sci. Rep. 10, 7391. https://doi.org/10.1038/s41598-020-64464-9.

Hwang, K.-S., Son, Y., Kim, S.S., Shin, D.-S., Lim, S.H., Yang, J.Y., Jeong, H.N., Lee, B.H., Bae, M.A., 2022. Size-dependent effects of polystyrene nanoparticles (PS-NPs) on behaviors and endogenous neurochemicals in zebrafish larvae. IJMS 23, 10682. https://doi.org/10.3390/ijms231810682.

Jenner, L.C., Rotchell, J.M., Bennett, R.T., Cowen, M., Tentzeris, V., Sadofsky, L.R., 2022. Detection of microplastics in human lung tissue using μFTIR spectroscopy. Sci. Total Environ. 831, 154907 https://doi.org/10.1016/j.scitotenv.2022.154907.

Jiang, B., Kauffman, A.E., Li, L., McFee, W., Cai, B., Weinstein, J., Lead, J.R., Chatterjee, S., Scott, G.I., Xiao, S., 2020. Health impacts of environmental contamination of micro- and nanoplastics: a review. Environ. Health Prev. Med. 25, 29. https://doi.org/10.1186/s12199-020-00870-9.

Kelpsiene, E., Ekvall, M.T., Lundqvist, M., Torstensson, O., Hua, J., Cedervall, T., 2022. Review of ecotoxicological studies of widely used polystyrene nanoparticles. Environ. Sci.: Processes Impacts 24, 8–16. https://doi.org/10.1039/D1EM00375E.

Kik, K., Bukowska, B., Sicińska, P., 2020. Polystyrene nanoparticles: sources, occurrence in the environment, distribution in tissues, accumulation and toxicity to various organisms. Environ. Pollut. 262, 114297 https://doi.org/10.1016/j.envpol.2020.114297.

Kik, K., Bukowska, B., Krokosz, A., Sicińska, P., 2021. Oxidative properties of polystyrene nanoparticles with different diameters in human peripheral blood mononuclear cells (in vitro study). IJMS 22, 4406. https://doi.org/10.3390/ijms22094406.

Kim, M.J., Shin, S., 2014. Toxic effects of silver nanoparticles and nanowires on erythrocyte rheology. Food Chem. Toxicol. 67, 80–86. https://doi.org/10.1016/j.fct.2014.02.006.

Klemeš, J.J., Fan, Y.V., Tan, R.R., Jiang, P., 2020. Minimising the present and future plastic waste, energy and environmental footprints related to COVID-19. Renew. Sust. Energ. Rev. 127, 109883 https://doi.org/10.1016/j.rser.2020.109883.

Koter, M., Franiak, I., Strychalska, K., Broncel, M., Chojnowska-Jezierska, J., 2004. Damage to the structure of erythrocyte plasma membranes in patients with type-2 hypercholesterolemia. Int. J. Biochem. Cell Biol. 36, 205–215. https://doi.org/10.1016/s1357-2725(03)00195-x.

Kuhlman, R.L., 2022. Letter to the editor, discovery and quantification of plastic particle pollution in human blood. Environ. Int. 167, 107400 https://doi.org/10.1016/j.envint.2022.107400.

Lehner, R., Weder, C., Petri-Fink, A., Rothen-Rutishauser, B., 2019. Emergence of Nanoplastic in the environment and possible impact on human health. Environ. Sci. Technol. 53, 1748–1765. https://doi.org/10.1021/acs.est.8b05512.

Leslie, H.A., van Velzen, M.J.M., Brandsma, S.H., Vethaak, A.D., Garcia-Vallejo, J.J., Lamoree, M.H., 2022. Discovery and quantification of plastic particle pollution in human blood. Environ. Int. 163, 107199 https://doi.org/10.1016/j.envint.2022.107199.

Li, S.-Q., Zhu, R.-R., Zhu, H., Xue, M., Sun, X.-Y., Yao, S.-D., Wang, S.-L., 2008. Nanotoxicity of TiO2 nanoparticles to erythrocyte in vitro. Food Chem. Toxicol. 46, 3626–3631. https://doi.org/10.1016/j.fct.2008.09.012.

Li, R., Cheng, M., Cui, Y., He, Q., Guo, X., Chen, L., Wang, X., 2020. Distribution of the soil PAHs and health risk influenced by coal usage processes in Taiyuan City. Northern China. IJERPH 17, 6319. https://doi.org/10.3390/ijerph17176319.

Loos, C., Syrovets, T., Musyanovych, A., Mailänder, V., Landfester, K., Nienhaus, G.U., Simmet, T., 2014. Functionalized polystyrene nanoparticles as a platform for studying bio–nano interactions. Beilstein J. Nanotechnol. 5, 2403–2412. https://doi.org/10.3762/bjnano.5.250.

Lu, Y., Zhang, Y., Deng, Y., Jiang, W., Zhao, Y., Geng, J., Ding, L., Ren, H., 2016. Uptake and accumulation of polystyrene microplastics in zebrafish (*Danio rerio*) and toxic effects in liver. Environ. Sci. Technol. 50, 4054–4060. https://doi.org/10.1021/acs.est.6b00183.

Malinowska, K., Bukowska, B., Piwoński, I., Foksiński, M., Kisielewska, A., Zarakowska, E., Gackowski, D., Sicińska, P., 2022. Polystyrene nanoparticles: the mechanism of their genotoxicity in human peripheral blood mononuclear cells. Nanotoxicology 1–21. https://doi.org/10.1080/17435390.2022.2149360.

Mattsson, K., Hansson, L.-A., Cedervall, T., 2015. Nano-plastics in the aquatic environment. Environ. Sci.: Processes Impacts 17, 1712–1721. https://doi.org/10.1039/C5EM00227C.

Mitrano, D.M., Wick, P., Nowack, B., 2021. Placing nanoplastics in the context of global plastic pollution. Nat. Nanotechnol. 16, 491–500. https://doi.org/10.1038/s41565-021-00888-2.

O'Neill, S.M., Lawler, J., 2021. Knowledge gaps on micro and nanoplastics and human health: a critical review. Case Studies in Chemical and Environmental Engineering 3, 100091. https://doi.org/10.1016/j.cscee.2021.100091.

Plastics Europe, 2022. https://plasticseurope.org/media/backgrounder-plastics-the-facts-2022/.

Poojari, C., Wilkosz, N., Lira, R.B., Dimova, R., Jurkiewicz, P., Petka, R., Kepczynski, M., Róg, T., 2019. Behavior of the DPH fluorescence probe in membranes perturbed by drugs. Chem. Phys. Lipids 223, 104784. https://doi.org/10.1016/j.chemphyslip.2019.104784.

Ragusa, A., Svelato, A., Santacroce, C., Catalano, P., Notarstefano, V., Carnevali, O., Papa, F., Rongioletti, M.C.A., Baiocco, F., Draghi, S., D'Amore, E., Rinaldo, D., Matta, M., Giorgini, E., 2021. Plasticenta: first evidence of microplastics in human placenta. Environ. Int. 146, 106274 https://doi.org/10.1016/j.envint.2020.106274.

Ramsperger, A.F.R.M., Jasinski, J., Völkl, M., Witzmann, T., Meinhart, M., Jérôme, V., Kretschmer, W.P., et al., 2022. Supposedly Identical Microplastic Particles Substantially Differ in Their Material Properties Influencing Particle-Cell Interactions and Cellular Responses. J. Hazard. Mater. 425, 127961. https://doi.org/10.1016/j.jhazmat.2021.127961.

Rawat, N., Singla-Pareek, S.L., Pareek, A., 2021. Membrane dynamics during individual and combined abiotic stresses in plants and tools to study the same. Physiol. Plant. 171, 653–676. https://doi.org/10.1111/ppl.13217.

Rossi, G., Barnoud, J., Monticelli, L., 2014. Polystyrene nanoparticles perturb lipid membranes. J. Phys. Chem. Lett. 5, 241–246. https://doi.org/10.1021/jz402234c.

Salvia, R., Rico, L.G., Bradford, J.A., Ward, M.D., Olszowy, M.W., Martínez, C., Madrid-Aris, Á.D., Grífols, J.R., Ancochea, Á., Gomez-Muñoz, L., Vives-Pi, M., Martínez-Cáceres, E., Fernández, M.A., Sorigue, M., Petriz, J., 2023. Fast-screening flow cytometry method for detecting nanoplastics in human peripheral blood. MethodsX 10, 102057. https://doi.org/10.1016/j.mex.2023.102057.

Sana, S.S., Dogiparthi, L.K., Gangadhar, L., Chakravorty, A., Abhishek, N., 2020. Effects of microplastics and nanoplastics on marine environment and human health. Environ. Sci. Pollut. Res. 27, 44743–44756. https://doi.org/10.1007/s11356-020-10573-x.

Sarma, D.K., Dubey, R., Samarth, R.M., Shubham, S., Chowdhury, P., Kumawat, M., Verma, V., Tiwari, R.R., Kumar, M., 2022. The biological effects of polystyrene nanoplastics on human peripheral blood lymphocytes. Nanomaterials 12, 1632. https://doi.org/10.3390/nano12101632.

Schwabl, P., Köppel, S., Königshofer, P., Bucsics, T., Trauner, M., Reiberger, T., Liebmann, B., 2019. Detection of various microplastics in human stool: a prospective case series. Ann. Intern. Med. 171, 453–457. https://doi.org/10.7326/M19-0618.

Snell, T.W., Hicks, D.G., 2011. Assessing toxicity of nanoparticles using Brachionus manjavacas (Rotifera). Environ. Toxicol. 26, 146–152. https://doi.org/10.1002/tox.20538.

Stasiuk, M., Kijanka, G., Kozubek, A., 2009. Zmiany kształtu erytrocytów i czynniki je wywołujące. Postępy Biochemii 55, 425–433.

Sun, X.-D., Yuan, X.-Z., Jia, Y., Feng, L.-J., Zhu, F.-P., Dong, S.-S., Liu, J., Kong, X., Tian, H., Duan, J.-L., Ding, Z., Wang, S.-G., Xing, B., 2020. Differentially charged nanoplastics demonstrate distinct accumulation in Arabidopsis thaliana. Nat. Nanotechnol. 15, 755–760. https://doi.org/10.1038/s41565-020-0707-4.

Sze, A., Erickson, D., Ren, L., Li, D., 2003. Zeta-Potential Measurement Using the Smoluchowski Equation and the Slope of the Current-Time Relationship in Electroosmotic Flow. J. Colloid Int. Sci. 261 (2), 402–410. https://doi.org/10.1016/S0021-9797(03)00142-5.

Tallec, K., Blard, O., González-Fernández, C., Brotons, G., Berchel, M., Soudant, P., Huvet, A., Paul-Pont, I., 2019. Surface functionalization determines behavior of nanoplastic solutions in model aquatic environments. Chemosphere 225, 639–646. https://doi.org/10.1016/j.chemosphere.2019.03.077.

Trpkovic, A., Todorovic-Markovic, B., Kleut, D., Misirkic, M., Janjetovic, K., Vucicevic, L., Pantovic, A., Jovanovic, S., Dramicanin, M., Markovic, Z., Trajkovic, V., 2010. Oxidative stress-mediated hemolytic activity of solvent exchange-prepared fullerene (C_{60}) nanoparticles. Nanotechnology 21, 375102. https://doi.org/10.1088/0957-4484/21/37/375102.

Wadhwa, R., Aggarwal, T., Thapliyal, N., Kumar, A., Priya Yadav, P., Kumari, V., Reddy, B.S.C., Chandra, P., Maurya, P.K., 2019. Red blood cells as an efficient in vitro model for evaluating the efficacy of metallic nanoparticles. 3 Biotech 9, 279. https://doi.org/10.1007/s13205-019-1807-4.

Wang, T., Bai, J., Jiang, X., Nienhaus, G.U., 2012. Cellular uptake of nanoparticles by membrane penetration: a study combining confocal microscopy with FTIR spectroelectrochemistry. ACS Nano 6, 1251–1259. https://doi.org/10.1021/nn203892h.

Xu, M., Halimu, G., Zhang, Q., Song, Y., Fu, X., Li, Yongqiang, Li, Yansheng, Zhang, H., 2019. Internalization and toxicity: a preliminary study of effects of nanoplastic particles on human lung epithelial cell. Sci. Total Environ. 694, 133794 https://doi.org/10.1016/j.scitotenv.2019.133794.

Zając, M., Kotyńska, J., Worobiczuk, M., Breczko, J., Naumowicz, M., 2022. The effect of submicron polystyrene on the electrokinetic potential of cell membranes of red blood cells and platelets. Membranes 12, 366. https://doi.org/10.3390/membranes12040366.

scientific reports

Check for updates

OPEN

The interactions of non-functionalized polystyrene nanoparticles with human albumin and erythrocyte proteins: implications and potential consequences

Kamil Płuciennik[1,2], Mariusz Szabelski[3], Katarzyna Miłowska[4], Karol Ciepluch[5], Piotr Duchnowicz[1], Anita Krokosz[1], Paulina Sicińska[1] & Bożena Bukowska[1]✉

The aim of the study was to determine the concentration- and size-dependent effects of ~30 nm, ~45 nm and ~70 nm non-functionalized polystyrene nanoparticles (PS-NPs) on human serum albumin (HSA) and human erythrocyte proteins in vitro. . HSA or human erythrocytes were exposed to PS-NPs at concentrations ranging from 0.001 to 100 µg/mL for 24 h. Any resulting changes in HSA secondary structure were investigated using circular dichroism (CD), fluorescence spectrum analysis, and fluorescence lifetime measurements. Incubation with 50 µg/mL and 100 µg/mL PS-NPs resulted in an increase in the hydrodynamic diameter of PS-NPs and caused significant alterations in HSA secondary structure for all tested nanoparticle sizes. Additionally, treatment with the ~30 nm and ~45 nm PS-NPs resulted in a more intense HSA fluorescence signal and changes in mean fluorescence lifetimes, indicating interactions between PS-NPs and HSA. Incubation with PS-NPs (0.1–1 µg/mL) also led to significant changes in relative viscosity and increased protein carbonyl content in erythrocytes (10–100 µg/mL); however, no significant changes in acetylcholinesterase (AChE) activity or methemoglobin levels were observed. The study confirms that non-functionalized polystyrene nanoparticles influence the structure and functional properties of human plasma and erythrocyte proteins under in vitro conditions, and their effects are clearly dependent on the size and concentration of the nanoparticles. It is likely that PS-NPs can modify the structure of albumin, which may indirectly potentiate plastic-related damage to erythrocytes in vivo. The potential influence of albumin modified by plastic particles on the properties of human erythrocytes in vivo was discussed.

Keywords Acetylcholinesterase, Albumin, Fluorescence, Methemoglobin, Nanoplastic, Protein oxidation, Secondary structure

It is estimated that global production of plastics will triple by 2060[1]. This poses a serious problem for the environment, as it is estimated that 75 to 79% of waste ends up in landfills[2]. While most data regarding environmental pollution concerns the seas and oceans, which receive 10 to 20 million tons of plastic annually[3]soils also receive large amounts of plastic pollution; this can be an equally serious problem, especially for agricultural soils[1].

[1]Department of Biophysics of Environmental Pollution, Faculty of Biology and Environmental Protection, University of Lodz, Pomorska 141/143, 90- 236 Lodz, Poland. [2]Doctoral School of Exact and Natural Sciences, University of Lodz, ul. Jana Matejki 21/23, 90-237 Lodz, Poland. [3]Department of Physics And Biophysics, Faculty of Food Science, University of Warmia and Mazury, 10-719 Olsztyn, Poland. [4]Department of General Biophysics, Faculty of Biology and Environmental Protection, University of Lodz, Pomorska 141/143, 90-236 Lodz, Poland. [5]Department of Basic Medical Sciences, Faculty of Medical Sciences and Health, Casimir Pulaski University of Radom, 26-600 Radom, Poland. ✉email: bozena.bukowska@biol.uni.lodz.pl

Plastic particles have been detected both in bodily excretions, i.e. feces[4] and urine[5]and in secretions, e.g. semen[6]. They are also present in human tissues, such as the lungs[7,8]colon[9]placenta[10]veins[11] and heart[12]. Most worryingly, plastic particles with diameters of 100–200 nm have been identified in human brain biopsy specimens, with the median mass being 4917 µg/g in 2024: a significantly increase compared to 3345 µg/g determined in 2016[13]. Micro- and nanoparticles concentrations in brain samples of healthy deceased were 7–30 times higher than concentrations observed in liver or kidney tissue. In addition, the plastic particle level was found to be higher in a cohort of brains from individuals with a documented diagnosis of dementia, with noticeable deposition recorded in the walls of brain vessels and immune cells.

Due to the increasingly widespread detection of plastic particles in human tissues, increasing research is being directed toward determining their effects on human health. Blood is of particular interest as a research medium as it can facilitate the entry of plastic into other cells and tissues, and indeed, numerous studies have concerned the presence of plastic particles in human blood[14–17]. Leonard et al. found microplastics to be present in 18 of 20 subjects, among whom the entire spectrum of 24 different plastics was detected, with the predominant plastic being polyethylene (4.65 µg/mL of blood)[17]. Another study showed the presence of microplastic particles in 32 of 36 volunteers (88.9%), with the mean number of particles being 4.2 per mL of blood tested; various microplastic particles were found, but the predominant form was polystyrene. Other studies have noted a link between the amount of plastic food packaging in the refrigerator and the amount of plastic particles in the blood[14]and have identified concentrations of plastic particles as high as 10 µg/mL in blood[15].

Due to methodological limitations, little data exists on the presence of plastic nanoparticles in human blood; however, a 2023 study on a Spanish population showed the presence of plastic nanoparticles in the blood of all 196 people tested, regardless of age and health status. Their results suggest that nanoplastics may account for as much as 99.7 to 99.9% of all plastic particles in human blood[16].

As blood and plasma contain a range of morphotic components that are essential in maintaining the physiological functions of the human body, it is very important to determine the possible influence of plastic particles . Previous studies have shown that plastic particles can interact with mononuclear human blood cells and erythrocytes, and that polystyrene nanoparticles can cause oxidative stress[18] and DNA single- and double-strand breaks[19]; in PBMCS, they can also induce apoptosis[20] and have cytotoxic effects[18,19]. The plastic particles typically exert their negative effects on nucleated cells by inducing oxidative stress and causing damage to the mitochondrial membrane[18,20].

Plastic nanoparticles are able to adhere to the surface of erythrocytes, the main cells of the blood system, leading to adverse effects related to erythrocyte aggregation and adhesion to blood vessels[21]. A study of the effects of polystyrene nanoparticles of different diameters (~30 nm, ~45 nm and ~70 nm) on hemolysis and cell morphology found the smallest nanoparticles (~30 nm) to have the greatest hemolytic effects[22]. This was probably due to the fact that these nanoparticles were packed more closely on a specific membrane surface and thus had a stronger interaction with plasma membrane components than the larger particles. In contrast, the largest particles (~70 nm) induced a change in shape from physiological discocytes to stomatocytes, even at the lowest concentrations tested, indicating that the larger particles had a strong physical interaction of with the cell membrane of the red blood cells.

Erythrocytes demonstrate considerable mechanical stability and deformability in vivo; this allows them to traverse capillaries with high levels of shear stress, which can reach values as high as 10 Pa in extreme conditions such as elevated cardiac output or hypertension[23,24]. This mechanical resilience is primarily maintained by human serum albumin (HSA), which preserving the shape, membrane integrity and deformability of red blood cells, and their resistance to shear-induced hemolysis[25,26]. Furthermore, HSA plays a regulatory role in metal ion homeostasis (e.g., Zn^{2+} transport), which influences hemoglobin function and overall erythrocyte physiology[27]. Albumin is characterized by *inter alia* biocompatibility, biodegradability, non-immunogenicity, long half-life, minimal toxicity, good stability and good reactivity[28]. Hence, it has a number of very important functions, such as the maintenance of osmotic pressure in blood vessels, i.e., maintenance of the tension and volume of blood vessels by regulating water pressure, and protecting the vascular endothelium[29]and supporting the transport, delivery, and removal of drugs, as well as uptake, storage and removal of potentially-harmful biological products, such as bilirubin, hormones, metals and vitamins. In addition, HSA binds free fatty acids, which can induce apoptosis of vascular smooth muscle cells, uncouple endothelial NO synthase and reduce endothelium-dependent vasodilation[30]. Furthermore, thanks to the presence of the thiol group Cys34, albumin can neutralize free radicals and reduce oxidative stress by scavenging reactive oxygen and nitrogen species[31,32]. Albumin can also buffer blood pH by neutralizing excess hydrogen ions, thus maintaining a stable environment for enzymes and other proteins in organisms[32,33].

The aim of this study was to examine the effects of polystyrene nanoparticles (PS-NPs) in human serum albumin (HSA), a model plasma protein, and erythrocyte proteins, representing a complex cellular system; although these proteins represent two complementary biological systems, they have seldom been jointly analysed to date. While previous research has typically focused either on isolated proteins (e.g., HSA, hemoglobin) or entire cells, the approach used in the present study encompasses both with the aim of identifying shared mechanisms of nanoparticle-induced toxicity and biointeractions. As HSA and erythrocytes are essential blood components and primary targets of nanoparticle exposure under in vivo conditions, their combined analysis allows for a more comprehensive mechanistic insight into how PS-NPs influence protein structure and function across different levels of biological complexity. Furthermore, given that conformational changes in albumin can potentially compromise membrane integrity by altering red blood cell stability, this study also discusses how PS-NP-induced alterations in HSA may modulate erythrocyte properties.

The study examines whether plastic particles can damage the free plasma proteins, such as albumin, resulting in protein corona formation, changes in secondary structure, fluorescence and lifetimes. The work also examines the influence of the particles on erythrocyte proteins by analyzing carbonyl group and methemoglobin levels,

acetylcholinesterase activity and erythrocyte intrinsic viscosity. We used a wide range of concentrations , ranging from 0.001 to 10 µg/mL, which can be found in humans [15,17,] up to high concentration of 100 µg/mL, to assess potential toxic effects.

Materials and methods

Reagents

Human serum albumin (purity ≥ 98%) was purchased from Sigma-Aldrich (Saint Louis, Mi, USA); non-functionalized PS-NPs of varying diameters (~ 30 nm, ~ 45 nm, and ~ 70 nm) were acquired from Bangs Laboratories (Fishers, Indiana, USA). A 1 g unit of individual nanoparticles contained the following: 7458×10^{16} nanoparticles/g (~ 30 nm); 2.842×10^{16} particles/g (~ 45 nm); 5.785×10^{15} particles/g (~ 70 nm). The carbonyl fluorometric assay kit was purchased from Cayman MI USA no. 701530-96. Phosphate buffer solutions with pH = 7.4 were used to prepare HSA and PSNP dilutions.

Physicochemical characterization of PS-NPs

The ζ-potential of the analysed non-functionalized PS-NPs, measured in water by our team, was negative, with values of − 40 ± 1 mV, − 38 ± 1 mV, and − 36 ± 1 mV for nanoparticles of approximately ~ 30 nm, ~ 45 nm, and ~ 70 nm, respectively[19]. However, when measured in Ringer's buffer, i.e. the medium in which erythrocytes are incubated, the ζ-potential varied depending on particle size: −29.68 ± 2.15 mV for the smallest particles (~ 30 nm), − 35.03 ± 3.31 mV for particles ~ 45 nm, and − 42.0 ± 1.52 mV for the largest particles (~ 70 nm)[22]. DLS measurements in water confirmed the particle sizes declared by the manufacturers[19]. Previous research based on a combination of AFM and SEM imaging found PS nanoparticles to predominantly form densely-packed aggregates due to strong interparticle and surface interactions, although individual particles were also occasionally observed[19].

Non-functionalized polystyrene nanoparticles (PS-NPs) are composed mainly of neutral, hydrophobic carbon chains and have limited surface charge: their surfaces lack specific functional groups. Their hydrophobic nature promotes protein adsorption via hydrophobic interactions, initiating the formation of a protein corona[34]. While the absence of functional groups limits specific chemical bonding, it does not prevent the physicochemical adsorption of albumin.

Dynamic light scattering

Particle size distribution was determined on a Anton Paar Particle Analyzer Litesizer™ 500. PS nanoplastics and HSA were diluted in PBS buffer (pH 7.4). The analysis was conducted under at a wavelength of 658 nm and measuring angles of 15°, 90°, and 175°. To measure the particle size, 1 mL of the PS solution (concentration 100 µg/mL) with different concentrations of HSA was placed in a polystyrene cuvette and measured at 25 °C. This process was repeated three times.

Circular dichroism (CD)

The circular dichroism spectra of HSA, in the presence or absence of PS-NPs, were measured using a Jasco J-815 CD spectropolarimeter (Jasco International Co., Ltd., Tokyo, Japan). The following conditions were used: measurement range 195–260 nm, 5 mm path-length quartz cuvettes. wavelength step of 1 nm, response time of 4 s, scan rate of 20 nm/min, with the temperature maintained at 25 °C. Each spectrum was taken as the mean of three repetitions and was analyzed for the content of α-helix and β-sheet structures using the *CDNN* software (Applied Photophysics, Leatherhead, UK). In this experiment, changes in the secondary structure of HSA in the presence and absence of PS-NPs were studied after 24 h of incubation at 37 °C. The CD spectra of the nanoparticles alone, at the same concentrations used in the HSA experiments, were recorded and used as baselines. These baseline spectra were automatically subtracted from those of the HSA–NPs complexes using CD analysis software. As such, the detected spectral changes reflect conformational modifications in HSA exclusively, without interference from the nanoparticles.

Steady state and time-resolved fluorescence measurements

All fluorescence spectroscopy measurements were carried out at 25 °C in a 1 × 1 cm quartz cuvette using the right-angle geometry. Emission spectra were measured using excitation wavelength 280 nm on a Varian Cary Eclipse Fluorescence Spectrophotometer, Agilent Technologies, Santa Clara, CA, USA. The study used solutions containing 2 µmol/L of HSA and 10 µg/mL of PS-NPs in PBS buffer. For each type of nanoparticle, at least three fluorescence spectrum measurements were taken and the results were averaged. The fluorescence emission decays were determined using a PicoQuant FluoTime 300 spectrometer equipped with an R3809U-50 microchannel plate photomultiplier MCP-PMT and a TimeHarp 260 PICO TCSPC module. The source of excitation was the SuperK EXTREME EXR-20 with a Super EXTEND-UV unit (Deep UV model, tuning range 265–345 nm) from NKT Photonics. The excitation wavelength was set at 280 nm and observation wavelength at 330 nm. The instrument response function (IRF) was recorded with Ludox, showing full width at half maximum (FWHM) around 72 ps. The data were analyzed with EasyTau version 2 software (PicoQuant, Germany), using the multiexponential intensity decay model as follows:

$$I(t) = \sum_i \alpha_i exp(-t/\tau_i)$$

where α_i and τ_i are pre-exponential factors and fluorescence lifetimes, respectively.

Erythrocyte isolation

Erythrocytes were isolated from a leukocyte buffy coat separated from blood, purchased from the Regional Center for Blood Donation and Treatment in Lodz; separation was performed according to Płuciennik et al. (2023). Erythrocytes with a hematocrit of 5% (approximately 630 million cells per mL) were incubated with polystyrene nanoparticles at concentrations ranging from 0.001 to 100 µg/mL at 37 °C for 24 h. The study was approved by the Bioethics Committee of the University of Lodz (Resolution No. 12/KEBN-UŁ/I/2022–23).

Internal viscosity of red blood cells

The rotational dynamics of TEMPAMINE (1 mM) were used to determine the internal viscosity of the erythrocytes. To reduce the signal from the spin label, which did not enter the cell, 120 mM $K_3Fe(CN)_6$ was used in the intercellular space. The analysis was conducted using a Brucker 300 ESR Spectrometer. Based on the spectrum obtained for TEMPAMINE in water and in erythrocytes, the rotational correlation time was determined according to the formula:

$$\tau = kW_0 \left[\left(\frac{h_0}{h_1} \right)^{\frac{1}{2}} - 1 \right]$$

where: k—constant for the nitroxide spin label, $k = 6.5 \times 10^{-9}$ s mT^{-1}, h_0—height of the center line, h_{-1}—height of high-field line, W_0—centerline width.

The relative viscosity was determined from the formula:

$$\frac{\tau R}{\tau B} = \frac{\eta C}{\eta B}$$

where: τ_R—rotational correlation time of the marker in erythrocytes, τ_B—rotational correlation time of the marker in PBS,η_C—internal viscosity of erythrocyte, η_B—PBS viscosity (value 1 was assumed).

The changes in the studied parameter were calculated and expressed as percentages of control.

Hemoglobin oxidation

The level of methemoglobin was measured by the Drabkin method[35]. Erythrocytes were incubated with PS-NPs and then treated with deionized water and centrifuged (3000 rpm, 10 min, 4 °C). Methemoglobin was determined by absorbance at 630 nm and 700 nm. Then, to obtain a positive control, a solution containing potassium ferricyanide (1 M Fe^{2+} : 3 M $K_3[Fe(CN)_6]$) was added to the hemolysate containing methemoglobin, and the samples were re-assayed for absorbance at the same wavelengths. The percentage share of methemoglobin was calculated by the following equation:

$$\mathrm{MetHb} \frac{(A_{630-A_{700})}}{(A_{100\%MetHb630} - A_{100\%MetHb700)}} \times 100\%.$$

where: A_{630}—absorbance of Hb in the sample tested at 630 nm, A_{700}—absorbance of Hb in the sample tested at 700 nm, $A_{100\%metHb630}$—absorbance of Hb at 630 nm after treatment with potassium ferricyanide, $A_{100\%metHb700}$—absorbance of Hb at 700 nm after treatment with potassium ferricyanide.

Activity of acetylcholinesterase

Acetylcholinesterase (AChE) activity was determined using the Ellman method[36] based on its potential to hydrolyse acetylthiocholine iodide. The erythrocyte suspension was diluted with phosphate buffer (pH 8) to a final hematocrit value of 0.05%, and 20 µL of 5,5'-dithio-bis-2-nitrobenzoic acid (DTNB) was added to 2 mL of the erythrocyte solution. The absorbance slope was measured over one minute at a wavelength of $\lambda = 412$ nm. The unit of AChE activity was defined as the amount of micromoles of acetylthiocholine hydrolyzed per minute by AChE present in 1 mL of erythrocytes at 100% hematocrit (packed cells).

Preparation of erythrocyte ghosts

Erythrocyte membranes were prepared according to Dodge et al. (1963), with modifications. The erythrocytes were hemolysed in 20 mM phosphate buffer, pH 7.4, containing 1 mM EDTA and 2% PMSF in ethanol as proteolytic inhibitors, and then centrifuged at 13,000 rpm for 15 min at 4 °C. The samples were subsequently washed several times under the same conditions with 10 mM phosphate buffer containing 1 mM EDTA, followed by washing with 5 mM buffer until hemoglobin was fully released. Protein concentration was determined using the Lowry method, with bovine serum albumin as a standard.

Protein carbonyl measurement The levels of oxidized proteins in tissue can be used as an indicator of oxidative stress. Protein carbonyl levels in the erythrocytes ghosts were measured using the commercial protein carbonyl fluorometric assay kit (Cayman Chemical Company, MI, USA). This test is based on the reaction of protein carbonyls with rhodamine B hydrazide (RBH), which leads to the production of protein carbonyl-RBH-hydrazone, whose fluorescence (at ex/em 560/585 nm) is greatly enhanced by guanidine-HCl.

Statistical analysis

Differences in the analysed parameters among erythrocytes following exposure to PS-NPs (29 nm, 44 nm and 72 nm) were assessed using analysis of variance. Depending on the distribution of variables, either the one-way

ANOVA test or the Kruskal–Wallis test was applied. For multiple comparisons, either Tukey's test or Dunn's test was used as a *post hoc* test. Statistical significance was set at $p < 0.05$. All analyses were performed with GraphPad Prism 8 software (GraphPad Software, San Diego, CA, USA).

Results

The effect of PS-NPs on model protein albumin (HSA)

Dynamic light scattering of PS-NPs incubated with HSA

The hydrodynamic diameter of the studied PS nanoparticles (~30, ~45 and ~70 nm at the concentration 100 µg/mL) with increasing HSA concentration is shown in Fig. 1. In the case of PS nanoparticles with a size of about ~30 nm, the obtained results are about ~24 ± 6 nm. The addition of HSA (10 and 50 µg/mL) to the nanoparticle solution did not increase the size; however, the addition of 150 µg/mL HSA resulted in a broadening of the peak, but with a similar maximum of about 24 ± 7 nm. For PS nanoparticles with an overall size of about ~45 nm, the obtained DLS result (volume weight) indicates 33 ± 6 nm. In the presence of 10 µg/mL HSA, the size remains the same. When the HSA concentration reached 50 µg/mL, the size of the PS-HSA complex was

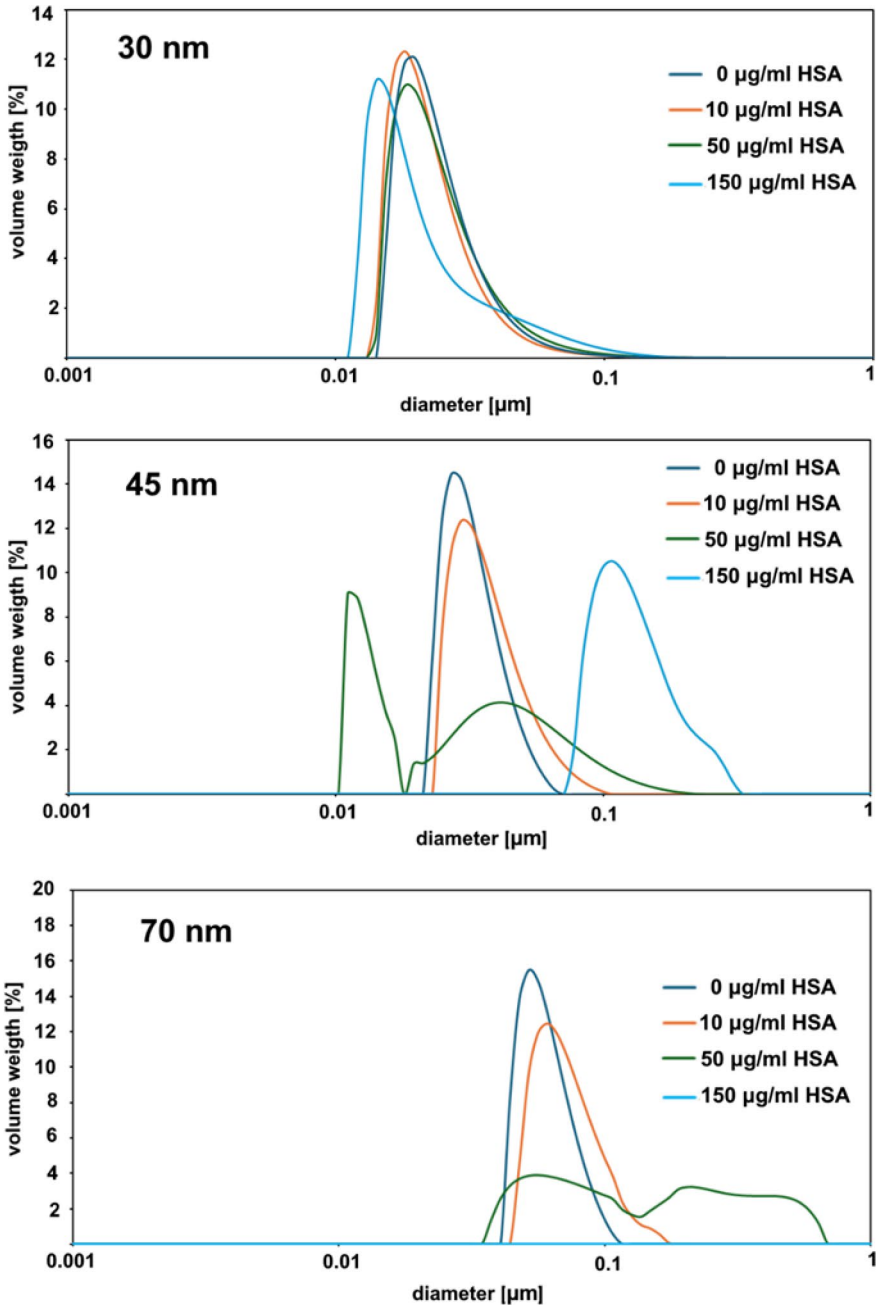

Fig. 1. Size distribution (volume, weight%) of PS nanoparticles (100 µg/mL) with increasing concentration of human serum albumin (HSA) in PBS buffer at 25 °C.

Concentrations of HSA / PS-NPs	0 µg/mL	10 µg/mL	50 µg/mL	150 µg/mL
~ 30 nm	25.4%	27.5%	26.7%	25.0%
~ 45 nm	5.5%	15.9%	22.9%	18.6%
~ 70 nm	3.8%	14.9%	25.0%	30.7%

Table 1. The polydispersity index (PI) of PS-NPs at the concentration 100 µg/mL with increasing concentration of human serum albumin (HSA) in PBS buffer at 25 °C.

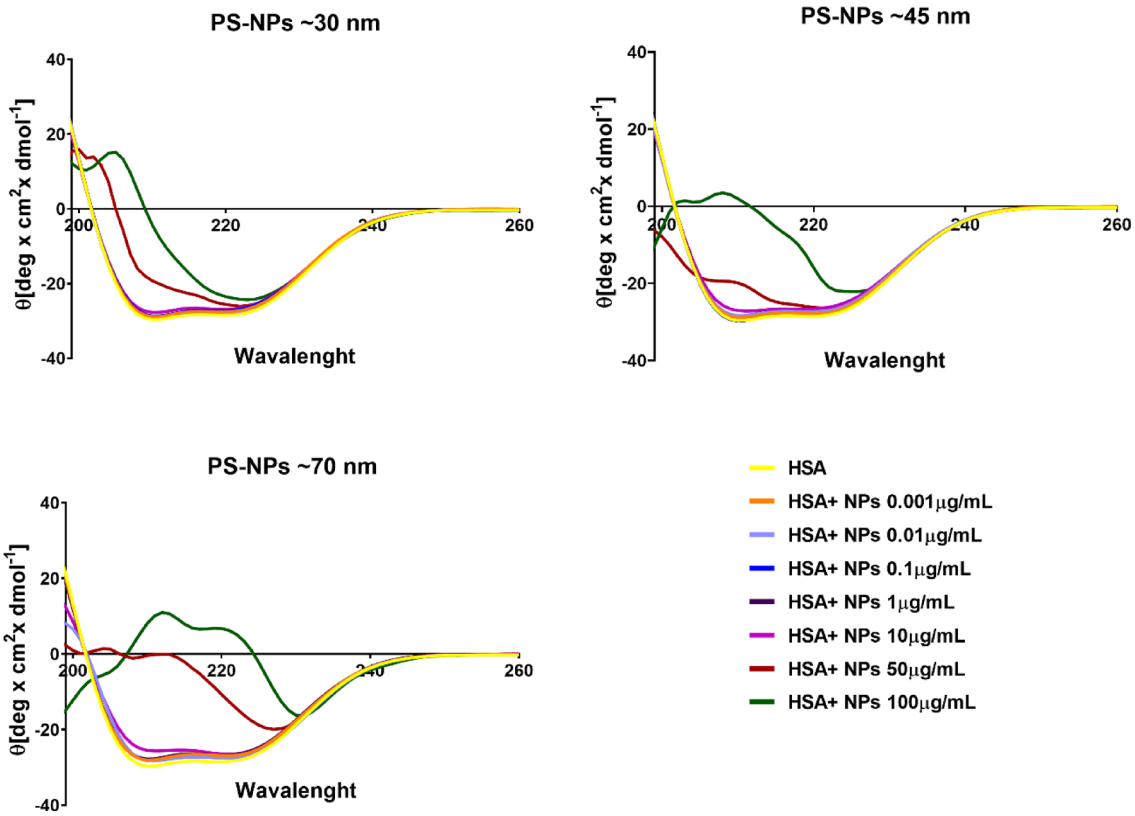

Fig. 2. Circular dichroism spectra (CD) of HSA treated with PS-NPs of ~ 30 nm, ~ 45 nm, and ~ 70 nm in diameter (0.001–100 µg/mL) for 24 h. Data are presented as mean ± SD, $n = 3$ to 6 independent experiments.

found to consist of two populations, one with a size distribution of 52 nm ± 20 nm and a smaller one of about 20 nm; however, this population occupies only 30% of the total volume intensity given by the software. The shape correlation function in this case indicates a very inhomogeneous sample.

For the highest HSA concentration (150 µg/mL), the particle size increases to 136 ± 40 nm. The PS nanoparticles with an overall size of about 70 nm, the size diameter given by the software shows 60 ± 10 nm. The presence of 10 µg/mL HSA slightly increases the size to 74 ± 16 nm. When the HSA concentration reaches 50 µg/mL, two populations with a size distribution of 70 ± 18 nm and 228 ± 50 nm can be observed, suggesting a very inhomogeneous sample. For the highest HSA concentration (150 µg/mL) the size is no longer measured due to the very large aggregates visible to the naked eye in the cuvette.

The polydispersity index (PI) of the studied suspensions was also evaluated. It was found that the samples were polydisperse after the addition of albumins, whereas the nanoparticle suspensions themselves exhibited polydispersity in the case of the ~ 30 nm nanoparticles, and monodispersity for the ~ 45 nm and ~ 70 nm nanoparticles (Table 1).

Circular dichroism

The changes occurring in the secondary structure of proteins incubated with PS-NPs were determined by circular dichroism (CD). Significant alterations in HSA secondary structure were observed for all sizes of tested non-functionalized PS-NP (~ 30 nm, ~ 45 nm, ~ 70 nm) at the two highest concentrations (50 µg/mL and 100 µg/mL) (Fig. 2). At these concentrations, a decrease in the amount of the α-helix structure was observed, from 60.86 ± 4.36 in the control sample to 45.38 ± 3.93* for ~ 30 nm NPs, 44.84 ± 11.73* for ~ 45 nm NPs, and 30.23 ± 2.74* at ~ 70 nm NPs at 50 µg/mL. For 100 µg/mL, the respective values were 25.26 ± 6.38*, 17.87 ± 6.46*, and 17.56 ± 1.96* (Table 2). A slight increase in the β-sheet structure was also observed, with values rising from

Concentration µg/mL	Helix	Antiparallel	Parallel	Beta-Turn	Rdm. coil
Control	60.86 ± 4.36	3.54 ± 0.54	3.96 ± 0.53	12.72 ± 0.61	17.56 ± 2.01
PS-NPs ~ 30 nm					
0.001	60.10 ± 1.51	3.63 ± 0.15	4.03 ± 0.15	12.87 ± 0.21	17.80 ± 0.62
0.01	61.37 ± 2.54	3.47 ± 0.32	3.90 ± 0.27	12.67 ± 0.32	17.27 ± 1.01
0.1	59.00 ± 0.92	3.73 ± 0.15	4.20 ± 0.10	12.97 ± 0.12	18.47 ± 0.40
1	60.57 ± 1.48	3.57 ± 0.15	4.00 ± 0.20	12.83 ± 0.06	17.70 ± 0.66
10	58.00 ± 0.10	3.87 ± 0.06	4.30 ± 0.00	13.10 ± 0.00	18.87 ± 0.12
50	45.38 ± 3.93*	5.23 ± 0.72	6.85 ± 1.32	14.10 ± 0.76	30.18 ± 7.15*
100	25.26 ± 6.38*	9.80 ± 2.19*	13.18 ± 3.23*	16.86 ± 1.16*	48.32 ± 7.66*
PS-NPs ~ 45 nm					
0.001	60.53 ± 3.23	3.57 ± 0.40	3.97 ± 0.40	12.77 ± 0.40	17.67 ± 1.48
0.01	59.17 ± 2.62	3.73 ± 0.35	4.13 ± 0.35	12.93 ± 0.35	18.20 ± 1.21
0.1	62.00 ± 1.99	3.43 ± 0.23	3.83 ± 0.23	12.57 ± 0.29	17.00 ± 0.87
1	57.20 ± 9.40	4.03 ± 1.21	4.50 ± 1.25	13.23 ± 1.25	19.40 ± 4.50
10	56.80 ± 9.11	4.07 ± 1.16	4.53 ± 1.21	13.27 ± 1.20	19.53 ± 4.31
50	44.84 ± 11.73*	6.10 ± 2.07	6.30 ± 2.02	14.92 ± 1.51*	25.38 ± 6.45
100	17.87 ± 6.46*	14.37 ± 3.93*	16.50 ± 4.60*	19.27 ± 1.69*	52.50 ± 9.11*
PS-NPs ~ 70 nm					
0.001	58.60 ± 2.30	3.80 ± 0.28	4.20 ± 0.28	13.00 ± 0.28	18.60 ± 1.31
0.01	56.00 ± 3.47	4,06 ± 0.51	4.56 ± 0.42	13.27 ± 0.51	19.93 ± 1.12
0.1	57.90 ± 4.28	3.80 ± 0.61	4.34 ± 0.50	13.00 ± 0.61	19.17 ± 1.55
1	58.90 ± 0.90	3.75 ± 0.015	4.20 ± 0.10	13.00 ± 0.10	18.50 ± 0.40
10	58.05 ± 0.35*	3.85 ± 0.05	4.30 ± 0.00	13.15 ± 0.05	18.75 ± 0.15
50	30.23 ± 2.74*	10.33 ± 1.59*	7.83 ± 0.29*	18.17 ± 1.18*	26.23 ± 1.01*
100	17.56 ± 1.96*	13.96 ± 1.26*	16.06 ± 1.34*	19.20 ± 0.50*	52.37 ± 2.72*

Table 2. Composition of the secondary structure of HSA exposed to PS-NPs studied. (*) Significantly different from control $p < 0.05$.

12.72 ± 0.61 in the control sample to 16.86 ± 1.16* (~ 30 nm NPs), 19.27 ± 1.69* (~ 45 nm), and 19.20 ± 0.50* (~ 70 nm) at a concentration of 100 µg/mL. Moreover, at concentrations of 50 and 100 µg/mL, the random coil increased for each tested nanoparticle.

Fluorescence of HSA

The HSA protein structure includes 1 Trp and 18 Tyr, both of which are able to absorb and emit light from the UV range; their spectra and excited state lifetimes depend on the microenvironment. The fluorescence emission spectra were measured for both HSA alone and solutions containing a mixture of HSA and PS-NPs (Fig. 3). The results reveal an increase in Tyr and Trp UV emission in HSA in the presence of PS-NPs of ~ 30 nm and ~ 45 nm, with the greatest increase in fluorescence seen for the smallest particles; no change in intensity was observed for the solution containing PS-NPs ~ 70 nm. In addition, the fluorescence decay over time was measured for each solution, and the lifetimes of their excited states were determined (Table 3). Similar to the emission spectra, the samples with PS-NPs of ~ 30 nm and ~ 45 nm demonstrated clear changes in mean lifetimes; the largest change was observed for ~30 nm PS-NPs, where it extended by 37 ps compared to the protein alone.

The effect of PS-NPs on erythrocyte proteins

Internal viscosity of human erythrocytes

After 24 h of incubation with erythrocytes and PS-NPs at concentrations ranging from 0.001 to 100 µg/mL, statistically significant alterations in the relative intracellular viscosity were observed for all tested PS-NPs. Notably, significant increases in viscosity were detected for PS-NPs with a diameter of approximately ~ 30 nm starting at a concentration of 0.1 µg/mL, and for particles of approximately ~ 45 nm and ~ 70 nm starting at 1 µg/mL (Fig. 4). The observed effect was dependent on both the concentration and the particle size of the PS-NPs.

Hemoglobin oxidation

After 24 h of incubation of erythrocytes with non-functionalized PS-NPs at concentrations ranging from 0.001 to 500 mg/mL, no increase in met-Hb levels was observed for any nanoparticle type (Fig. 5).

The activity of acetylcholinesterase present in erythrocyte membrane

No statistically significant changes in erythrocyte acetylcholinesterase activity were observed following 24-hour incubation with non-functionalized PS-NPs of ~ 30 nm, ~ 45 nm, and ~ 70 nm in diameter, across the concentration range of 0.001 to 100 µg/mL (Fig. 6).

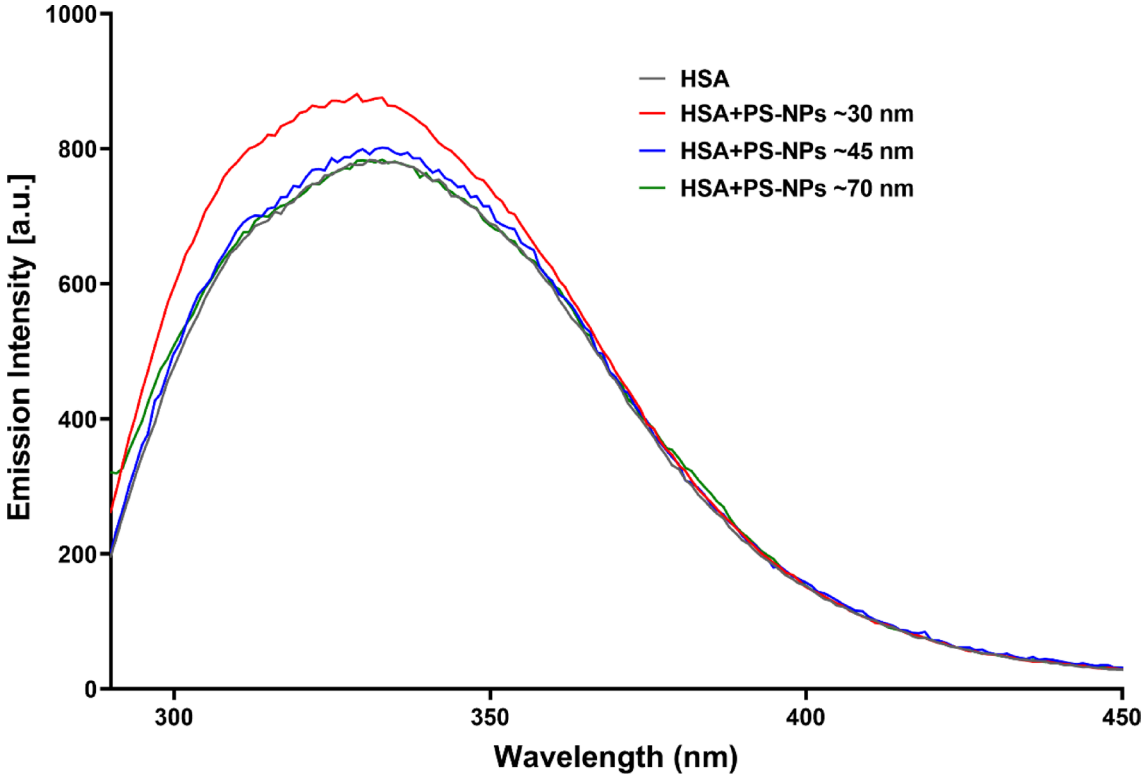

Fig. 3. Fluorescence emission spectra of HSA in the presence of PS-NPs at a concentration of 10 µg/mL were recorded upon excitation at 280 nm.

	τ_1 (ns)	α_1 (%)	τ_2 (ns)	α_2 (%)	τ_3 (ns)	α_3 (%)	$\bar{\tau}$ (ns)
HSA	0.455 ± 0.032	38.6 ± 1.6	2.070 ± 0.130	37.5 ± 0.8	5.890 ± 0.110	24.0 ± 1.1	4.230 ± 0.015
HSA + PS-NP ~ 30	0.439 ± 0.019	37.6 ± 0.8	2.309 ± 0.062	38.5 ± 0.4	5.929 ± 0.083	24.1 ± 1.1	4.267 ± 0.013
HSA + PS-NP ~ 45	0.435 ± 0.030	41.5 ± 1.0	2.230 ± 0.120	37.2 ± 0.5	6.066 ± 0.069	21.5 ± 0.8	4.252 ± 0.014
HSA + PS-NP ~ 70	0.460 ± 0.039	38.8 ± 0.9	2.140 ± 0.110	38.3 ± 0.7	5.966 ± 0.083	23.1 ± 0.9	4.232 ± 0.013

Table 3. Fluorescence lifetime (τ_i), pre-exponential factor (α_i), mean fluorescence lifetime ($\bar{\tau}$) computed for HSA with PS-NPs (10 µg/mL) in PBS buffer.

Protein carbonyl level in the erythrocyte membrane

An increase in protein carbonyl content was observed in erythrocytes incubated for 24 h with polystyrene nanoparticles (PS-NPs), particularly the smallest diameter (~ 30 nm), at a concentration of 10 µg/mL. For PS-NPs with diameters of 45 nm and 72 nm, a significant increase was noted at 100 µg/mL. The mean protein carbonyl level in control samples after 24 h of incubation was 2.78 ± 1.14 nmol/mg protein. The observed effect was dependent on both the concentration and the size of the PS-NPs (Fig. 7).

Discussion

Effect of PS-NPs on the structure of HSA

Nano- and microplastics can form protein-coated complexes with biomolecules, a *protein corona*, which may have unforeseen toxic effects. This corona alters the biological identity of the particles, facilitating their translocation from the bloodstream to organs such as the liver and intestines, and allowing them to interact with erythrocytes and other blood cells[37]. It can also modulate the immune response, enabling plastic particles to evade detection and persist in circulation[37]. Furthermore, the corona affects the physicochemical properties of the particles, including their solubility, agglomeration and cellular interactions[38]thus influencing their transport, uptake, distribution, biotransformation, and toxicity[39,40].

Protein coronas can be *soft* (i.e. loosely-bound proteins) or *hard* (i.e. strongly-adsorbed proteins)[41,42]. Their formation on plastic particles is mainly studied for its impact on toxicity[43,44]. Therefore, the present study examined the hydrodynamic diameter of non-functionalized PS-NPs (~ 30 nm, ~ 45 nm and ~ 70 nm) after

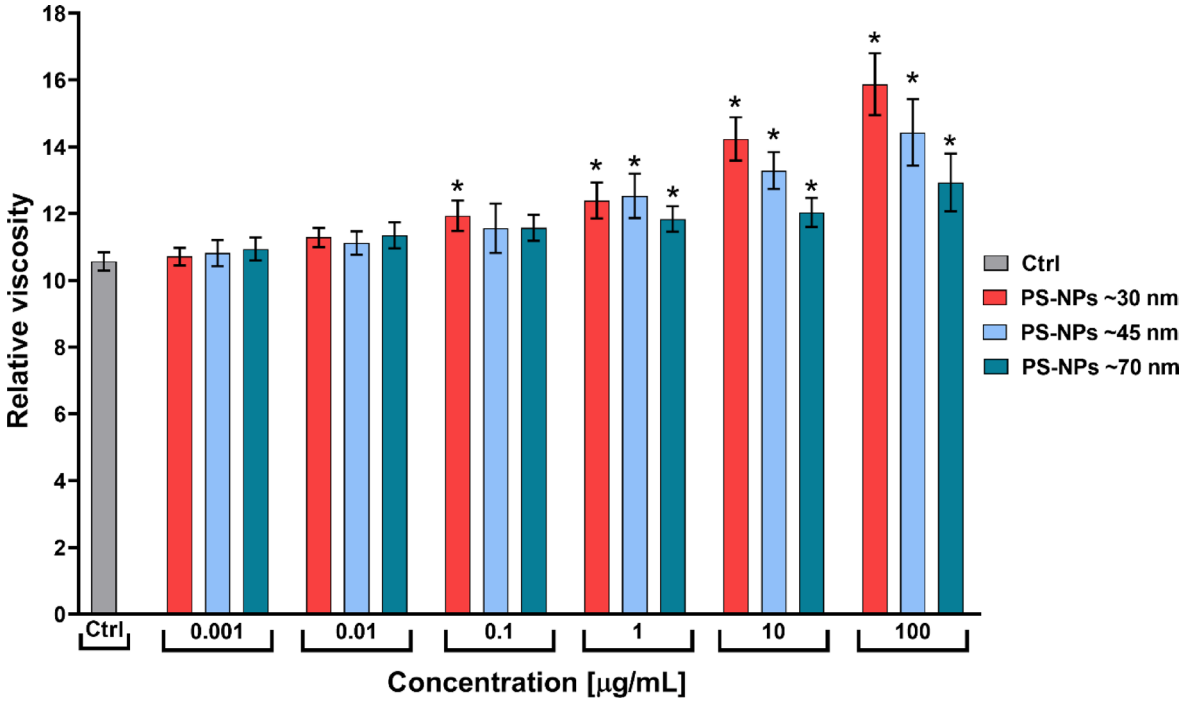

Fig. 4. The relative internal viscosity in control erythrocytes and erythrocytes incubated with PS-NPs of ~30 nm, ~45 nm, and ~70 nm in diameter at concentrations ranging from 0.001 to 100 μg/mL for 24 h. Data are presented as mean ± SD, $n = 4$ independent experiments. Significant differences from control ($^*p < 0.05$). Statistical analysis was conducted using one-way ANOVA or Kruskal-Wallis test.

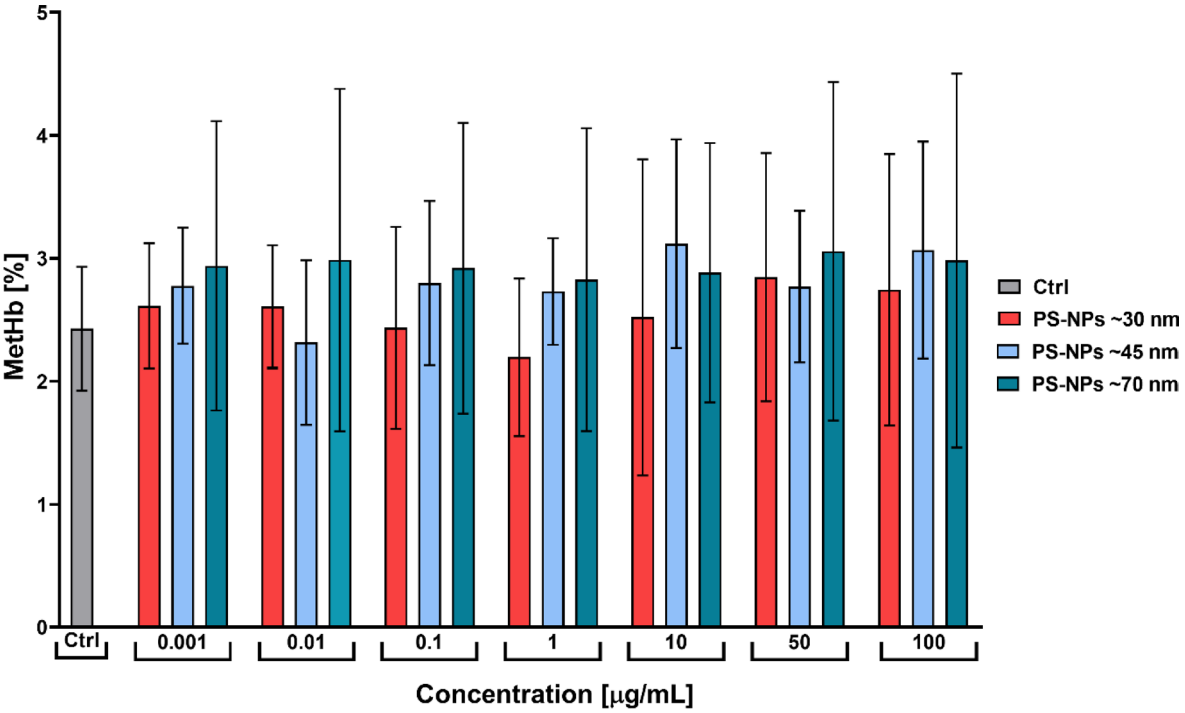

Fig. 5. Changes in methemoglobin level in control erythrocytes and erythrocytes incubated with PS-NPs of ~30 nm, ~45 nm, and ~70 nm in diameter at concentrations ranging from 0.001 to 100 μg/mL for 24 h. Data are presented as mean ± SD, $n = 5$ independent experiments. Statistical analysis was conducted using one-way ANOVA or Kruskal–Wallis test.

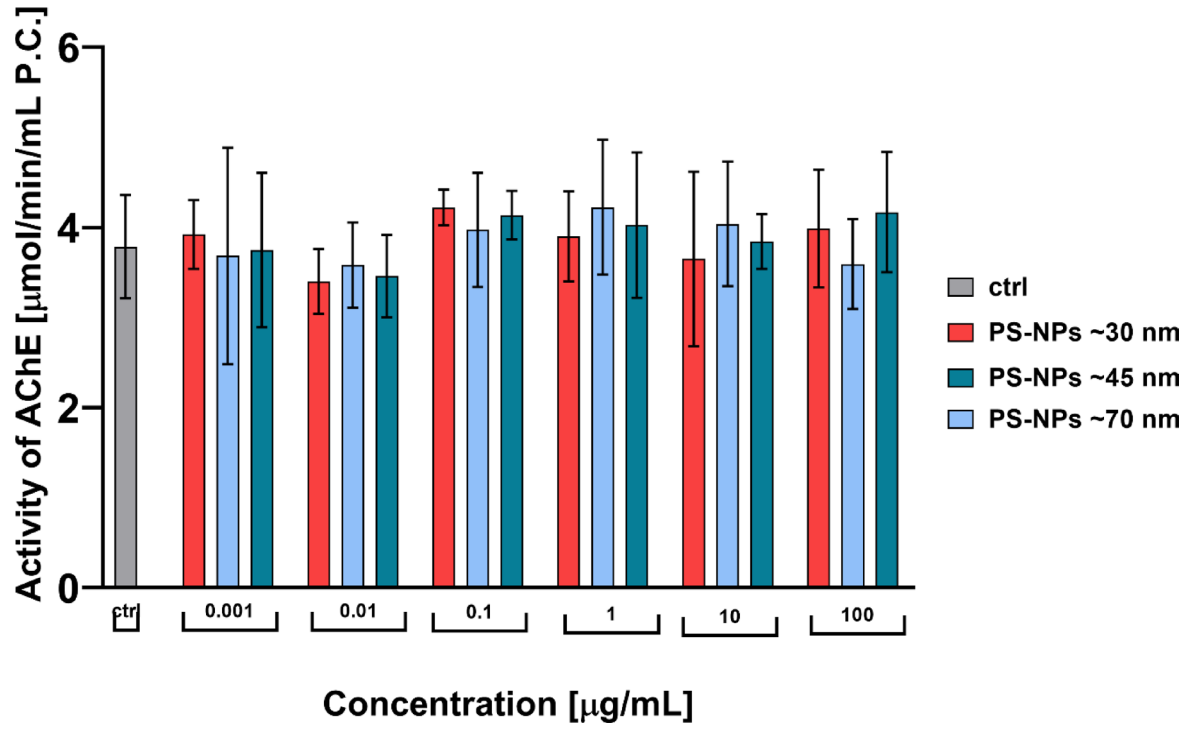

Fig. 6. Activity of AChE in control erythrocytes and erythrocytes incubated with PS-NPs of ~ 30 nm, ~ 45 nm, and ~ 70 nm in diameter at concentrations ranging from 0.001 to100 μg/mL for 24 h. Data are presented as mean ± SD, $n = 5$ independent experiments. Statistical analysis was conducted using one-way ANOVA or Kruskal–Wallis test.

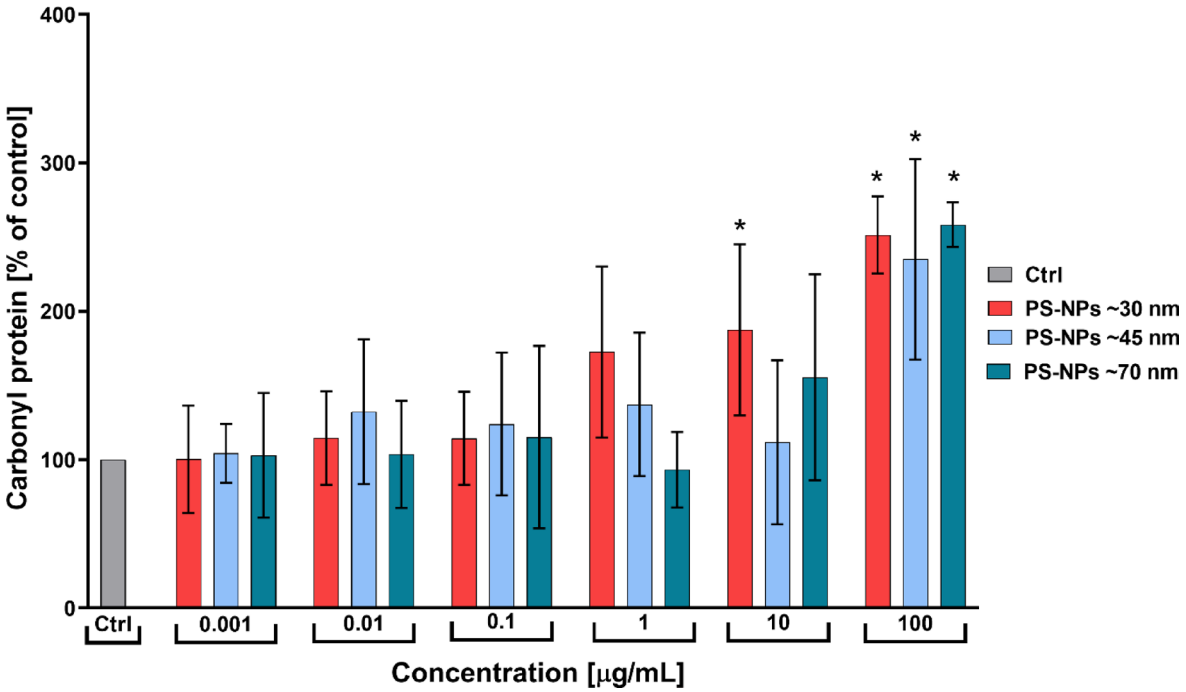

Fig. 7. The protein carbonyl level in the membrane of human erythrocytes incubated with PS-NPs of ~ 30 nm, ~ 45 nm, and ~ 70 nm in diameter at concentrations ranging from 0.001 to 100 μg/mL for 24 h. Data are presented as mean ± SD, $n = 3$ to 4 independent experiments. Significant differences from control (*)$p < 0.05$. Statistical analysis was conducted using one-way ANOVA or Kruskal-Wallis test.

interacting with from HSA (human serum albumin) which is believed to result in the formation of a protein corona. It also investigates the effect of plastic particles on the secondary structure of HSA; our data indicate that incubation of plastic nanoparticles with diameters of ~45 nm and ~70 nm with different concentrations of albumin results in the formation of structures with increased hydrodynamic diameter (Fig. 1).

Our findings indicate that while no protein corona formed on the very small plastic particles, or that the size was below detection by DLS, it was observed on large particles. This could have several causes: firstly, larger particles have a larger total surface area, so they can attract more proteins and adsorb them, and it is difficult for protein to be stabilized on very small particles[45,46]. Secondly, small particles have high curvature and are therefore unlikely to form a protein corona[47]. Finally, proteins have more favorable adsorption energy when deposited on larger particles than on small particles[48].

Therefore, it can be concluded that the observed changes in the hydrodynamic diameter result from the formation of a protein corona. To investigate the nature of this corona, the study examined the effect of PS-NP type on the secondary structure of albumin: the presence of changes in the secondary structure indicates the formation of a "hard" corona, while a lack of changes indicates a "soft" corona[42]. Our findings confirm changes in the secondary structure for all tested non-functionalized polystyrene nanoparticles (~30 nm, ~45 nm, ~70 nm) at the two highest concentrations (50 µg/mL and 100 µg/mL), indicating the formation of a hard corona (Fig. 2; Table 2). The smallest changes were observed for the smallest particles. The changes manifested as a decrease in the amount of the α-helix structure, an increase in the β-sheet structure and an increase in random coils (Table 2). Protein particles in the hard corona are strongly adsorbed on the surface of PS-NPs and lose their biological activity. Proteins forming a "soft" corona have also been found to demonstrate reduced enzymatic activity[42,49].

Kihara et al.[49] studied HSA corona formation on polystyrene particles with different sizes and charges. Their observations indicate a smaller increase in hydrodynamic diameter for negatively-charged particles (32–34 nm, 226–230 nm) than positively-charged ones (39–5000 nm, 229–315 nm), indicating the presence of soft and hard coronas, respectively. As in the present study, binding to a positively-charged PS reduced α-helix content, suggesting hard corona formation[50].

Another study confirmed the formation of soft and hard coronas on 50 nm and 210 nm PS-NPs[50]. The AFM and DLS analysis found that corona size depends on particle diameter and protein type: HSA formed a ~1 nm corona on 50 nm particles and a ~30 nm, multilayer corona on 210 nm particles, while transferrin formed a bilayer on 50 nm NPs. Strong aggregation (500–700 nm) was seen for 50 nm particles with HSA and transferrin. These findings support our present findings: larger PS-NPs (~70 nm) formed larger albumin coronas than smaller ones (~45 nm) (Fig. 1).

In conclusion, as the concentration of albumin increases, the secondary structure becomes less stable, and the hydrodynamic diameter of the plastic particles increases. This suggests the formation of a hard protein corona on non-functionalized PS-NPs (Figs. 1 and 2; Table 2). The formation of a hard protein corona with negatively-charged albumin[51] around plastic nanoparticles with a negative zeta potential is mainly due to hydrophobic interactions and local electrostatic interactions. Although albumin has a net negative charge, it can bind stably to the nanoparticle surface due to its positive domains and its amphipathic nature[48,52]. Also in silico simulations show rapid protein adsorption takes place on PS surfaces via hydrophobic interactions with amino acid side chains (e.g., alanine, histidine, threonine, valine)[50].

The interaction of plastic nanoparticles with albumin is also evidenced by studies of HSA fluorescence emission spectra (Fig. 3) and analysis of fluorescence decay over time (Table 3). Changes in the fluorescence signal of Tyr and Trp in HSA indicate an interaction between the protein and PS-NPs. Changing the microenvironment of these amino acids to a more non-polar one results in increased quantum yield of fluorescence and a longer excited state lifetime[53,54]. These results perfectly complement the DLS data (Fig. 1); they also indicate that proteins interact with PS-NPs with sizes of ~30 nm and ~45 nm and at a low concentration of 10 µg/mL. For small nanoparticles, no protein corona is formed. However, this does not mean a lack of interaction with the protein; in such cases, the small size and high curvature of the particles favor interaction with proteins, for example, by allowing the particle to fit better into cavities in the protein structure. This will alter the spectra and lifetimes of the two amino acids Tyr and Trp by altering the conformation of the protein[55,56] and/or directly affecting their microenvironment.

The fact that such interactions are more likely for the smallest nanoparticles is clearly visible in the DLS measurements. Figure 1 shows a change in the particle size distribution; two maxima can be observed for PS-NPs ~30 nm at a protein concentration of 150 µg/mL, one on the smaller side and one on the larger diameter side. A similar situation can be seen for PS-NPs ~45 nm at a protein concentration of 50 µg/mL. The study used commercial mixtures of particles with an mean size of ~30 nm or ~45 nm, i.e. the mixture included various PS-NPs that ranged in size from those that were smaller than the mean diameter stated by the manufacturer, to much larger ones. As such, two types of interactions with albumin take place, causing the formation of small PS-NP-albumin complexes for small particles (visible in fluorescence measurements) as well as protein corona for large particles visible in DLS measurements[50,57].

Numerous studies have investigated the toxicity of protein-crowned microplastics. Uncontrolled protein corona (PC) formation has been found to potentially increase or inhibit cellular uptake, interfere with active targeting, or promote passive targeting. It may also modulate immune responses and either attenuate or exacerbate cytotoxicity[58]. The PC thus acts as a "toxicity modulator" for micro- and nanoplastics, often increasing toxicity by altering internalization, inducing oxidative stress, or triggering inflammation[40]. Corona composition has been found to significantly influence blood-brain barrier penetration in striped danios[59]and to influence absorption and toxicity associated with oxidative damage and impaired digestion due to aggregation and prolonged intestinal retention[44].

However, in some cases, the corona can reduce toxicity by forming a protective barrier that limits direct interaction with cell membranes[45,60]. Photo-aging has been found to alter the corona protein profiles of PS-NPs in bronchoalveolar lavage fluid (BALF), increasing hydrophilicity and uptake by lung macrophages due to stronger binding of negatively-charged proteins[57]. Gopinath et al.[37] found that coronas causing greater protein conformational changes led to higher genotoxicity and hemolysis (up to 91% at 5 µg/mL vs. 22% for virgin NPs), indicating enhanced blood toxicity. Conversely, Saha et al.[61] and Kihara et al.[62] report that protein coronas, especially soft coronas, can protect red blood cells and reduce cytotoxicity. Overall, corona-related toxicity depends on protein composition, cell type, and experimental conditions.

Effect of PS-NPs on erythrocyte proteins

As the tested NPs demonstrated a strong interaction with HSA, the next stage of the study focused on the interaction of PS-NPs with erythrocyte proteins. The shape and rheological properties of erythrocytes are ideally suited to gas exchange, their main physiological function. As such, their main interior protein is the oxygen transport molecule, hemoglobin, which also transports approx. 23% of carbon dioxide, the final product of metabolism, from the tissues to the lungs for elimination from the body[63]. In addition to this primary role, erythrocytes also take part in maintaining the acid-base balance, regulating blood flow by modulating nitric oxide bioavailability, and playing important roles in the redox balance and the immune response. Erythrocytes also affect hemostasis and thrombosis by altering blood viscosity, blood flow dynamics and interactions with platelets and by governing red blood cell aggregation and blood clotting factor activation[64].

As they have such an important role, any disruption in erythrocyte function can result in adverse health effects. The present study investigated the effects of PS-NPs on erythrocyte proteins after 24-hour incubation of red cells with PS-NPs. First, the relative viscosity of the erythrocyte interior was evaluated, with the results revealing a significant increase in each of the PS-NPs tested. The smallest nanoparticles (~ 30 nm) increased the relative viscosity even at a NPs concentration of 0.1 µg/mL (Fig. 4). The observed changes in interior viscosity may be due to the interaction of NPs with hemoglobin, via a similar mechanism to that observed for adsorption of hemoglobin to polyethylene[65]. Gennaro et al.[66] propose that Hb determines the degree of microviscosity of the erythrocyte interior, and hence, the microviscosity of the erythrocyte interior can serve as an indicator of any changes in Hb concentration or structure; this can result in altered interactions between protein molecules. Hemoglobin has been shown to be a key determinant of the microviscosity of the erythrocyte interior, resulting in altered interactions between protein molecules. As such, changes in its concentration or structure can be determined by measuring the microviscosity of the cell contents[66]. Hemoglobin has also been found to demonstrate high affinity to various polymeric surfaces[67]and more recently, Rajendran and Chandrasekaran[41] note that polystyrene alters the structure and functional properties of Hb. Therefore, it seems that Hb is able to adsorb onto a polymer surface, thus altering its interactions. Such changes could also lead to an increase in the interior viscosity of an erythrocyte, resulting in decreased deformability and reorganization of the erythrocyte cytoskeleton, as confirmed by previous data indicating intense stomatocyte formation in the presence of NPs[22].

However, in the NP concentration range of 0.001–100 µg/mL, no possible adsorption of Hb to NPs was found to result in the oxidation of Hb to methemoglobin (Fig. 5); such a disruption would prevent the cell from transporting oxygen, and result in the accelerated removal of the erythrocyte from the bloodstream[68]. Therefore, it is unlikely that plastic nanoparticles found in human bodies induce direct oxidation of hemoglobin.

The next step examined the effect of nanoparticles on proteins present in erythrocyte membranes, i.e. the oxidation of membrane proteins and their influence on the activity of AChE: a protein anchored to phosphatidylinositol in the erythrocyte membrane. The level of erythrocyte AChE in the body correlates positively with AChE in the brain, which is a target for neurotoxins; hence, it can serve as a biomarker of the effects of exposure to neurotoxins, such as pesticides[69] and lead[70]. In addition, the activity of AChE in the erythrocyte membrane is considered a biomarker of membrane integrity, as well as erythrocyte aging and the onset of inflammation. Erythrocyte AChE activity has also been found to be related to various clinical and biophysical parameters associated with health disorders, and has been used to identify congenital colonic amenorrhea or Hirschsprung's disease[71,72]. Our analyses showed no change in erythrocyte AChE activity following 24-hour exposure to PS-NPs in the range of 0.001–100 µg/mL (Fig. 6).

An elevated level of carbonyl groups was observed on the membrane proteins in the human erythrocytes. These changes occurred at concentrations of 10 µg/mL (PS-NPs with a diameter of 30 nm) and 100 µg/mL (PS-NPs with diameters of ~ 40 and ~ 70 nm) (Fig. 7). These changes can be explained by the plastic particles exerting direct physical pressure on the cell membrane, altering its fluidity and influencing stomatocyte formation[22]. This would result in damage to the membrane proteins, and an increased risk of their oxidation; which would be exacerbated by increased exposure to molecular oxygen.

The role of albumin in erythrocyte integrity and modulation by PS-NPs

The approach taken in the present study allowed a detailed analysis of the conformational changes (Fig. 2; Table 2) and molecular-level interactions (Fig. 3; Table 3) taking place in HSA, which are challenging to observe directly in the more complex cellular context of erythrocytes. Conversely, findings from the erythrocyte model confirmed the biological relevance of these interactions and enabled evaluation of their functional consequences, such as changes in viscosity (Fig. 4) or oxidative stress (Figs. 5 and 7). Integrating the molecular- and cellular-level analyses provides a more comprehensive understanding of the overall impact of PS-NPs on blood constituents and and proper functioning of the cardiovascular system .

Albumin plays a vital role in maintaining the structural integrity and functionality of erythrocytes, particularly within their immediate plasma environment. It is the most abundant protein in plasma, and is needed to preserve the biconcave shape of red blood cells, which is essential for maintaining their deformability

and capillary passage[30,73]. Indeed, crystalline bovine serum albumin has been found to enhance erythrocyte resistance to mechanical damage and protect against oxidative or physical hemolysis[74].

Albumin and other plasma proteins adsorb onto erythrocyte surfaces, forming a protective layer that modifies the cells' zeta potential and facilitates membrane repair following mechanical stresses, such as blood shear or passage through high-resistance vascular regions[75,76]. In vitro and ex vivo findings indicate that albumin also improves erythrocyte mechanical properties—including elasticity, shear modulus, and surface viscosity—enhancing adaptation to hemodynamic forces[77].

In its native conformation, albumin stabilizes erythrocyte membranes through electrostatic interactions, elevates zeta potential, and reduces cell aggregation and endothelial adhesion[25]. Additionally, it functions as an osmotic and mechanical buffer, protecting erythrocytes from deformation and premature senescence[26,78]. However, conditions such as pH shifts, high temperature, oxidation, glycation, exposure to salts, or freezing can induce its partial unfolding. This exposes hydrophobic regions that interact strongly with erythrocyte lipid bilayers[79,80,81]disrupting membrane structure, altering lipid asymmetry, increasing permeability, and favouring morphological transformation into stomatocytes[25]. Such changes lead to increased membrane rigidity, reduced deformability, and enhanced hemolytic susceptibility[82,83].

Polystyrene nanoparticles (PS-NPs) play a particularly relevant role: by interacting and binding to albumin (Figs. 1 and 3; Table 3) they can be seen to alter its secondary structure (Fig. 2; Table 2) and impair its protective functions. These interactions may yield denatured albumin forms that destabilize erythrocyte membranes. PS-NPs also induce inflammatory responses[84,85]alter plasma albumin levels, and promote post-translational modifications (e.g., oxidation, glycation), which further undermine erythrocyte stability and membrane interactions[86,87]. Misfolded albumin not only loses its protective role, it may actively contribute to structural and functional deterioration in erythrocytes; indeed, structural perturbations of albumin have been shown to affect erythrocyte shape and viability[79,82,83]. Structural disruptions stemming from oxidation, glycation, drug binding, or nanoparticle interactions can impair the ligand-binding and redox-active sites in albumin, altering its allosteric regulation and antioxidant capacity. For example, compromised heme-binding and scavenging functions elevate free heme levels, exacerbating oxidative stress in erythrocytes and undermining membrane stability[88].

The secondary-structure changes in albumin observed in vitro (Fig. 2; Table 2), and the formation of a protein corona (Fig. 1), can significantly perturb erythrocyte homeostasis in vivo. The exposure with PS-NPs may alter the functional properties of erythrocyte membranes, thus indirectly enhancing any detrimental effects observed with plastic. These alterations may lead to premature erythrocyte degradation, reduced deformability, and increased vulnerability to mechanical stress and hemolysis, and can ultimately affect cardiovascular function, especially under conditions of elevated oxidative or mechanical stress.

These suggestions are consistent with those given in a previous review[41]which reported that exposure to plastic nanoparticles is associated with an increased risk of life-threatening diseases due to enhanced plasma protein denaturation, hemolysis, reduced immunity, thrombosis, blood clotting, and vascular endothelial damage. Some of the key mechanisms involved in these toxic effects include protein corona formation, oxidative stress, cytokine changes, inflammation, and cyto- and genotoxicity. Micro- and nanoparticles alter the secondary structure of plasma proteins, thus preventing their them from transporting *inter alia* nutrients, drugs and oxygen. They increase the aggregation of red blood cells and platelets, as well as their adhesion to endothelial cells, which can increase the risk of thrombosis and cardiovascular disease.

Conclusion

Our study takes an original approach based on the integration of molecular and cellular approaches to assess the interactions of polystyrene nanoparticles (PS-NPs) within the blood environment. Its findings demonstrate that structural alterations in HSA and functional changes in erythrocytes occur even at very low concentrations of plastic nanoparticles (0.1–10 μg/mL); this observation is highly relevant for future risk assessment and exposure studies, as most previous research has focused on higher, less physiologically-relevant concentrations which are unlikely to occur under in vivo conditions.

Effects on albumin: Non-functionalized polystyrene nanoparticles (PS-NPs) alter the spatial structure of human serum albumin (HSA) , which may affect its biological function. These changes were dependent on both the concentration (50–100 μg/mL) and the size of the nanoparticles (30, 45, and 70 nm). Spectroscopic studies showed that PS-NPs caused an increase in HSA fluorescence and changes in its mean fluorescence lifetime, confirming interactions between the protein and the nanoparticles.

Effects on erythrocytes: PS-NPs did not affect the activity of acetylcholinesterase (AChE) in the erythrocyte membrane. However, they did cause oxidation of membrane proteins, possibly due to the physical pressure exerted by the nanoparticles on the membrane. In addition, exposure also altered the viscosity of the erythrocyte interior, which probably resulted from the interaction of the NPs with hemoglobin. However, the PS-NPs did not oxidize the hemoglobin molecules.

Our results reveal pronounced alterations in the secondary structure of HSA following exposure, indicating direct binding between PS-NPs and albumin. These findings support the hypothesis that PS-NPs also interact with proteins on the erythrocyte surface. Furthermore, in addition to protein corona formation, the interaction between PS-NPs and HSA may also disrupt the integrated protein–cell system in peripheral blood. Mechanistic correlations were observed in both the HSA and erythrocyte models, indicating that both nanoparticle concentration and size influence the effects of PS-NPs exposure.

It is possible that the structural changes in albumin induced by PS-NPs may indirectly alter the rheological properties of erythrocytes in vivo, potentially impairing their functionality within the circulatory system.

Data availability

The datasets used and/or analysed during the current study available from the corresponding author on reasonable request.

Received: 11 June 2025; Accepted: 7 August 2025
Published online: 17 August 2025

References

1. Yates, J. et al. Plastics matter in the food system. *Commun. Earth Environ.* **6**, 176 (2025).
2. Saudrais, F. et al. The impact of Virgin and aged microstructured plastics on proteins: The case of hemoglobin adsorption and oxygenation. *Int. J. Mol. Sci.* **25**, 7047 (2024).
3. Fayshal, M. A. Current practices of plastic waste management, environmental impacts, and potential alternatives for reducing pollution and improving management. *Heliyon* **10**, e40838 (2024).
4. Schwabl, P. et al. Detection of various microplastics in human stool: A prospective case series. *Ann. Intern. Med.* **171**, 453–457 (2019).
5. Pironti, C. et al. First evidence of microplastics in human urine, a preliminary study of intake in the human body. *Toxics* **11**, 40 (2022).
6. Zhao, Q. et al. Detection and characterization of microplastics in the human testis and semen. *Sci. Total Environ.* **877**, 162713 (2023).
7. Amato-Lourenço, L. F. et al. Presence of airborne microplastics in human lung tissue. *J. Hazard. Mater.* **416**, 126124 (2021).
8. Jenner, L. C. et al. Detection of microplastics in human lung tissue using μFTIR spectroscopy. *Sci. Total Environ.* **831**, 154907 (2022).
9. Ibrahim, Y. S. et al. Detection of microplastics in human colectomy specimens. *JGH Open.* **5**, 116–121 (2021).
10. Ragusa, A. et al. Plasticenta: first evidence of microplastics in human placenta. *Environ. Int.* **146**, 106274 (2021).
11. Rotchell, J. M. et al. Detection of microplastics in human saphenous vein tissue using μFTIR: A pilot study. *PLOS ONE* **18**, e0280594 (2023).
12. Yang, Y. et al. Detection of various microplastics in patients undergoing cardiac surgery. *Environ. Sci. Technol.* **57**, 10911–10918 (2023).
13. Nihart, A. J. et al. Bioaccumulation of microplastics in decedent human brains. *Nat. Med.* **31**, 1114–1119 (2025). https://doi.org/10.1038/s41591-024-03453-1
14. Lee, D. W. et al. Microplastic particles in human blood and their association with coagulation markers. *Sci. Rep.* **14**, 30419 (2024).
15. Leslie, H. A. et al. Discovery and quantification of plastic particle pollution in human blood. *Environ. Int.* **163**, 107199 (2022).
16. Salvia, R. et al. Fast-screening flow cytometry method for detecting nanoplastics in human peripheral blood. *MethodsX* **10**, 102057 (2023).
17. Leonard, V. L. Microplastics in human blood: Polymer types, concentrations and characterisation using μFTIR. *Environ. Int.* **188**, 108751 (2024).
18. Kik, K., Bukowska, B., Krokosz, A. & Sicińska, P. Oxidative properties of polystyrene nanoparticles with different diameters in human peripheral blood mononuclear cells (in vitro study). *Int. J. Mol. Sci.* **22**, 4406 (2021).
19. Malinowska, K. et al. Polystyrene nanoparticles: the mechanism of their genotoxicity in human peripheral blood mononuclear cells. *Nanotoxicology* **16**(6-8), 791–811 (2022). https://doi.org/10.1080/17435390.2022.2149360
20. Malinowska, K., Sicińska, P., Michałowicz, J. & Bukowska, B. The effects of non-functionalized polystyrene nanoparticles of different diameters on the induction of apoptosis and mTOR level in human peripheral blood mononuclear cells. *Chemosphere* **335**, 139137 (2023).
21. Remigante, A. et al. Internalization of nano- and micro-plastics in human erythrocytes leads to oxidative stress and estrogen receptor-mediated cellular responses. *Free Radic Biol. Med.* **223**, 1–17 (2024).
22. Płuciennik, K. et al. The effects of non-functionalized polystyrene nanoparticles with different diameters on human erythrocyte membrane and morphology. *Toxicol. Vitro* **91**, 105634 (2023).
23. Gural, A., Pajić-Lijaković, I. & Barshtein, G. Mechanical stimulation of red blood cells aging: Focusing on the microfluidics application. *Micromachines* **16**, 259 (2025).
24. Dao, M., MacDonald, I. & Asaro, R. J. Erythrocyte flow through the interendothelial slits of the splenic venous sinus. *Biomech. Model. Mechanobiol.* **20**, 2227–2245 (2021).
25. Pajic-Lijakovic, I., Milivojevic, M., Barshtein, G. & Gural, A. The mechanical properties of erythrocytes are influenced by the conformational state of albumin. *Cells* **14**(15), 1139 (2025). https://doi.org/10.3390/cells14151139
26. Reinhart, W. H. et al. Washing stored red blood cells in an albumin solution improves their morphologic and hemorheologic properties. *Transfus. (Paris)* **55**, 1872–1881 (2015).
27. Ashraf, S. et al. Unraveling the versatility of human serum albumin—a comprehensive review of its biological significance and therapeutic potential. *Curr. Res. Struct. Biol.* **6**, 100114 (2023).
28. Hutapea, T. P. H. et al. Albumin: source, preparation, determination, applications, and prospects. *J. Sci. Adv. Mater. Devices* **8**, 100549 (2023).
29. Bihari, S., Bannard-Smith, J. & Bellomo, R. Albumin as a drug: its biological effects beyond volume expansion. *Crit. Care Resusc.* **22**, 257–265 (2020).
30. Van De Wouw, J. & Joles, J. A. Albumin is an interface between blood plasma and cell membrane, and not just a sponge. *Clin. Kidney J.* **15**, 624–634 (2022).
31. Watanabe, K. et al. Antioxidant properties of albumin and diseases related to obstetrics and gynecology. *Antioxidants* **14**, 55 (2025).
32. Belinskaia, D. A., Voronina, P. A. & Goncharov, N. V. Integrative role of albumin: Evolutionary, biochemical and pathophysiological aspects. *J. Evol. Biochem. Physiol.* **57**, 1419–1448 (2021).
33. Bern, M., Sand, K. M. K., Nilsen, J., Sandlie, I. & Andersen, J. T. The role of albumin receptors in regulation of albumin homeostasis: Implications for drug delivery. *J. Controlled Release*. **211**, 144–162 (2015).
34. Bashiri, G. et al. Nanoparticle protein corona: From structure and function to therapeutic targeting. *Lab. Chip* **23**, 1432–1466 (2023).
35. Drabkin, D. L. Spectrophotometric studies; the crystallographic and optical properties of the hemoglobin of man in comparison with those of other species. *J. Biol. Chem.* **164**, 703–723 (1946).
36. Ellman, G. L., Courtney, K. D., Andres, V. & Featherstone, R. A new and rapid colorimetric determination of acetylcholinesterase activity. *Biochem. Pharmacol.* **7**, 88–95 (1961).
37. Gopinath, P. M. et al. Assessment on interactive prospectives of nanoplastics with plasma proteins and the toxicological impacts of virgin, coronated and environmentally released-nanoplastics. *Sci. Rep.* **9**, 8860 (2019).
38. Dawson, A. L., Bose, U., Ni, D. & Nelis, J. Unravelling protein Corona formation on pristine and leached microplastics. *Microplasti. Nanoplast.* **4**, 9 (2024).

39. Brouwer, H., Porbahaie, M., Boeren, S., Busch, M. & Bouwmeester, H. The in vitro Gastrointestinal digestion-associated protein Corona of polystyrene nano- and microplastics increases their uptake by human THP-1-derived macrophages. *Part. Fibre Toxicol.* **21**, 4 (2024).
40. Wang, J. et al. Nanoplastic-protein corona interactions and their biological effects: A review of recent advances and trends. *TrAC Trends Anal. Chem.* **166**, 117206 (2023).
41. Rajendran, D. & Chandrasekaran, N. Molecular interaction of functionalized nanoplastics with human hemoglobin. *J. Fluoresc.* **33**, 2257–2272 (2023).
42. Kihara, S. et al. Soft and hard interactions between polystyrene nanoplastics and human serum albumin protein corona. *Bioconjug. Chem.* **30**, 1067–1076 (2019).
43. Ducoli, S. et al. A different protein Corona cloaks true-to-life nanoplastics with respect to synthetic polystyrene nanobeads. *Environ. Sci. Nano* **9**, 1414–1426 (2022).
44. Luo, H., Du, Q., Zhong, Z., Xu, Y. & Peng, J. Protein-coated microplastics Corona complex: An underestimated risk of microplastics. *Sci. Total Environ.* **851**, 157948 (2022).
45. Lundqvist, M. et al. Nanoparticle size and surface properties determine the protein Corona with possible implications for biological impacts. *Proc. Natl. Acad. Sci.* **105**, 14265–14270 (2008).
46. Walkey, C. D., Olsen, J. B., Guo, H., Emili, A. & Chan, W. C. Nanoparticle size and surface chemistry determine serum protein adsorption and macrophage uptake. *J. Am. Chem. Soc.* **134**, 2139–2147 (2012).
47. Gonzalez Solveyra, E., Thompson, D. H. & Szleifer, I. Proteins adsorbing onto surface-modified nanoparticles: Effect of surface curvature, pH, and the interplay of polymers and proteins acid–base equilibrium. *Polymers* **14**, 739 (2022).
48. Pinals, R. L., Chio, L., Ledesma, F. & Landry, M. P. Engineering at the nano-bio interface: Harnessing the protein corona towards nanoparticle design and function. *Analyst* **145**, 5090–5112 (2020).
49. Kihara, S. et al. Structure of soft and hard protein corona around polystyrene nanoplastics—particle size and protein types. *Biointerphases* **15**, 051002 (2020).
50. Meesaragandla, B. et al. Interaction of polystyrene nanoparticles with supported lipid bilayers: Impact of nanoparticle size and protein Corona. *Macromol. Biosci.* **23**, 2200464 (2023).
51. Nattich-Rak, M., Dąbkowska, M. & Adamczyk, Z. Microparticle deposition on human serum albumin layers: Unraveling anomalous adsorption mechanism. *Colloids Interfaces* **4**, 51 (2020).
52. Panico, S. et al. Biological features of nanoparticles: Protein Corona formation and interaction with the immune system. *Pharmaceutics* **14**, 2605 (2022).
53. Guzow, K. et al. Photophysical properties of tyrosine and its simple derivatives in organic solvent studied by time-resolved fluorescence spectroscopy and global analysis. *Photochem. Photobiol.* **81**(3), 697–704 (2005) https://doi.org/10.1562/2004-03-02-RA-095
54. Lakowicz, J.L. *Principles of Fluorescence Spectroscopy* (Springer US, 2006). https://doi.org/10.1007/978-0-387-46312-4.
55. Zhdanova, N. G., Maksimov, E. G., Arutyunyan, A. M., Fadeev, V. V. & Shirshin, E. A. Tyrosine fluorescence probing of conformational changes in tryptophan-lacking domain of albumins. *Spectrochim Acta Mol. Biomol. Spectrosc.* **174**, 223–229 (2017).
56. Zhdanova, N. G. et al. Tyrosine fluorescence probing of the surfactant-induced conformational changes of albumin. *Photochem. Photobiol Sci.* **14**, 897–908 (2015).
57. Du, T. et al. Aging of nanoplastics significantly affects protein Corona composition thus enhancing macrophage uptake. *Environ. Sci. Technol.* **57**, 3206–3217 (2023).
58. Liu, N., Tang, M. & Ding, J. The interaction between nanoparticles-protein Corona complex and cells and its toxic effect on cells. *Chemosphere* **245**, 125624 (2020).
59. Kopatz, V. et al. Micro- and nanoplastics breach the blood–brain barrier (BBB): Biomolecular corona's role revealed. *Nanomaterials* **13**, 1404 (2023).
60. Casals, E., Pfaller, T., Duschl, A., Oostingh, G. J. & Puntes, V. Time evolution of the nanoparticle protein corona. *ACS Nano.* **4**, 3623–3632 (2010).
61. Saha, K., Moyano, D. F. & Rotello, V. M. Protein coronas suppress the hemolytic activity of hydrophilic and hydrophobic nanoparticles. *Mater. Horiz.* **1**, 102–105 (2014).
62. Kihara, S. et al. Cellular interactions with polystyrene nanoplastics—the role of particle size and protein corona. *Biointerphases* **16**, 041001 (2021).
63. Ahmed, M. H., Ghatge, M. S., Safo, M. K. & Hemoglobin Structure, function and allostery. in *Vertebrate and Invertebrate Respiratory Proteins, Lipoproteins and Other Body Fluid Proteins* (eds Hoeger, U. & Harris, J. R.) vol. 94 345–382 (Springer International Publishing, Cham, 2020).
64. Litvinov, R. I. & Weisel, J. W. Role of red blood cells in haemostasis and thrombosis. *ISBT Sci. Ser.* **12**, 176–183 (2017).
65. Horbett, T. A., Weathersby, P. K. & Hoffman, A. S. The preferential adsorption of hemoglobin to polyethylene. *J. Bioeng.* **1**, 61–77 (1977).
66. Gennaro, A. M., Luquita, A. & Rasia, M. Comparison between internal microviscosity of low-density erythrocytes and the microviscosity of hemoglobin solutions: An electron paramagnetic resonance study. *Biophys. J.* **71**, 389–393 (1996).
67. Horbett, T. A., Weathersby, P. K. & Hoffman, A. S. Hemoglobin adsorption to three polymer surfaces. *Thromb. Res.* **12**, 319–329 (1978).
68. Ashraf, M. F. et al. Acute severe methemoglobinemia caused by accidental liquid shoe shiner ingestion: A case report and review of literature. *Med. Rep.* **11**, 100187 (2025).
69. Sosnowska, B., Huras, B., Krokosz, A. & Bukowska, B. The effect of bromfenvinphos, its impurities and chlorfenvinphos on acetylcholinesterase activity. *Int. J. Biol. Macromol.* **57**, 38–44 (2013).
70. Nwobi, N. L., Nwobi, J. C., Ogunbona, R. A., Adetunji, A. O. & Anetor, J. I. Erythrocyte acetylcholinesterase as a biomarker of environmental lead exposure. in *Biomarkers in Toxicology* (eds Patel, V. B., Preedy, V. R. & Rajendram, R.) 39–61 (Springer International Publishing, Cham, 2023). https://doi.org/10.1007/978-3-031-07392-2_4.
71. Saldanha, C. Human erythrocyte acetylcholinesterase in health and disease. *Molecules* **22**, 1499 (2017).
72. Freitas Leal, J. K., Adjobo-Hermans, M. J. W., Brock, R. & Bosman, G. J. Acetylcholinesterase provides new insights into red blood cell ageing in vivo and in vitro. *Blood Transfus. Trasfus Sangue* **15**, 232–238 (2017).
73. Kamada, T., McMillan, D. E., Sternlieb, J. J., Björk, V. O. & Otsuji, S. Albumin prevents erythrocyte crenation in patients undergoing extracorporeal circulation. *Scand. J. Thorac. Cardiovasc. Surg.* **22**, 155–158 (1988).
74. Williams, A. R. The effect of bovine and human serum albumins on the mechanical properties of human erythrocyte membranes. *Biochim. Biophys. Acta BBA - Biomembr.* **307**, 58–64 (1973).
75. Sümpelmann, R., Schürholz, T., Marx, G. & Zander, R. Protective effects of plasma replacement fluids on erythrocytes exposed to mechanical stress. *Anaesthesia* **55**, 976–979 (2000).
76. Kameneva, M. V. et al. Mechanisms of red blood cell trauma in assisted circulation. Rheologic similarities of red blood cell transformations due to natural aging and mechanical stress. *ASAIO J. Am. Soc. Artif. Intern. Organs*. **1992 41**, M457–460 (1995).
77. Luquita, A., Gennaro, A. & Rasia, M. Influence of adsorbed plasma proteins on erythrocyte rheological properties: In vitro and ex vivo studies. *Pflüg Arch.* **443**, 78–83 (2001).
78. McLaughlin, S. The electrostatic properties of membranes. *Annu. Rev. Biophys. Biophys. Chem.* **18**, 113–136 (1989).
79. Dobson, J. et al. Inducing protein aggregation by extensional flow. *Proc. Natl. Acad. Sci.* **114**, 4673–4678 (2017).

80. Raghav, A., Ahmad, J. & Alam, K. Impact of glycation on structural and antioxidant function of human serum albumin: Relevance in diabetic complications. *Diabetes Metab. Syndr. Clin. Res. Rev.* **10**, 96–101 (2016).
81. Kawakami, A. et al. Identification and characterization of oxidized human serum albumin: A slight structural change impairs its ligand-binding and antioxidant functions. *FEBS J.* **273**, 3346–3357 (2006).
82. Pretini, V. et al. Red blood cells: chasing interactions. *Front Physiol.* **10** (2019).
83. Ranade, S. S., Syeda, R. & Patapoutian, A. Mechanically activated ion channels neuron. **87**, 1162–1179 (2015).
84. Xiong, Z., Kong, Q., Hua, J., Chen, Q. & Wang, D. Cardiotoxicity of polystyrene nanoplastics and associated mechanism of myocardial cell injury in mice. *Ecotoxicol. Environ. Saf.* **290**, 117712 (2025).
85. Zhang, T. et al. Multi-dimensional evaluation of cardiotoxicity in mice following respiratory exposure to polystyrene nanoplastics. *Part Fibre Toxicol.* **20** (2023).
86. Soeters, P. B., Wolfe, R. R. & Shenkin, A. Hypoalbuminemia: Pathogenesis and clinical significance. *J. Parenter. Enter. Nutr.* **43**, 181–193 (2019).
87. Zhang, C. et al. Research progress and value of albumin-related inflammatory markers in the prognosis of non-small cell lung cancer: A review of clinical evidence. *Ann. Med.* **55**, 1294–1307 (2023).
88. De Simone, G., Varricchio, R., Ruberto, T. F., Di Masi, A. & Ascenzi, P. Heme scavenging and delivery: The role of human serum albumin. *Biomolecules* **13**, 575 (2023).

Author contributions

Author Contributions Statement: Conceptualization: K.P; B.B; Methodology K.P., M.S., K.M., K.C, P.D., Formal analysis: K.P., M.S., K.M., K.C, P.D., B.B.; Visualization K.P; M.S., K.C, B.B.; Writing—original draft: K.P., M.S., K.M., K.C, P.D., A.K., B.B. Supervision,: B.B., A.K., P.S.; Writing—review & editing: K.P., M.S., K.M., K.C, P.D., A.K., B.B.

Funding

This manuscript was supported by research funding granted to the Department of Biophysics of Environmental Pollution, Faculty of Biology and Environmental Protection, University of Lodz, Poland (grant no. B2511000000191.01), as well as by the University of Lodz Doctoral School of Exact and Natural Sciences (Grant No. B2410000000013.05).

Declarations

Competing interests

.No potential conflict of interest was reported by the author(s).

Additional information

Correspondence and requests for materials should be addressed to B.B.

Reprints and permissions information is available at www.nature.com/reprints.

Publisher's note Springer Nature remains neutral with regard to jurisdictional claims in published maps and institutional affiliations.

Terms and Conditions

Springer Nature journal content, brought to you courtesy of Springer Nature Customer Service Center GmbH (“Springer Nature”).
Springer Nature supports a reasonable amount of sharing of research papers by authors, subscribers and authorised users (“Users”), for small-scale personal, non-commercial use provided that all copyright, trade and service marks and other proprietary notices are maintained. By accessing, sharing, receiving or otherwise using the Springer Nature journal content you agree to these terms of use (“Terms”). For these purposes, Springer Nature considers academic use (by researchers and students) to be non-commercial.
These Terms are supplementary and will apply in addition to any applicable website terms and conditions, a relevant site licence or a personal subscription. These Terms will prevail over any conflict or ambiguity with regards to the relevant terms, a site licence or a personal subscription (to the extent of the conflict or ambiguity only). For Creative Commons-licensed articles, the terms of the Creative Commons license used will apply.
We collect and use personal data to provide access to the Springer Nature journal content. We may also use these personal data internally within ResearchGate and Springer Nature and as agreed share it, in an anonymised way, for purposes of tracking, analysis and reporting. We will not otherwise disclose your personal data outside the ResearchGate or the Springer Nature group of companies unless we have your permission as detailed in the Privacy Policy.
While Users may use the Springer Nature journal content for small scale, personal non-commercial use, it is important to note that Users may not:

1. use such content for the purpose of providing other users with access on a regular or large scale basis or as a means to circumvent access control;
2. use such content where to do so would be considered a criminal or statutory offence in any jurisdiction, or gives rise to civil liability, or is otherwise unlawful;
3. falsely or misleadingly imply or suggest endorsement, approval , sponsorship, or association unless explicitly agreed to by Springer Nature in writing;
4. use bots or other automated methods to access the content or redirect messages
5. override any security feature or exclusionary protocol; or
6. share the content in order to create substitute for Springer Nature products or services or a systematic database of Springer Nature journal content.

In line with the restriction against commercial use, Springer Nature does not permit the creation of a product or service that creates revenue, royalties, rent or income from our content or its inclusion as part of a paid for service or for other commercial gain. Springer Nature journal content cannot be used for inter-library loans and librarians may not upload Springer Nature journal content on a large scale into their, or any other, institutional repository.
These terms of use are reviewed regularly and may be amended at any time. Springer Nature is not obligated to publish any information or content on this website and may remove it or features or functionality at our sole discretion, at any time with or without notice. Springer Nature may revoke this licence to you at any time and remove access to any copies of the Springer Nature journal content which have been saved.
To the fullest extent permitted by law, Springer Nature makes no warranties, representations or guarantees to Users, either express or implied with respect to the Springer nature journal content and all parties disclaim and waive any implied warranties or warranties imposed by law, including merchantability or fitness for any particular purpose.
Please note that these rights do not automatically extend to content, data or other material published by Springer Nature that may be licensed from third parties.
If you would like to use or distribute our Springer Nature journal content to a wider audience or on a regular basis or in any other manner not expressly permitted by these Terms, please contact Springer Nature at

onlineservice@springernature.com

Taylor & Francis
Taylor & Francis Group

Nanotoxicology

Polystyrene nanoparticles and death of erythrocytes: does exposure induce eryptosis?

Submission ID	259032716
Article Type	Research Article
Keywords	erythrocytes, eryptosis, calpain, polystyrene nanoparticles, phosphatidylserine externalization
Authors	Paulina Sicińska, Kamil Płuciennik, Bożena Bukowska

For any queries please contact:

INAN-peerreview@journals.tandf.co.uk

Note for Reviewers:

To submit your review please visit https://mc.manuscriptcentral.com/tnan

Polystyrene nanoparticles and death of erythrocytes: does exposure induce eryptosis?

Kamil Płuciennik[1,2] , Bożena Bukowska [1], Paulina Sicińska [1]*

Kamil Płuciennik[1,2] ORCID 0000-0003-4866-7464

[1]Department of Biophysics of Environmental Pollution, Faculty of Biology and Environmental Protection, University of Lodz, Pomorska 141/143, 90- 236 Lodz, Poland.

[2]Doctoral School of Exact and Natural Sciences, University of Lodz, ul. Jana Matejki 21/23, 90-237 Lodz, Poland.

Bożena Bukowska [1], ORCID 0000-0003-3044-2953

[1]Department of Biophysics of Environmental Pollution, Faculty of Biology and Environmental Protection, University of Lodz, Pomorska 141/143, 90- 236 Lodz, Poland.

Paulina Sicińska [1]*, ORCID 0000-0002-6139-2613

[1]Department of Biophysics of Environmental Pollution, Faculty of Biology and Environmental Protection, University of Lodz, Pomorska 141/143, 90- 236 Lodz, Poland.

*Corresponding author: paulina.sicinska@biol.uni.lodz.pl

Graphical abstract

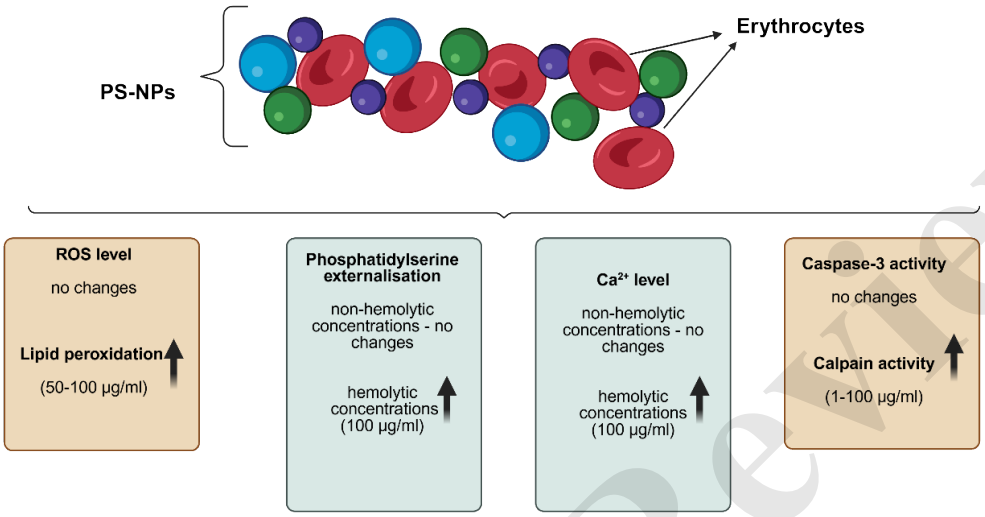

Polystyrene nanoparticles and death of erythrocytes: does exposure induce eryptosis?

Kamil Płuciennik[1,2] , Bożena Bukowska [1], Paulina Sicińska [1]*

[1]Department of Biophysics of Environmental Pollution, Faculty of Biology and Environmental Protection, University of Lodz, Pomorska 141/143, 90- 236 Lodz, Poland.

[2]Doctoral School of Exact and Natural Sciences, University of Lodz, ul. Jana Matejki 21/23, 90-237 Lodz, Poland.

*Corresponding author: paulina.sicinska@biol.uni.lodz.pl

Abstract

The widespread presence of polystyrene nanoparticles (PS-NPs) in the human body has raised concerns about their potential biological toxicity. When assessing the safety of nanoparticles and other xenobiotics, a key aspect is their effect on blood cells, particularly erythrocytes, which experience the most direct exposure to nanoparticles circulating in the bloodstream. The present study evaluated the impact of non-functionalized PS-NPs with diameters of ~30 nm, ~45 nm, and ~70 nm on human red blood cells after 24 hours of incubation.

The studied PS-NPs did not influence intracellular Ca^{2+} ion levels or caspase 3 activity, and did not induce phosphatidylserine translocation at pre-hemolytic concentrations (below 100 µg/mL). Also, exposure did not increase reactive oxygen species (ROS) levels at any tested concentration, indicating that their mechanism of action in human erythrocytes is not related to oxidative stress. The results suggest that PS-NPs primarily interact with the erythrocyte membrane mechanically, which may result in increased calpain activity (already at a concentration of 1 µg/mL) and lipid peroxidation (from a concentration of 50 µg/mL).

These effects suggest that PS-NP toxicity may primarily act through red blood cell membrane destabilization; however, this requires further study, especially in *in vivo* models that incorporate physiological blood flow conditions and protein corona formation, which could modify the interactions between nanoparticles and cells.

Keywords: erythrocytes; polystyrene nanoparticles; eryptosis; calpain; phosphatidylserine externalization

1. Introduction

The most numerous cells in the human circulatory system, and the entire body, are erythrocytes.(Sender et al., 2016). Their primary function is to transport oxygen to peripheral tissues, thus enabling the maintenance of mitochondrial aerobic metabolism and the overall functioning of the body (Nemkov et al., 2018).However, these cells also perform a number of additional roles, such as regulating blood flow, and maintaining haemostasis and redox balance. Furthermore, a growing body of evidence indicates that erythrocytes may act as part of the immune system, thanks to their ability to capture and store cytokines (Tkachenko, 2024; Tkachenko et al., 2025).

Due to their lack of mitochondria and other organelles, erythrocytes cannot undergo classical apoptosis; however, both old and damaged cells are eliminated from the bloodstream in a process of programmed death known as eryptosis (Tkachenko et al., 2025). Eryptosis is characterized by a series of morphological and biochemical changes such as cell shrinkage, exposure of phosphatidylserine (PS) on the outer surface of the membrane, and the activation of proteases such as calpain and caspase-3. During eryptosis, the cell experiences an influx of Ca^{2+} ions through cation channels, leading to the activation of potassium Ca^{2+} channels (Gardos channels, K_Ca3.1), in turn resulting in an efflux of K^+ and Cl^-, water loss, and cell shrinkage (Föller and Lang, 2020). An increase in Ca^{2+} concentration inhibits flipases (enzymes that maintain membrane asymmetry) and activates scramblase, which is responsible for the movement of PS to the cell membrane surface (Alghareeb et al., 2023). In turn, the high levels of intracellular Ca^{2+} activate calpain-1, a cysteine protease that breaks down cytoskeletal elements, leading to the formation of cell membrane blebs (Zhang et al., 2022). Eryptosis can also be induced by caspase-3, especially under oxidative stress (ROS), which also promotes PS externalization (Lang and Lang, 2015; Tkachenko et al., 2025).

Excessive eryptosis can disrupt the functioning of the body, especially the cardiovascular system, resulting in anaemia with tissue hypoxia, as well as sickle cell anaemia, heart failure, and arthritis. In addition, excessive activation can be observed in other diseases, such as chronic inflammation, diabetes, renal failure, liver failure and sepsis (Bissinger et al., 2016; Jarosiewicz et al., 2019; Restivo et al., 2022; Tkachenko et al., 2025).

Erythrocytes are known to bind and transport xenobiotics, and evidence indicates that plastic additives, such as bisphenols, phthalates (Maćczak et al., 2016;Sicińska, 2018) or

brominated flame retardants (Jarosiewicz et al., 2019) are able to induce eryptosis. Hence, there is a need to better understand the potential impact of the presence of plastic particles in the bloodstream.

Leslie et al.,(2022) report the concentration of polystyrene (PS) in the bloodstream to reach up to 4.8 µg/ml. Worryingly, these plastic particles are known to influence erythrocytes: previous research confirms that they can cause rheological changes, lead to the formation of echinocytes (Remigante et al., 2024) and stomatocytes, increase the internal microviscosity of red blood cells, oxidize erythrocyte membrane proteins, and ultimately cause haemolysis at high concentrations (Płuciennik et al., 2023, 2025)

Therefore, the aim of this study was to determine whether 24-hour exposure to polystyrene nanoparticles (PS-NPs) with three different diameters (~30 nm, ~45 nm, ~70 nm) induces eryptosis in human erythrocytes and whether this effect depends on particle size and concentration. A comprehensive assessment of eryptosis was made based on key biochemical parameters: reactive oxygen species (ROS) levels, intracellular Ca^{2+} ion concentration, lipid peroxidation, phosphatidylserine (PS) exposure, and caspase-3 and calpain activation.

2. Materials and Methods

2.1. Chemicals

Standards of non-functionalized polystyrene nanoparticles (PS-NPs) were purchased from Bangs Laboratories (Fishers, Indiana, USA). 1 g of individual nanoparticles contained the following: 9.24116 × 1016 nanoparticles/g (~30 nm); 2.13516 × 1016 particles/g (~45 nm); 5.78515 × 1015 particles/g (~70 nm). Annexin V was purchased from ThermoFisher (Waltham, MA, USA). The FITC-DEVD-FMK, 2',7'-dichlorodihydrofluorescein diacetate (H2DCFDA) caspase 3-detection kit and Fluo 3-AM were purchased from Merck (Darmstadt, Germany). Ionomycin calcium salt, betulinic , phosphate buffer saline tablets and Hank's Balanced Salt Solution (HBSS) were obtained from Merck (Darmstadt, Germany) , while NaCl, NaOH, TRIS, sodium acetate and HEPES were purchased from POCh (Gliwice, Poland) and Roth (Karlsruhe, Germany).

2.2. Isolation of red blood cells

Erythrocytes were isolated from a leukocyte buffy coat collected from the blood of healthy volunteers. The blood samples were purchased from the Regional Center for Blood Donation and Treatment in Lodz. Erythrocytes with a haematocrit of 5% were incubated with PS-NPs at concentrations ranging from 0.001 to 100 µg/mL at 37 °C for 24 hours. The study was approved by the Bioethics Committee of the University of Lodz (Resolution No. 12/KEBN-UŁ/I/2022–23).

2.3. Measurement of reactive oxygen species.

Reactive oxygen species (ROS) levels were determined by H_2DCFDA (2',7'-dichlorodihydrofluorescein) assay. The H_2DCFDA penetrates the erythrocyte membrane and is hydrolysed by esterases to H_2DCF; it is then oxidized in the presence of ROS to the highly fluorescent 2',7'-dichlorofluorescein (DCF). Erythrocytes were incubated with PS-NPs of different diameters (~30 nm, ~45 nm and 70 nm) in the concentration range 0.001-100 µg/ml for 24 hours. After incubation, the cells were washed and resuspended in Ringer buffer (final density 1 × 106 cells/mL). H2DCF-DA was added to the samples to the final concentration of 5 µM. Samples with stain were incubated for 15 minutes at 37 ºC in total darkness. Fluorescence was measured using an FACSymphony™ A1, flow cytometer (Becton Dickinson, USA) at excitation wavelength λ = 488 nm and emission wavelength λ = 530 nm. The data were recorded for a total of 10 000 events per sample.

2.4. Lipid peroxidation

The level of lipid peroxidation was then determined in erythrocytes incubated with PS-NPs (diameters ~30 nm, ~45 nm and ~70 nm) using the fluorescent probe Bodipy 581/591 C11. After 24-hour incubation of cells with polystyrene nanoparticles, a marker was added to 0,3 µM final concentration and the mixture was incubated for one hour in the dark at 37°C. After incubation, the samples were centrifuged (2000 rpm. 10min) and diluted to 2.5 % haematocrit. Fluorescence was measured using an FACSymphony™ A1 flow cytometer (Becton Dickinson, USA) at excitation wavelength λ = 488 nm and emission wavelength λ = 510 nm. The data were recorded for a total of 10 000 events per sample. Luperox was used as a positive control.

2.5. Analysis of phosphatidylserine (PS) externalization

During apoptosis, the phosphatidylserine (PS) present in the internal layer of the plasma membrane moves to the external layer. These cells, expressing PS on their surface, can be

bound by annexin V conjugated with fluorescein isothiocyanate (FITC). The resulting green fluorescence of the annexin-FITC complex indicates the presence of PS. The cells were incubated with PS-NPs of different diameters (~30 nm, ~45 nm and ~70 nm) in the concentration range 0.001-100 µg/ml. After incubation, the cells were centrifuged at 3000 rpm for 10 min at 4 °C and diluted with Ringer buffer (density $1x10^6$ cells/ml), then in Annexin V-binding buffer, and stained with Annexin V-FITC (1 µM) for 20 min at room temperature in total darkness. The analysis was performed for 10 000 cells at excitation/emission wavelengths of 488 nm and 530 nm, respectively, using an FACSymphony™ A1, flow cytometer (Becton Dickinson, USA). Betulinic acid (10 µM) was used as positive control.

2.6. Analysis of intracellular calcium ion level

Cytosolic ion levels were measured by complexation of calcium ions by Fluo-3/AM stain. Fluo3/AM passes through membrane of living cells, where it is cleaved by intracellular esterases to Fluo-3 which exhibits green fluorescence after complexation with calcium ions. The erythrocytes were treated with PS-NPs with different diameters and incubated for 24 hours at 37 °C in total darkness. The cells were suspended in Fluo-3/AM solution (1 µM) and incubated for 20 min at 37°C in total darkness. Following this, HBSS with 1% of bovine serum albumin (BSA) was added and incubated again for 40 minutes at 37 ºC in total darkness. After incubation the cells were centrifuged at 1500 rpm. for 10 minutes at 4 °C, and washed twice with the HEPES buffer. Fluorescence was measured using an FACSymphony™ A1 flow cytometer (Becton Dickinson USA) at 490 nm (excitation) and 528 nm (emission). The data were recorded for a total of 10 000 events per sample. Calcium ionomycin (1 µM) was used as a positive control.

2.7. Caspase 3-activity

Caspase-3 activity was determined by flow cytometry using the caspase-3-specific substrate FITC-DEVD-FMK directly conjugated to fluorescein isothiocyanate (FITC). The fluorescence intensity of the stain released from the substrate is proportional to caspase-3 activity. The analysis was conducted according to the manufacturer's protocol. After 24-hour incubation of erythrocytes with PS-NPs in different diameters (~30 nm, ~45 nm and ~70 nm) in the concentration range 10-100 µg/ml, the cells were centrifuged at 3000 rpm for 10 min at 4 ºC and diluted with Ringer buffer (density 1 × 106 cells/mL). The erythrocytes were treated with

caspase-3 substrate (FITC-DEVD-FMK), which binds to activated caspase-3 (2 µg/ml, 60 min, 37 ºC, total darkness). Then the cells were centrifuged at 3000 rpm for 10 min at 4 ºC, washed in wash solution and analysed. Fluorescence was measured at 495 nm (excitation) and 525 nm (emission). The samples were also preincubated with caspase-3 inhibitor (Z-VAD-FMK) at 1 µl/ml to measure the non-specific hydrolysis of the substrate.

2.8. Calpain activity

The calpain activity of the erythrocytes was determined using a commercial calpain assay (QIA120, Merck) following 24-hour incubation with the PS-NPs (~30 nm, ~45 nm and ~70 nm) at 0.1-100 µg/ml. The cells were diluted to a density of $5x10^6$ cells/ml, and 50 µL of sample was loaded in duplicate, in either 100 µL of activator buffer or 100 µL of inhibitor buffer, in a 96-well plate, as per the manufacturer's instructions. Following this, 50 µL of diluted substrate was added in the dark into each well, and the plate was incubated for 15 minutes. The plate was then read at 370 nm (excitation) and 450 nm (emission).

2.9. Statistical analysis

Statistical analysis was performed with GraphPad Prism version 8.3.4 for Windows (GraphPad Software, San Diego, CA, USA) The obtained results were presented as mean ± SD. The mean differences between groups were subjected to multiple comparisons by one-way analysis of variance (ANOVA) followed by Tukey's post hoc test. Statistical significance was assumed for $p < 0.05$.

3.Results

3.1. Reactive Oxygen Species

No statistically-significant changes in ROS levels were observed following 24-hour erythrocyte incubation with PS-NPs (30 nm, 45 nm and 70 nm) (Fig. 1).

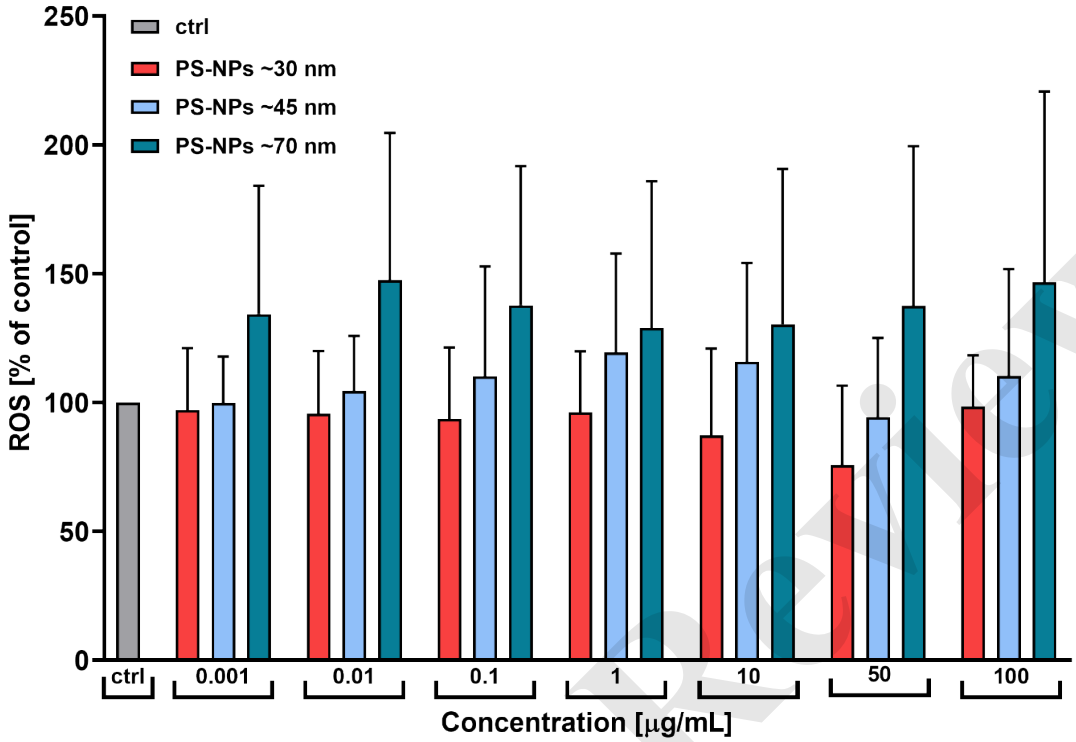

Fig. 1. Effects on ROS formation in human erythrocytes after 24 hours of incubation with PS-NPs of different diameters (concentration range 0.001–100 μg/mL). Each value represents the mean ± SD obtained from 8 independent experiments. An asterisk indicates a significant difference from control (*) $P < 0.05$; one-way ANOVA and a Tukey post hoc test.

3.2. Lipid peroxidation

At a PS-NP concentration of 50 μg/mL, significant increase in lipid peroxidation relative to the control (100%) was observed for NPs measuring ~30 nm and ~70 nm (133% and 119.35% of control values, respectively). At the highest concentration, i.e. 100 μg/mL, a significant increase was also noted for all diameters: 151.53% (30 nm), 121.38% (45 nm), and 120.56% (70 nm) (Fig. 2). Thus, the smallest nanoparticles induced the greatest increase in lipid peroxidation.

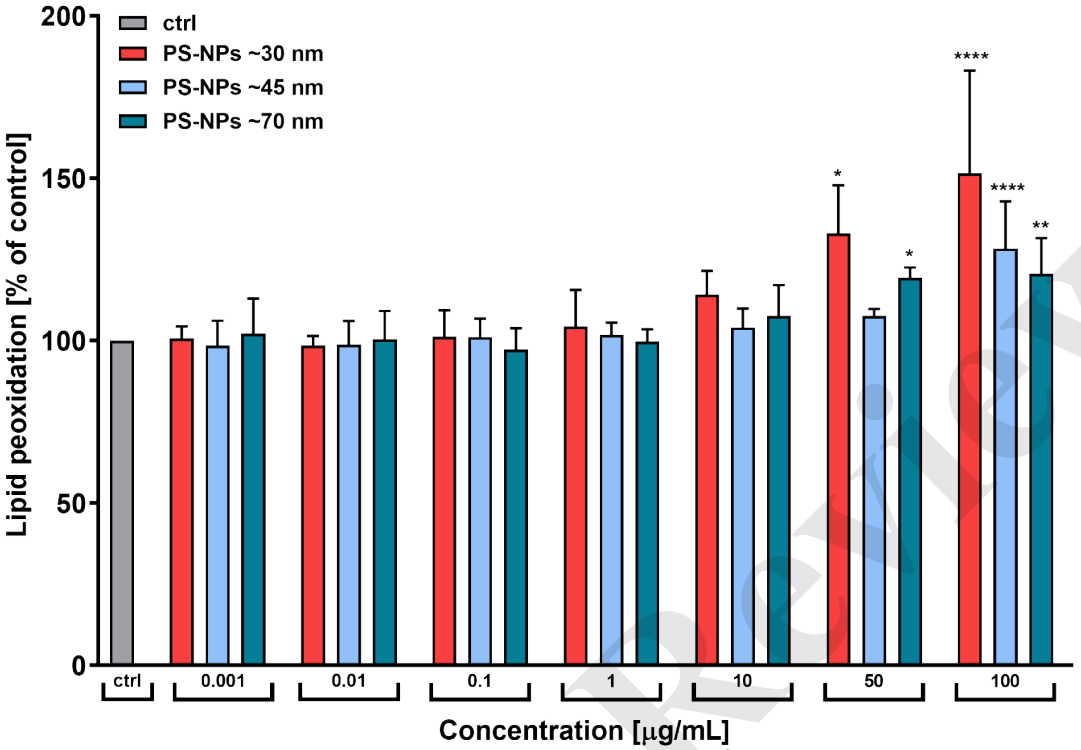

Fig. 2. Changes in lipid peroxidation in human erythrocytes after 24 hours of incubation with PS-NPs of different diameters (concentration range 0.001–100 μg/mL). Each value represents the mean ± SD obtained from 4-6 independent experiments. The asterisk (*) indicates significant differences from control values ($P < 0.05$); one-way ANOVA and a Tukey post hoc test.

3.3. Phosphatidylserine externalisation

After 24-hour incubation, only the smallest PS-NPs (30 nm) at the highest concentration of 100 μg/mL induced a significant increase in phosphatidylserine translocation. For this significant sample, the mean FITC fluorescence reached 180.75% (Fig. 3).

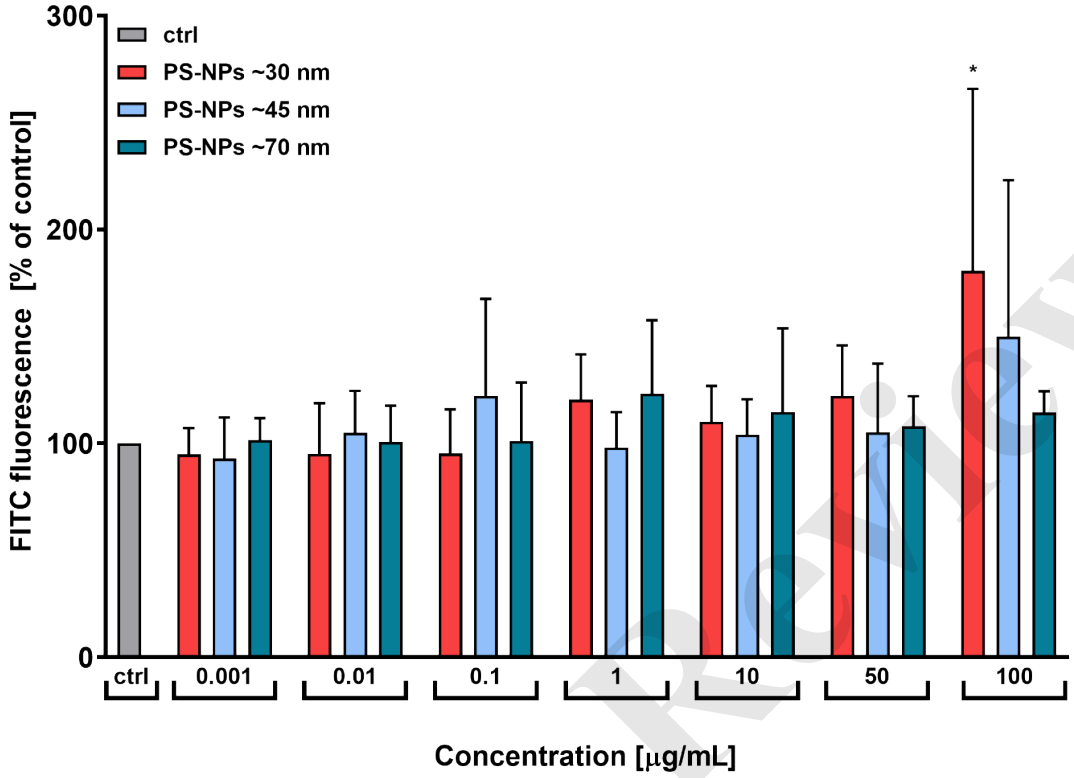

Fig. 3. Effects of phosphatidylserine externalisation in human erythrocytes after 24 hours of incubation with PS-NPs of different diameters (concentration range 0.001–100 μg/mL). Each value represents the mean ± SD obtained from 4-5 independent experiments. The asterisk (*) indicates significant differences from control values ($P < 0.05$); one-way ANOVA and a Tukey post hoc test.

3.4. Intracellular calcium ion level

Following 24-hour incubation, the smaller nonfunctionalized PS-NPs (30 nm and 45 nm) induced a significant increase in intracellular Ca^{2+} levels in human erythrocytes, but only at the highest tested concentration (100 μg/mL). The ~30 nm particles demonstrated a greater increase in intracellular Ca^{2+} mL (mean 166.6% of controls) than the ~45 nm particles (mean 124.13% of controls). No such effect was observed for the largest PS-NPs (~70 nm) at any concentration (Fig. 4).

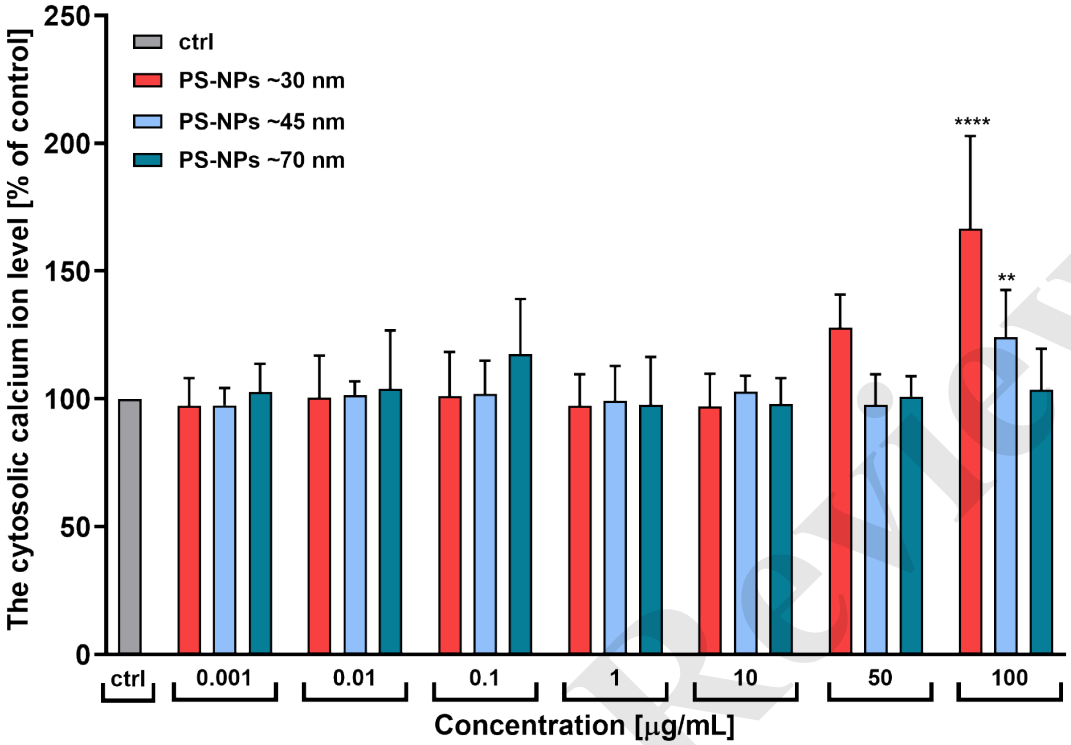

Fig. 4. Changes in cytosolic calcium ion level in human erythrocytes after 24 hours of incubation with PS-NPs of different diameters (concentration range 0.001–100 µg/mL). Each value represents the mean ± SD obtained from 6 independent experiments. The asterisk (*) indicates significant differences from control values ($P < 0.05$); one-way ANOVA and a Tukey post hoc test.

3.5. Caspase 3 activity

No statistically significant changes indicative of caspase-3 activity were observed in human erythrocytes after 24 hours of incubation, irrespective of NP diameter or concentration (10–100 µg/mL) (Fig. 5).

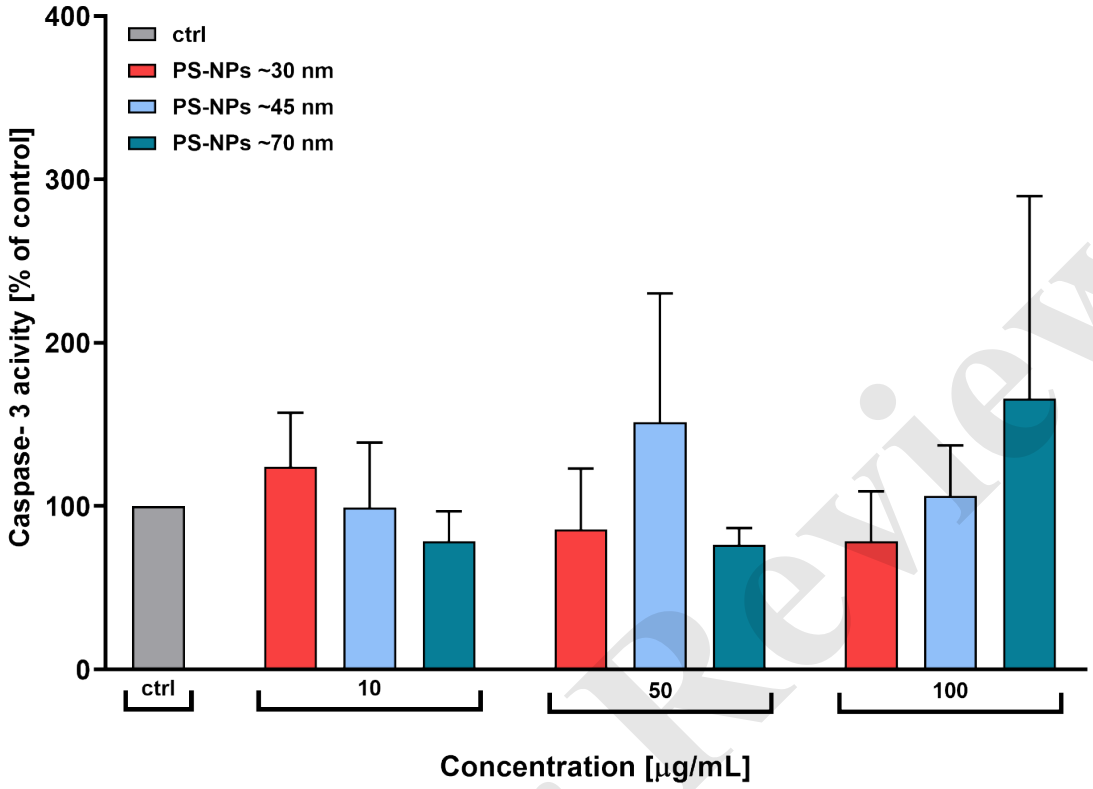

Fig 5. Changes in Caspase-3 activity in human erythrocytes after 24 hours of incubation with PS-NPs of different diameters (concentration range 10–100 μg/mL). Each value represents the mean ± SD obtained from 3 independent experiments. The asterisk (*) indicates significant differences from control values ($P < 0.05$); one-way ANOVA and a Tukey post hoc test.

3.6. Calpain activity

Changes in calpain activity were observed, depending on the size of the NPs. The PS-NPs approximately 45 nm demonstrated changes starting from the lowest concentration (1 μg/mL), the smallest PS-NPs (~30nm) starting at 50 μg/mL, and the largest PS-NPs (~70 nm) only at the highest concentration (100 μg/mL) (Fig. 6).

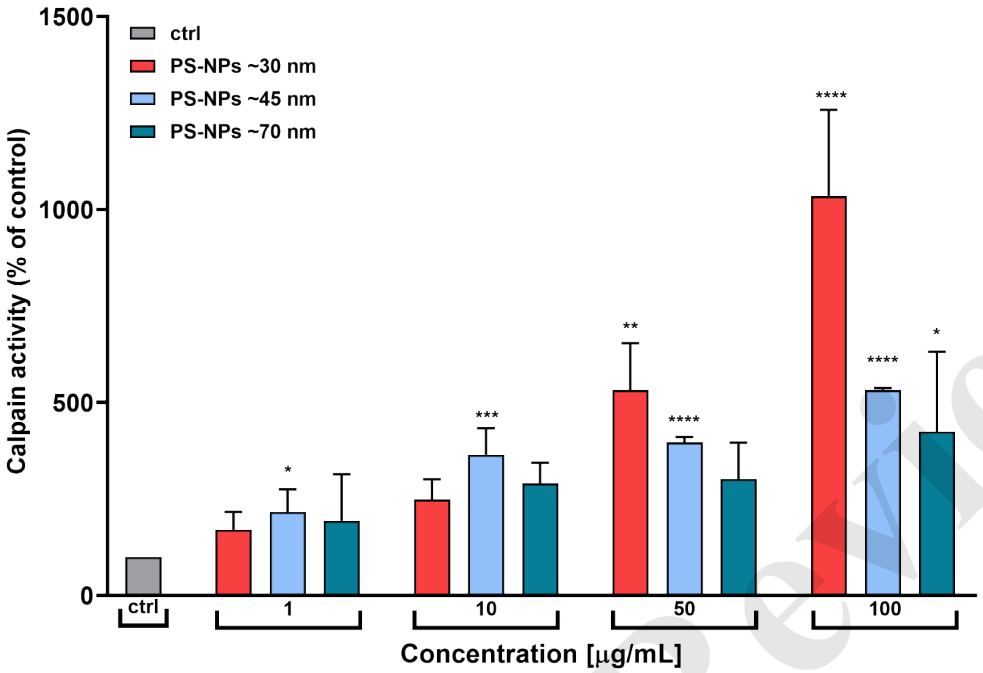

Fig 6. Changes in calpain activity of human erythrocytes after 24 hours of incubation with PS-NPs of different diameters (concentration range 1–100 μg/mL). Each value represents the mean ± SD obtained from 3 independent experiments. The asterisk (*) indicates significant differences from control values ($P < 0.05$); one-way ANOVA and a Tukey post hoc test.

4. Discussion

Polystyrene nanoparticles (PS-NPs) are one of the most widespread forms of synthetic nanomaterials, and are widely used in industry, biotechnology, and medicine (Neagu et al., 2017). However, recent years have seen growing interest in their potential harm, especially regarding their presence in the environment and their potential accumulation in living organisms, including humans (Kik et al., 2020)

One main element of xenobiotic safety assessment is determining their interaction with blood. To reflect this, the present study examined the effect of PS-NPs on erythrocytes; these constitute the most plentiful cell type in blood and play an important role in the transport of oxygen and carbon dioxide. They are also particularly vulnerable to contact with nanoparticles if they are present in the circulation. Due to the lack of a nucleus and organelles, erythrocytes cannot activate typical defence mechanisms like nucleated cells can, which makes them a good model for studying the direct effects of nanoparticles on the cell membrane and redox balance (Lang et al., 2012).

Our previous research indicates that PS-NPs become localized in the cell membrane of human erythrocytes. From there, they alter cell fluidity and shape, induce oxidation of membrane proteins, and ultimately hemolysis; however, cell death is only observed at very high concentrations of 100 µg/mL (30 nm nanoparticles) and 200 µg/mL (45 and 70 nm nanoparticles) (Płuciennik et al., 2025, 2023). Literature data indicate that selected xenobiotics and plastic additives can induce eryptosis, but the effect of plastic nanoparticles on programmed erythrocyte death remains poorly understood.

Therefore, the aim of this study was to evaluate the effect of non-functionalized polystyrene nanoparticles (PS-NPs) with diameters of ~30 nm, ~45 nm, and ~70 nm on the induction of eryptosis. This was achieved by analysing typical markers of this process, *viz.* reactive oxygen species (ROS) levels, lipid peroxidation, phosphatidylserine translocation, intracellular calcium ion concentration, and caspase-3 and calpain activity, following 24-hour exposure to PS-NPs.

Our research has shown indicate that 24-hour incubation of erythrocytes with non-functionalized Ps-NPs (diameters of ~30 nm, ~45 nm, and ~70 nm) did not result in any significant changes in ROS level compared to controls (Fig. 1). These results are consistent with previous research indicating no changes in haemoglobin oxidation by PS-NPs as the main source of ROS in erythrocytes (Płuciennik et al., 2025). This lack of increase in ROS levels may be related to the specificity of erythrocytes, which are devoid of mitochondria and hence may be less susceptible to oxidative damage than nucleated cells. It is known that in nucleated cells, PS-NP-related changes in the mitochondrial membrane result in oxidative stress and an increase in ROS levels (Liu et al., 2022; Xu et al., 2019). However, it should be noted that, contrary to our results, Remigante et al.,(2024) report an increase in ROS levels under the influence of non-functionalized nano- and micro-polystyrene in human erythrocytes, resulting in increased lipid peroxidation and protein sulfhydryl group oxidation. Oxidative stress was also associated with altered band 3 ion transport activity and increased concentrations of oxidized haemoglobin. However, this study was based on particles with a much larger diameter (100 nm and 1000 nm) than in the present study.

While no changes in ROS levels were noted, our results indicate a significant increase in lipid peroxidation, particularly in the case of the smallest nanoparticles (~30 nm); this increase was observed at both 50 µg/ml and the highest concentration tested (100 µg/ml) for all particle sizes (Fig. 2). Similar effects were reported by (Remigante et al., 2024) Smaller

particles may have a stronger effect, which may result from their higher surface-to-volume ratio, which increases their reactivity and potential to destabilize the membrane structure

Another characteristic marker of eryptosis is the translocation of phosphatidylserine to the outer layer of the cell membrane (Lang et al., 2012).In the present study, a significant increase in phosphatidylserine externalization was noted, but only at a NP concentration of 100 µg/ml and only for the smallest particles (30 nm; Fig. 3). However, it should be noted that these changes occurred at a level at which approximately 12% hemolysis was already observed (Płuciennik et al., 2023) this suggests that the observed increase in phosphatidylserine externalization is associated with hemolytic cell membrane destabilization rather than directly with the process of eryptosis.

Therefore, the next stage of the study evaluated eryptosis markers generally occurring at concentrations lower than PS externalization (Jarosiewicz et al., 2019; Maćczak et al., 2016; Sicińska, 2018). It was found that PS-NPs with diameters of ~30 nm and ~45 nm caused a significant increase in Ca^{2+} concentration inside erythrocytes, but only at the highest concentration (100 µg/ml), with the effect being clearly stronger for the smallest particles (Fig. 4). Increased calcium ion influx is considered a key factor inducing eryptosis, leading to potassium channel activation, cell shrinkage, and phosphatidylserine exposure (Alghareeb et al., 2023; Föller and Lang, 2020; Repsold and Joubert, 2018). However, as in the case of PS externalization, the observed changes in calcium ion levels probably resulted from haemolytic changes and not eryptosis, as they only took place at haemolytic concentrations.

Another eryptosis marker, caspase 3 activity, did not change across the entire range of concentrations analysed, further implying that PS-NPs with diameters of 30, 45, and 70 nm do not induce eryptosis in human erythrocytes (Fig. 5). However, changes in calpain activity were observed, even at low pre-haemolytic concentrations, i.e. 1-50 µg/mL (Fig. 6). Therefore, it is possible that PS-NPs may interact with the erythrocyte cell membrane primarily by mechanical means, without triggering classic eryptotic pathways.

Out findings indicate no changes in intracellular Ca^{2+} level, caspase activity, reactive oxygen species (ROS) generation, or phosphatidylserine (PS) externalization on the cell surface at pre-haemolytic concentrations, suggesting no induction of eryptosis. Interestingly, however, increased calpain activity was observed at low nanoparticle concentrations, indicating that PS-NPs may cause subtle structural disturbances at the membrane level. Indeed, previous studies indicate that PS-NPs can physically interact with the membrane

through adsorption, partial penetration into the lipid bilayer, or generation of local stresses(Hollóczki and Gehrke, 2019; Łazarski et al., 2025). This type of mechanical interaction can lead to microdefects in the erythrocyte cytoskeleton. However, calpains, being highly sensitive to cytoskeletal organization disturbances, are likely to be sensitized to activation under conditions of membrane deformation (e.g., reorganization of ankyrin or spectrin), which lowers the calcium activation threshold (Suzuki and Sorimachi, 1998; Von Reyn et al., 2012; Wieschhaus et al., 2012) It is possible that membrane deformation by PS-NPs may induce local changes in the conformation of calpain or its displacement to the vicinity of cofactors, thus causing its activation. This would not require an increase in the global Ca^{2+} level, which was not observed in the present study: a local "micro-shift" near the membrane would suffice. In erythrocytes, where typical calcium signals are low, mechanical stimuli can induce minimal but detectable calpain activity, e.g., by shifting phospholipids and lowering the Ca^{2+} concentration necessary for autolysis and thus for calpain activity (Pontremoli et al., 1985).

In summary, at pre-haemolytic concentrations, no phosphatidylserine externalization, calcium ion influx or changes in caspase-3 activity were noted, nor any increase in ROS levels. This further confirms that eryptosis was not triggered, and the observed effect of increased calpain activity is likely related to the micromechanical response of the cytoskeleton to the interaction with nanoparticles.

Author Contributions

Statement: Conceptualization: K.P., P.S. Methodology K.P., P.S Formal analysis: K.P., B.B., P.S. Visualization K.P., B.B., P.S. Writing—original draft: K.P., B.B., P.S. Supervision: P.S., Writing—review & editing: K.P., B.B., P.S.

Disclosure statement

No potential conflict of interest was reported by the author(s).

Funding

This manuscript was supported by research funding granted to the Department of Biophysics of Environmental Pollution, Faculty of Biology and Environmental Protection, University of Lodz, Poland (grant no. B2511000000191.01), as well as by the University of Lodz Doctoral School of Exact and Natural Sciences (Grant No. B2410000000013.05).

Data availability statement

Data available on request

References

Alghareeb, S.A., Alfhili, M.A., Fatima, S., 2023. Molecular Mechanisms and Pathophysiological Significance of Eryptosis. Int. J. Mol. Sci. 24, 5079. https://doi.org/10.3390/ijms24065079

Bissinger, R., Schumacher, C., Qadri, S.M., Honisch, S., Malik, A., Götz, F., Kopp, H.-G., Lang, F., 2016. Enhanced eryptosis contributes to anemia in lung cancer patients. Oncotarget 7, 14002–14014. https://doi.org/10.18632/oncotarget.7286

Föller, M., Lang, F., 2020. Ion Transport in Eryptosis, the Suicidal Death of Erythrocytes. Front. Cell Dev. Biol. 8, 597. https://doi.org/10.3389/fcell.2020.00597

Hollóczki, O., Gehrke, S., 2019. Nanoplastics can change the secondary structure of proteins. Sci. Rep. 9, 16013. https://doi.org/10.1038/s41598-019-52495-w

Jarosiewicz, M., Michałowicz, J., Bukowska, B., 2019. In vitro assessment of eryptotic potential of tetrabromobisphenol A and other bromophenolic flame retardants. Chemosphere 215, 404–412. https://doi.org/10.1016/j.chemosphere.2018.09.161

Kik, K., Bukowska, B., Sicińska, P., 2020. Polystyrene nanoparticles: Sources, occurrence in the environment, distribution in tissues, accumulation and toxicity to various organisms. Environ. Pollut. 262, 114297. https://doi.org/10.1016/j.envpol.2020.114297

Lang, E., Lang, F., 2015. Triggers, Inhibitors, Mechanisms, and Significance of Eryptosis: The Suicidal Erythrocyte Death. BioMed Res. Int. 2015, 1–16. https://doi.org/10.1155/2015/513518

Lang, F., Lang, E., Föller, M., 2012. Physiology and Pathophysiology of Eryptosis. Transfus. Med. Hemotherapy 39, 308–314. https://doi.org/10.1159/000342534

Łazarski, G., Rajtar, N., Romek, M., Jamróz, D., Rawski, M., Kepczynski, M., 2025. Interaction of Polystyrene Nanoplastic with Lipid Membranes. J. Phys. Chem. B 129, 4110–4122. https://doi.org/10.1021/acs.jpcb.5c00738

Leslie, H.A., Van Velzen, M.J.M., Brandsma, S.H., Vethaak, A.D., Garcia-Vallejo, J.J., Lamoree, M.H., 2022. Discovery and quantification of plastic particle pollution in human blood. Environ. Int. 163, 107199. https://doi.org/10.1016/j.envint.2022.107199

Liu, T., Hou, B., Wang, Z., Yang, Y., 2022. Polystyrene microplastics induce mitochondrial damage in mouse GC-2 cells. Ecotoxicol. Environ. Saf. 237, 113520. https://doi.org/10.1016/j.ecoenv.2022.113520

Maćczak, A., Cyrkler, M., Bukowska, B., Michałowicz, J., 2016. Eryptosis-inducing activity of bisphenol A and its analogs in human red blood cells (in vitro study). J. Hazard. Mater. 307, 328–335. https://doi.org/10.1016/j.jhazmat.2015.12.057

Neagu, M., Piperigkou, Z., Karamanou, K., Engin, A.B., Docea, A.O., Constantin, C., Negrei, C., Nikitovic, D., Tsatsakis, A., 2017. Protein bio-corona: critical issue in immune nanotoxicology. Arch. Toxicol. 91, 1031–1048. https://doi.org/10.1007/s00204-016-1797-5

Nemkov, T., Reisz, J.A., Xia, Y., Zimring, J.C., D'Alessandro, A., 2018. Red blood cells as an organ? How deep omics characterization of the most abundant cell in the human

body highlights other systemic metabolic functions beyond oxygen transport. Expert Rev. Proteomics 15, 855–864. https://doi.org/10.1080/14789450.2018.1531710

Płuciennik, K., Sicińska, P., Duchnowicz, P., Bonarska-Kujawa, D., Męczarska, K., Solarska-Ściuk, K., Miłowska, K., Bukowska, B., 2023. The effects of non-functionalized polystyrene nanoparticles with different diameters on human erythrocyte membrane and morphology. Toxicol. In Vitro 91, 105634. https://doi.org/10.1016/j.tiv.2023.105634

Płuciennik, K., Szabelski, M., Miłowska, K., Ciepluch, K., Duchnowicz, P., Krokosz, A., Sicińska, P., Bukowska, B., 2025. The interactions of non-functionalized polystyrene nanoparticles with human albumin and erythrocyte proteins: implications and potential consequences. Sci. Rep. 15, 30076. https://doi.org/10.1038/s41598-025-15422-w

Pontremoli, S., Melloni, E., Sparatore, B., Salamino, F., Michetti, M., Sacco, O., Horecker, B.L., 1985. Role of phospholipids in the activation of the Ca2+-dependent neutral proteinase of human erythrocytes. Biochem. Biophys. Res. Commun. 129, 389–395. https://doi.org/10.1016/0006-291X(85)90163-9

Remigante, A., Spinelli, S., Gambardella, L., Bozzuto, G., Vona, R., Caruso, D., Villari, V., Cappello, T., Maisano, M., Dossena, S., Marino, A., Morabito, R., Straface, E., 2024. Internalization of nano- and micro-plastics in human erythrocytes leads to oxidative stress and estrogen receptor-mediated cellular responses. Free Radic. Biol. Med. 223, 1–17. https://doi.org/10.1016/j.freeradbiomed.2024.07.017

Repsold, L., Joubert, A.M., 2018. Eryptosis: An Erythrocyte's Suicidal Type of Cell Death. BioMed Res. Int. 2018, 1–10. https://doi.org/10.1155/2018/9405617

Restivo, I., Attanzio, A., Tesoriere, L., Allegra, M., Garcia-Llatas, G., Cilla, A., 2022. Anti-Eryptotic Activity of Food-Derived Phytochemicals and Natural Compounds. Int. J. Mol. Sci. 23, 3019. https://doi.org/10.3390/ijms23063019

Sender, R., Fuchs, S., Milo, R., 2016. Revised Estimates for the Number of Human and Bacteria Cells in the Body. PLOS Biol. 14, e1002533. https://doi.org/10.1371/journal.pbio.1002533

Sicińska, P., 2018. Di-n-butyl phthalate, butylbenzyl phthalate and their metabolites induce haemolysis and eryptosis in human erythrocytes. Chemosphere 203, 44–53. https://doi.org/10.1016/j.chemosphere.2018.03.161

Suzuki, K., Sorimachi, H., 1998. A novel aspect of calpain activation. FEBS Lett. 433, 1–4. https://doi.org/10.1016/S0014-5793(98)00856-4

Tkachenko, A., 2024. Apoptosis and eryptosis: similarities and differences. Apoptosis 29, 482–502. https://doi.org/10.1007/s10495-023-01915-4

Tkachenko, A., Alfhili, M.A., Alsughayyir, J., Attanzio, A., Al Mamun Bhuyan, A., Bukowska, B., Cilla, A., Quintanar-Escorza, M.A., Föller, M., Havranek, O., Jilani, K., Onishchenko, A., Pretorius, E., Prokopiuk, V., Restivo, I., Tesoriere, L., Virzì, G.M., Wieder, T., 2025. Current understanding of eryptosis: mechanisms, physiological functions, role in disease, pharmacological applications, and nomenclature recommendations. Cell Death Dis. 16, 467. https://doi.org/10.1038/s41419-025-07784-w

Von Reyn, C.R., Mott, R.E., Siman, R., Smith, D.H., Meaney, D.F., 2012. Mechanisms of calpain mediated proteolysis of voltage gated sodium channel α-subunits following *in vitro* dynamic stretch injury. J. Neurochem. 121, 793–805. https://doi.org/10.1111/j.1471-4159.2012.07735.x

Wieschhaus, A., Khan, A., Zaidi, A., Rogalin, H., Hanada, T., Liu, F., De Franceschi, L., Brugnara, C., Rivera, A., Chishti, A.H., 2012. Calpain-1 knockout reveals broad effects on erythrocyte deformability and physiology. Biochem. J. 448, 141–152. https://doi.org/10.1042/BJ20121008

Xu, M., Halimu, G., Zhang, Q., Song, Y., Fu, X., Li, Yongqiang, Li, Yansheng, Zhang, H., 2019. Internalization and toxicity: A preliminary study of effects of nanoplastic particles on human lung epithelial cell. Sci. Total Environ. 694, 133794. https://doi.org/10.1016/j.scitotenv.2019.133794

Zhang, Y., Xu, Y., Zhang, S., Lu, Z., Li, Y., Zhao, B., 2022. The regulation roles of Ca2+ in erythropoiesis: What have we learned? Exp. Hematol. 106, 19–30. https://doi.org/10.1016/j.exphem.2021.12.192

OŚWIADCZENIE WSPÓŁAUTORÓW PUBLIKACJI WCHODZĄCYCH W SKŁAD ROZPRAWY DOKTORSKIEJ

Łódź, 16.12.2025 r.

mgr Kamil Płuciennik

Katedra Biofizyki Skażeń Środowiska
Uniwersytet Łódzki

OŚWIADCZENIE WSPÓŁAUTORA

Oświadczam, że w opublikowanej pracy:

Płuciennik K., Sicińska P., Misztal W., Bukowska B., *Important Factors Affecting Induction of Cell Death, Oxidative Stress and DNA Damage by Nano- and Microplastic Particles In Vitro* Cells 2024 13(9) DOI:10.3390/cells13090768

mój udział polegał na opracowaniu koncepcji pracy przeglądowej, zebraniu danych literaturowych i przygotowaniu wstępnej wersji artykułu, redagowaniu roboczej wersji manuskryptu, opracowaniu i przygotowaniu rysunków, przygotowaniu ostatecznej wersji artykułu oraz odpowiedzi na recenzje.

Kamil Płuciennik

Mgr Kamil Płuciennik

(podpis)

Oświadczam, że w opublikowanej pracy:

Płuciennik K., Sicińska P., Duchnowicz P, Bonarska-Kujawa D., Męczarska K., Solarska-Ściuk K., Miłowska K., Bukowska B., *The effects of non-functionalized polystyrene nanoparticles with different diameters on human erythrocyte membrane and morphology.* Toxicology in Vitro 2023 91(1) DOI:10.1016/j.tiv.2023.105634

mój udział polegał na opracowaniu koncepcji badań, zaplanowaniu i wdrożeniu części metodycznej, wykonania eksperymentów (izolacja erytrocytów z kożuszków leukocytarno-płytkowych, analiza stopnia hemolizy erytrocytów, przygotowanie prób do oceny płynności błony komórkowej erytrocytów metodą ERP, ocena wpływu nanocząstek polistyrenu na morfologię erytrocytów), analizie, opracowaniu i interpretacji wyników; wizualizacji wyników, przygotowaniu wstępnej wersji manuskryptu, redagowaniu roboczej wersji manuskryptu i zatwierdzeniu ostatecznej wersji pracy.

Kamil Płuciennik

Mgr Kamil Płuciennik

(podpis)

Łódź, 16.12.2025 r.

mgr Kamil Płuciennik

Katedra Biofizyki Skażeń Środowiska
Uniwersytet Łódzki

Oświadczam, że w opublikowanej pracy:

Płuciennik K., Szabelski M., Miłowska K., Ciepluch K., Duchnowicz P., Krokosz A., Sicińska P., Bukowska B. *The interactions of non-functionalized polystyrene nanoparticles with human albumin and erythrocyte proteins: implications and potential consequences.* Scientific Reports 2025 15(1), DOI:10.1038/s41598-025-15422-w

mój udział polegał na opracowaniu koncepcji badań, wykonaniu eksperymentów (izolacja erytrocytów, izolacja błon erytrocytarnych, analiza z udziałem dichroizmu kołowego, wykonanie badań dotyczących fluorescencji stacjonarnej, utlenianie hemoglobiny, aktywność acetylocholinoesterazy erytrocytarnej, pomiar poziomu grup karbonylowych w białkach, przygotowanie próbek do oceny mikrolepkości wnętrza erytrocytów metodą EPR), analizie, opracowaniu i interpretacji wyników, wizualizacji zdecydowanej większości wyników, przygotowaniu wstępnej wersji manuskryptu, redagowaniu roboczej wersji manuskryptu, przygotowaniu odpowiedzi dla recenzentów, przygotowaniu i zatwierdzeniu ostatecznej wersji artykułu.

Kamil Płuciennik.

Mgr Kamil Płuciennik

(podpis)

Oświadczam, że w manuskrypcie artykułu:

Płuciennik K., Sicińska P., Bukowska B. *Polystyrene nanoparticles and death of erythrocytes: does exposure induce eryptosis?*

mój udział polegał na opracowaniu koncepcji badań, wykonaniu wszystkich eksperymentów, wykonaniu analizy statystycznej i interpretacji wyników, wizualizacji wszystkich wyników, przygotowaniu wstępnej wersji manuskryptu, redagowaniu roboczej wersji manuskryptu, przygotowaniu roboczej wersji artykułu i zatwierdzeniu ostatecznej wersji pracy.

Kamil Płuciennik.

Mgr Kamil Płuciennik

(podpis)

Łódź, 16.12.2025 r.

prof. dr hab. Bożena Bukowska

Katedra Biofizyki Skażeń Środowiska
Uniwersytet Łódzki

OŚWIADCZENIE WSPÓŁAUTORA

Oświadczam, że w opublikowanej pracy:

Płuciennik K., Sicińska P., Misztal W., **Bukowska B.**, *Important Factors Affecting Induction of Cell Death, Oxidative Stress and DNA Damage by Nano- and Microplastic Particles In Vitro* Cells 2024 13(9) DOI:10.3390/cells13090768

mój udział polegał na opracowaniu koncepcji pracy przeglądowej, redagowaniu roboczej wersji manuskryptu, przygotowaniu koncepcji rycin, przygotowaniu i zatwierdzeniu ostatecznej wersji artykułu oraz odpowiedzi na recenzje.

B Bukowska

prof. dr hab. Bożena Bukowska
(*podpis)*

Oświadczam, że w opublikowanej pracy:

Płuciennik K., Sicińska P., Duchnowicz P, Bonarska-Kujawa D., Męczarska K., Solarska-Ściuk K., Miłowska K., **Bukowska B.**, *The effects of non-functionalized polystyrene nanoparticles with different diameters on human erythrocyte membrane and morphology.* Toxicology in Vitro 2023 91(1), DOI:10.1016/j.tiv.2023.105634

mój udział polegał na opracowaniu koncepcji badań, zapewnieniu dostępu do materiałów badawczych, redagowaniu roboczej wersji manuskryptu, wprowadzeniu poprawek merytorycznych i przygotowaniu odpowiedzi dla recenzentów.

B Bukowska

prof. dr hab. Bożena Bukowska
(*podpis)*

Łódź, 16.12.2025 r.

prof. dr hab. Bożena Bukowska

Katedra Biofizyki Skażeń Środowiska
Uniwersytet Łódzki

OŚWIADCZENIE WSPÓŁAUTORA

Oświadczam, że w opublikowanej pracy:

Płuciennik K., Szabelski M., Miłowska K., Ciepluch K., Duchnowicz P., Krokosz A., Sicińska P., **Bukowska B.** *The interactions of non-functionalized polystyrene nanoparticles with human albumin and erythrocyte proteins: implications and potential consequences. Scientific* Reports 2025 15(1), DOI:10.1038/s41598-025-15422-w

mój udział polegał na opracowaniu koncepcji badań, zaplanowaniu i wdrożeniu części metodycznej, zapewnieniu dostępu do materiałów badawczych, redagowaniu roboczej wersji manuskryptu, przygotowaniu odpowiedzi dla recenzentów, przygotowaniu ostatecznej wersji artykułu.

B Bukowska

prof. dr hab. Bożena Bukowska
(podpis)

Oświadczam, że w manuskrypcie artykułu:

Płuciennik K., Sicińska P., **Bukowska B.** *Polystyrene nanoparticles and death of erythrocytes: does exposure induce eryptosis?*

mój udział polegał na opracowaniu koncepcji badań, zapewnieniu dostępu do materiałów badawczych, przygotowaniu roboczej wersji artykułu i zatwierdzeniu ostatecznej wersji pracy.

B Bukowska

prof. dr hab. Bożena Bukowska
(podpis)

Łódź, 16.12.2025 r.

dr hab. Paulina Sicińska

Katedra Biofizyki Skażeń Środowiska
Uniwersytet Łódzki

OŚWIADCZENIE WSPÓŁAUTORA

Oświadczam, że w opublikowanej pracy:

Płuciennik K., **Sicińska P.,** Misztal W., Bukowska B., *Important Factors Affecting Induction of Cell Death, Oxidative Stress and DNA Damage by Nano- and Microplastic Particles In Vitro* Cells 2024 13(9), DOI:10.3390/cells13090768

mój udział polegał na nadzorze merytorycznym nad przygotowaniem artykułu i zatwierdzeniu ostatecznej wersji manuskryptu.

Paulina Sicińska

dr hab. Paulina Sicińska
(podpis)

Oświadczam, że w opublikowanej pracy:

Płuciennik K., **Sicińska P.,** Duchnowicz P, Bonarska-Kujawa D., Męczarska K., Solarska-Ściuk K., Miłowska K., Bukowska B., *The effects of non-functionalized polystyrene nanoparticles with different diameters on human erythrocyte membrane and morphology.* Toxicology in Vitro 2023 91(1), DOI:10.1016/j.tiv.2023.105634

mój udział polegał na wykonaniu części badań dotyczących płynności błony za pomocą znaczników fluorescencyjnych, nadzorze nad badaniami dotyczącymi zmian morfologicznych, analizie, opracowaniu i interpretacji wyników; przygotowaniu roboczej wersji artykułu i zatwierdzeniu ostatecznej wersji manuskryptu.

Paulina Sicińska

dr hab. Paulina Sicińska
(podpis)

Łódź, 16.12.2025 r.

dr hab. Paulina Sicińska

Katedra Biofizyki Skażeń Środowiska
Uniwersytet Łódzki

Oświadczam, że w opublikowanej pracy:

Płuciennik K., Szabelski M., Miłowska K., Ciepluch K., Duchnowicz P., Krokosz A., **Sicińska P.,** Bukowska B. *The interactions of non-functionalized polystyrene nanoparticles with human albumin and erythrocyte proteins: implications and potential consequences. Scientific* Reports 2025 15(1), DOI:10.1038/s41598-025-15422-w

mój udział polegał na nadzorze nad wykonaniem doświadczeń dotyczących oceny poziomu met-Hb, przygotowaniu roboczej wersji artykułu i zatwierdzeniu ostatecznej wersji pracy.

Paulina Sicińska

dr hab. Paulina Sicińska
(podpis)

Oświadczam, że w manuskrypcie artykułu:

Płuciennik K., **Sicińska P.,** Bukowska B. *Polystyrene nanoparticles and death of erythrocytes: does exposure induce eryptosis?*

mój udział polegał na opracowaniu koncepcji badań, zaplanowaniu i wdrożeniu części metodycznej, nadzorze nad wykonaniem doświadczeń, opracowaniu i interpretacji wyników, przygotowaniu roboczej wersji artykułu i zatwierdzeniu ostatecznej wersji pracy.

Paulina Sicińska

dr hab. Paulina Sicińska
(podpis)

Łódź, 21.11.2025 r.

Dr hab. Piotr Duchnowicz

Katedra Biofizyki Skażeń Środowiska
Uniwersytet Łódzki

OŚWIADCZENIE WSPÓŁAUTORA

Oświadczam, że w opublikowanej pracy:

Płuciennik K., Sicińska P., **Duchnowicz P,** Bonarska-Kujawa D., Męczarska K., Solarska-Ściuk K., Miłowska K., Bukowska B., *The effects of non-functionalized polystyrene nanoparticles with different diameters on human erythrocyte membrane and morphology.* Toxicology in Vitro 2023 91(1), DOI:10.1016/j.tiv.2023.105634

mój udział polegał na wykonaniu pomiarów płynności błony erytrocytów metodą elektronowego rezonansu paramagnetycznego oraz wizualizacji wyników i zatwierdzeniu ostatecznej wersji manuskryptu.

.

Dr hab. Piotr Duchnowicz
(*podpis*)

Oświadczam, że w opublikowanej pracy:

Płuciennik K., Szabelski M., Miłowska K., Ciepluch K., **Duchnowicz P.,** Krokosz A., Sicińska P., Bukowska B. *The interactions of non-functionalized polystyrene nanoparticles with human albumin and erythrocyte proteins: implications and potential consequences. Scientific* Reports 2025 15(1), DOI:10.1038/s41598-025-15422-w

mój udział polegał na wykonaniu pomiarów mikrolepkości wnętrza erytrocytów za pomocą elektronowego rezonansu paramagnetycznego, analizie wyników z tej metody i zatwierdzeniu ostatecznej wersji manuskryptu.

Dr hab. Piotr Duchnowicz
(*podpis*)

Łódź, 21.11.2025 r.

Dr hab. Anita Krokosz, prof. UŁ

Katedra Biofizyki Skażeń Środowiska
Uniwersytet Łódzki

OŚWIADCZENIE WSPÓŁAUTORA

Oświadczam, że w opublikowanej pracy:

Płuciennik K., Szabelski M., Miłowska K., Ciepluch K., Duchnowicz P., **Krokosz A.,** Sicińska P., Bukowska B. *The interactions of non-functionalized polystyrene nanoparticles with human albumin and erythrocyte proteins: implications and potential consequences. Scientific* Reports 2025 15(1), DOI:10.1038/s41598-025-15422-w

mój udział polegał na zaplanowaniu i pomocy w ustawieniu metody badawczej dotyczącej utleniania białek, redagowaniu roboczej wersji manuskryptu, odpowiedziach na recenzję i zatwierdzeniu ostatecznej wersji manuskryptu.

Dr hab. Anita Krokosz, prof. UŁ
(*podpis*)

Łódź, 21.11.2025 r.

Dr hab. Katarzyna Miłowska, prof. UŁ

Katedra Biofizyki Ogólnej
Uniwersytet Łódzki

OŚWIADCZENIE WSPÓŁAUTORA

Oświadczam, że w opublikowanej pracy:

Płuciennik K., Sicińska P., Duchnowicz P, Bonarska-Kujawa D., Męczarska K., Solarska-Ściuk K., **Miłowska K.,** Bukowska B., *The effects of non-functionalized polystyrene nanoparticles with different diameters on human erythrocyte membrane and morphology.* Toxicology in Vitro 2023 91(1), DOI:10.1016/j.tiv.2023.105634

mój udział polegał na wykonaniu badań dotyczących oceny potencjału ζ nanocząstek polistyrenu zawieszonych w buforze Ringera, pomocy w redagowaniu roboczej wersji manuskryptu i zatwierdzeniu ostatecznej wersji artykułu.

Dr hab. Katarzyna Miłowska, prof. UŁ
(*podpis*)

Łódź, 21.11.2025 r.

Dr hab. Katarzyna Miłowska, prof. UŁ

Katedra Biofizyki Ogólnej
Uniwersytet Łódzki

OŚWIADCZENIE WSPÓŁAUTORA

Oświadczam, że w opublikowanej pracy:

Płuciennik K., Szabelski M., **Miłowska K.**, Ciepluch K., Duchnowicz P., Krokosz A., Sicińska P., Bukowska B. *The interactions of non-functionalized polystyrene nanoparticles with human albumin and erythrocyte proteins: implications and potential consequences. Scientific* Reports 2025 15(1), DOI:10.1038/s41598-025-15422-w

mój udział polegał na zaplanowaniu i pomocy w ustawieniu metody badawczej dotyczącej dichroizmu kołowego (CD), opracowaniu i interpretacji wyników z CD, pomocy w redagowaniu roboczej wersji manuskryptu, odpowiedziach na recenzje i zatwierdzeniu ostatecznej wersji artykułu.

Dr hab. Katarzyna Miłowska, prof. UŁ
(*podpis*)

Łódź, 21.11.2025 r.

Dr hab. Dorota Bonarska-Kujawa, prof. UPWr

Katedra Fizyki i Biofizyki
Uniwersytet Przyrodniczy we Wrocławiu

OŚWIADCZENIE WSPÓŁAUTORA

Oświadczam, że w opublikowanej pracy:

Płuciennik K., Sicińska P., Duchnowicz P, **Bonarska-Kujawa D.**, Męczarska K., Solarska-Ściuk K., Miłowska K., Bukowska B., *The effects of non-functionalized polystyrene nanoparticles with different diameters on human erythrocyte membrane and morphology.* Toxicology in Vitro 2023 91(1), DOI:10.1016/j.tiv.2023.105634

mój udział polegał na sprawowaniu nadzoru nad wykonaniem badań dotyczących płynności błony za pomocą znaczników fluorescencyjnych, przygotowaniu roboczej wersji artykułu, odpowiedziach na recenzje i zatwierdzeniu ostatecznej wersji manuskryptu.

Dorota Bonarska-Kujawa

Dr hab. Dorota Bonarska-Kujawa, prof. UPWr
(podpis)

Łódź, 21.11.2025 r.

mgr Katarzyna Męczarska

Katedra Fizyki i Biofizyki
Uniwersytet Przyrodniczy we Wrocławiu

OŚWIADCZENIE WSPÓŁAUTORA

Oświadczam, że w opublikowanej pracy:

Płuciennik K., Sicińska P., Duchnowicz P, Bonarska-Kujawa D., **Męczarska K.**, Solarska-Ściuk K., Miłowska K., Bukowska B., *The effects of non-functionalized polystyrene nanoparticles with different diameters on human erythrocyte membrane and morphology.* Toxicology in Vitro 2023 91(1), DOI:10.1016/j.tiv.2023.105634

mój udział polegał na wykonaniu części badań dotyczących płynności błony za pomocą znaczników fluorescencyjnych.

Katarzyna Męczarska

Mgr Katarzyna Męczarska
(podpis)

Łódź, 21.11.2025 r.

Dr Katarzyna Solarska-Ściuk
Katedra Fizyki i Biofizyki
Uniwersytet Przyrodniczy we Wrocławiu
Obecnie:
Wydział Biotechnologii
Collegium Medicum
Uniwersytet Rzeszowski

OŚWIADCZENIE WSPÓŁAUTORA

Oświadczam, że w opublikowanej pracy:

Płuciennik K., Sicińska P., Duchnowicz P, Bonarska-Kujawa D., Męczarska K., **Solarska-Ściuk K.,** Miłowska K., Bukowska B., *The effects of non-functionalized polystyrene nanoparticles with different diameters on human erythrocyte membrane and morphology.* Toxicology in Vitro 2023 91(1), DOI:10.1016/j.tiv.2023.105634

mój udział polegał na wykonaniu części badań dotyczących płynności błony za pomocą znaczników fluorescencyjnych.

Katarzyna Solarska-Ściuk

Dr Katarzyna Solarska-Ściuk
(podpis)

Łódź, 21.10.2025 r

Dr hab. Karol Ciepluch prof. URad

Katedra Podstawowych Nauk Medycznych
Uniwersytet Radomski im. Kazimierza Pułaskiego

OŚWIADCZENIE WSPÓŁAUTORA

Oświadczam że w opublikowanej pracy:

Płuciennik K., Szabelski M., Miłowska K., **Ciepluch K.**, Duchnowicz P., Krokosz A., Sicińska P., Bukowska B. *The interactions of non-functionalized polystyrene nanoparticles with human albumin and erythrocyte proteins: implications and potential consequences* Scientific Reports 2025 15(1), DOI:10.1038/s41598-025-15422-w

mój udział polegał na zaplanowaniu i nadzorze wykonania pomiaru dynamicznego rozpraszania światła, analizie, opracowaniu i interpretacji wyników, wizualizacji wyników, redagowaniu roboczej wersji manuskryptu, odpowiedziach na recenzje i zatwierdzeniu ostatecznej wersji artykułu.

Karol Ciepluch

Dr hab. Karol Ciepluch, prof. URad.
(*podpis*)

Signed by / Podpisano przez:

Karol Eugeniusz Ciepluch
Uniwersytet Radomski im. Kazimierza Pułaskiego

Date / Data: 2025-12-09 13:48

Łódź, 21.11.2025 r.

Dr hab. Mariusz Szabelski, prof. UWM

Katedra Fizyki i Biofizyki
Uniwersytet Warmińsko Mazurski w Olsztynie

OŚWIADCZENIE WSPÓŁAUTORA

Oświadczam, że w opublikowanej pracy:

Płuciennik K., **Szabelski M.,** Miłowska K., Ciepluch K., Duchnowicz P., Krokosz A., Sicińska P., Bukowska B. *The interactions of non-functionalized polystyrene nanoparticles with human albumin and erythrocyte proteins: implications and potential consequences. Scientific* Reports 2025 15(1), DOI:10.1038/s41598-025-15422-w

mój udział polegał na zaplanowaniu i ustawieniu badań dotyczących fluorescencji stacjonarnej i czasów życia fluorescencji, analizie i interpretacji wyników z tej metody, wizualizacji wyników, redagowaniu roboczej wersji manuskryptu, odpowiedziach na recenzje i zatwierdzeniu ostatecznej wersji manuskryptu.

PODPIS ZAUFANY
Mariusz
SZABELSKI
28.11.2025 11:43:08 GMT+1
Dokument podpisany elektronicznie
podpisem zaufanym

Mariusz Szabelski

Dr hab. Mariusz Szabelski, prof. UWM.
(*podpis*)

Łódź, 21.11.2025 r.

Weronika Misztal

Katedra Biofizyki Skażeń Środowiska
Uniwersytet Łódzki

OŚWIADCZENIE WSPÓŁAUTORA

Oświadczam, że w opublikowanej pracy:

Płuciennik K., Sicińska P., **Misztal W.**, Bukowska B., *Important Factors Affecting Induction of Cell Death, Oxidative Stress and DNA Damage by Nano- and Microplastic Particles In Vitro* Cells 2024 13(9), DOI:10.3390/cells13090768

mój udział polegał na zebraniu danych literaturowych do dwóch rozdziałów pracy przeglądowej dotyczących uszkodzenia DNA i stresu oksydacyjnego indukowanego przez cząstki mikroplastiku.

Weronika Misztal

Weronika Misztal
(podpis)